Porirua Harbour - Modelling for Whaitua Collaborative Modelling Group

The expert in **WATER ENVIRONMENTS**

Porirua Harbour - Modelling for Whaitua Collaborative Modelling Group

| Prepared for | Greater Wellington Regional Council |
| Represented by | Brent King |

Te Awarua-o-Porirua

Project manager	John Oldman

Project number	44800943
Approval date	6th June.2019
Revision	Final
Classification	Open

CONTENTS

The expert in **WATER ENVIRONMENTS**

1 Executive Summary

For Te Awarua-o-Porirua Whaitua Collaborative Modelling Project (CMP), a suite of hydrodynamic, wave, sediment transport and contaminant dispersion models have been calibrated against available field data.

These models have been used to assess Porirua Harbour attributes relating to sedimentation, suspended sediment concentration, pathogens, water column nutrients and bed-sediment metal concentrations under existing land use.

The models have then been used to determine how alternative management scenarios (involving land use change, contaminant source control and implementation of stormwater treatment devices) may improve the attribute states for the contaminants being considered in the context of current land use. These scenarios are a Business as Usual (BAU) scenario representative of current potential land use changes implemented using existing approaches to catchment management, and a Water Sensitive scenario representing land use changes using contaminant source control and stormwater treatment devices within the catchment.

This modelling approach has helped inform the Whaitua decision-making process around making recommendations for coastal objectives and approaches to land and water management in the catchment.

Sediments

The focus of the calibration of the sediment transport model was to ensure that the catchment-freshwater-marine modelling approach used for the Whaitua CMP could provide a good quantitative understanding of the basin-wide and subestuary deposition rates that may occur in relation to potential changes in catchment derived sediment loads. Underpinning this is the need to understand the dynamics of the legacy sediments in the harbour – how much existing sediment is there on the seabed, and how are those sediments resuspended by the action of waves and currents and where they are transported to and from under different conditions in the harbour. To provide an understanding of the dynamics of sediments in the harbour, both event-based modelling and an annual simulation have been carried out. This provided an understanding of the variability of the dynamics of sediment entering the harbour under different conditions and widely varying catchment loads. For the annual simulation, 2010 was chosen as it was considered to be representative in terms of sediment loads delivered to the harbour, winds and waves and therefore provided a good overview of the long-term patterns and rates of deposition and erosion that may occur within the harbour.

For each of the scenarios considered, a sediment budget was developed which quantified given catchment sediment inputs, the mass of sediment exported from the harbour, and the mass deposited within each of the arms of the harbour. Under the existing land use, the sediment budget derived is in good agreement with estimates from earlier work when the inter-annual variability of sediment loads is considered.

In much of the harbour, there is a relatively good match between observed trends in deposition and erosion (from sediment plate data and survey data) and those predicted by the model for the year 2010.

The model does not predict very low erosion rates (< 1mm) observed in some of the sub-tidal areas of the harbour towards Browns Bay and the eastern shores of the Onepoto Arm. A

significant amount of work would be required to improve the model calibration for these areas without degrading the overall predictive capability of the model in other parts of the harbour.

Model results indicate that the mass of sediment exported from the harbour is not significantly affected by the scenarios considered, with just over 2000 tonnes of sediment exported per year from the harbour. This compares to the present-day deposition within the harbour of around 6,250 tonnes per year.

The Water Sensitive scenario results in a 40% reduction in sediment load to the harbour. This results in a reduction in the mass of sediment being deposited within the harbour to 2,140 tonnes per year.

The areas that see the biggest reductions in deposition are those closest to the largest subcatchment – the southern sector of the Onepoto Arm and the eastern areas of the Pauatahanui Inlet.

There are localised improvements in suspended sediment concentrations near the catchment outlets but further from the catchment outlets the suspended sediment concentrations are dominated by the resuspension of legacy sediments resulting in limited reductions in suspended sediment concentrations in the wider harbour.

The largest reductions in muddiness are seen in the fringing subestuaries of the Pauatahanui Inlet and in the southern sector of the Onepoto Arm, which are associated with significant reductions in sediment load from the Porirua Mouth subcatchment.

Overall, the reductions in sediment loads associated with the Water Sensitive Scenario lead to reductions in mean annual deposition rates from around 4 mm/yr (in both the Onepoto Arm and Pauatahanui Inlet) to less than 2 mm/yr in the Pauatahanui Inlet and less than 1 mm/yr in the Onepoto Arm.

Nutrients

Currently, there are no major concerns with regard to nutrient issues in either the Onepoto Arm or Pauatahanui Inlet.

Modelling the input, uptake, export and chemical processes involved in Nitrogen and Phosphorous dynamics in a marine system is complex.

For the Whaitua CMP, we adopted a relatively simplified approach where both Total Nitrogen and Total Phosphorus were modelled using a first-order decay approach. This simplifies all the complexities of the nutrient dynamics into quantifying the amount of catchment derived nutrient lost from the harbour – either via export from the harbour through tidal exchange or through losses into the sediment and/or uptake in the water column.

This approach provides relatively good estimates of the observed long-term average water column concentrations of Total Nitrogen and Phosphorus in the harbour and therefore the modelling approach provides some context for assessing the potential influence of scenarios with respect to nutrient levels in the harbour.

Under the alternative scenarios considered, nutrient loads are reduced leading to an overall reduction in predicted nutrient concentrations which is most apparent in the immediate vicinity of the catchment outlets.

Pathogens

No overlapping field data was available to calibrate the pathogen model for the Whaitua CMP. This is because the period chosen to model for the Whaitua CMP was 2004-2014 and regular monitoring of the recreational water quality in Porirua Harbour has only been done since 2015.

However, GWRC have had ongoing work in the harbour developing a water quality forecast model. It has been shown that the water quality forecast model (which forms the basis of the Whaitua CMP model) is a very good predictor of high alert levels for recreational waters.

Model outputs for the Whaitua CMP will therefore provide a good basis for assessing how alternative scenarios may improve water quality in the context of recreational contact. This is done by determining what attribute state may be achieved (ranging from Excellent to Poor) at key sites within the harbour.

For the BAU scenario, there are only limited improvements to the attribute state for pathogens across the key sites.

Improvements to the attribute state for pathogens occurred at all key sites under the Water Sensitive Scenario except at the Waka Ama site, which remained Poor.

Metals

The metal accumulation model assumes that the metal loads being delivered to the harbour are associated with fine cohesive sediments. Understanding the dynamics of the sediments therefore provides a good basis for understanding the potential for the long-term build-up of metals in the harbour.

Despite the model not being calibrated, it can still be used to identify which areas of the harbour may (sometime in the future) have metal accumulation levels that could approach (or exceed) sediment quality guidelines. This will aid with the development of future monitoring strategies and provide some focus for identifying areas in the catchment where combinations of sediment and metal load reductions may provide improvements to metal accumulation in the harbour.

It is unlikely that overall metal accumulation in the Pauatahanui Inlet or the northern sector of the Onepoto Arm will exceed sediment quality guidelines or accelerate under the alternative scenarios.

However, under the BAU scenario, metal accumulation accelerated in the southern sector of the Onepoto Arm due to the simultaneous decreases in sediment loads and increases in metal loads. Under the Water Sensitive Scenario there is likely to be an improvement in Zinc accumulation in this sector of the harbour, but potentially higher levels of Copper accumulation associated with relative decreases in sediment loads and metal loads under this scenario.

2 Introduction

This report provides details of the marine receiving environment models used as part of Te Awarua-o-Porirua Whaitua Collaborative Modelling Project (CMP). The marine receiving environment models cover both the Pauatahanui Inlet and Onepoto Arm of Porirua Harbour and the area immediately offshore of the entrance to the Harbour (Figure 2-1).
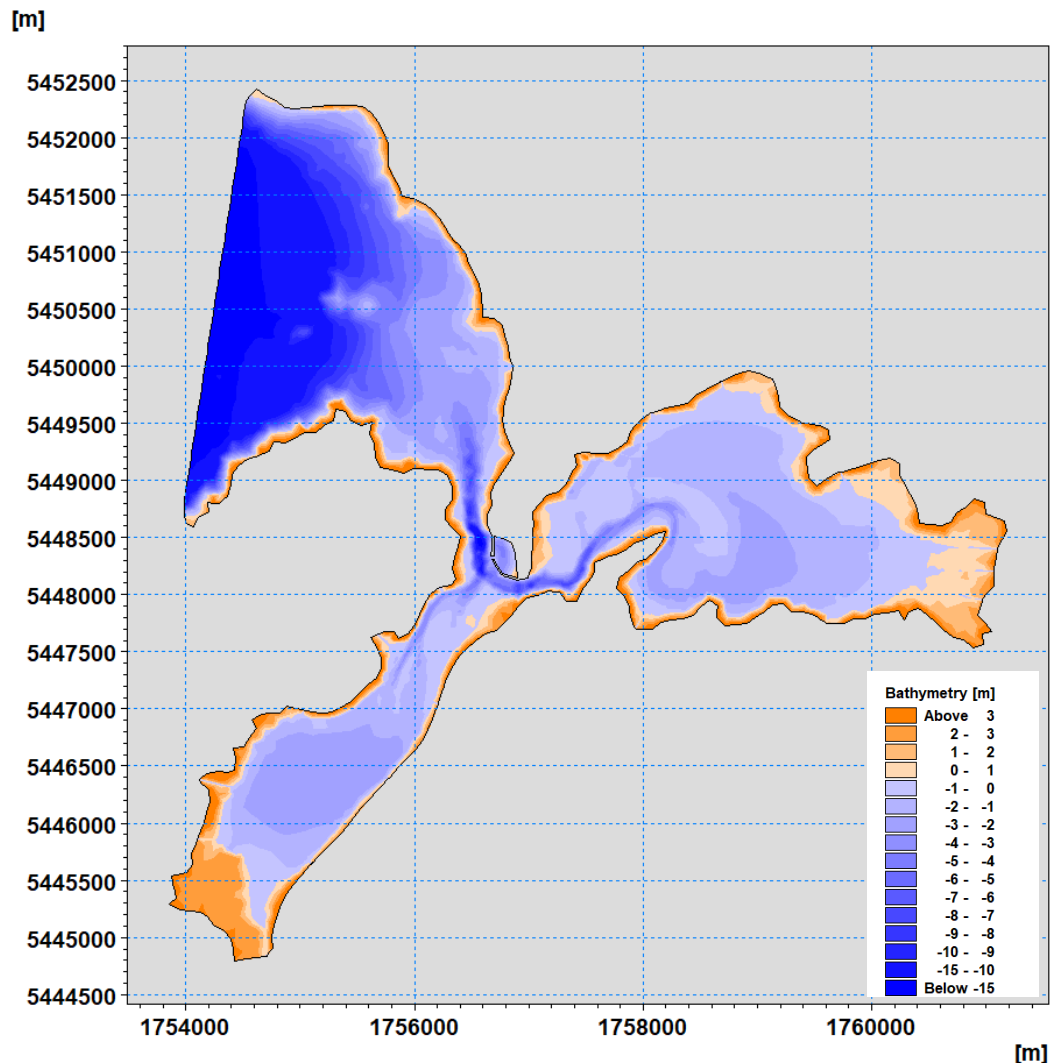
Figure 2-1.   Extent of the marine receiving environment bathymetric mesh used for Te Awarua-o-Porirua Whaitua Collaborative Modelling Project. Depths relative to mean sea level and coordinates in New Zealand Transverse Mercator.

The modelling for Te Awarua-o-Porirua Whaitua Collaborative Modelling Project builds on the modelling that was carried out for the Transmission Gully Motorway assessment (SKM, 2011) which was well calibrated against measured water level, current, wave and suspended sediment concentrations. Refinement and further calibration of these models has been done for the Whaitua CMP based on using the inputs from the catchment and freshwater models (Jacobs, 2019a,b) with the focus on quantifying harbour attributes in relation to the contaminants being considered – sediments, nutrients, pathogens and heavy metals.

The overall framework for the Collaborative Modelling Project included catchment modelling (Moores et al. 2017, Semadeni-Davies and Kachhara, 2017) that provided predictions of catchment diffuse source contaminant loads under alternative land and water management

scenarios. These loads were then transported through the stream network in the catchment to be delivered to the marine receiving environment models. Details of the stream network modelling are provided in Jacobs (2019a,b).

Three different scenarios have been considered, as follows:

- Baseline scenario representing current land use conditions,

- Business as Usual (BAU) scenario representing land use changes and existing approaches to catchment management, and

- Water Sensitive scenario representing land use changes and implementation of contaminant source control and stormwater treatment devices.

The modelling did not consider the timed staging of any of the development of the scenarios but assumed only a fully developed scenario. The modelling did not include the long-term influences of climate change (sea-level rise and change in weather patterns) or the potential effects that the long-term infilling of harbour may have on physical processes that may alter the transport of contaminants within the harbour.

Outputs from the marine receiving environment models and overall characteristics of the scenarios have been used by the Whaitua Committee to carry out an assessment of how marine receiving environment attributes respond to alternative management scenarios involving land use change, contaminant source control and implementation of stormwater treatment devices. This has helped inform the decision-making process around making recommendations for coastal objectives and approaches to land and water management in the catchment.

The scope of work for the marine receiving environment models included establishing a hydrodynamic model and a sediment-transport model which are used together to quantify suspended-sediment concentrations, storm event sediment deposition rates, annual sedimentation rates and changes in sediment texture with time.

The sediment transport model included an advection–dispersion model coupled to an underlying hydrodynamic model. The coupled models transport sediment in the marine receiving environment. Using the same coupled models, the transport of both nutrients and pathogens have been simulated.

For pathogens, the advection–dispersion model applied an inactivation rate which, along with the physical dilution achieved in the marine receiving environment, provided good estimates of the public health risk - particularly at sites remote from the source of contamination (in this case the stream outlets).

The same approach was applied to nutrients to provide good estimates of the long-term average water-column nutrient concentrations.

In addition, outputs from the sediment transport model have been used to provide estimates of the long-term (i.e. 50-100 year) build-up of Zinc and Copper in surface sediments in the Harbour. This has been done using a simple mass balance calculation, in which inputs of new sediments from the subcatchment outlets (with known metal concentration) are mixed with existing bed sediments (with an assumed background level of metal concentration). This approach was applied at a subestuary scale to provide an insight into how metals may accumulate in the different areas of the Harbour.

The report is divided into an overview of catchment load inputs for the scenarios considered (Section 3), a section on model calibration, where the calibration process for each contaminant is discussed (Section 5), and a section where the marine model outputs are presented for each contaminant for each of the scenarios considered (Section 6).

3 Catchment Inputs to Harbour

The marine models were run for three scenarios, the Baseline scenario representing current land use conditions, the Business as Usual (BAU) scenario representing land use changes and existing approaches to catchment management, and the Water Sensitive scenario representing land use changes and implementation of contaminant source control and stormwater treatment devices. Details of the land use changes and mitigations applied for each of these scenarios are provided in Jacobs (2019a).

Daily predictions of flow and contaminant concentrations from the freshwater and catchment modelling (Jacobs, 2019a,b) for the three scenarios have been used as inputs to the marine receiving environment models. The catchment outlets are shown in Figures 3-1 through to 3-3.

In reality, development within a catchment is phased over time and occurs within different parts of the catchment through time. However, it has been assumed that each scenario is representative of a fully developed state. This allows a direct comparison of model results to be made without the complexities of considering when and how a scenario may evolve over time or when it may reach a state of being fully developed.

The sequence and magnitude of rain within the catchment directly determines the freshwater inflows to the marine receiving environment and is also the major driver for contaminant generation and runoff within the catchment. Therefore, to provide a direct comparison between each of the fully developed scenarios, the same representative period of rainfall has been modelled for each fully developed scenario. Jacobs (2019a) identified that the period between 2005 and 2014 provides such a representative range of climatic conditions.

Figure 3-4 shows the annual total (i.e., from all catchment outlets) freshwater inflow to the Harbour (cubic metres per year) for each year in the period 1975 to 2016. It can be seen that the ten-year running average for the period 2005-2014 is close to the long term average value and that there is sequence of higher than average inflows followed by lower than average inflows throughout the period 2005-2014. Of interest is the period of higher than average inflows prior to 1983 and a period of lower than average inflows during the early 1990's. Also, to note are the high inflows that occurred in 2004.

Figure 3-5 shows the annual total (i.e., from all catchment outlets) sediment load (tonnes per year) for each year in the period 1975 to 2016. It can be seen that the highest annual sediment load under the Baseline scenario occurs in 2004. As discussed below, it is therefore important to include sediment loads from 2004 to provide more representative model estimates.

Table 3-1 shows the average annual total (i.e., from all catchment outlets) sediment load (tonnes per year) for different periods between 1975-2016. These are (1) the full catchment load period; 1975–2016, (2) the representative climatic period; 2005-2014, (3) the period between recent bathymetric surveys of the harbour used by DML (2014) to estimate sedimentation rates; 2009–2014, (4) the period between 1974–2009, which was analysed by Gibb (2009) to estimate sedimentation rates, (5) and the period 2004–2015, which is the period considered by the Whaitua CMP for sediment loads.

Table 3-1.   Annual total sediment load (tonnes per year) averaged over different historic periods.

Period	Annual average sediment load (tonnes/year)
2005-2014 (Original period considered for sediments)	9104
Complete record (1975-2016)	12868
Period between previous DML bathymetric surveys (2009-2014)	6156
Gibb (2009) analysis period (1974-2009)	12253
Whaitua Period with addition of 2004	13873

Figure 3-5 and Table 3-1 show the importance of considering 2004 with regard to sediment inputs to the harbour. Over the period 2005–2014 (considered to be climatically representative), the annual sediment load delivered to the harbour was 9,104 tonnes/year averaged but, with the inclusion of the year 2004, this increased to 13,873 tonnes/year. This is close to the annual load averaged over the period 1974–2009 analysed by Gibb (2009).

Further analysis of the input data shows that majority of sediment is delivered during individual events. Individual events in 2004, 2005, 2006, and 2013 were modelled to quantify event-based estimates and a full annual simulation was carried out for 2010 to provide representative annual estimates. The sediment loads for the individual events (as a percentage of the 2010 annual sediment load) are shown in Table 3-2.

Table 3-2.   Total (i.e., from all outlets) sediment load (as a percentage of 2010 annual load) for the individual events shown in Figures 3-6. to 3-12.

Event	Sediment load (% of 2010 load)
2004 Event	590%
2005 Event	59%
2006 Event	223%
2013 Event	107%

Figure 3-1.   Onepoto Arm catchment outlets (all contaminants).

Figure 3-2.   Taupo Stream catchment outlet (pathogens only).
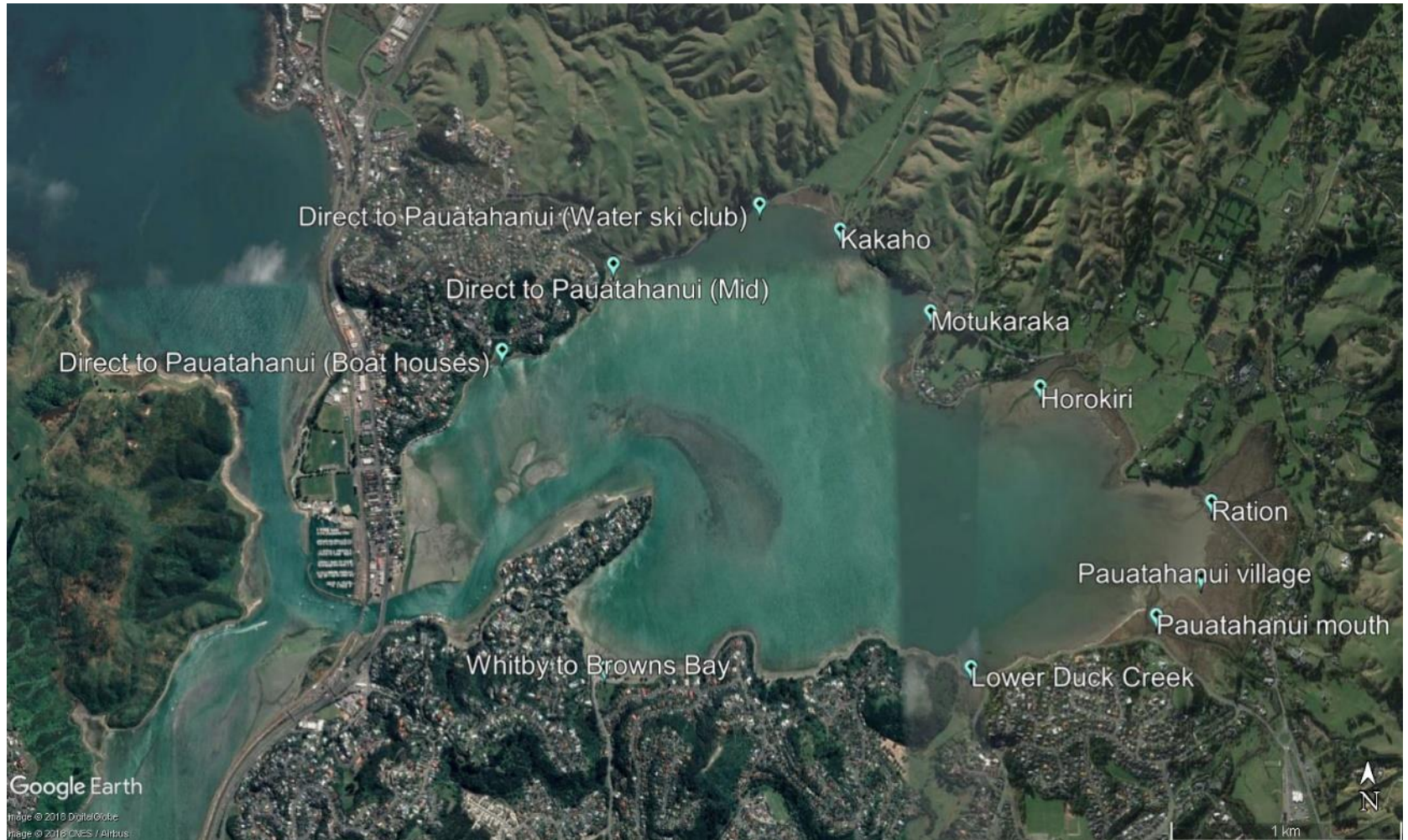
Figure 3-3.   Pauatahanui Inlet catchment outlets (all contaminants).
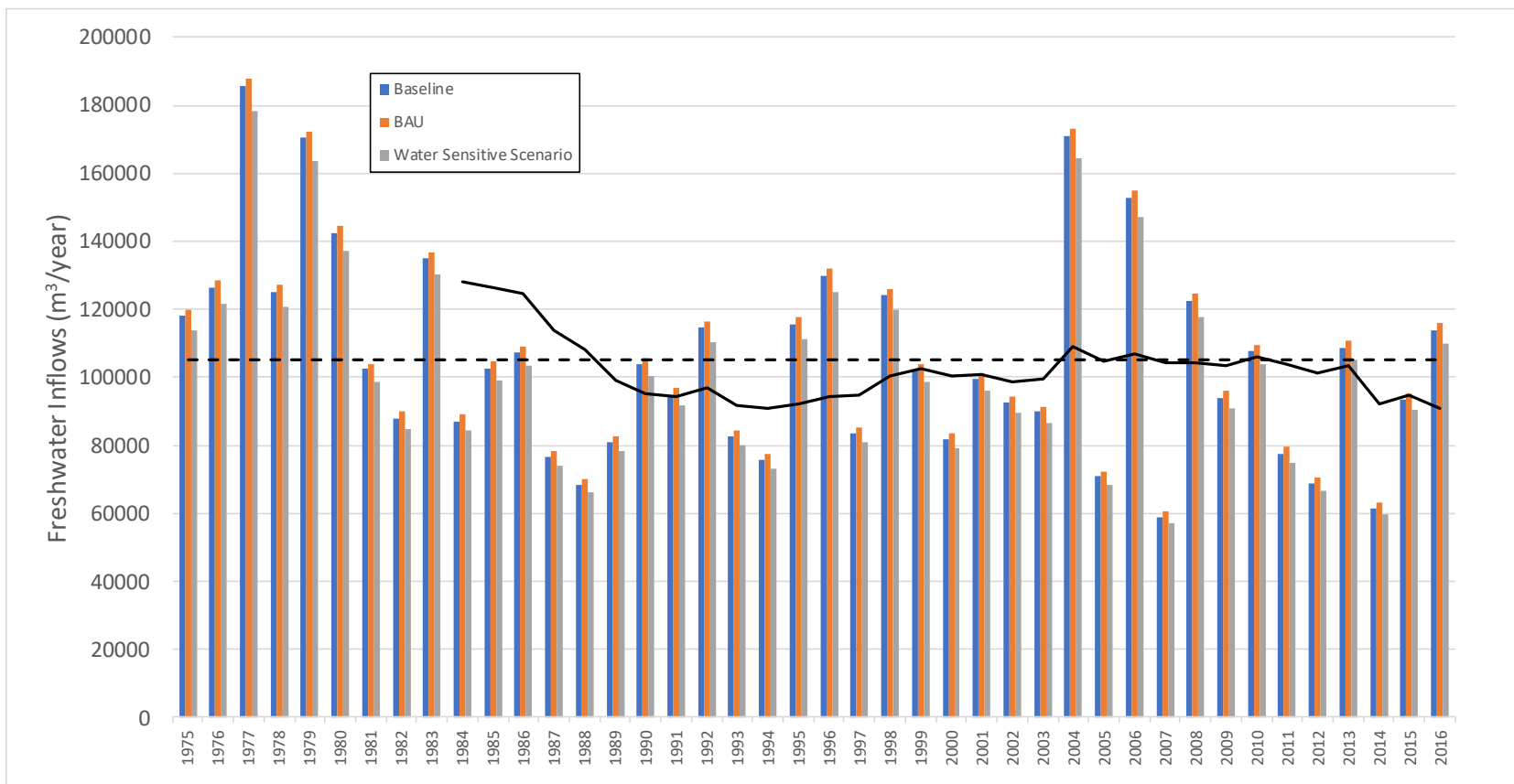
Figure 3-4.   Annual total inflow to the Porirua Harbour (m³/year) for each year in the period 1975–2016. Solid black line shows the ten-year running average inflow (m³/year) while the dashed line shows the average over the full record (1975-2016).
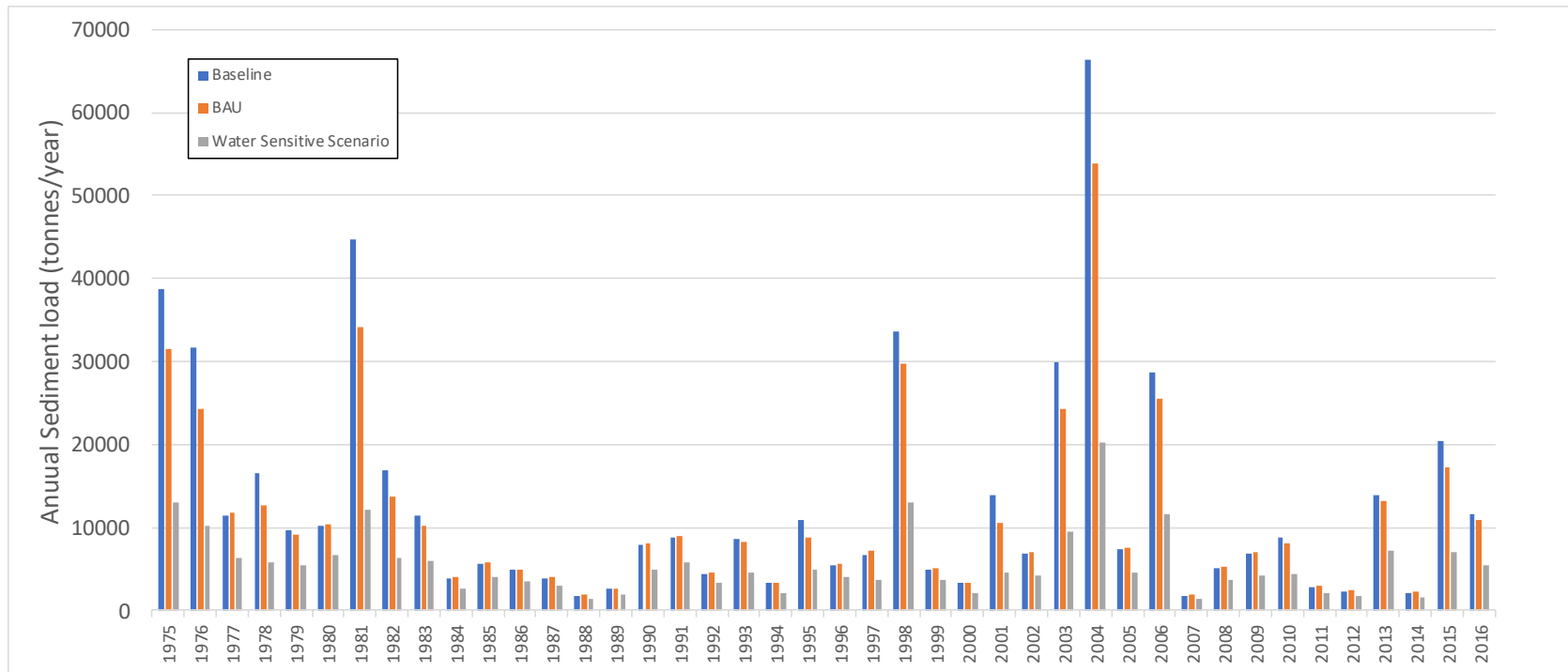
Figure 3-5.   Annual sediment load (tonnes/year) delivered to the Porirua Harbour for each year in the period 1975–2016.

Figures 3-6. to 3-12 show the predicted freshwater inflows to the harbour during the events and for 2010. In addition, the figures show the offshore tidal boundary conditions and the observed wind speed and directions over the period of the events and for 2010.

For the 2004 event, the peak of the hydrograph (and therefore contaminant delivery) occurs during a neap tide (Figure 3-6) a secondary peak in the hydrograph occurs 12 days after the first during a mean tide. Winds over the period (Figure 3-7) peak at over 20 m/s (from the north-east) and regularly exceed 10 m/s (from a range of directions).

The single peak of the hydrograph for the 2005 event (Figure 3-8) occurs during a neap tide. Peak wind speeds of around 10 m/s occur over the simulation period (Figure 3-9) and winds are generally from the north.

For the 2006 event, the peak of the hydrograph (and therefore contaminant delivery) occurs during a mean tide (Figure 3-10) with a number of smaller secondary peaks in the hydrograph. Winds over the period (Figure 3-11) peak at around 18 m/s (from the south) and regularly exceed 10 m/s (from a range of directions).

For the 2013 event, the peak of the hydrograph (and therefore contaminant delivery) occurs during a neap tide (Figure 3-12) with a smaller secondary peak in the hydrograph occurs around a week later on a spring tide. Peak winds (of greater than 15 m/s from the south) correspond to the peaks in the hydrograph (Figure 3-13).

For completeness, Figures 3-14 and 3-15 show the time series data for all of 2010. Figure 3-14 shows that the majority of the sediment load delivered in 2010 (~two-thirds of the annual average load) is distributed across several events over the winter period.

Figures 3-16 to 3-19 show the annual Total Nitrogen, Total Phosphorous, Total Zinc and Total Copper loads (all kg/year) delivered to the harbour and Figure 3-20 shows the mean daily *E. Coli* count (cfu/100 mL) averaged over all catchment outlets and for each year in the period 2005-2014[1]. Loads for 2010 for these contaminants are very close to the average catchment input record (2005-2014).

To put the relative loads from each catchment outlet in context, Table 3-3 shows the relative contribution of each of the catchment outlets in terms of freshwater inflows, loads for sediments, Total Nitrogen, Total Phosphorous, Total Zinc and Total Copper and the mean subcatchment daily *E. Coli count* (cfu/100 mL). In addition, Table 3-4 shows a summary of the changes associated with each contaminant and freshwater inflow under the fully developed BAU and Water Sensitive Scenario.

---

[1] Note that wastewater overflows were only modelled 2005-2014 (Jacobs, 2019a).
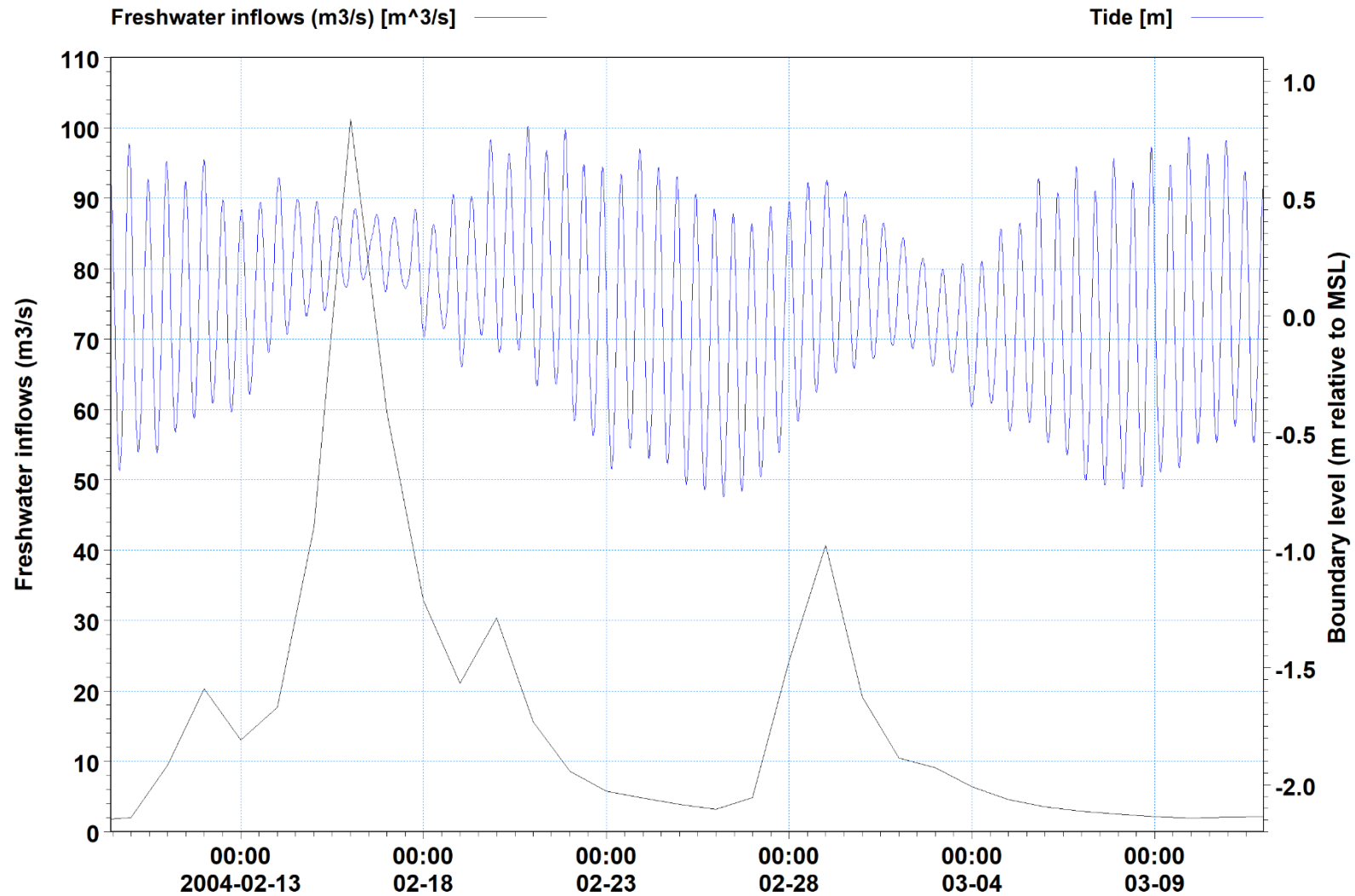
Figure 3-6.   Time series of total (i.e., from all outlets) freshwater inputs (black line) and offshore tidal boundary conditions (blue line) for the 2004 event. The offshore tidal boundary condition is derived from a combination of the predicted tide at the model boundary (Figure 2-1) adjusted for barometric pressure.
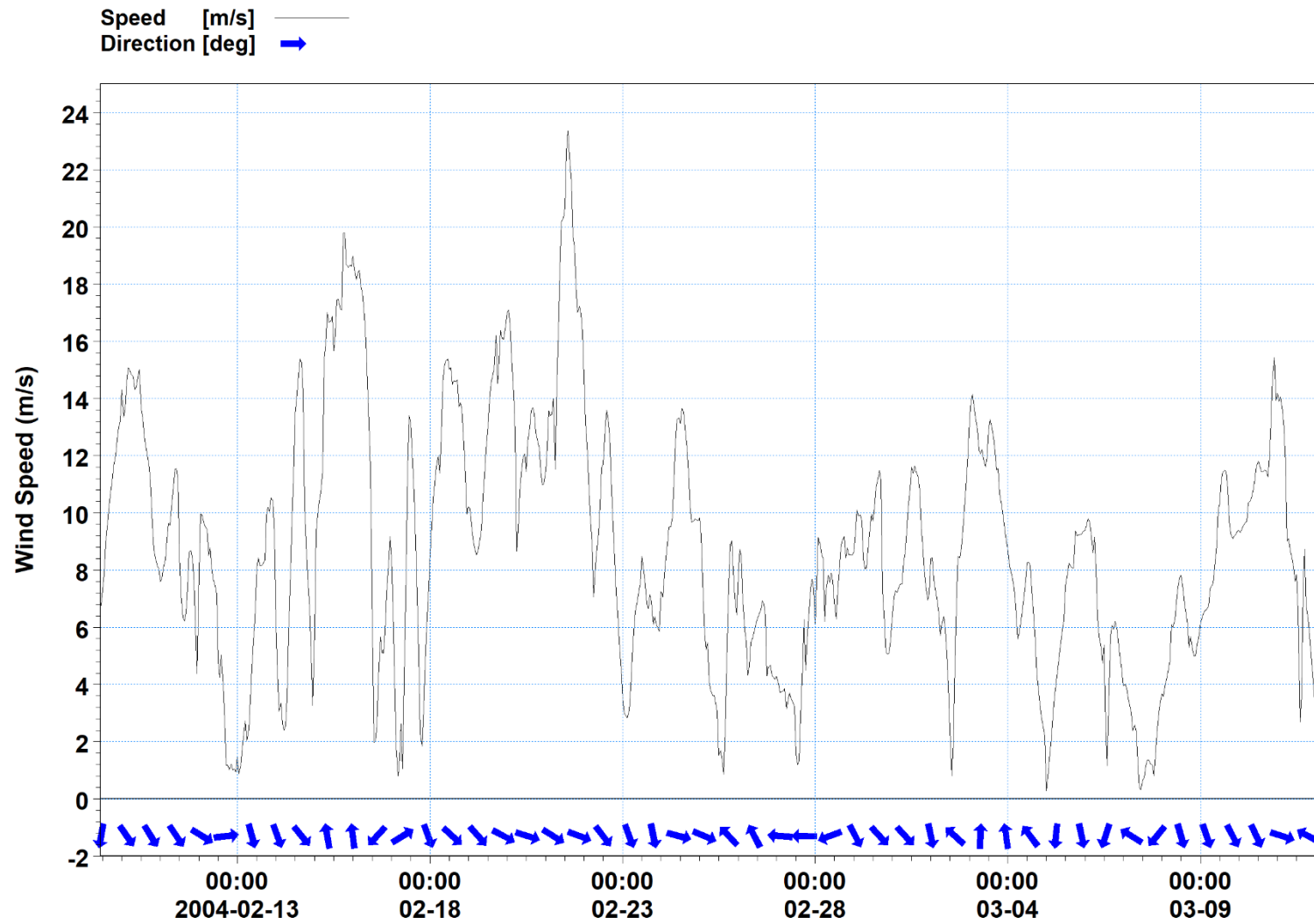
Figure 3-7.   Wind speed and direction from the Mana Island automated weather station during the 2004 event.
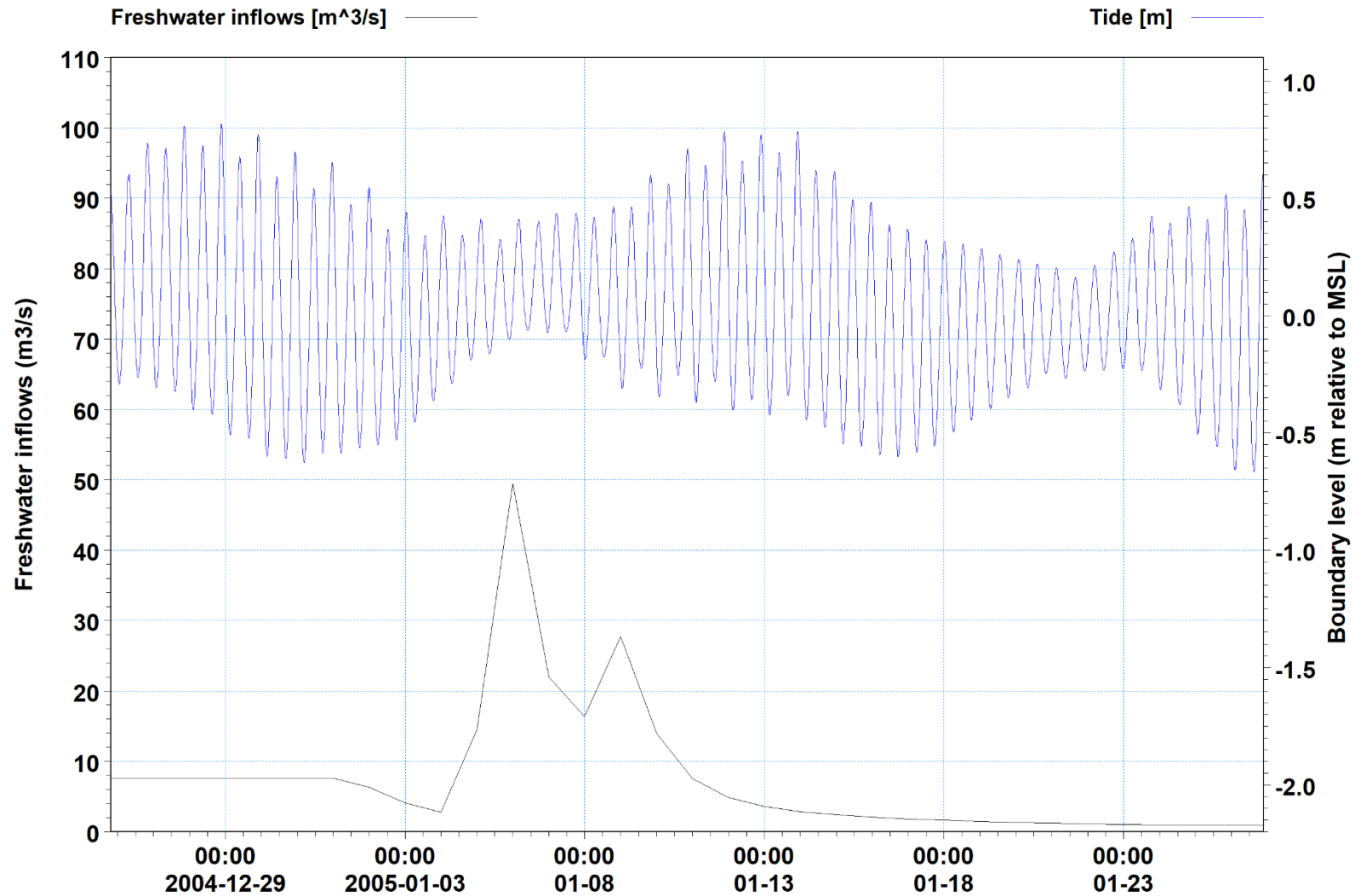
Figure 3-8. Time series of total (i.e., from all outlets) freshwater inputs (black line) and offshore tidal boundary conditions (blue line) for the 2005 event. The offshore tidal boundary condition is derived from a combination of the predicted tide at the model boundary (Figure 2-1) adjusted for barometric pressure.
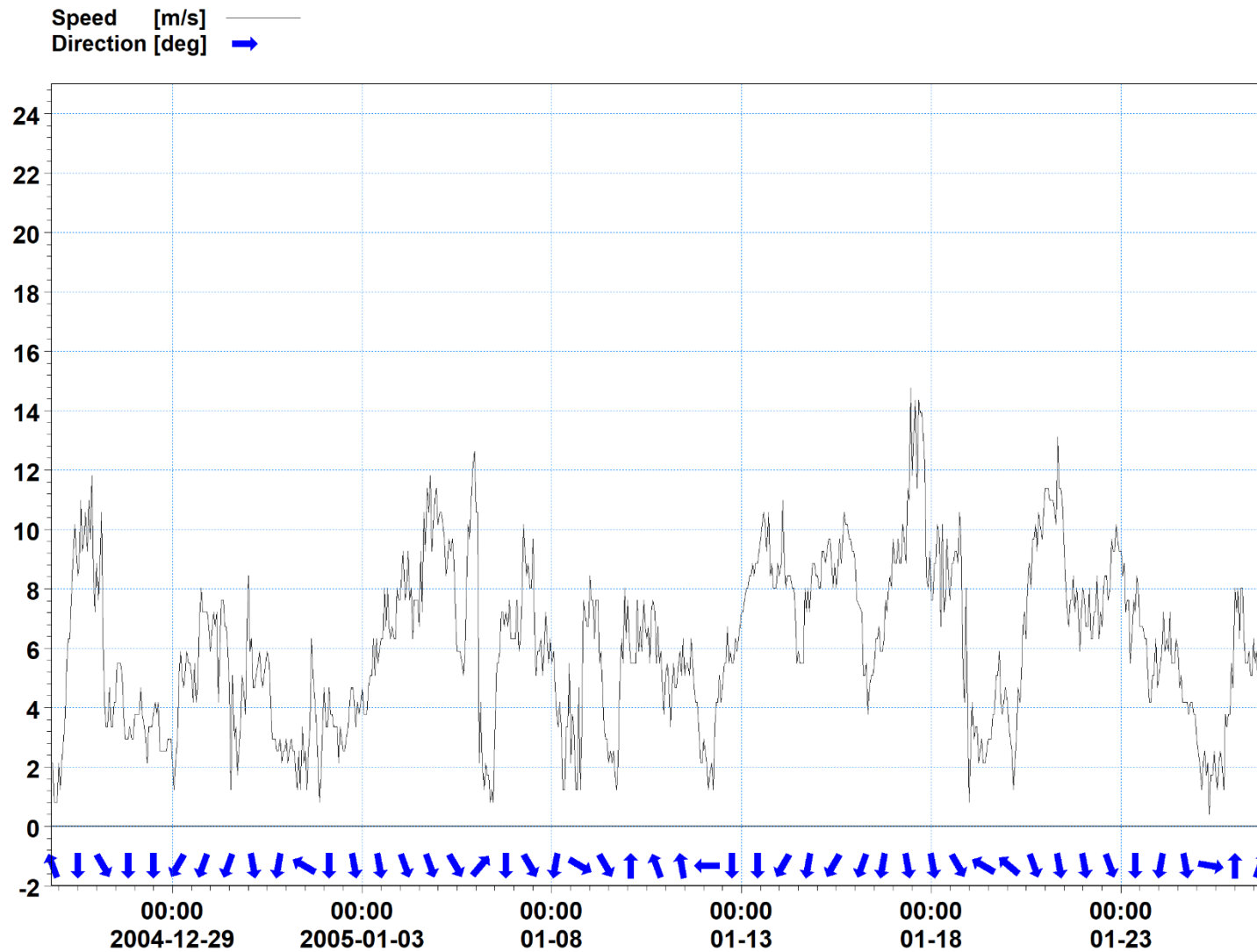
Figure 3-9.   Wind speed and direction from the Mana Island automated weather station during the 2005 event.
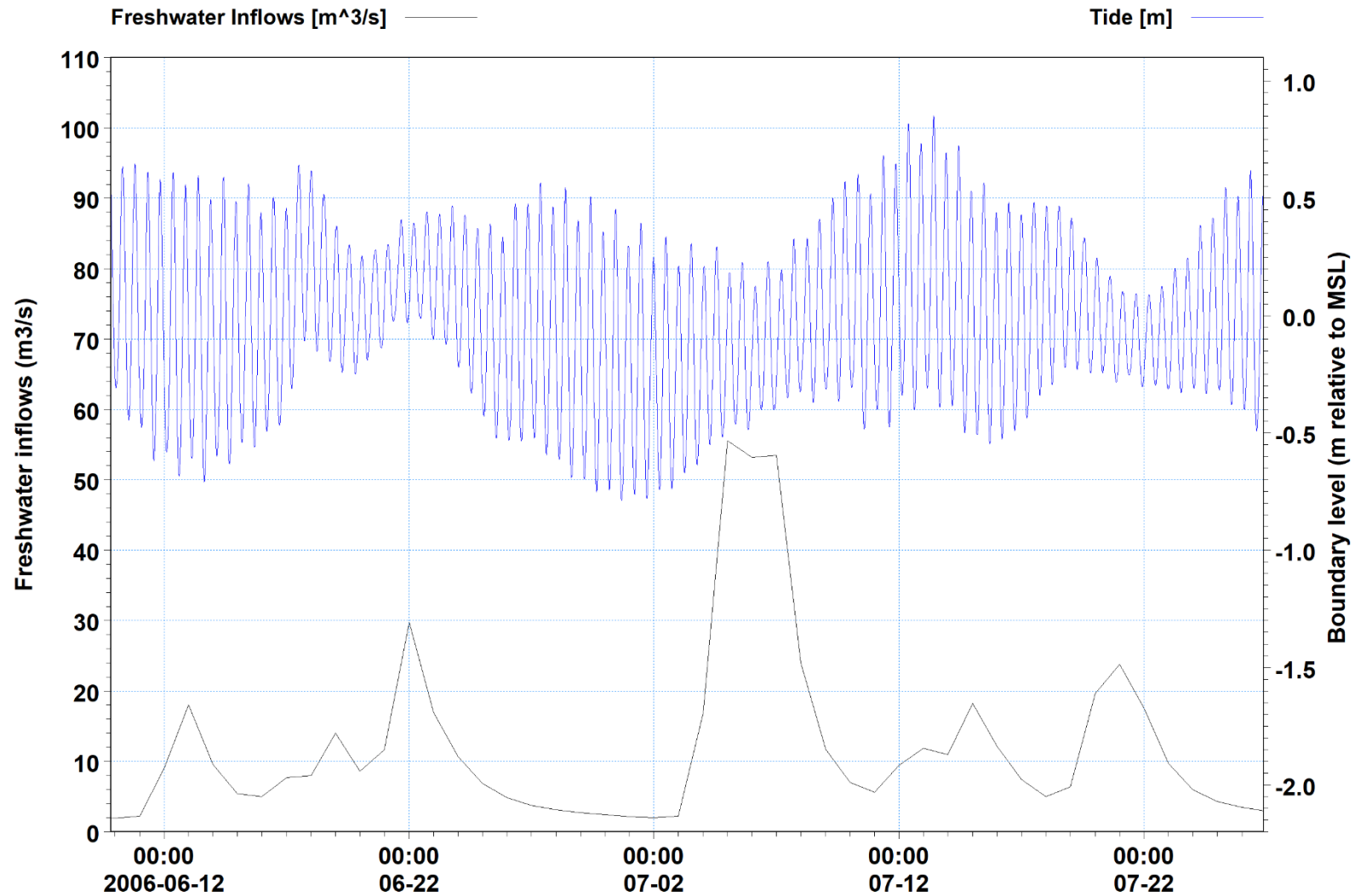
Figure 3-10.   Time series of total (i.e., from all outlets) freshwater inputs (black line) and offshore tidal boundary conditions (blue line) for the 2006 event. The offshore tidal boundary condition is derived from a combination of the predicted tide at the model boundary (Figure 2-1) adjusted for barometric pressure.
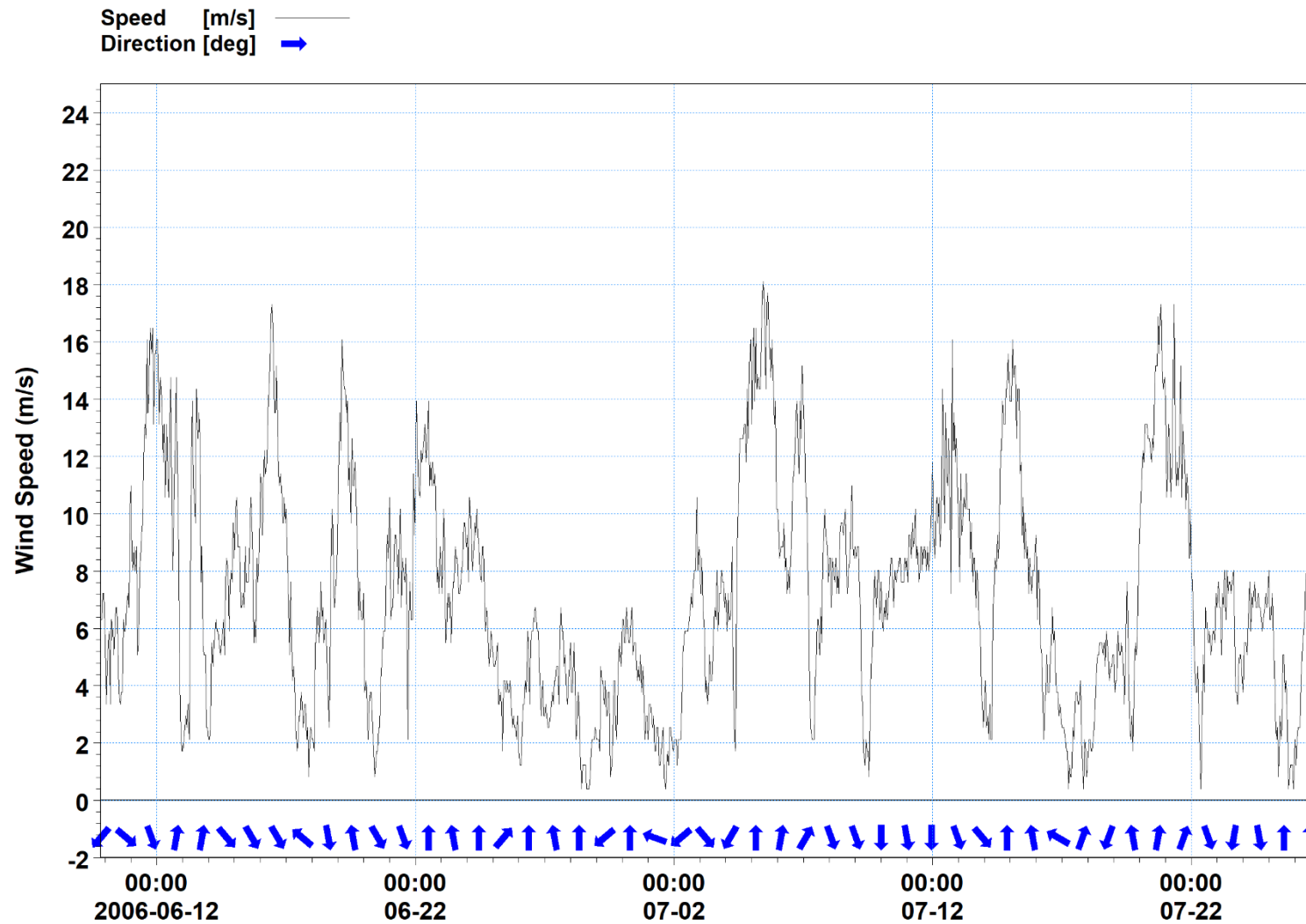
Figure 3-11.   Wind speed and direction from the Mana Island automated weather station during the 2006 event.

jwo / 15.11.2018
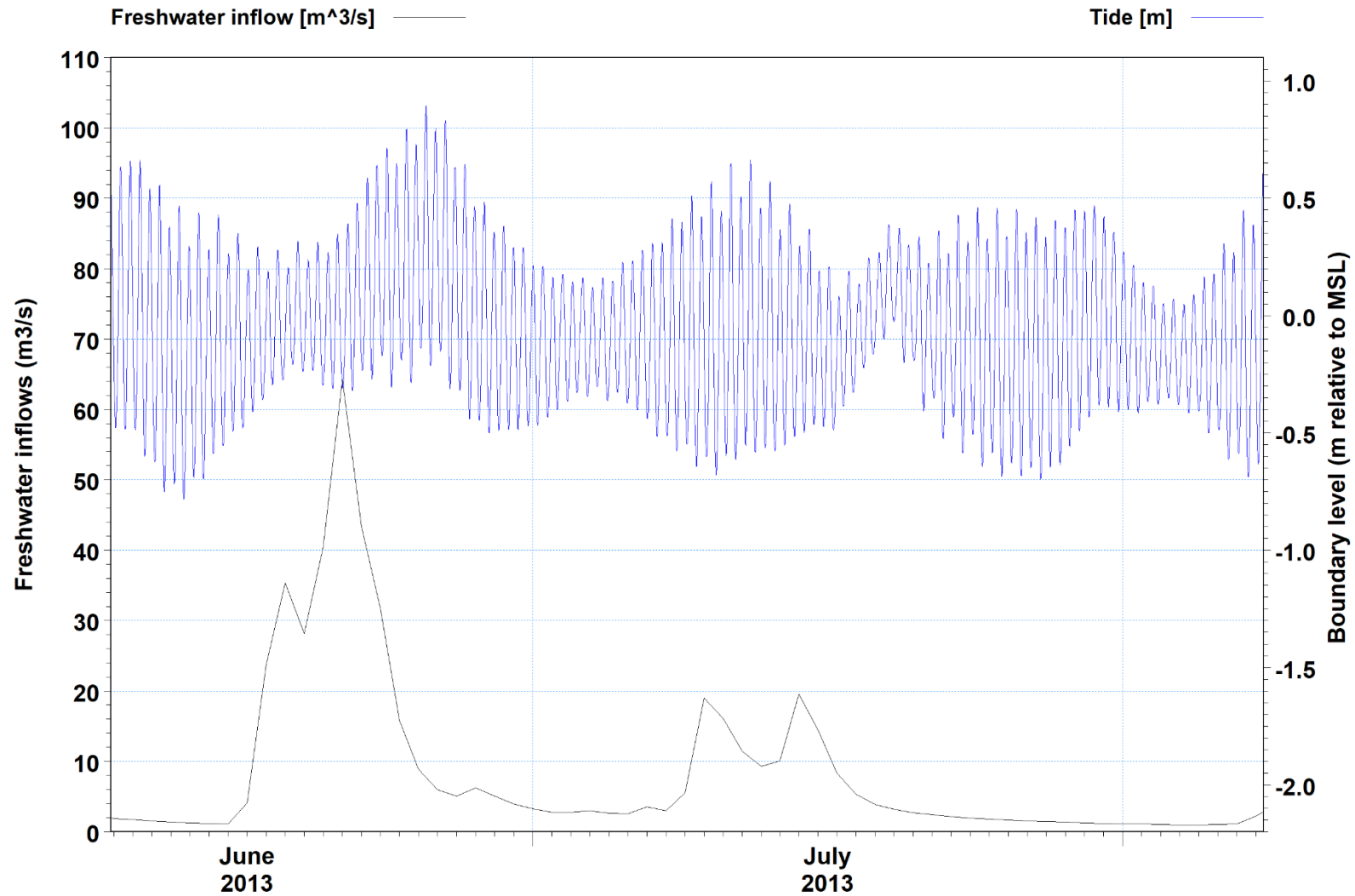
Figure 3-12. Time series of total (i.e., from all outlets) freshwater inputs (black line) and offshore tidal boundary conditions (blue line) for the 2013 event. The offshore tidal boundary condition is derived from a combination of the predicted tide at the model boundary (Figure 2-1) adjusted for barometric pressure.
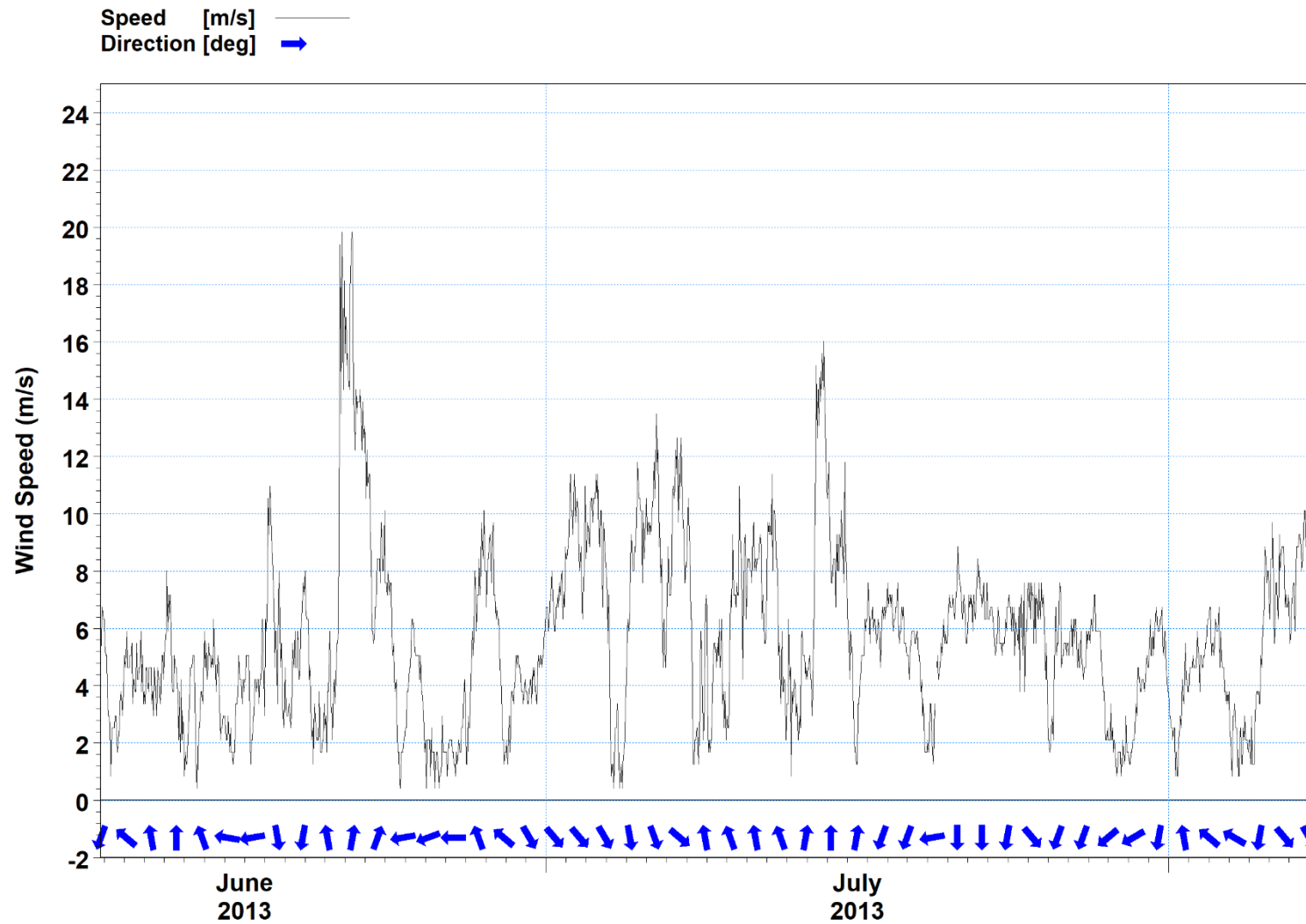
Figure 3-13.   Wind speed and direction from the Mana Island automated weather station during the 2013 event.

jwo / 15.11.2018
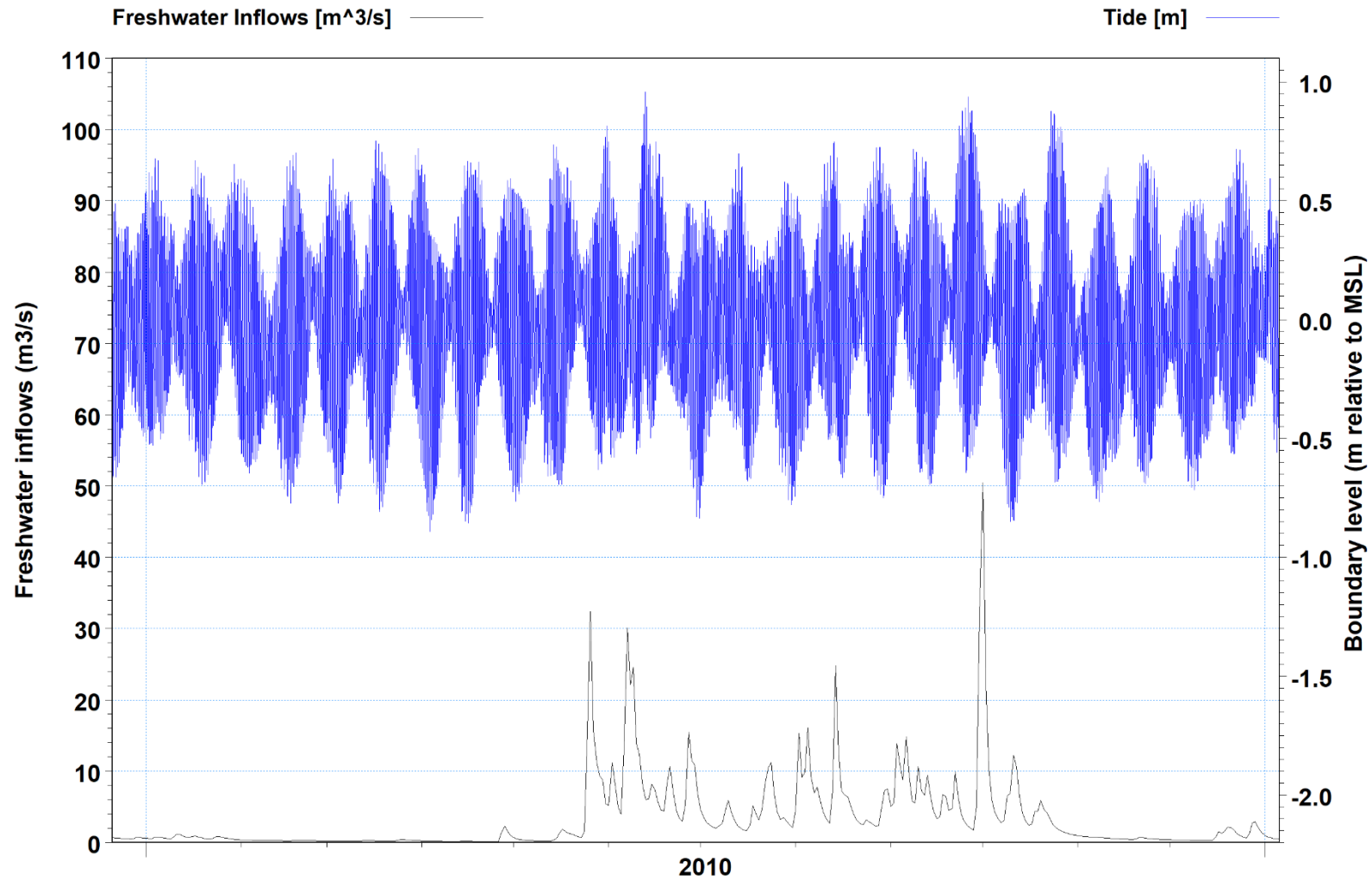
Figure 3-14.   Time series of total (i.e., from all outlets) freshwater inputs (black line) and offshore tidal boundary conditions (blue line) for the 2010. The offshore tidal boundary condition is derived from a combination of the predicted tide at the model boundary (Figure 2-1) adjusted for barometric pressure
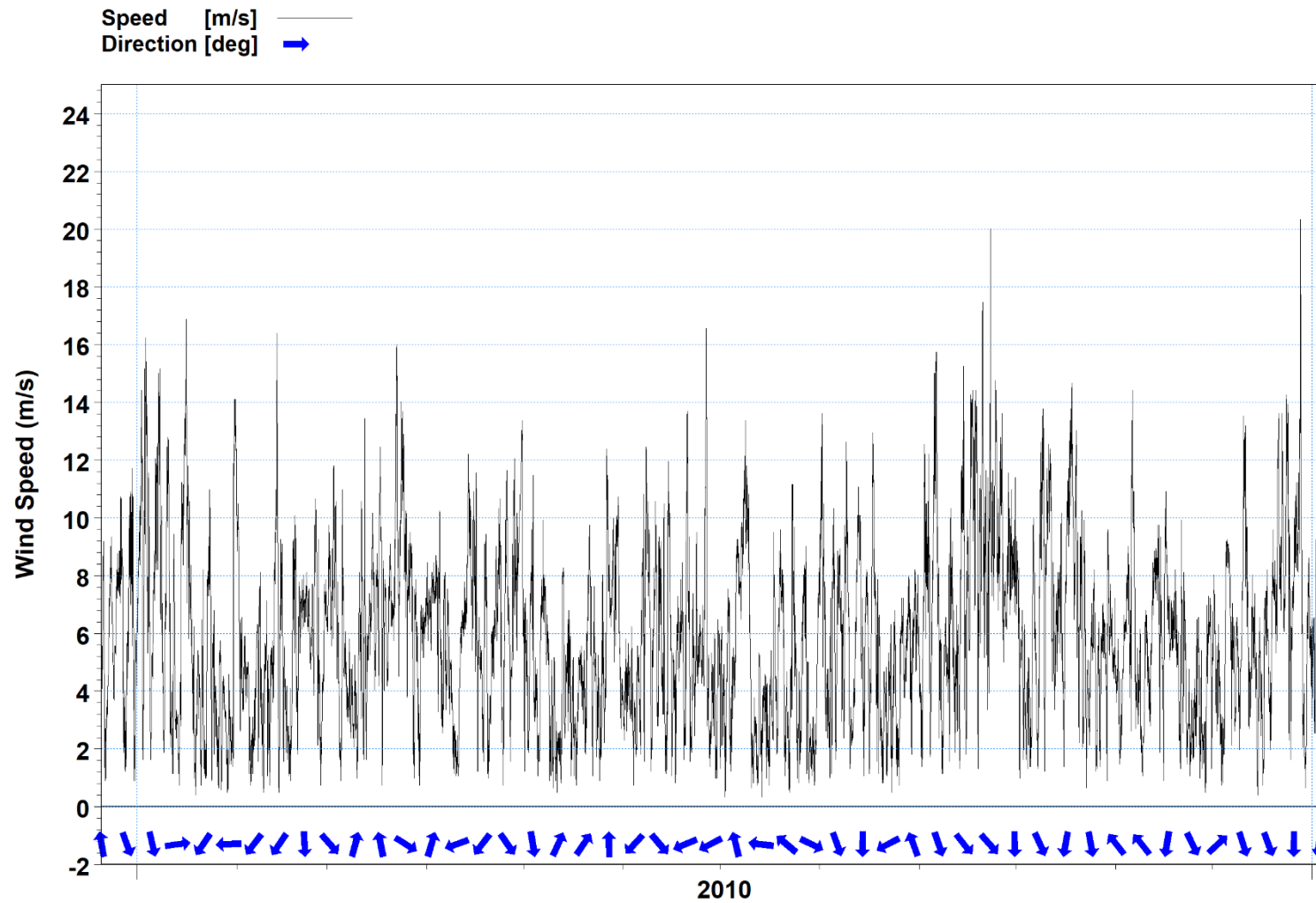
Figure 3-15. Wind speed and direction from the Mana Island automated weather station during 2010.
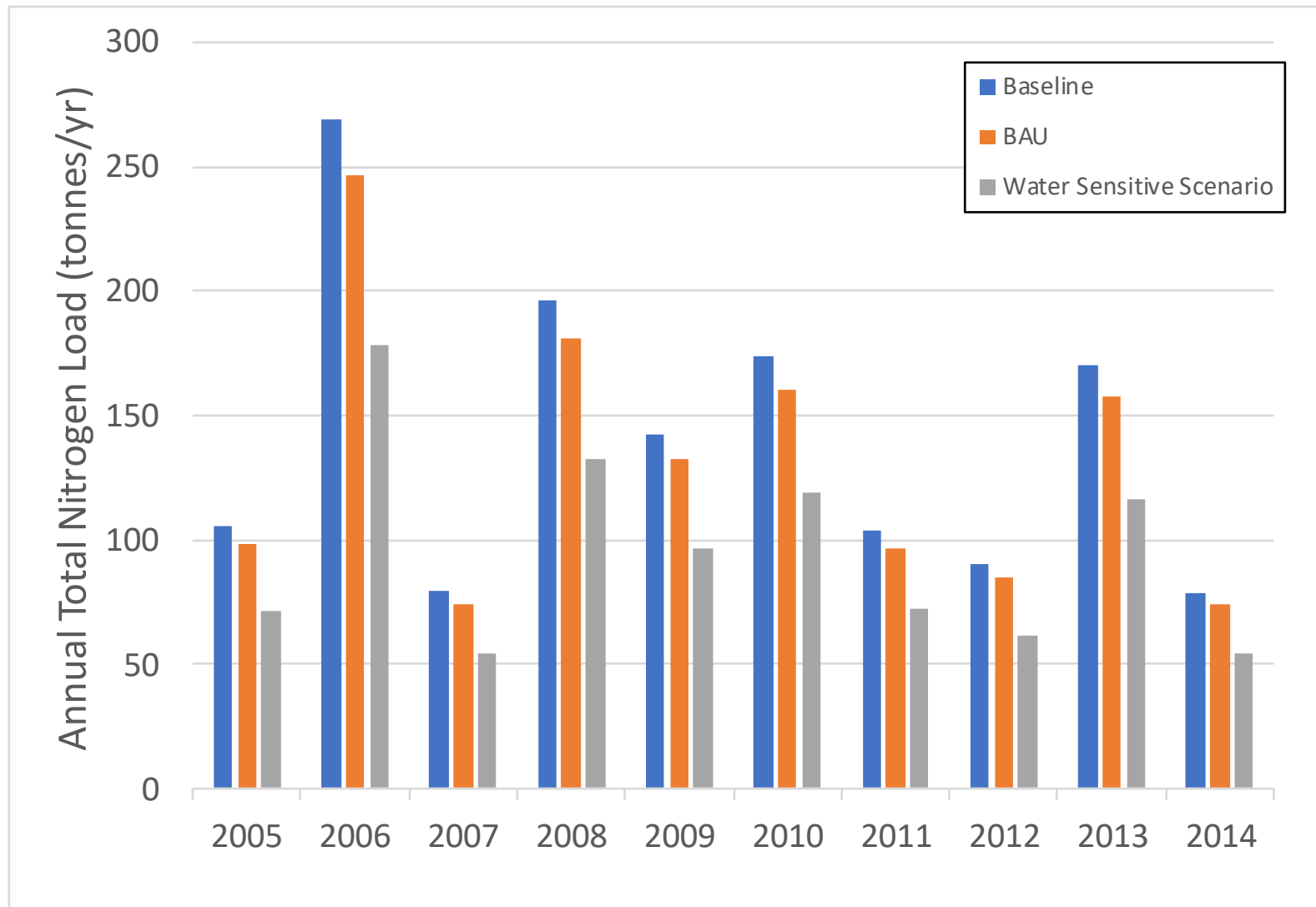
Figure 3-16.   Annual Total Nitrogen load (tonnes/yr) delivered to the Porirua Harbour.
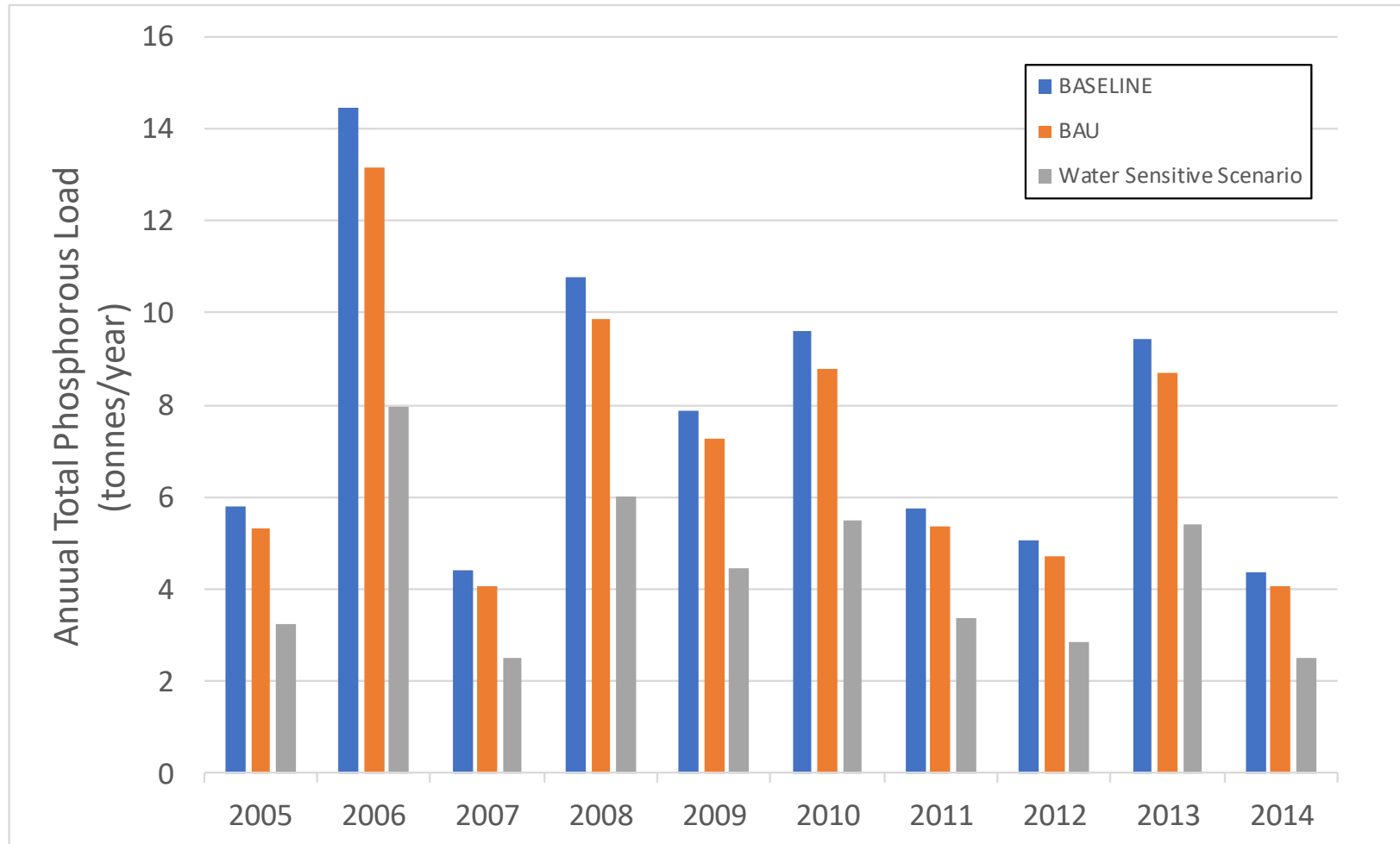
Figure 3-17.   Annual Total Phosphorous load (tonnes/yr) delivered to the Porirua Harbour.
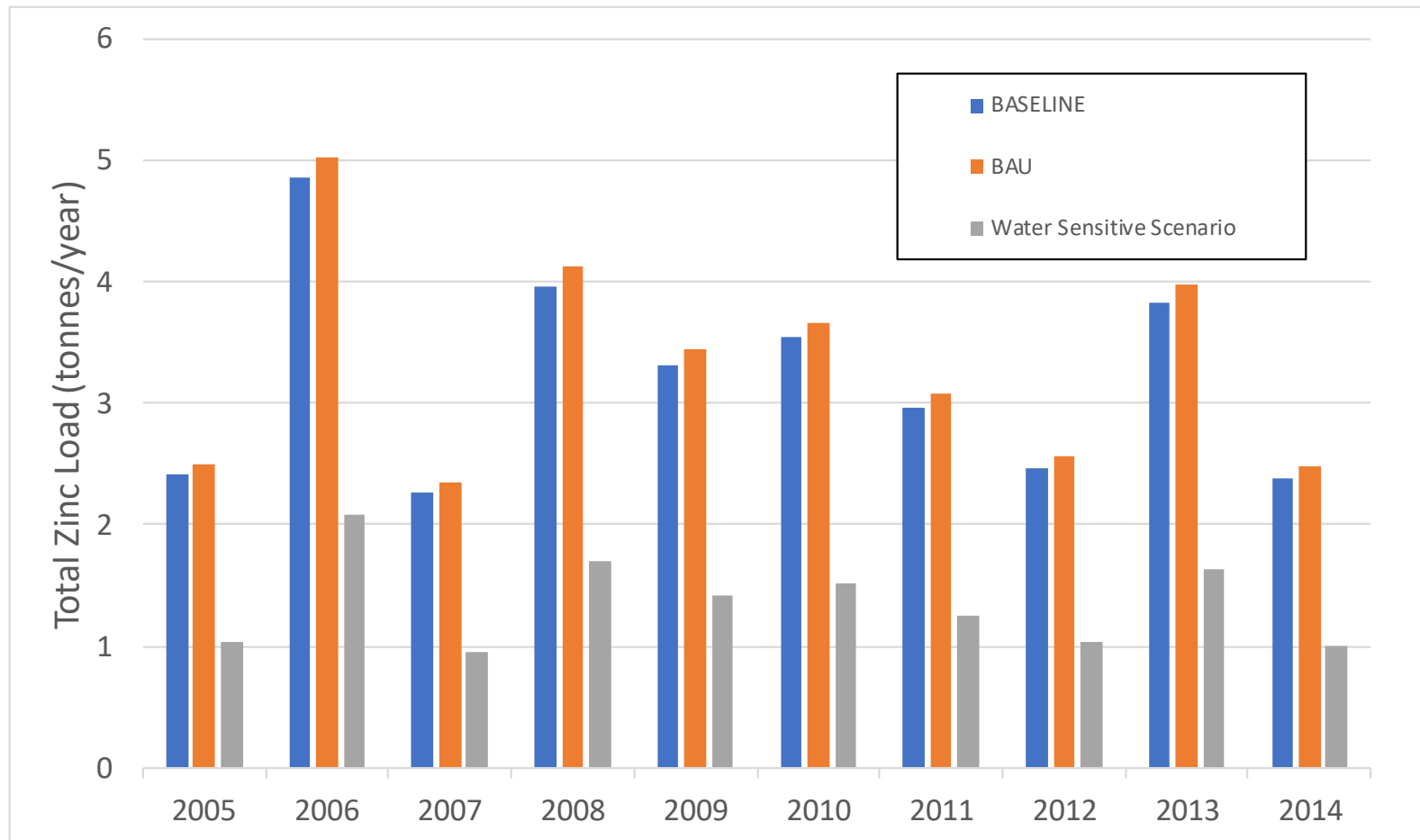
Figure 3-18.   Annual Total Zinc load (tonnes/yr) delivered to the Porirua Harbour.
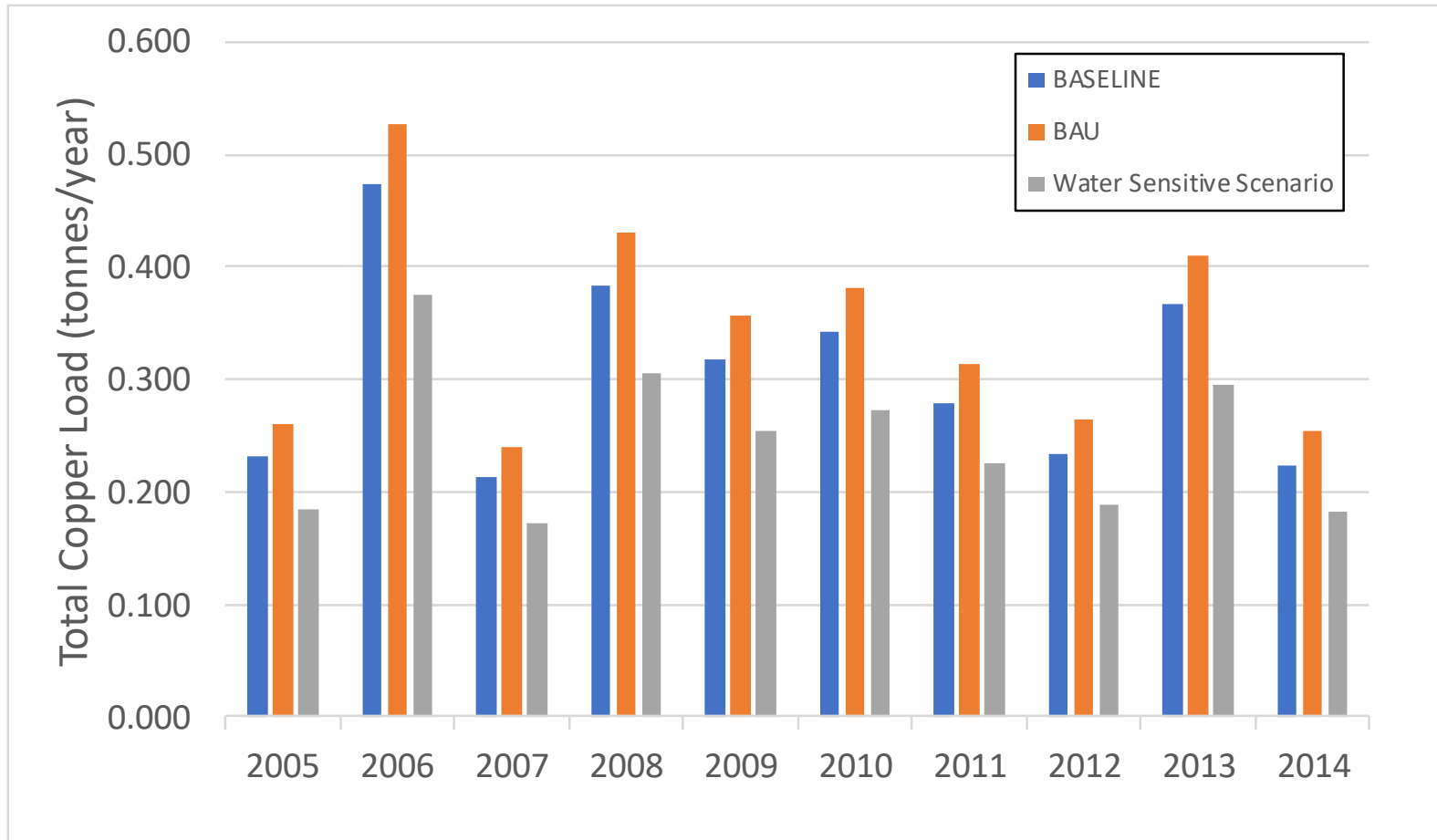
Figure 3-19.   Annual Total Copper load (tonnes/yr) delivered to the Porirua Harbour.

jwo / 15.11.2018
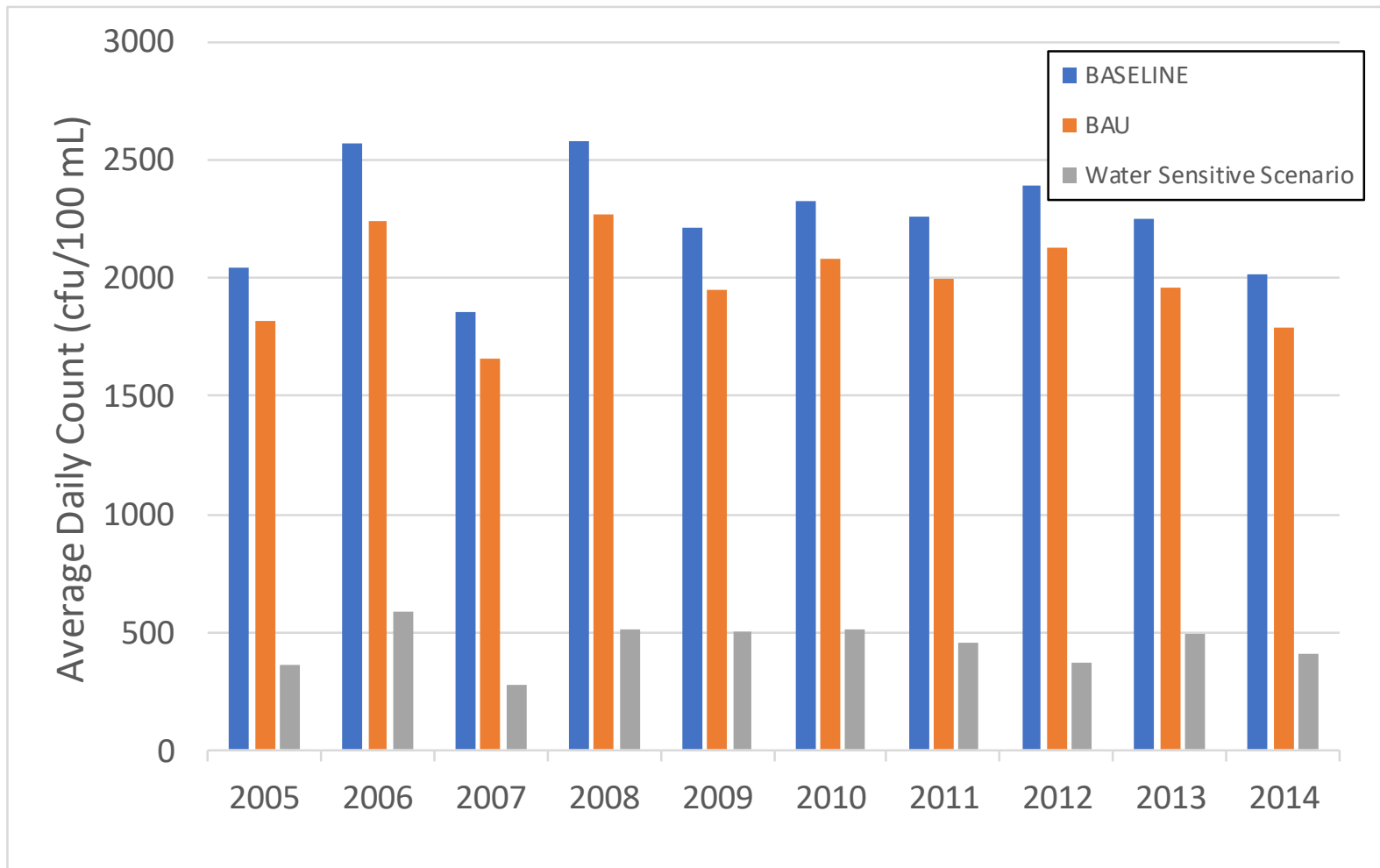
Figure 3-20.   Average daily *E. coli* count (cfu/100 mL) across all catchment outlets.

Table 3-3. Relative contaminant loads and average E. Coli count (cfu/100 mL) from each of the catchment outlets for the Baseline scenario.

Catchment Outlet	% of Mean Annual Sediment Load (2004-2014)	% of Mean Annual Flow (2004-2014)	% of Mean Annual Zinc Load (2005-2014)	% of Mean Annual Copper Load (2005-2014)	% of Mean Annual TN Load (2005-2014)	% of Mean Annual TP Load (2005-2014)	Mean E. Coli count (cfu/100 ml) (2005-2014)
Whitby to Browns Bay	0.55%	0.81%	2.37%	2.06%	0.96%	1.11%	2412
Pauatahanui village	0.08%	0.22%	0.12%	0.14%	0.43%	0.37%	2271
Lower Duck Creek	6.60%	5.31%	5.81%	5.44%	6.29%	6.84%	1479
Horokiri	11.99%	22.46%	2.15%	3.61%	18.23%	15.95%	547
Kakaho	3.08%	6.67%	0.83%	1.42%	9.87%	9.62%	1530
Onepoto fringe Elsdon	0.25%	1.01%	5.91%	4.48%	0.63%	0.69%	1740
Direct to Onepoto (South)	0.46%	0.23%	0.47%	0.73%	0.65%	1.01%	7998
Next to Mahinawa	0.12%	0.62%	2.31%	2.00%	0.46%	0.50%	1587
Hukarito	0.13%	0.39%	0.57%	0.59%	0.44%	0.42%	1759
Kahetoa (Onepoto Park)	0.11%	0.84%	2.83%	2.94%	0.96%	1.22%	4147
Whitireia/Te Onepoto	0.15%	0.35%	0.17%	0.16%	0.60%	0.48%	1987
Direct to Onepoto (North)	0.14%	0.52%	1.75%	1.66%	0.56%	0.66%	2648
Direct to Onepoto (Mid)	0.18%	0.54%	1.50%	1.92%	0.68%	0.81%	2887
Pauatahanui mouth	40.32%	22.91%	5.14%	7.71%	16.88%	19.44%	568
Direct to Pauatahanui (Mid)	0.02%	0.23%	0.54%	0.53%	0.35%	0.34%	2985
Motukaraka	0.03%	0.22%	0.07%	0.08%	0.46%	0.39%	2117

Catchment Outlet	% of Mean Annual Sediment Load (2004-2014)	% of Mean Annual Flow (2004-2014)	% of Mean Annual Zinc Load (2005-2014)	% of Mean Annual Copper Load (2005-2014)	% of Mean Annual TN Load (2005-2014)	% of Mean Annual TP Load (2005-2014)	Mean E. Coli count (cfu/100 ml) (2005-2014)
Direct to Pauatahanui (Water ski club)	0.02%	0.10%	0.04%	0.08%	0.25%	0.22%	2476
Direct to Pauatahanui (Boat houses)	0.02%	0.21%	0.67%	0.62%	0.21%	0.31%	3106
Porirua Mouth	33.31%	31.45%	66.45%	63.37%	35.80%	35.75%	1461
Ration	2.46%	4.92%	0.30%	0.45%	5.29%	3.87%	864
Taupo Stream	-	-	-	-	-	-	1581
Mahinawa	-	-	-	-	-	-	1397
Mean Annual	13,873 tonnes	98,942 m^3	3.2 tonnes	0.3 tonnes	141.0 tonnes	7.8 tonnes	-

Table 3-4   Percentage change in loads and daily *E. Coli* count (cfu/100 mL) for the BAU and Water Sensitive Scenario. Positive value indicates a reduction compared to the Baseline. Negative value indicates an increase compared to the Baseline.

Scenario	Change in Mean Sediment Load (%) (2004-2014)	Change in Mean Freshwater Input (%) (2004-2014)	Change in Mean Zn Load (%) (2005-2014)	Change in Mean Cu Load (%) (2005-2014)	Change in Mean TN Load (%) (2005-2014)	Change in Mean TP Load (%) (2005-2014)	Change in Mean E. Coli count (%) (2005-2014)
BAU	1.6	-2.1	-3.9	-12.3	7.3	7.7	11.6
Water Sensitive Scenario	39.0	3.4	57.5	19.6	31.9	43.4	80.3

4   Wind Data

Wind data from the Mana Island automated weather station was used for the study. Figure 4-1 shows the wind rose for the period modelled for the Whaitua CMP and shows the dominance of winds from the north and south sectors. Data in Table 4-1 shows the percentile estimates for wind speed while Table 4-2 provides a summary of the distribution of wind speeds and directions between 2004 and 2014. This distribution of wind speeds can be compared to those using just the wind record from 2010 (Table 4-3). Overall there is a very similar pattern of wind speeds compared to that from the period 2004-2014. Therefore, as well as being typical in terms of the mean annual loads and freshwater inputs delivered to the harbour, 2010 is representative of the long-term wind climate.

Table 4-1.   Percentile wind speeds based on the Mana Island automated weather station data 2004-2014.

Percentile	Wind Speed (m/s)
50	5.5
60	6.3
70	7.2
80	8.4
90	9.8
95	11.4
99	13.9
99.9	16.9
99.99	19.4
99.999	20.9
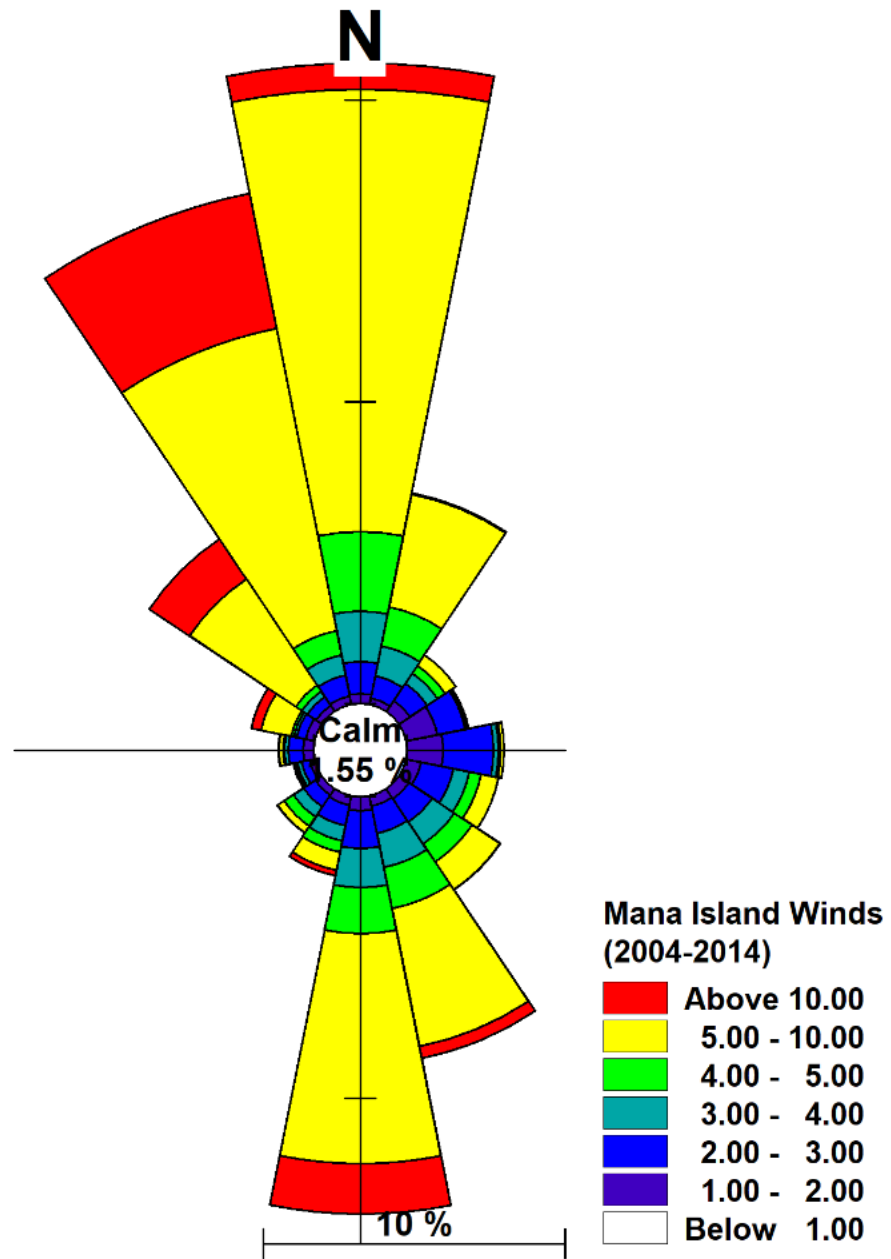
Figure 4-1.   Wind rose over the period considered for the Whaitua CMP (2004-2014) wind record from the Mana Island automated weather station.

Table 4-2.   Distribution of winds based on the Mana Island automated weather station data 2004-2014. Table shows percentage of winds within given sector and wind speed band.

Wind Speed Range (m/s)	>= 0 < 45	>= 45 < 90	>= 90 < 135	>= 135 < 180	>= 180 < 225	>= 225 < 270	>= 270 < 315	>= 315 < 360
<1	0.141%	0.169%	0.176%	0.171%	0.159%	0.132%	0.145%	0.130%
>=1 & < 2	0.479%	0.552%	0.582%	0.563%	0.467%	0.328%	0.456%	0.527%
>=2 & < 3	0.833%	0.963%	1.212%	1.059%	0.605%	0.364%	0.618%	0.957%
>=3 & < 4	1.376%	0.789%	1.580%	1.860%	0.872%	0.314%	0.661%	1.762%
>=4 & < 5	1.485%	0.537%	1.206%	2.148%	0.769%	0.256%	0.619%	2.253%
>=5 & < 6	1.381%	0.391%	0.822%	2.412%	0.855%	0.189%	0.678%	2.928%
>=6 & < 7	1.157%	0.264%	0.519%	2.232%	0.791%	0.143%	0.720%	3.393%
>=7 & < 8	1.092%	0.150%	0.309%	2.080%	0.800%	0.101%	0.862%	3.737%
>=8 & < 9	0.939%	0.088%	0.170%	1.712%	0.747%	0.075%	0.961%	3.757%
>=9 & < 10	0.751%	0.044%	0.099%	1.407%	0.732%	0.041%	1.033%	3.575%
>=10 & < 12	0.950%	0.031%	0.075%	1.919%	1.140%	0.037%	1.874%	5.500%
>=12 & < 15	0.444%	0.007%	0.023%	1.207%	0.973%	0.013%	1.599%	3.945%
>=15 & < 20	0.102%	0.000%	0.007%	0.389%	0.350%	0.006%	0.532%	1.236%
>= 20	0.002%	0.000%	0.000%	0.014%	0.022%	0.000%	0.014%	0.068%

Table 4-3.   Distribution of winds based on the Mana Island automated weather station data from 2010. Table shows percentage of winds within given sector and wind speed band

Wind Speed Range (m/s)	>= 0 < 45	>= 45 < 90	>= 90 < 135	>= 135 < 180	>= 180 < 225	>= 225 < 270	>= 270 < 315	>= 315 < 360
<1	0.057%	0.149%	0.092%	0.161%	0.069%	0.034%	0.092%	0.092%
>=1 & < 2	0.356%	1.344%	0.712%	0.551%	0.632%	0.391%	0.402%	0.471%
>=2 & < 3	1.045%	2.022%	1.620%	0.919%	0.896%	0.505%	0.517%	0.919%
>=3 & < 4	0.930%	0.735%	1.505%	1.677%	1.332%	0.597%	0.253%	1.309%
>=4 & < 5	1.447%	0.241%	0.804%	2.561%	1.516%	0.333%	0.103%	1.344%
>=5 & < 6	2.194%	0.172%	0.884%	3.228%	1.424%	0.264%	0.138%	2.068%
>=6 & < 7	2.470%	0.069%	0.620%	2.791%	1.114%	0.195%	0.103%	2.906%
>=7 & < 8	2.458%	0.115%	0.402%	2.182%	0.988%	0.069%	0.356%	3.894%
>=8 & < 9	1.849%	0.011%	0.230%	1.872%	0.666%	0.115%	0.391%	3.951%
>=9 & < 10	1.126%	0.011%	0.149%	1.574%	0.747%	0.069%	0.482%	4.342%
>=10 & < 12	0.540%	0.023%	0.069%	1.861%	1.126%	0.057%	1.022%	5.054%
>=12 & < 15	0.092%	0.011%	0.069%	1.367%	0.873%	0.046%	0.804%	3.813%
>=15 & < 20	0.011%	0.000%	0.011%	0.322%	0.218%	0.000%	0.345%	2.068%
>= 20	0.000%	0.000%	0.000%	0.023%	0.011%	0.000%	0.046%	0.034%

5   Model Setup and Calibration and Validation

The basis for the modelling for the Whaitua Collaborative Modelling Project was the work carried out for the Transmission Gully (TG) project. For the TG project a hydrodynamic, wave and sediment transport model was built and calibrated against an extensive field dataset. Details of the calibration of those models are provided in SKM (2011) as summarised in Appendix A.

For the Whaitua Collaborative Modelling Project, the model mesh was refined around each of the catchment outlets (Figures 3-1 through to 3-3) and using the inputs from the catchment/freshwater models (Section 3), validated against observed deposition rates and water column nutrient data. Note that further calibration against suspended sediment concentration was not carried out as this was done in full for the TG project.

For pathogens, analysis of available *Enterococci* and *E. Coli* monitoring data from GWRC and Wellington Water (Oliver and Conwell, 2019) indicated that the *E. coli* inputs used in the freshwater modelling could be used as a surrogate for *Enterococci* concentrations in the marine receiving environment. A representative decay rate for *Enterococci* was applied based on the ongoing work relating to the water quality forecast model for Porirua Harbour (DHI, 2018).

For metals, less than 5 years of monitoring data was available for bed-sediment metal concentrations which meant that it was not possible to quantify any long-term trends in relation to metal accumulation in the harbour. There was no information or data on historic metal catchment load inputs. So, no calibration of the metal equilibrium model was possible. In addition, as discussed in Jacobs (2019a), the total metal freshwater model is uncalibrated.

Details of model calibration procedures are provided in the following sections.

5.1 Sediments

As discussed in the Introduction, the sediment transport model used for the Whaitua work is based on the model developed for the Transmission Gully project (SKM, 2011). The focus of the TG study was to quantify the potential effects of the construction phase of the motorway development in the context of whole catchment sediment delivery. Observed water levels, currents, waves, suspended sediment concentrations and basin-wide deposition rates compared favourably with model predictions. Details of the calibration process are provided in SKM (2011).

For the CMP, the focus was on developing an understanding of subestuary deposition rates and the overall sediment budget of the Onepoto Arm and the Pauatahanui Inlet for alternative scenarios in the context of the current state of the harbour.

For the Transmission Gully work (SKM, 2011), a single cohesive sediment grain size fraction (medium-silt) and two non-cohesive (fine sand) fractions were used. Non-cohesive sediments are considered to be those with a grain size of greater than 64 microns while cohesive sediments are considered those with a grain size of less than 64 microns.

For the CMP, additional cohesive sediment grain sizes were included in the model to get a more representative distribution of the known portions of fine, medium and coarse cohesive sediments and fine non-cohesive sands being delivered to the harbour from the catchment. This was required to be able to quantify the potential change in seabed sediment texture under the different scenarios being considered. A review of the data in Sorensen and Milne (2009) and Stevens and Robertson (2016) showed that a more appropriate grainsize distribution could be achieved by having five cohesive sediment grain sizes and two (non-cohesive) sand size fractions - as summarised in Table 5-1.

Table 5-1. Sediment fractions, assumed portion of total sediment load and settling velocities used in the calibrated sediment transport model.

Fraction Description	Settling Velocity Coefficient[2]	Assumed Proportion of Cohesive Sediment (%)	Fall Velocity[3] (mm/s)	Equivalent Sediment Grain Size (Microns)
Clay	2	10	0.02	5
Fine Silt	3	20	0.10	10
Medium Silt	5	40	0.24	16
	10	20	0.39	21
Coarse Silt	20	10	0.48	23

Experimental studies (e.g. Heath et al., 2016) have found that, above a certain suspended sediment concentration, settling velocity for cohesive sediments increases as a function of concentration. This is due to the formation of flocs (or aggregates) of individual particles.

At very high concentrations (typically 2.5 kg/m³), the interactions between individual flocs becomes important and leads to a reduction in settling velocity and ultimately the formation of fluid mud layers. Input data from the catchment and freshwater modelling indicates that such levels of suspended sediment concentration may only occur at a limited number of the

[2] Factor used to derive fall velocity from the predicted concentration following Burt (1986).

[3] These are the spatial and temporal average fall velocities from the 2010 Baseline model simulation for the specified settling velocity coefficients (*k*).

catchment outlets and for less than 0.5% of the time. As such, the effects of hindered settling have been ignored in the sediment transport model.

Within the MIKE3 sediment transport model, the formula of Burt (1986) is adopted which relates the fall velocity (w_s) of cohesive sediments to the suspended sediment concentration (c in kg/m³), as follows;

$$w_s = k\frac{c}{\rho_{sed}}$$

Where k is the settling velocity coefficient for each of the cohesive sediment fractions being considered (as shown in Table 5-1) and ρ_{sed} is the density of the sediment grains (assumed to be 2650 kg/m³).

Table 5-1 also shows the assumed proportion of each of the cohesive sediment fractions based on the review of available sediment data within the harbour.

The spatially and temporal averaged fall velocities from the 2010 Baseline simulation are also shown in Table 5-1. These values are in good agreement with the fall velocity data from extensive sampling in Auckland catchments (Semadeni-Davies (2009) as shown in Figure 5-1.

Finally, for context only, Table 5-1 provides the equivalent grain size of the cohesive sediment fractions based on the Wentworth grade scale (Schlee, 1973).

Table 5-2 shows the assumed fall velocity and grain size data for the two non-cohesive sediment fractions.

Table 5-3 shows the proportional split between the cohesive sediments and non-cohesive sediments at each of the catchment outlets as derived from the Transmission Gully work (SKM, 2011).
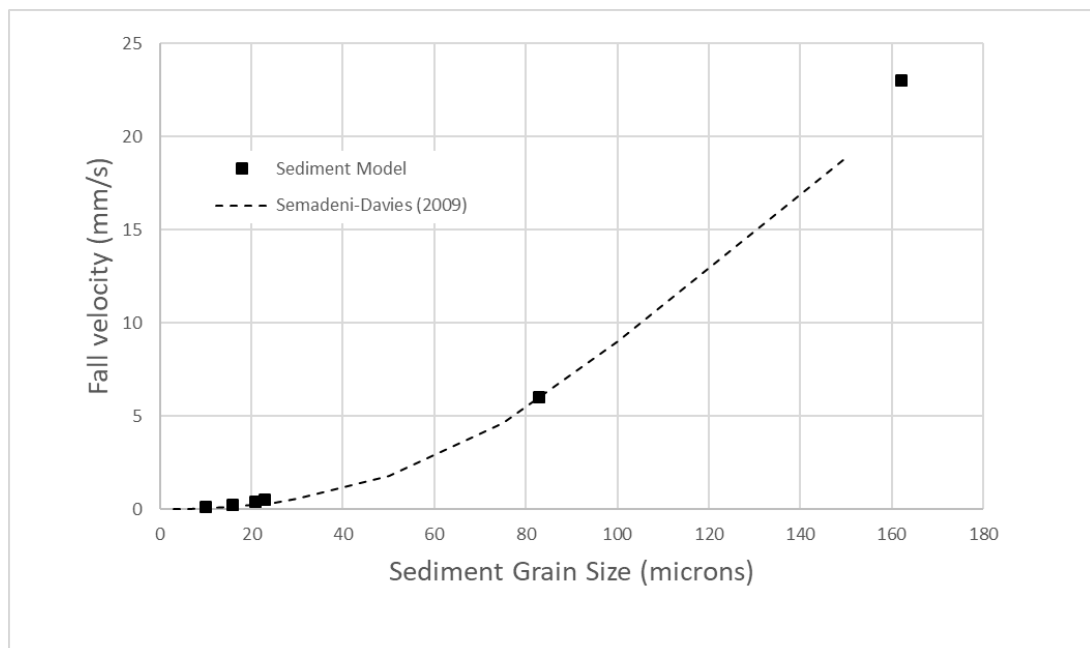
Figure 5-1.   Fall velocity (mm/s) as a function of sediment grain size (microns) derived from the calibrated sediment transport model and data from Semadeni-Davies (2009). The model data is the average predicted fall velocity over the whole model domain over the full 2010 model simulation. The data from Semadeni-Davies (2009) is derived from sampling within several Auckland urban catchments.

Table 5-2.   Non-cohesive sediment fractions used in the calibrated sediment transport model.

Fraction Description	Fall Velocity (mm/s)	Sediment Grain Size (Microns)
Very Fine Sand	6	83
Fine Sand	23	162

Table 5-3.   Proportional split between non-cohesive and cohesive sediments for each catchment outlet.

Fraction Description	Percent cohesive	Percent non-cohesive
Whitby to Browns Bay	79	21
Pauatahanui village	83	17
Lower Duck Creek	81	19
Horokiri	86	14
Kakaho	88	12
Onepoto fringe Elsdon	82	18
Direct to Onepoto (South)	80	20
Next to Mahinawa	81	19
Hukarito	80	20
Kahetoa (Onepoto Park)	80	20
Whitireia/Te Onepoto	85	15
Direct to Onepoto (North)	80	20
Direct to Onepoto (Mid)	80	20
Pauatahanui mouth	87	13
Direct to Pauatahanui (Mid)	80	20
Motukaraka	85	15
Direct to Pauatahanui (Water ski club)	91	9
Direct to Pauatahanui (Boat houses)	79	21
Porirua Mouth	82	18
Ration	87	13

To validate the sediment transport model, data from the most recent bathymetric survey of the harbour carried out by Discovery Marine Ltd (DML, 2015) and monitoring data from sediment plates (Stevens and Robertson, 2016) have been used.

Figures 5-3 and 5-4 show the comparison between the 2010 model predictions and the DML survey data between 2014 and 2009. Daily estimates of sediment load and inflows for 2010 (Figure 3-14) were input to the model at each of the catchment outlets in the marine receiving environment model (Figures 3-1 to 3-3). The total sediment load was split amongst the seven grain sizes based on the data in Tables 5-1 to 5-3. The distribution of sediments on the seabed of the model were determined by a series of spin up model runs. An initial estimate of bed sediment layer thickness was derived from a combination of sedimentation rate estimates in Swales et al. (2005), Gibb (2009) and Green et al. (2014), data in Stevens and Robertson (2016) and model estimates from the TG project (SKM, 2011). The 2010 model simulation was then rerun a number of times to give the bed thickness map shown in Figure 5-2. The maps give an indication of the areas that act as sinks for sediments (i.e. where the thickest bed sediments occur) and areas around the fringes of the harbour where waves play an important role in resuspended sediments (i.e. lowest initial bed thickness).

This process provides the starting conditions for the bed-sediments for all the subsequent model simulations.
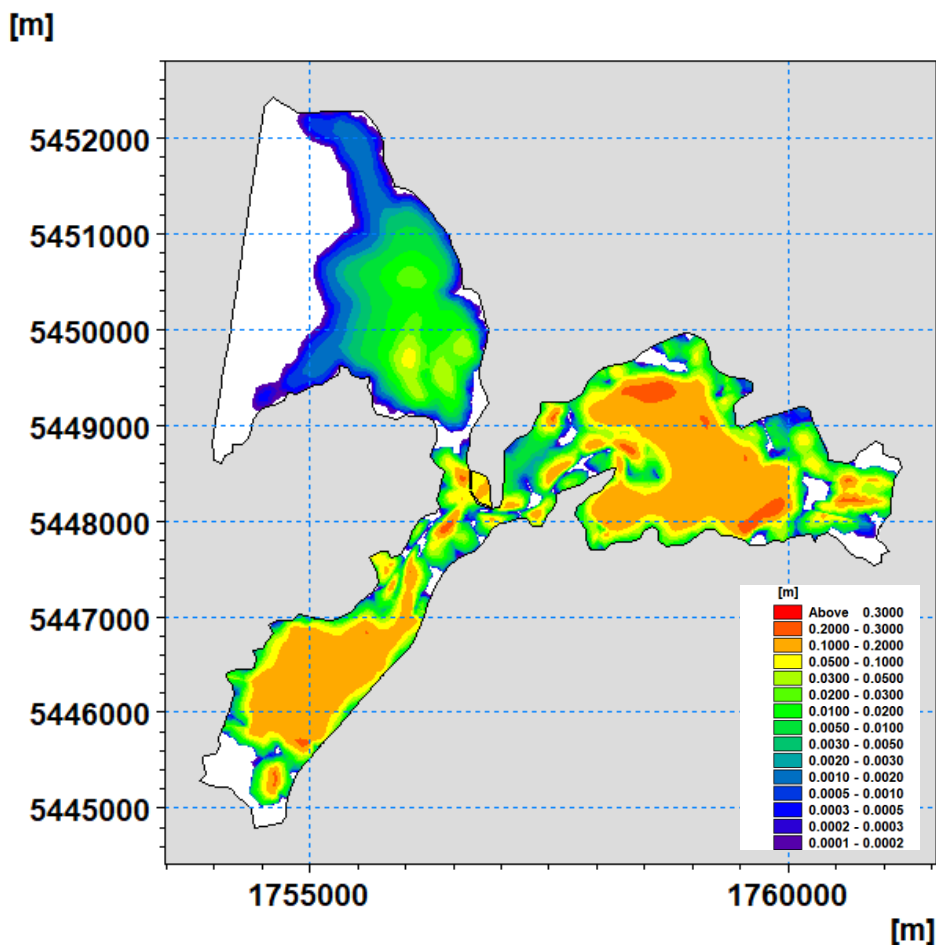
Figure 5-2.   Initial bed thickness (m) based on a series of iterations of the 2010 sediment transport model.

A full quantitative calibration of the model against the DML survey data could only be done if the model was run for the full period between the surveys (which was not possible within the timeframes of the Whaitua project). However, we know that the predicted sediment load delivered to the harbour in 2010 is 8,839 tonnes while the predicted average annual sediment load delivered to the harbour between the DML survey dates is 6,156 tonnes/year (Table 3-1) which is 80% of the 2010 sediment load.

Data in DML (2015) indicate that infilling of the inner parts of the Pauatahanui Inlet (Zones 2-7, Table 2 in DML, 2015) is estimated to be 22,625 m^3/yr which compares with the 25,150 m^3/yr of infilling predicted by the model in 2010. Scaling the model prediction by the ratio of the 2010 sediment load and the average annual sediment load between the DML surveys would provide an estimated infilling rate of 19,267 m^3/yr from the model. Similarly, the observed infilling of the southern part of the Onepoto Arm (Zones 2-4, Table 2 in DML, 2015) is estimated to be 17,594 m^3/yr compared to 24,535 m^3/yr of infilling predicted by the model in 2010. Scaling this value by the load ratios would give a predicted infilling value of 18,795 m^3/yr from the model.

The overall match of the modelled (Figure 5-3) and observed (Figure 5-4) areas of deposition and erosion is reasonably good.

This indicates that, at a very broad scale, the erosion and deposition thresholds used to calibrate the model (0.12 N/m^2 and 0.30 N/m^2 respectively[4]) and the fall velocities applied for each grain size fraction are appropriate in terms of the overall physical setting of both the Onepoto Arm and Pauatahanui Inlet. Areas of observed deposition match those predicted by the model and areas where net erosion on the fringes of the harbour are well matched by the model.

The two areas where the model does not seem match the DML survey data are the subtidal area in the south-west sector of the Pauatahanui Inlet and the eastern shoreline of the Onepoto Arm.

---

[4] These determine when sediment can be eroded from or deposited to the bed.
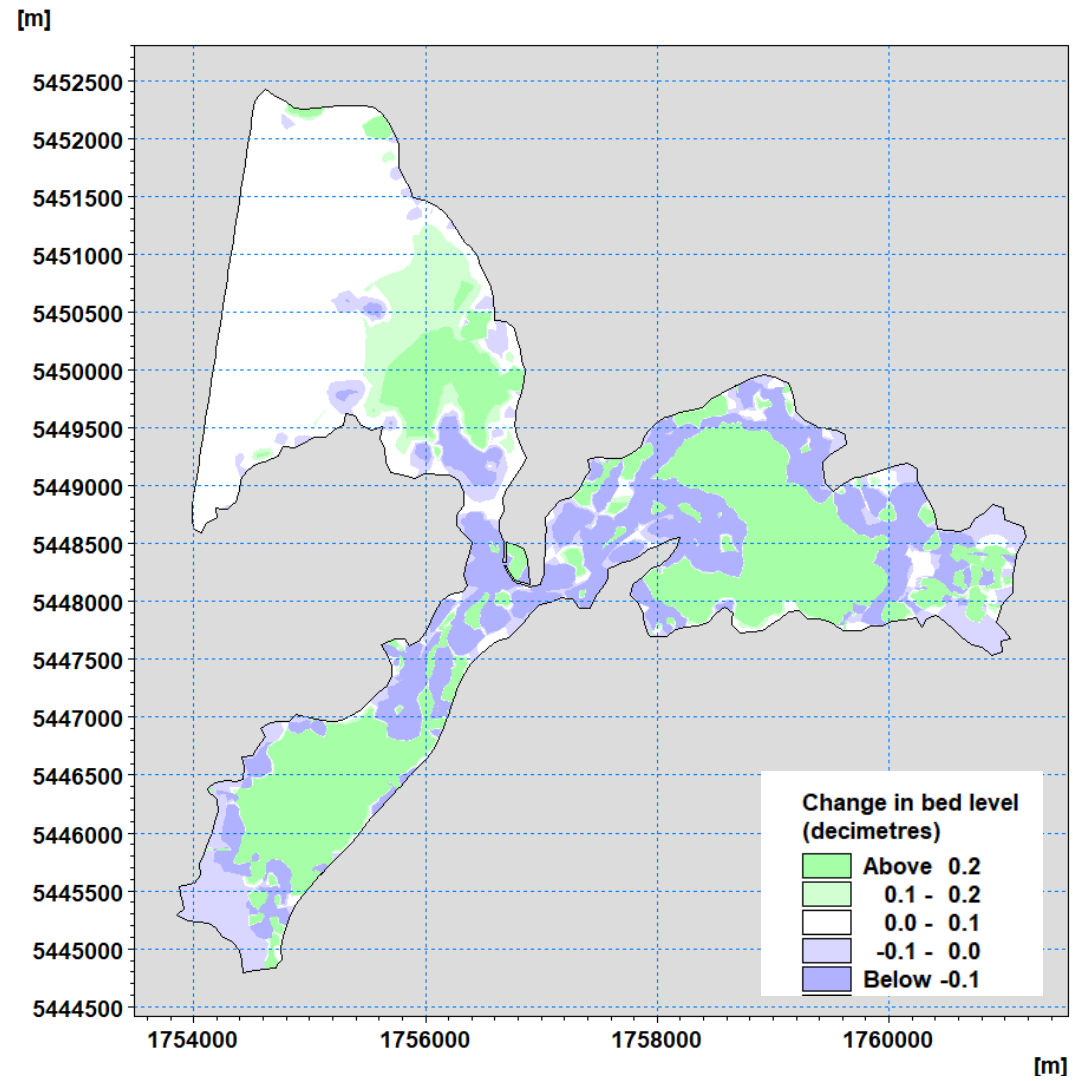
Figure 5-3.   Annual erosion and deposition rates (decimetres/year) from the calibrated sediment transport model for 2010. Areas of deposition are shown as green, areas of erosion are shown as blue.
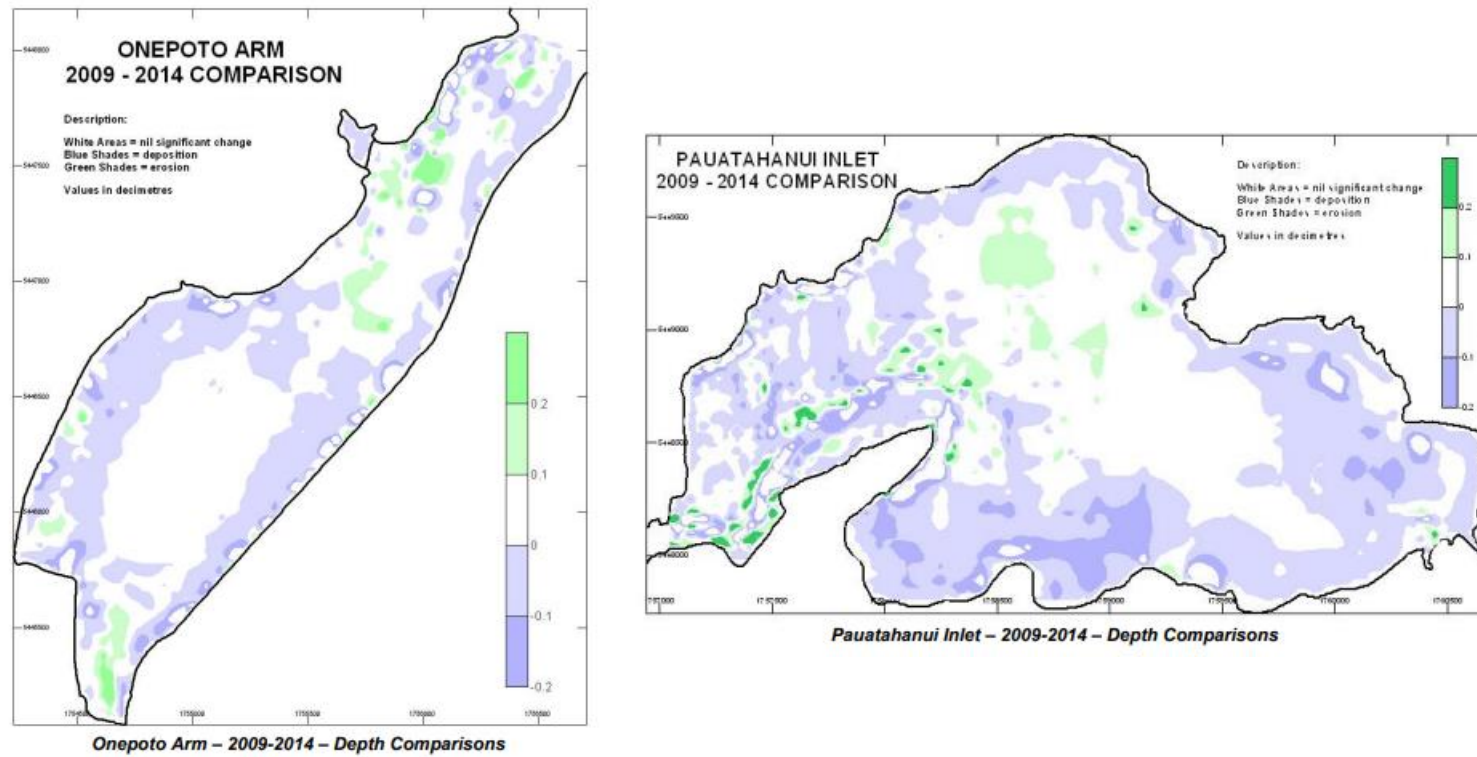
Figure 5-4. Annual erosion and deposition rates (decimetres/year) within the Onepoto Arm (left panel) and Pauatahanui Inlet (right panel) from the DML surveys of 2014 and 2009. Areas of deposition are shown as white or green, areas of erosion are shown as blue.

A more detailed calibration of the sediment transport model involved using data from the sediment plate data at sites in both the Onepoto Arm (Figure 5-5) and Pauatahanui Inlet (Figure 5-6). Predicted changes in bed level from the 2010 simulation have been compared to the trend data from the sediment plates (Figure 5-7). That is, the observed net erosion or accretion over the period that plate data has been collected (January 2009-Jaunary 2017) is compared to the predicted net bed level change from the model at the end of the 2010 simulation.

Overall there is a very good match across highly erosional sites (e.g. S8 Papakowhai) through to depositional sinks (e.g. S1 Kakaho and S2 Horokiri). The two sites where the model does not perform well are the S7 Onepoto site (where the model does not predict the observed erosion) and the S3 Duck Creek site (where the model over predicts the observed deposition).

Further validation of the model could be made by carrying out a year-by-year comparison of the sediment plate data but this would have to include an extension of the catchment outlet data from the end of 2015 through to the present day.

As noted above, the two areas where the model does not seem to perform well are in the south-west sector of the Pauatahanui Inlet and the eastern shoreline of the Onepoto Arm.

The predicted band of erosion along the eastern shoreline of the Onepoto Arm from the model (Figure 5-3) is much narrower than that derived from the DML surveys (Figure 5-4). This suggests that more sub-tidal erosion has occurred in between the period of the two surveys compared to that predicted by the model in 2010.

Similarly, data from the DML survey shows that the south-west sector of the Pauatahanui Inlet (particularly in the area immediately offshore of Bradeys Bay) is predominantly an area of net erosion.

The predicted mean deposition rate across this area from 2010 simulation is around 0.8 mm/yr whereas the DML survey data indicates the majority of the area has a net erosion rate of less than 2 mm/yr (0.1 decimetres over 5 years - Figure 5-4).

At both these sites, the differences between the modelled and observed changes in bed levels are likely to be due to the different sediment loads entering the system for each year between the survey and the potential differences in wave dynamics over the period 2009-2014 compared to 2010. This is discussed further in Section 6.1.

Elsewhere, the overall match between the sediment plate data and the DML survey data indicates that the sediment transport model provides good robust estimates of subestuary scale deposition and erosion rates, especially considering the uncertainties associated with post-processing the survey data and the "upstream" uncertainties associated with the catchment/freshwater modelling.

Further validation of the model could be done to determine if the discrepancies between the 2010 model results and the DML survey data relate to erosional events between the survey dates (2009-2014). If this was not the case, further calibration of the model would be required to provide a better match between the observed and predicted sub-tidal erosion rates to the east on the Onepoto Arm and the south-west sector of the Pauatahanui Inlet.
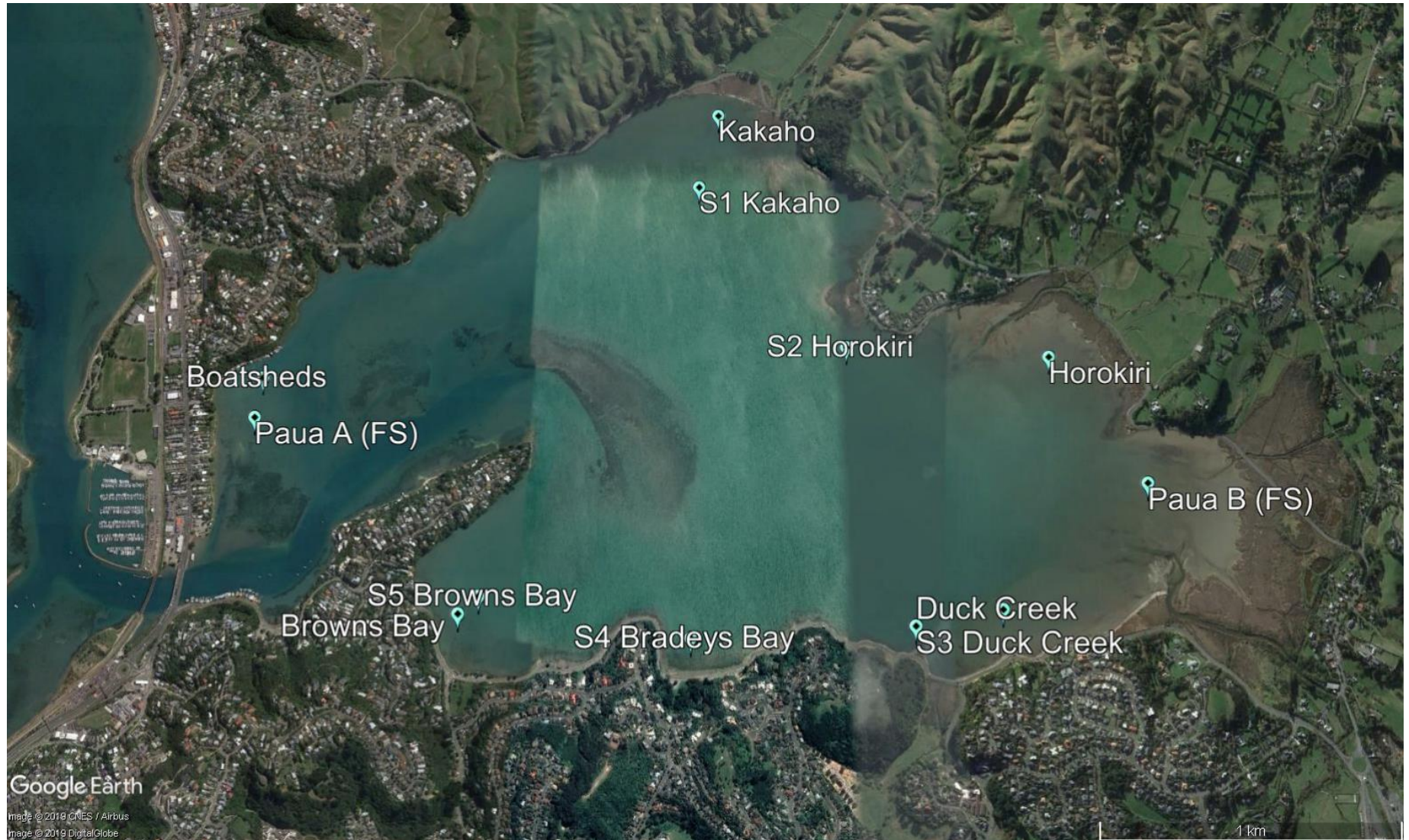
Figure 5-5.　　Location of sediment plate monitoring sites within the Pauatahanui Inlet.

Figure 5-6. Location of sediment plate monitoring sites within the Onepoto Arm.
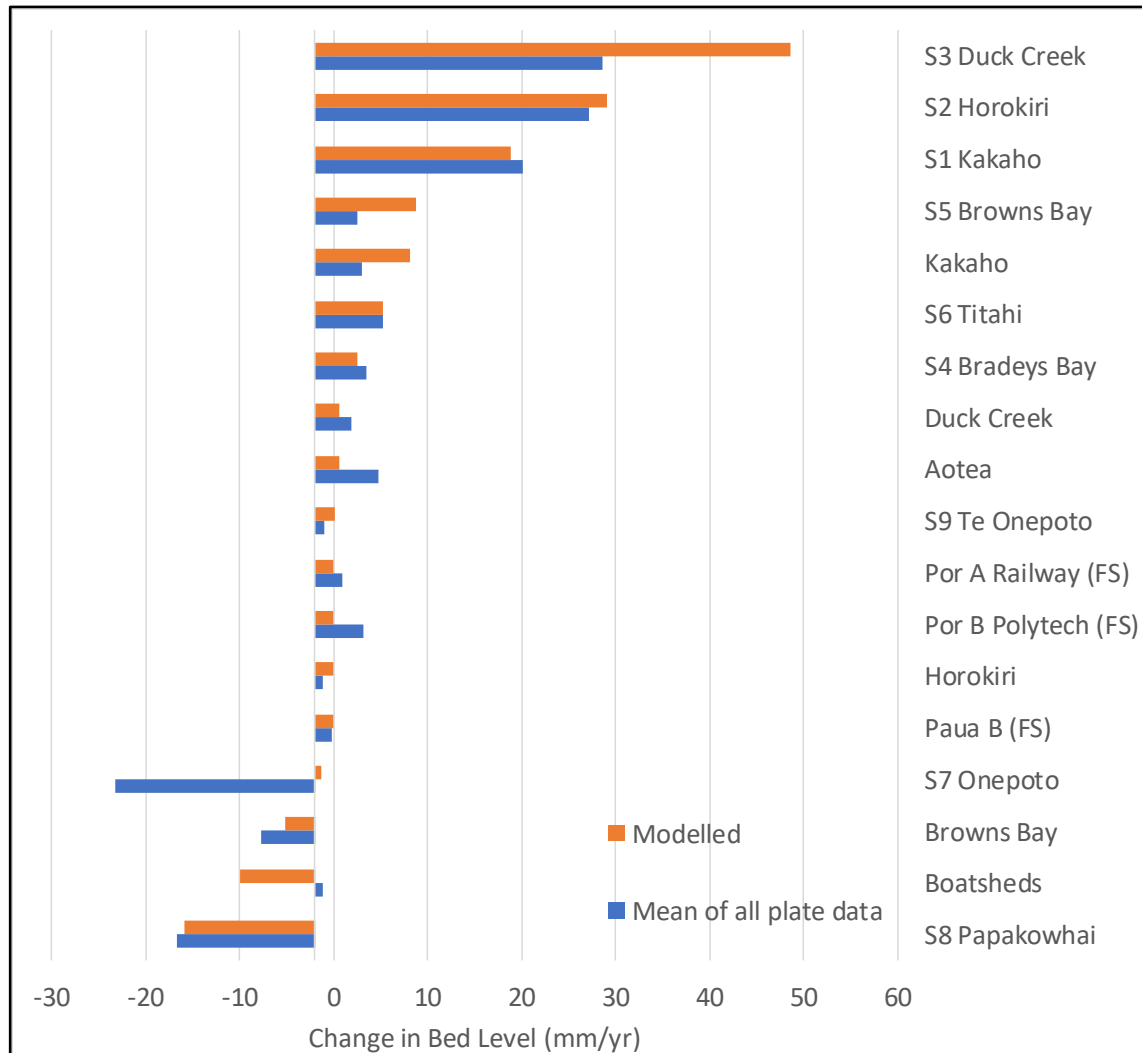
Figure 5-7.　Average change in bed level (mm/yr) from sediment plate data and from the 2010 model simulation.

5.2   Nutrients

To model the full dynamics of nutrients in an estuary setting, a coupled biophysical model is required.

This consists of 1) a hydrodynamic model 2) an advection-dispersion model and 3) a eutrophication model. Such coupled models are often referred to as biophysical, ecosystem health or eutrophication models. Typically, these models simulate the time and space varying dynamics of the following state variables;

- Phytoplankton Carbon, Nitrogen and Phosphorous,

- Chlorophyll-a,

- Zooplankton,

- Detrital Carbon, Nitrogen and Phosphorous,

- Inorganic Nitrogen and Phosphorus,

- Dissolved oxygen, and

- Benthic vegetation carbon.

For each variable, a numerical representation of its dynamics is used in the eutrophication model.

For example, the rate at which phytoplankton carbon changes is the sum of the production (i.e. growth rate - driven by temperature, nutrient levels and light levels), grazing (determined by zooplankton population dynamics), mortality rate (which relate to species-specific population dynamics) and the rate at which phytoplankton sink to the seabed (which relates to their inability to maintain buoyancy under nutrient-stress conditions). Similarly, for phytoplankton, phosphorous and nitrogen a rate of uptake replaces the production term for the carbon variable.

In addition, the interactions between all the variables are simulated as shown in Figure 5-8.

1. production, phytoplankton	8. mineralisation of suspended detritus
2. sedimentation, phytoplankton	9. sedimentation of detritus
3. grazing	10. mineralisation of detritus
4. extinction, phytoplankton	11. accumulation in sediment
5. excretion, zooplankton	12. production, benthic vegetation
6. extinction, zooplankton	13. extinction, benthic vegetation
7. respiration, zooplankton	14. exchange with surrounding waters

Figure 5-8.   Flow diagram of the interactions included within a eutrophication model (DHI, 2019).

Because of the interactive nature of eutrophication processes, the calibration of a eutrophication model is very complex. Firstly, the underlying hydrodynamics (including variations in temperature and salinity) must be well represented. The calibration of a eutrophication model itself requires a significant amount of field data collected over number of sites within the area of interest and that data must capture both seasonal and inter-annual variability. For example, Edelvang et al. (2004) calibrated a eutrophication model of the Baltic and North Sea based on data collected over a four-year period at 12 sites within the Baltic and North Seas and analysis of satellite imagery data. Recent work carried out in the Marlborough Sounds (Broekhuizen et al. 2015), used a three-year dataset to calibrate a fully coupled biophysical model. This provided a model that could reproduce the majority of the long-term averages of the state variables but did not accurately simulate the timing of the observed seasonality.

More simplified approaches to modelling nutrients (in relation to aquaculture developments) have recently been adopted in New Zealand (e.g. Gillespie et al. 2011, Knight et al., 2014) whereby simulation of tracers in the water column have been used to quantify "potential" nitrogen loading from sources. This approach ignores any loss in the system of the nutrients being modelled (i.e. to the net result of the interactions and processes simulated in the full eutrophication model). That is, simulating the transport of a passive tracer (that does not decay) provides an estimate of the upper limit of the concentration that may be achieved within the receiving environment.

For the Whaitua CMP we elected to use the simplified approach adopted by Gillespie et al. (2011) and Knight et al. (2014) but improve the accuracy of their approach by calibrating the model by applying a fixed (spatial and temporal) decay rate for both Total Nitrogen and Phosphorus.

As discussed below, this approach provides relatively good estimates of the observed long-term average water column observations of Total Nitrogen and Phosphorus in the harbour and as such provides some context for assessing the potential influence of changes to nutrient loading in the harbour under the scenarios considered.

For the Whaitua CMP, the transport of nutrients uses the same advection-dispersion model as used for the sediments. The decay rate applied to the Total Nitrogen and Total Phosphorous in the water column acts as an overall loss term for the net effect of the all the processes and interactions simulated using a full dynamic eutrophication model.

For the calibration, the time-series data from the 2010 simulation of Total Nitrogen and Phosphorous were extracted at the six monitoring sites in the harbour (Figure 5-9). These were then compared to the monthly observations that had been made between 2011 and 2013.

Figure 5-9.   Nutrient monitoring sites (monthly sampling, January 2001-2013).

A series of model runs were carried out where the decay rate for Total Nitrogen and Total Phosphorous were adjusted to achieve the lowest root mean square error across all the monitoring sites between the mean of the observed concentrations and the mean of the modelled concentrations over the duration of the 2010 simulation.

Figure 5-10 shows the comparison between the observed and predicted mean and maximum concentrations at the monitoring sites for Total Nitrogen and Figure 5-11 shows the comparison between the observed and predicted mean and maximum concentrations at the monitoring sites for Total Phosphorous.

For the mean concentrations there is a good fit between the observed and predicted values apart from the predicted Total Nitrogen at the monitoring site PH-E1 (located just outside the entrance). Work carried out in relation to Pathogens identified an additional source of contamination from Taupo Stream which was not included in the nutrient model. The poor fit at the PH-E1 site for Total Nitrogen indicates the presence of a potential Nitrogen source from the Taupo Stream.

The maximum concentrations are reasonably well matched by the model except at site PH-01 (near the Rowing Club) where the model predicts a lower maximum than has been observed. This suggests that an unmodelled source of nutrients may be present during periods of high nutrient load delivery (given the mean predicted value is good at this site).

The best overall fit was achieved with a T_{90} decay rate of 45 days for Total Phosphorous and a T_{90} decay rate of 24 days for Total Nitrogen. The decay rate for the Total Nitrogen compares favourably with T_{90} decay rate used by Vant and Williams (1992) of 20 days and Black et al. (1995) of 25 days in the Manukau Harbour in relation to the discharge of Nitrogen from the Mangere wastewater treatment plant.
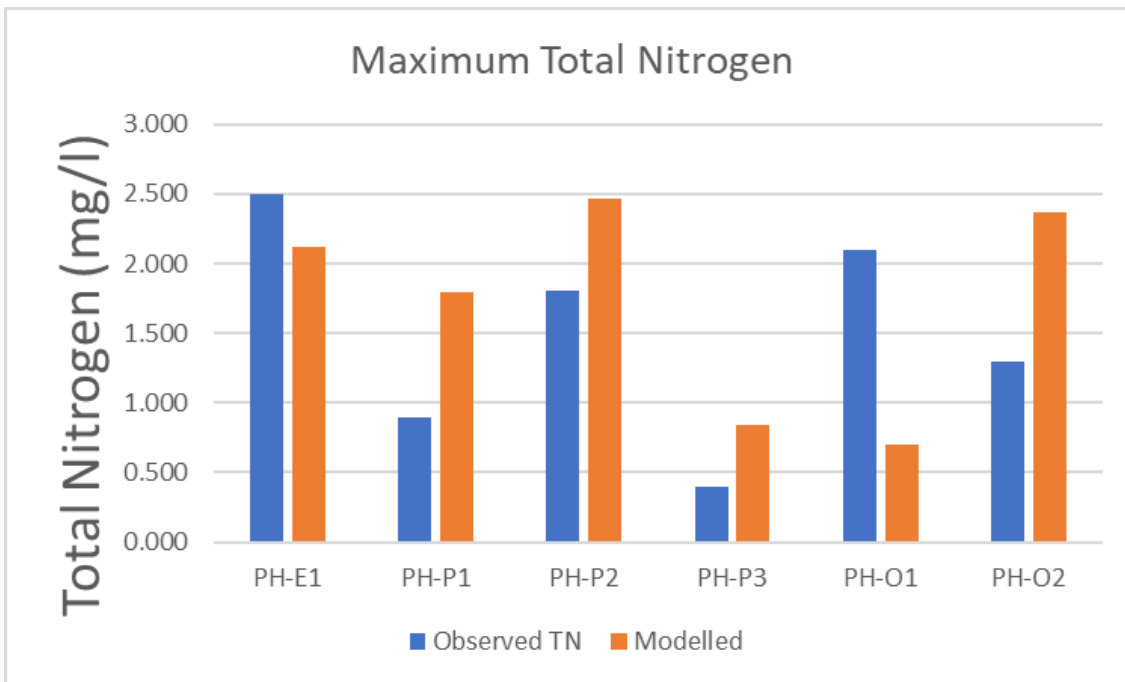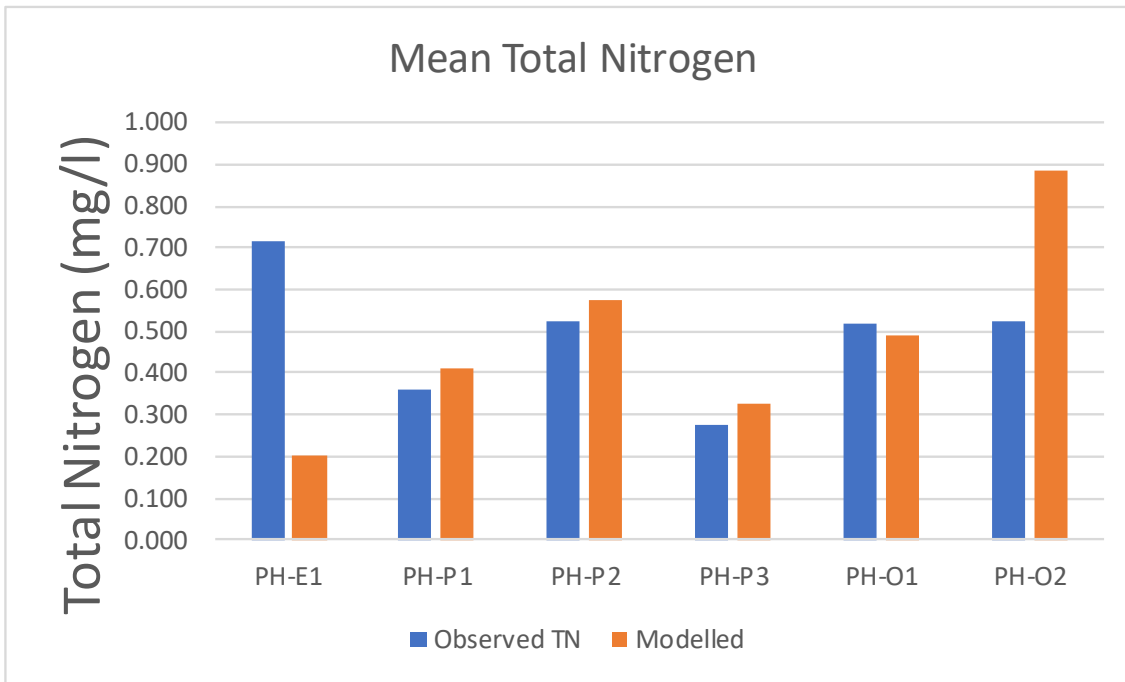
Figure 5-10. Mean (top panel) and maximum (bottom panel) of observed Total Nitrogen (monthly sampling, January 2011-January 2013) and predicted depth-averaged water column concentration from the 2010 model simulation.
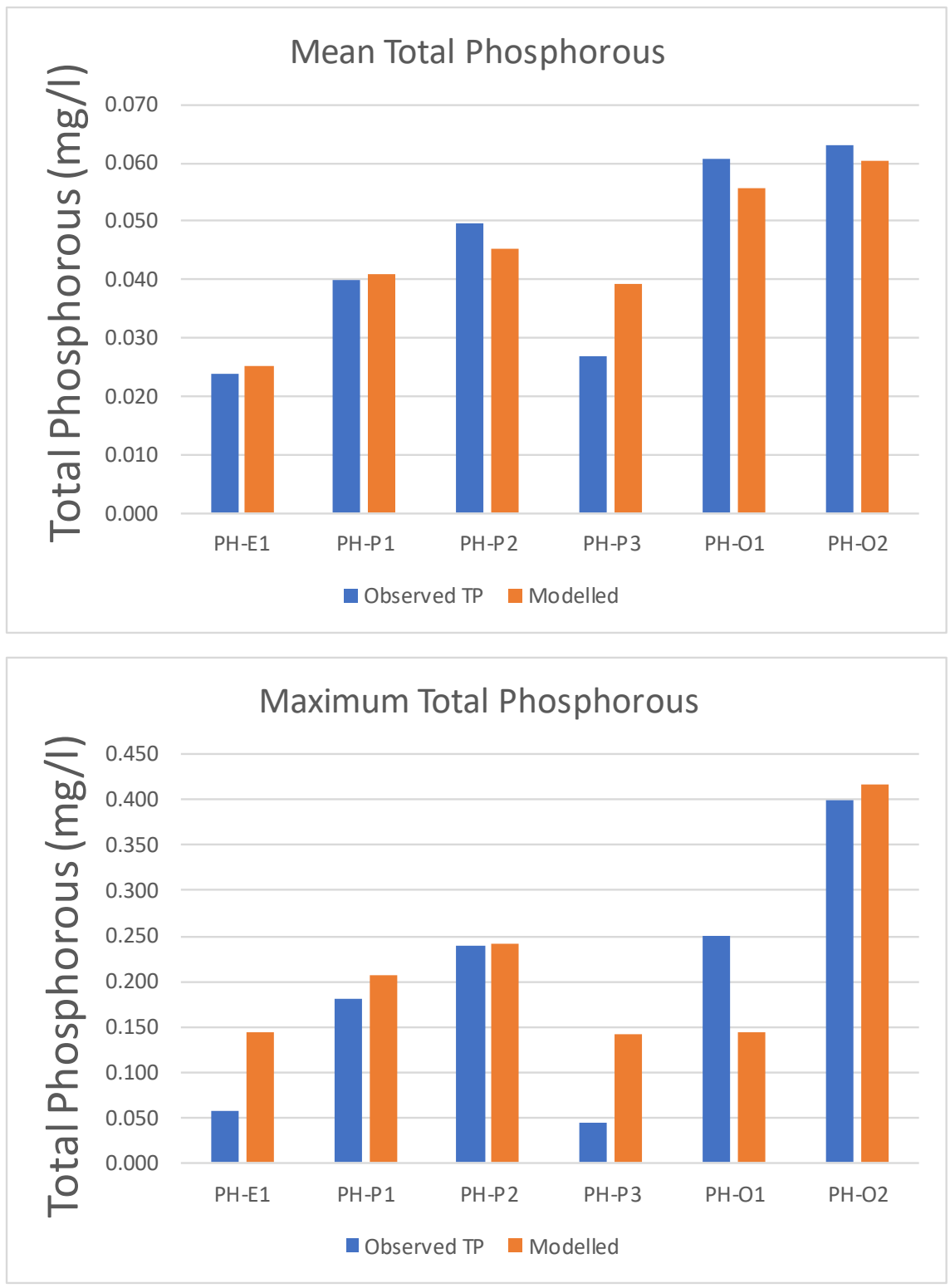
Figure 5-11. Mean (top panel) and maximum (bottom panel) of observed Total Phosphorous (monthly sampling, January 2011-January 2013) and predicted depth-averaged water column concentration from the 2010 model simulation.

5.3 Pathogens

The transport of pathogens uses the same advection-dispersion model as that used for the sediments and nutrients.

For the Whaitua CMP, the modelling of pathogens is based on the ongoing developing of the Porirua Harbour water quality forecast model (DHI, 2018). The focus of the calibration of the Porirua Harbour water quality forecast model has been to provide an accurate forecast of when *Enterococci* concentrations exceed specific criteria (as set out in Ministry for Environment, 2002). This has been achieved by comparing both routine and event-based monitoring of *Enterococci* levels within the harbour at a number of monitoring sites. Based on the prediction of events when a compliance alert mode may occur (i.e. a concentration of more than 280 counts/100 ml), the model performs very well. For example, at the Rowing Club site the model was considered to be accurate 97% of the time, achieved 76% accuracy at the Waka Ama site and 88% accuracy at South Beach.

The three key components that influence the calibration of the forecast model are 1) having a well calibrated hydrodynamic model 2) validation of load input data (i.e. flows and *Enterococci* concentrations - particularly during wet weather events) and 3) setting an appropriate inactivation rate.

As detailed in SKM (2011), the hydrodynamic model of the harbour is well calibrated and is used as the basis of both the Whaitua CMP and the water quality forecast model.

The two models differ in the load estimates they use. The Porirua Harbour water quality forecast model uses load estimates from statistical relationships of *Enterococci* and catchment rainfall, whereas the Whaitua CMP uses daily loads from Jacobs (2019a) catchment model. The accuracy of the marine based pathogen predictions is therefore directly reliant on the calibration of the catchment and freshwater models which, as documented in Jacobs (2019a), performs very well and provides a good fit of the overall distribution of pathogen concentrations at the four sites considered in their calibration.

For the Whaitua CMP the inactivation rate for *Enterococci* in the marine receiving environment was the same as that used for the water quality forecast model (0.0595 h^{-1}). Sinton et al. (1994) derived *Enterococci* dark inactivation rates of 0.05 h^{-1} to 0.08 h^{-1} and a daylight hour inactivation rate of 0.36 h^{-1}. Integrating these values over a typical year (considering daylight hours and cloudiness) gives a mean inactivation rate of 0.071 h^{-1}, which is in good agreement with the values used for the Whaitua CMP.

Overlapping load input data and in-harbour *Enterococci* monitoring data (as has been done for the Porirua Harbour water quality forecast model) has not been collected for the Whaitua CMP model. Therefore, calibration of the pathogen model for the Whaitua CMP is not possible. However, each of the key components that influence the pathogen model calibration are individually well calibrated. For this reason, they are considered reasonable for use in the Whaitua CMP model.

5.4 Metals

The metal accumulation model is based on the methodology adopted in a number of studies in the Auckland Region (Green, 2008, Green 2016).

One of the major assumptions in the metal accumulation model is the current day metal concentrations in the sediments. These are a function of historic land use and deposition patterns and rates over many decades.

To fully calibrate the metal accumulation model, it needs to be run in hindcast mode (i.e. from some point in the past to current day) using historic sediment and metal load data. This allows the model parameters to be adjusted to provide good estimates of the current day metal concentrations in the sediments.

Results from a calibrated metal accumulation model (and of course, long term monitoring data) give an indication if current day metal concentration are at or near an equilibrium state or are still increasing due to historic inputs of metals and sediments into the system.

One of the major parameters used to calibrate the metal accumulation model is a Metal Reduction Factor (Green, 2008). This factor (which can vary between 40 and 70%, Green 2008) removes a certain fraction of the metal load to account for the movement of metals from the particulate to dissolved phase. The other parameters used in the metal accumulation model are the depth to which sediments are mixed in the top few centimetres of the seabed and the mass of new sediment (and metal) arriving within a given subestuary in a given year.

Since historic sediment and metal load data was not available, it was not possible to carry out a calibration of the metal accumulation model for the Whaitua work. Instead, we adopted the approach of Green (2016) who assumed that 1) there was no loss of seabed metals to the dissolved phase 2) all the metal load was particulate and 3) current observed metal concentrations in the harbour do not represent equilibrium conditions. This approach provides worst case predictions (i.e. upper bounds) of how metal concentrations will increase over time and a valid methodology for providing quantification of the relative changes in metal accumulation under different land use scenarios.

In addition to a current day metal concentration, the metal accumulation model assumes there is a surface mixed layer of sediments that is uniformly mixed to a certain depth (the surface mixed layer depth - SML) during the course of each year. Effectively, it is assumed that at the end of each year, sediment in the surface mixed layer consists of a combination of new sediment deposited during the course of the year mixed uniformly with previously deposited sediments.

At the beginning of the simulation period the metal concentration in the surface mixed layer is assumed to be C_0 (defined in units of mg metal/kg sediment).

Outputs from the sediment transport model are used to quantify the sediment accumulation rate (SAR) within a given subestuary. The model data is post-processed to only consider the SAR due to catchment derived sediments and not the transport of pre-existing sediment from other parts of the harbour into the subestuary being considered. To do so would require a full process-based model that tracked the

exchange of sediments and metals between subestuaries as well as the sediments and metals from the catchment. This is not feasible over the time-frames that need to be considered for the metal accumulation. In terms of the metal accumulation results, this means that there would some "smoothing out" of the model results at a subestuary level. The exchange of pre-existing sediments between a subestuary with higher predicted metal accumulation and one with a lower level of metal accumulation would result in slightly higher levels in the "low" subestuaries and an equivalent reduction in the "high" subestuary. In a similar way, within each subestuary there will be areas with higher rates of deposition than the subestuary-wide SAR. Here, higher levels of metal accumulation will occur than predicted by the metal accumulation model. Conversely, there will be areas with lower rates of deposition than the subestuary wide SAR where lower levels of metal accumulation will occur than predicted by the metal accumulation model. Finally, there will be areas within each subestuary where there will be net erosion where the build-up of metals is unlikely to be of concern. Thus, the metal accumulation model provides an indication of which subestuaries may, over time, be more susceptible to metal accumulation but not the absolute level of metal accumulation or the spatial distribution of metal accumulation within that subestuary.

The predicted change in bed-level due to the catchment derived sediments at the end of the 2010 model simulation are then averaged over a given subestuary to provide the mean sedimentation rate within that subestuary.

Information from the catchment load data is used to define the metal concentration associated with the new sediment arriving into the subestuary each year (C_c defined in units of mg metal/kg sediment).

Based on a mass balance approach, the following can be derived. Details of the approach are given in Appendix B. Where C_i is the concentration in a given year and C_{i-1} is the metal concentration in the previous year.

$$C_i = [SML*Cc + (SML-SAR)*C_{i-1}]/SML$$

Thus, for year one of the metal model simulation the metal concentration in the SML is

$$C_1 = [SML*Cc + (SML-SAR)*C_0]/SML$$

In year two of the metal model simulation the metal concentration in the SML is

$$C_2 = [SML*Cc + (SML-SAR)*C_1]/SML$$

Essentially, the sediment transport model is used to define the connectivity of each of the subestuaries to each of the catchment sources and to define the mass of new sediment that is arriving in each subestuary. This then provides the necessary inputs to the metal accumulation model at the subestuary scale.

6 Results

In this section, the key results from the modelling are presented for the hydrodynamics of the harbour, the wave model simulations and for each of the contaminants considered.

6.1 Hydrodynamics and Wave Summary

The following section of the report gives an overview of the hydrodynamics and wave dynamics of the harbour.

6.1.1 Hydrodynamics

Figure 6-1 and Figure 6-2 show typical peak ebb and peak flood tide currents respectively within the harbour. Highest flows occur near the entrances to the two arms of the harbour. In this area of the harbour, tidal currents are of sufficient strength to prevent the long-term deposition of sediments. Lowest current speeds occur within the southern basin of the Onepoto Arm and the south-east sector of the Pauatahanui Arm around Browns Bay, Duck Creek and the Pauatahanui Creek.

Figure 6-3 shows the average current speed over the full duration of the 2010 model simulation. It shows areas where tidal flows dominate (in the vicinity of the entrances) and also where the larger catchment outlets contribute to higher current speeds.

Figure 6-4 shows the maximum current speed that is predicted to occur at any time during the 2010 simulation. This shows the influence of the highest freshwater inflows that occur throughout the year (enhancing flows near the catchment outlets) plus the enhanced effect of waves on currents in the shallower fringes of the harbour. Of note are the areas of lowest maximum currents in both the Onepoto Arm and Pauatahanui Inlet which correspond to the depositional sinks identified in Green et al. (2016).
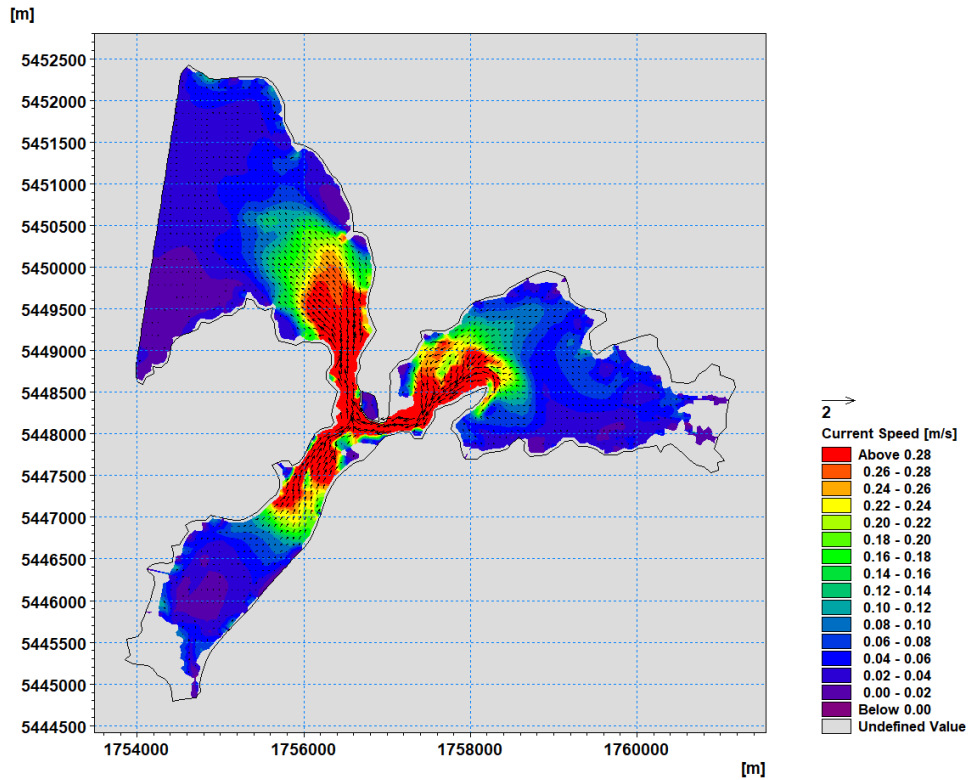
Figure 6-1.   Typical peak ebb tide currents across the harbour. Vectors are interpolated onto a regular grid for ease of visualisation.
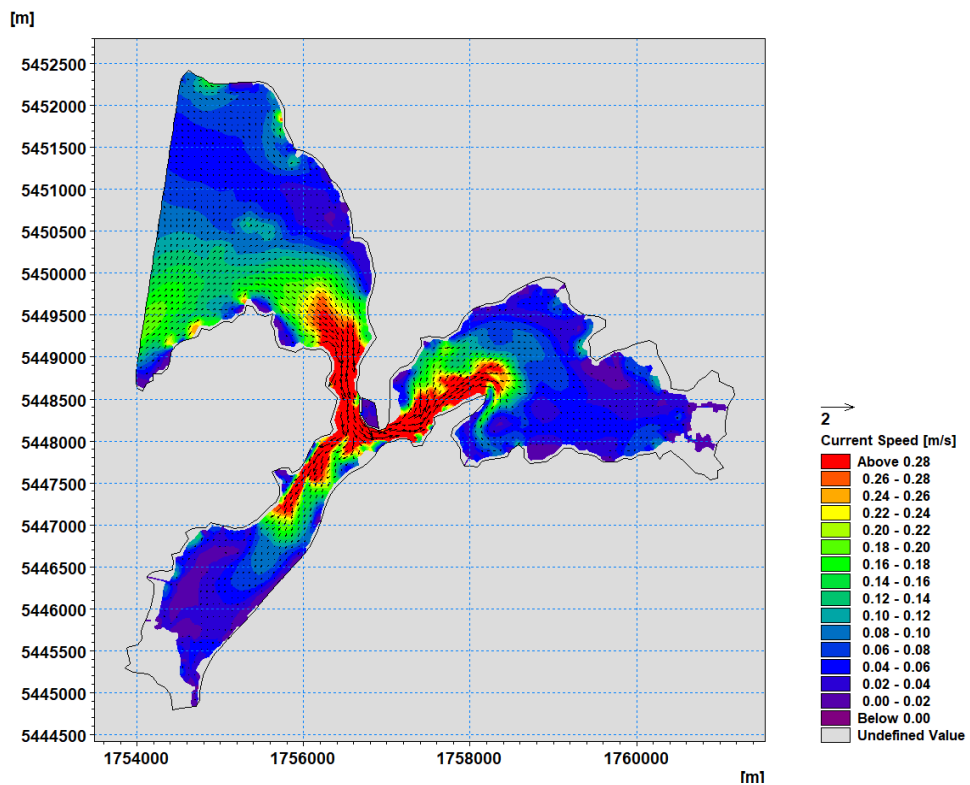
Figure 6-2.   Typical peak flood tide currents across the harbour. Vectors are interpolated onto a regular grid for ease of visualisation.
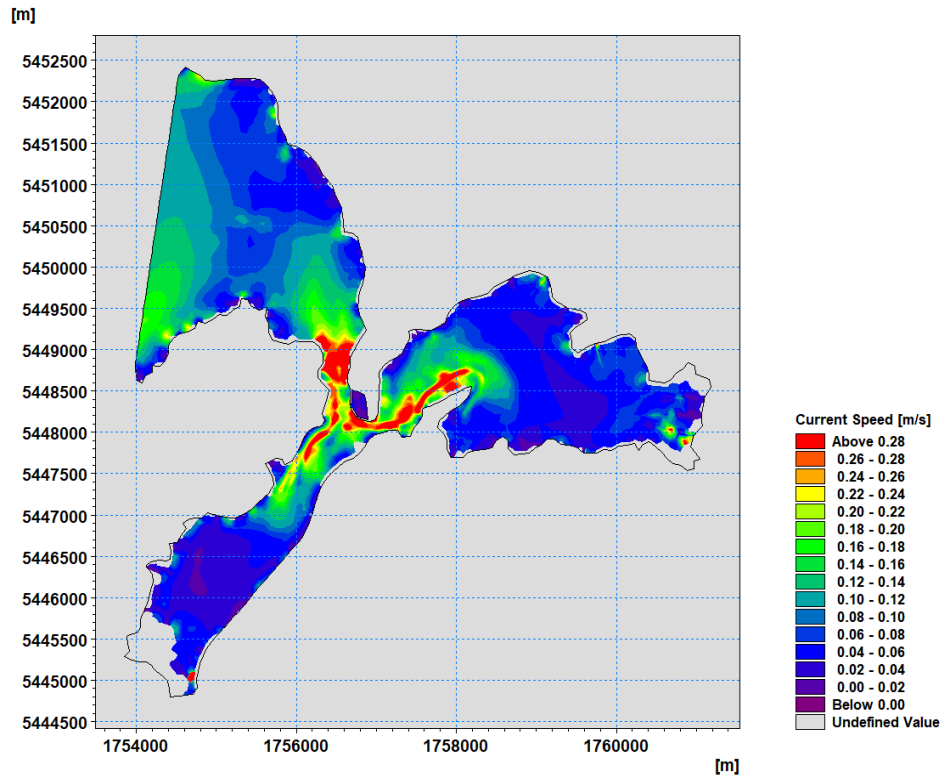
Figure 6-3.   Average current speed over the duration of the 2010 model simulation.
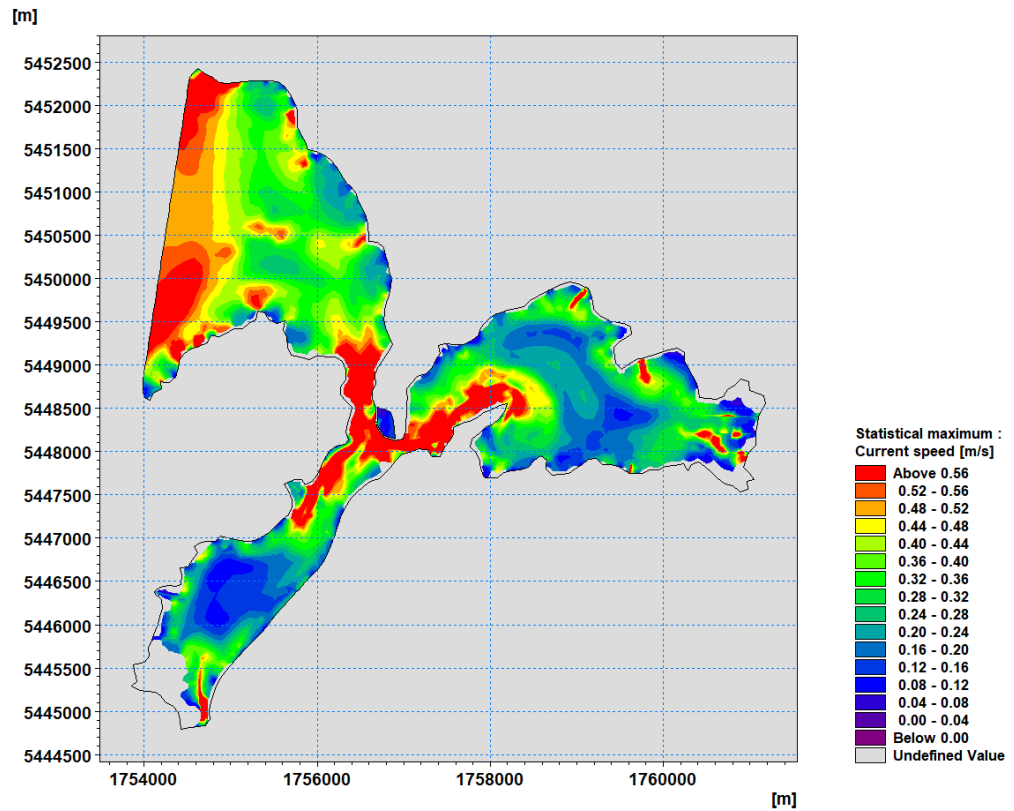
Figure 6-4.   Maximum predicted current speed over the duration of the 2010 model simulation.

6.1.2   Waves

Penetration of swell waves into the Onepoto Arm and Pauatahanui Inlet will be minimal so the wave model only considers wind generated waves.

Table 6-1 provides a summary of the predicted waves at the central Pauatahanui site (Figure 6-5) and Figures 6-6 to 6-10 show the maximum predicted wave heights across the model domain over the period for each of the events and for all of the 2010 model simulation. It can be seen that, at times, wind generated waves in excess of 0.5 m are predicted to occur immediate offshore of the harbour (e.g. Figure 6-10). Swell waves will also influence this area resulting in much larger waves than those predicted by the wave model. This would lead to greater erosion of any offshore sediments, but such dynamics are likely to have little influence on the overall sediment budget or dynamics within the harbour.

Table 6-1.   Summary of predicted waves at the central Pauatahanui site (Figure 6-5).

Simulation	Ratio of Hs over the simulation period to the Hs for the period 2004-2014	Percentage of time 0.1 m waves are exceeded
2004 Event	1.66	29%
2005 Event	0.90	2%
2006 Event	1.57	21%
2010 Annual	0.98	4%
2013 Event	0.93	5%
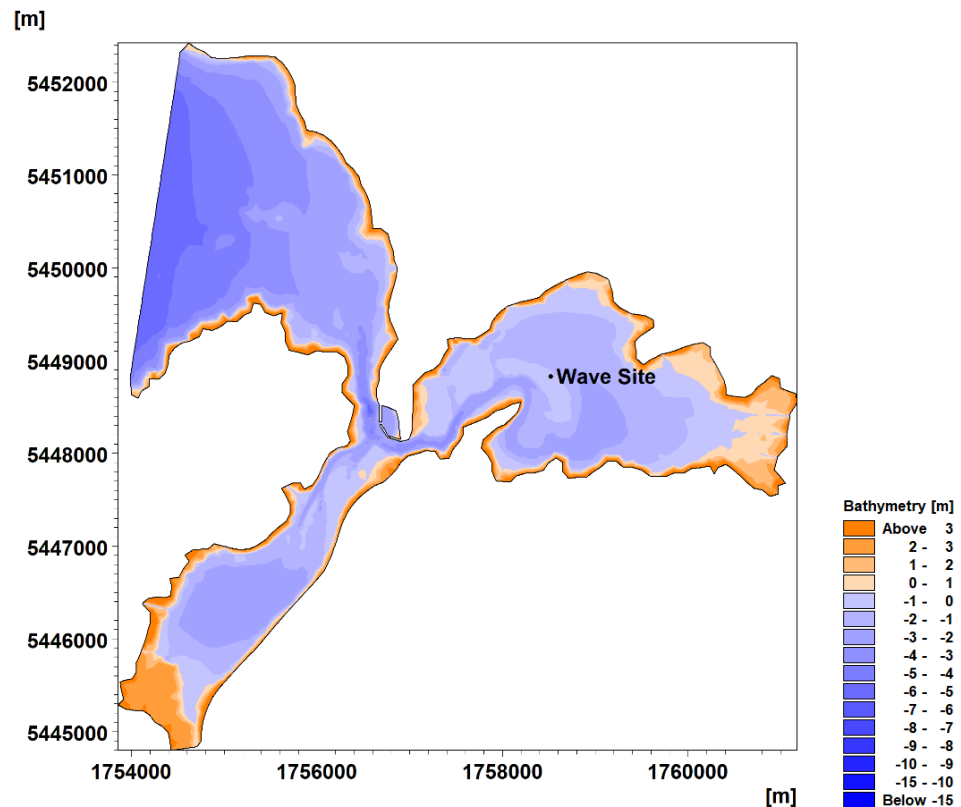
Figure 6-5.   Central Pauatahanui site where wave data has been extracted from the model simulations.

To provide an overview of the different wave climates during the selected events, the time series of predicted waves at the central site in the Pauatahanui Inlet (Figure 6-5) have been extracted from the model and plotted against the input hydrographs for the 2004, 2005, 2006 and 2013 events. These are shown in Figures 6-11 to 6-14.

During the 2004 event (Figure 6-11), the largest waves correspond to the peak of the event hydrograph (when winds exceed 20 m/s, Figure 3-8) and wave height decreases to less than 0.10 m a few days after the peak of the hydrograph. Wave activity increases again during the secondary peak of the hydrograph (when wind speeds again approach 20 m/s) towards the end of January. Overall, this event consists of a number of larger wave events and the overall Hs at the central Pauatahanui site for the period being modelled is over 60% higher than the long-term average significant wave height at the site.

During the 2005 event (Figure 6-12), winds are rarely over 10 m/s (Figure 3-9) and as such waves never exceed 0.10 m. Overall, this event is characterised by low wave energy.

During the 2006 event (Figure 6-13), smaller wave events (>0.10 m) coincide with the peaks in the hydrographs as is the case for the 2013 event (Figure 6-13). Overall, the 2006 event is very similar to the 2004 event in terms of waves and the 2013 event has similar wave conditions as the 2010 simulation period (Figure 6-14).

Figure 6-15 shows the comparison between the annual sediment load delivered to the harbour and the predicted significant wave height at a site immediately offshore of Bradeys Bay for the period between the DML surveys. The figure shows the high degree of inter-annual variability of both sediment load and wave activity in the period between the DML surveys and that 2010 is representative in terms of both average loads and wave activity that occurred between the DML surveys
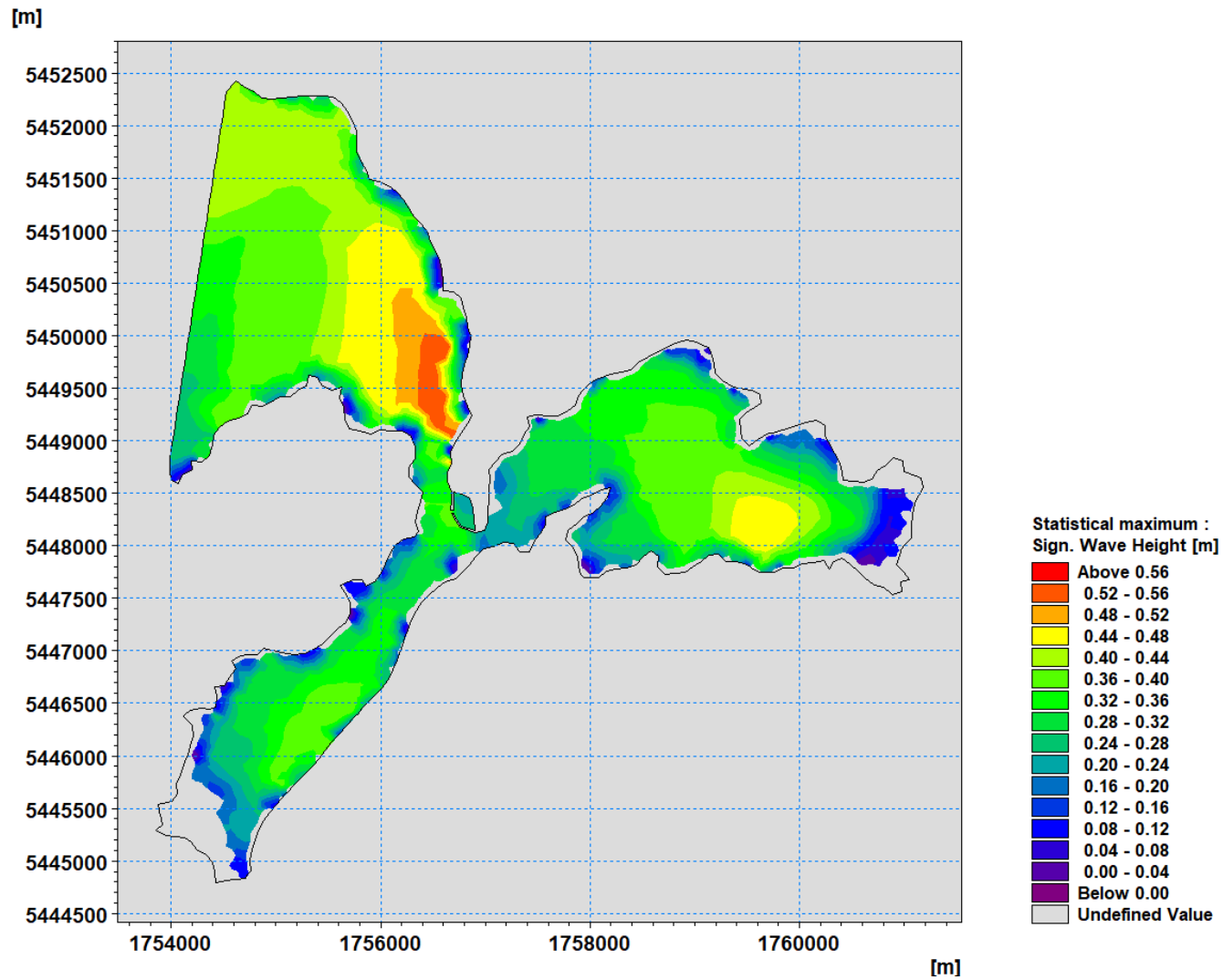
Figure 6-6.   Maximum predicted wave height during the 2004 event.
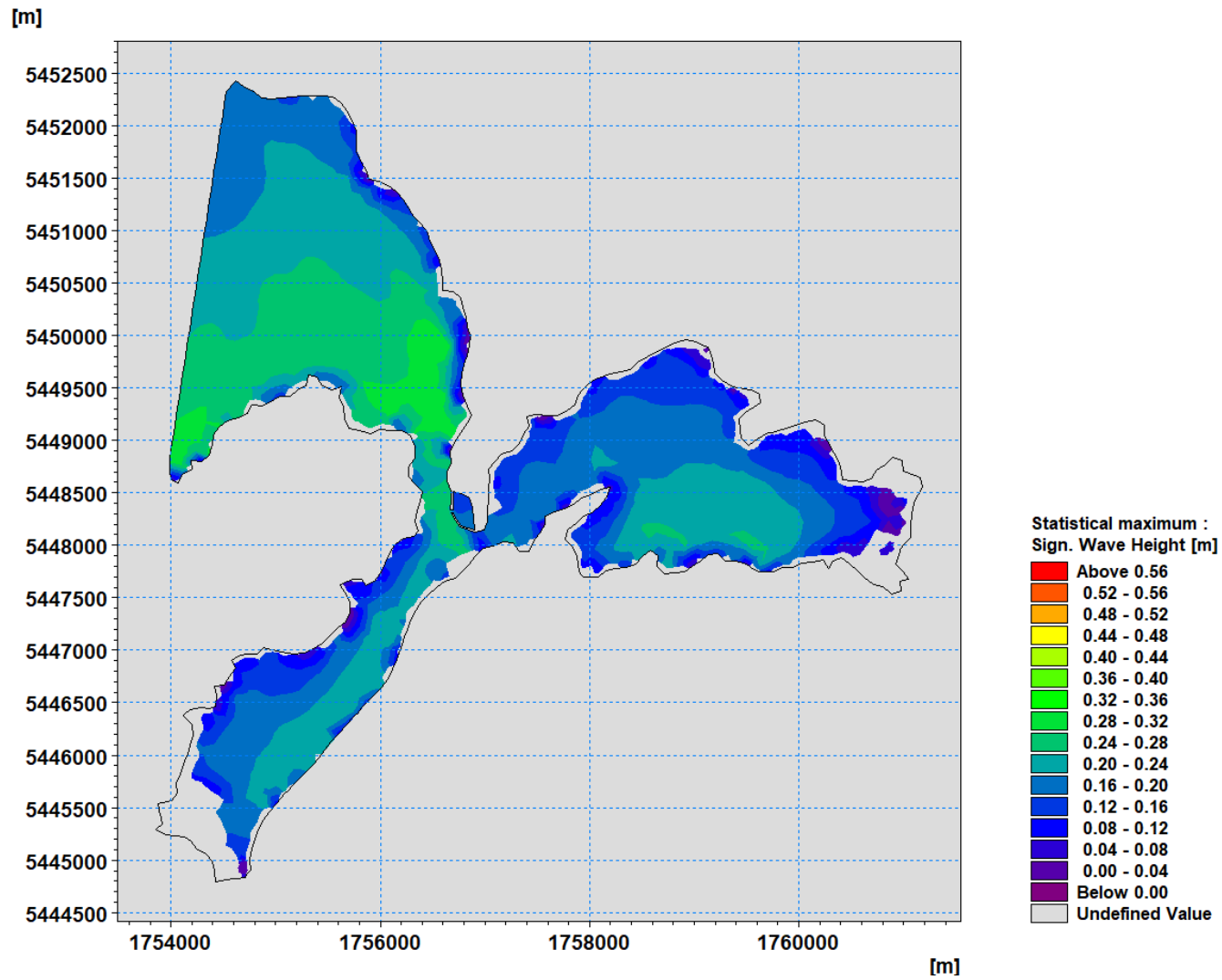
Figure 6-7.   Maximum predicted wave height during the 2005 event.
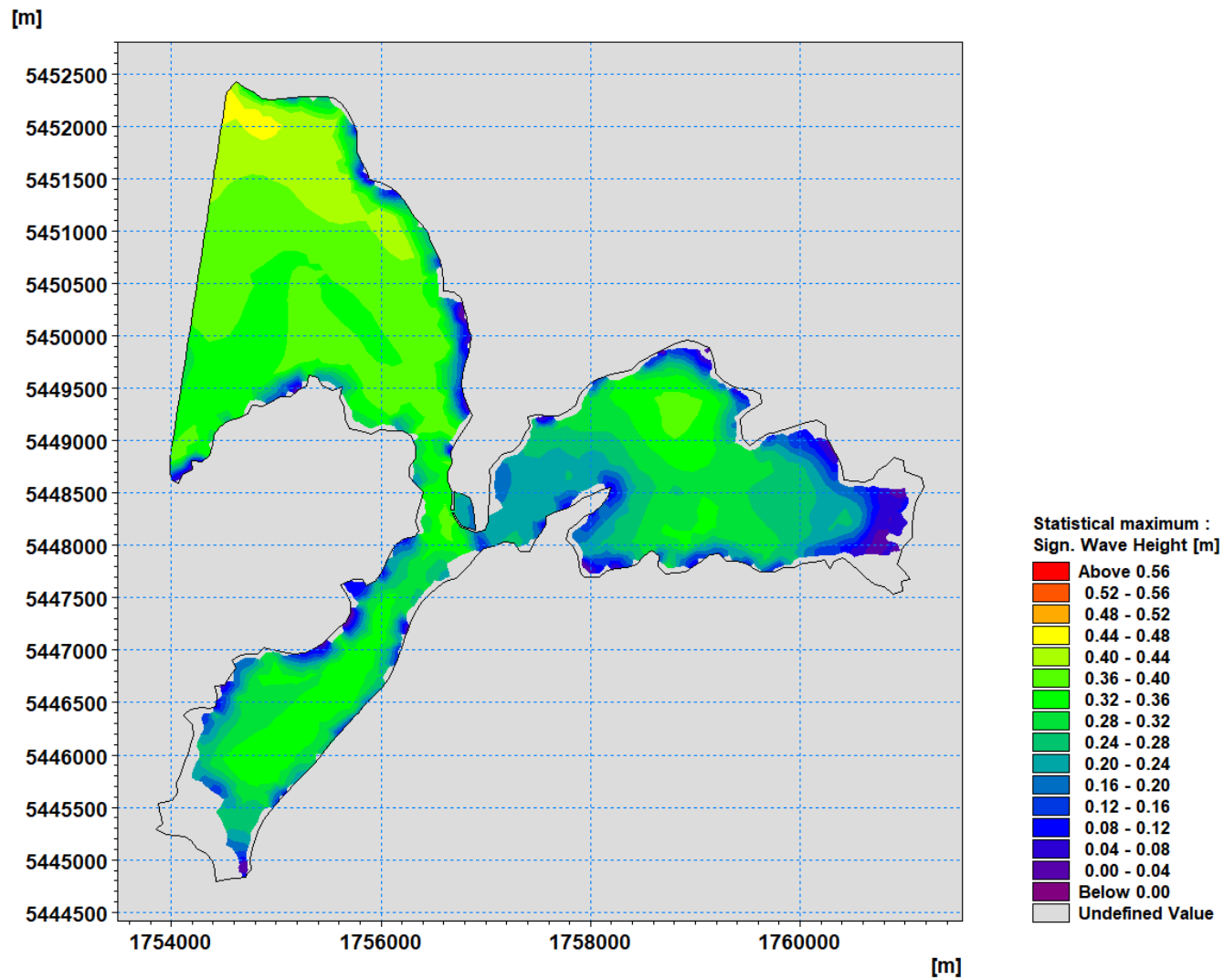
Figure 6-8.   Maximum predicted wave height during the 2006 event.
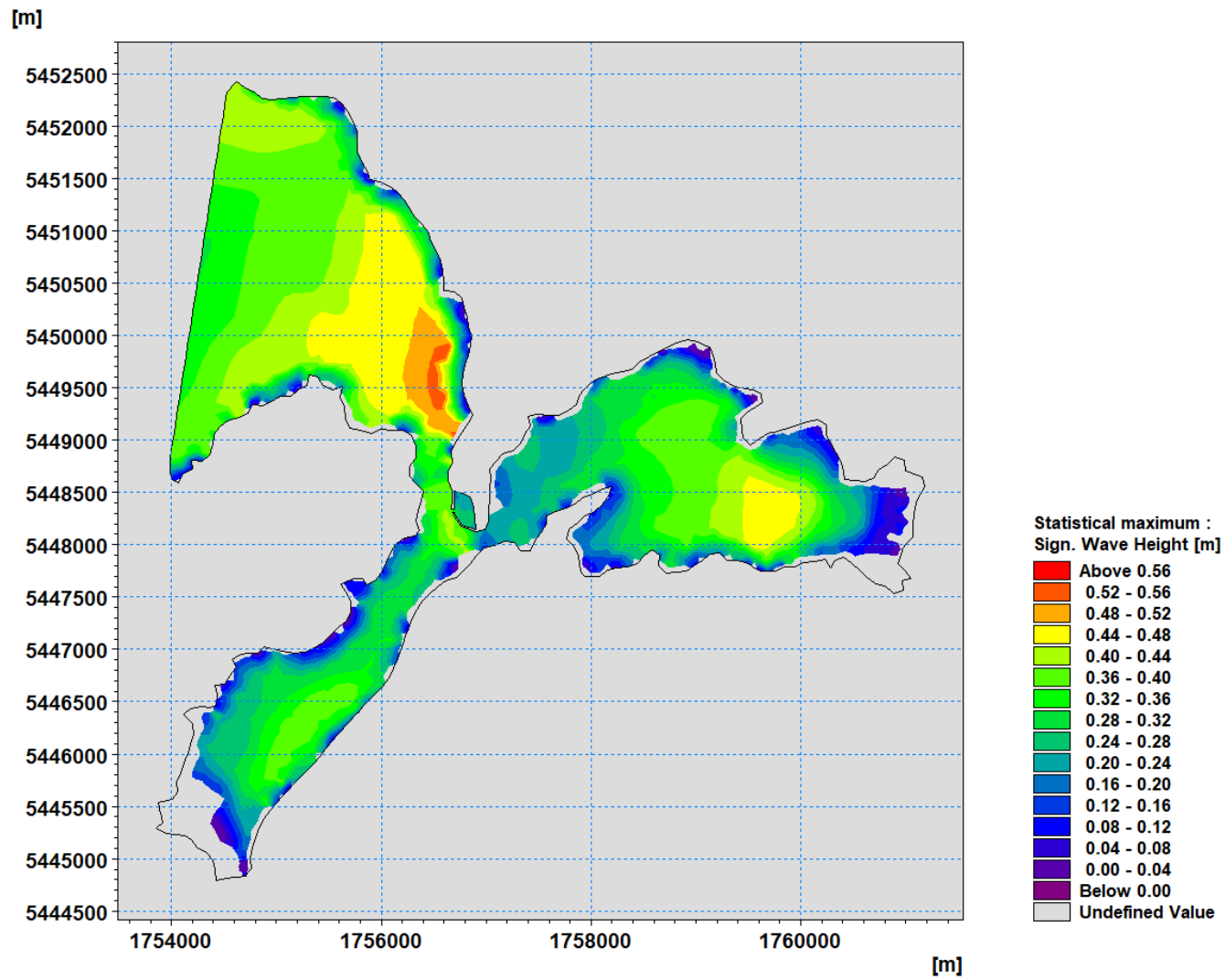
Figure 6-9.   Maximum predicted wave height over the full duration of the 2010 model simulation.
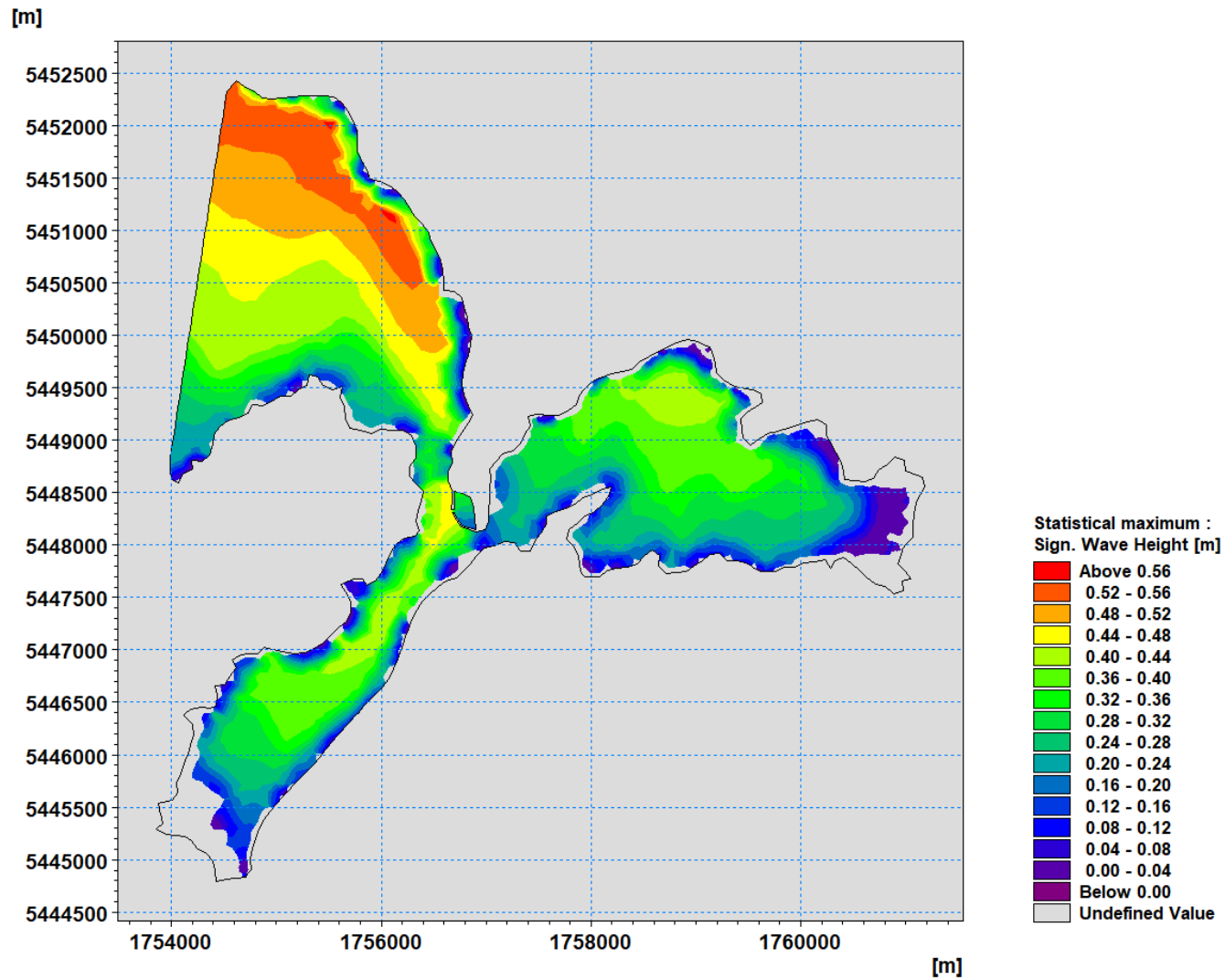
Figure 6-10.   Maximum predicted wave height during the 2013 event.
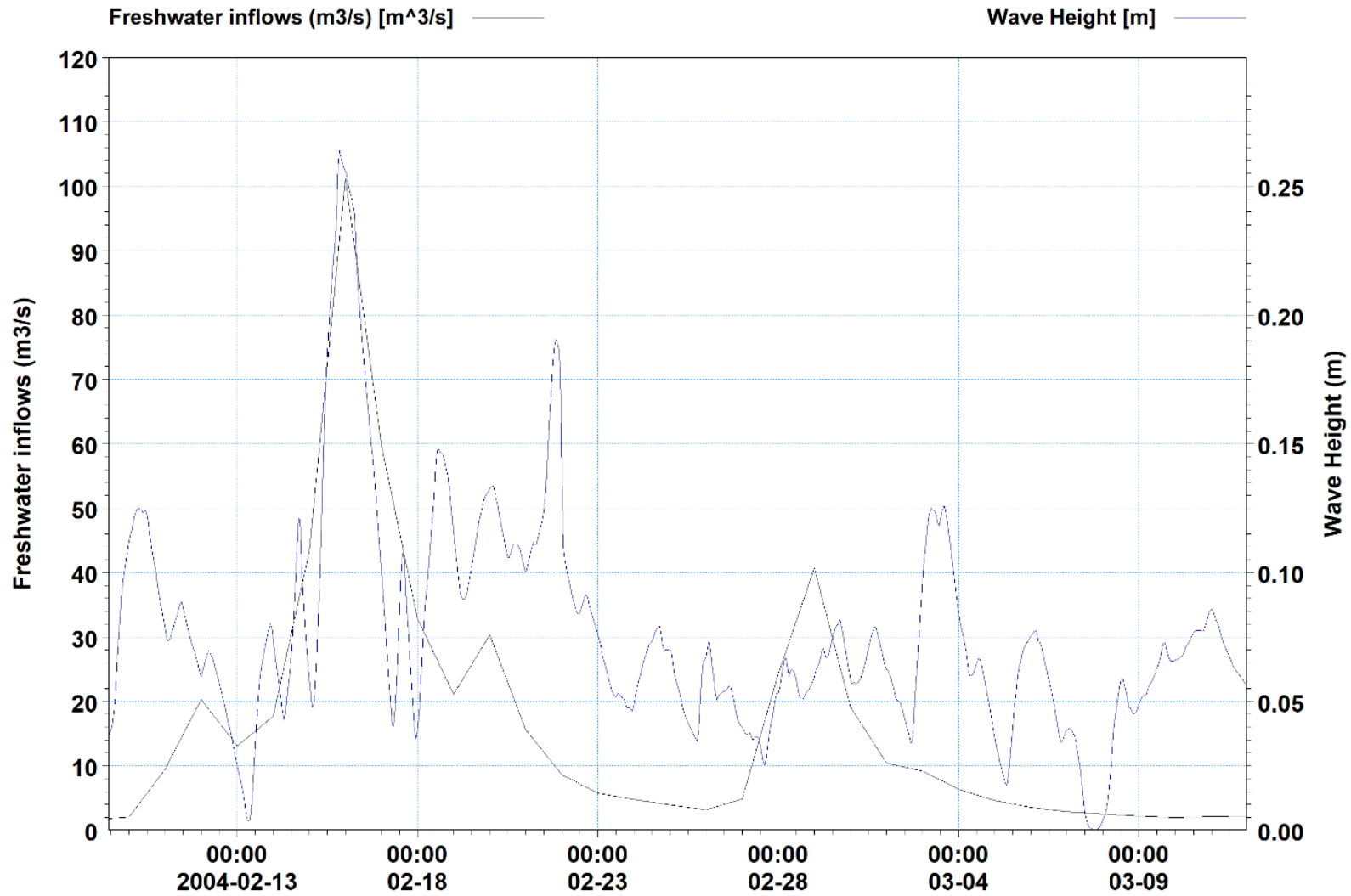
Figure 6-11.   Time-series of predicted wave height at the central Pauatahanui site (Figure 6-5) and sum of all catchment freshwater inputs for the 2004 event.
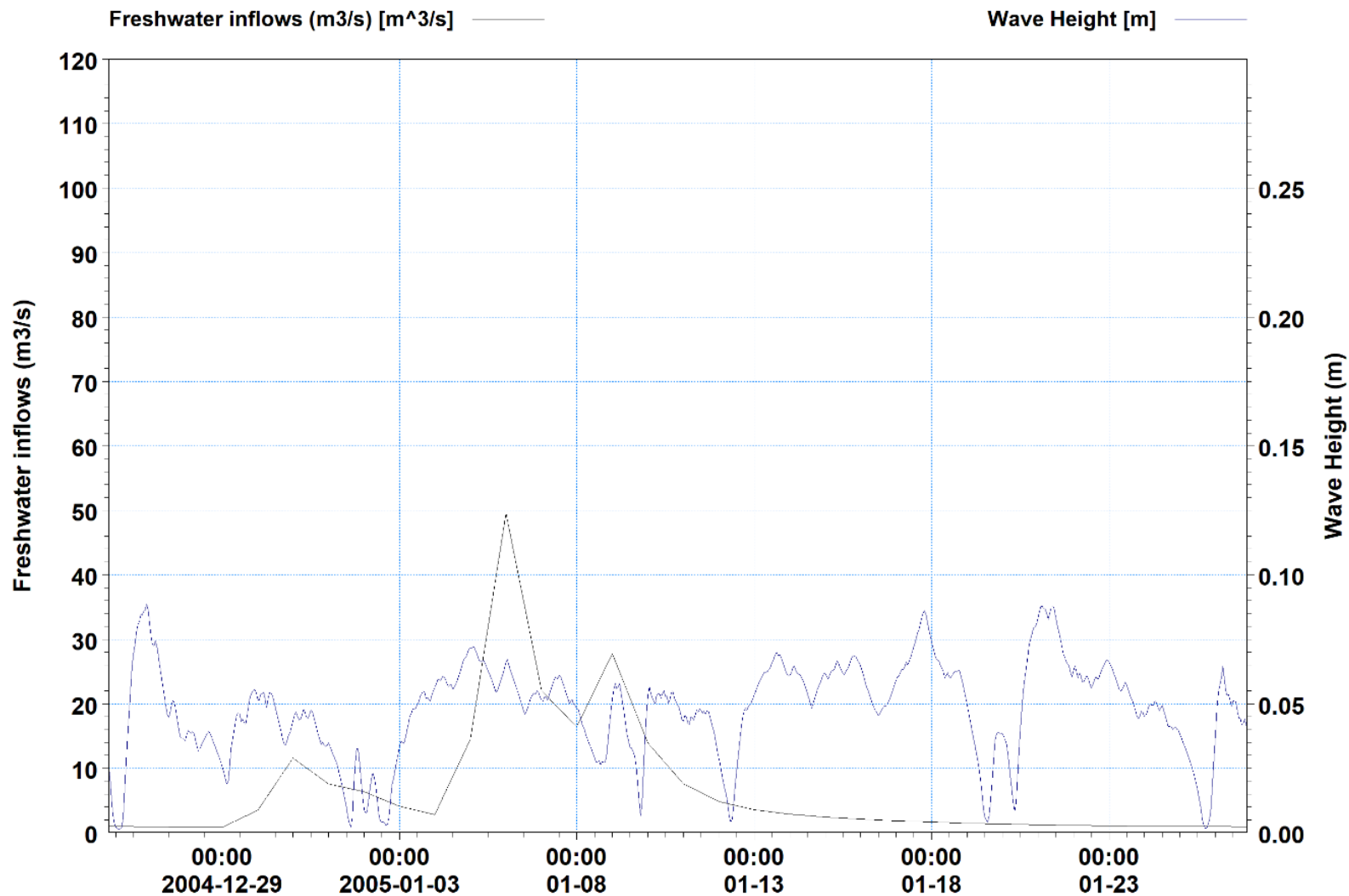
Figure 6-12.   Time-series of predicted wave height at the central Pauatahanui site (Figure 6-5) and sum of all catchment freshwater inputs for the 2005 event.
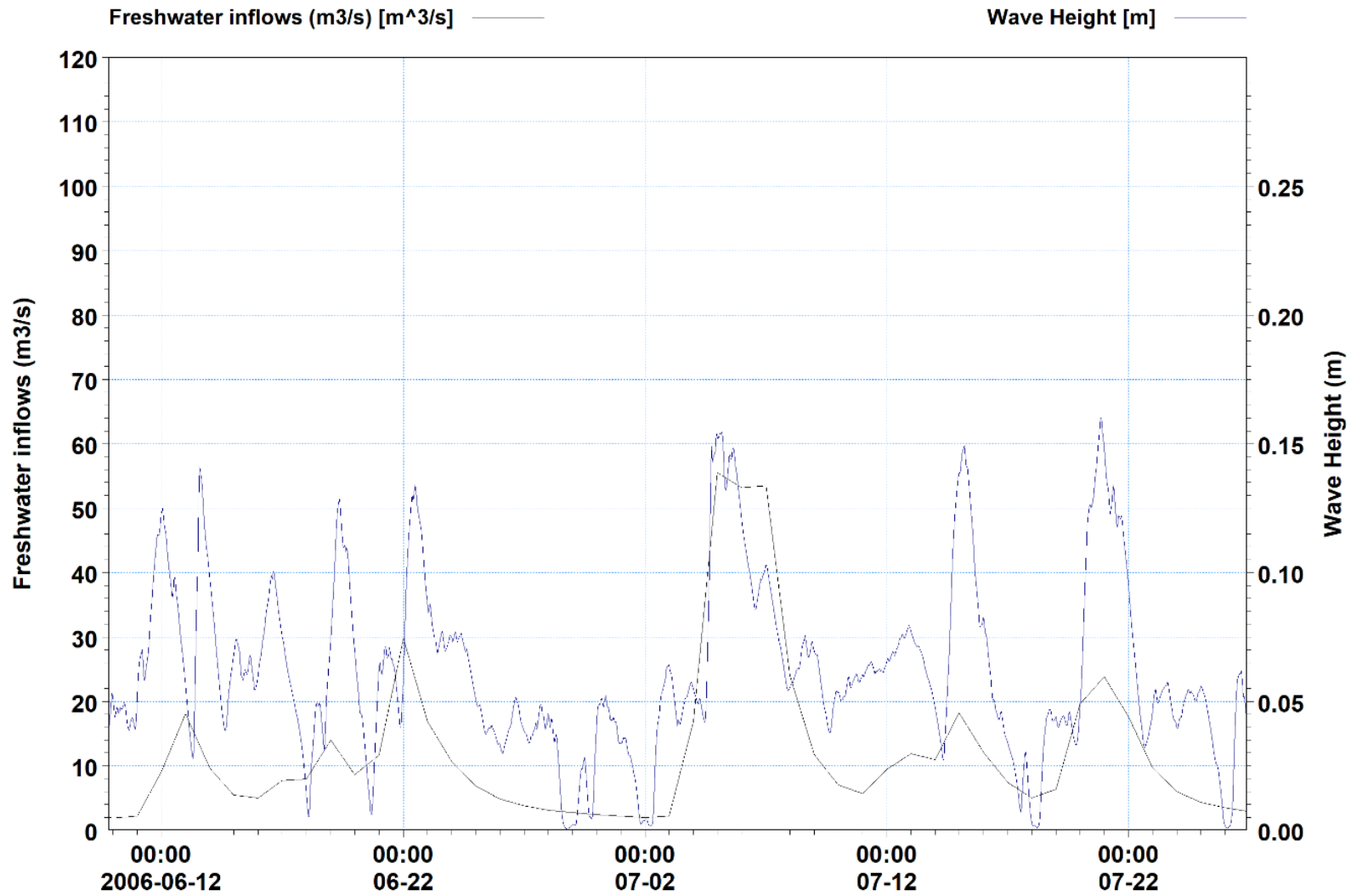
Figure 6-13. Time-series of predicted wave height at the central Pauatahanui site (Figure 6-5) and sum of all catchment freshwater inputs for the 2006 event.
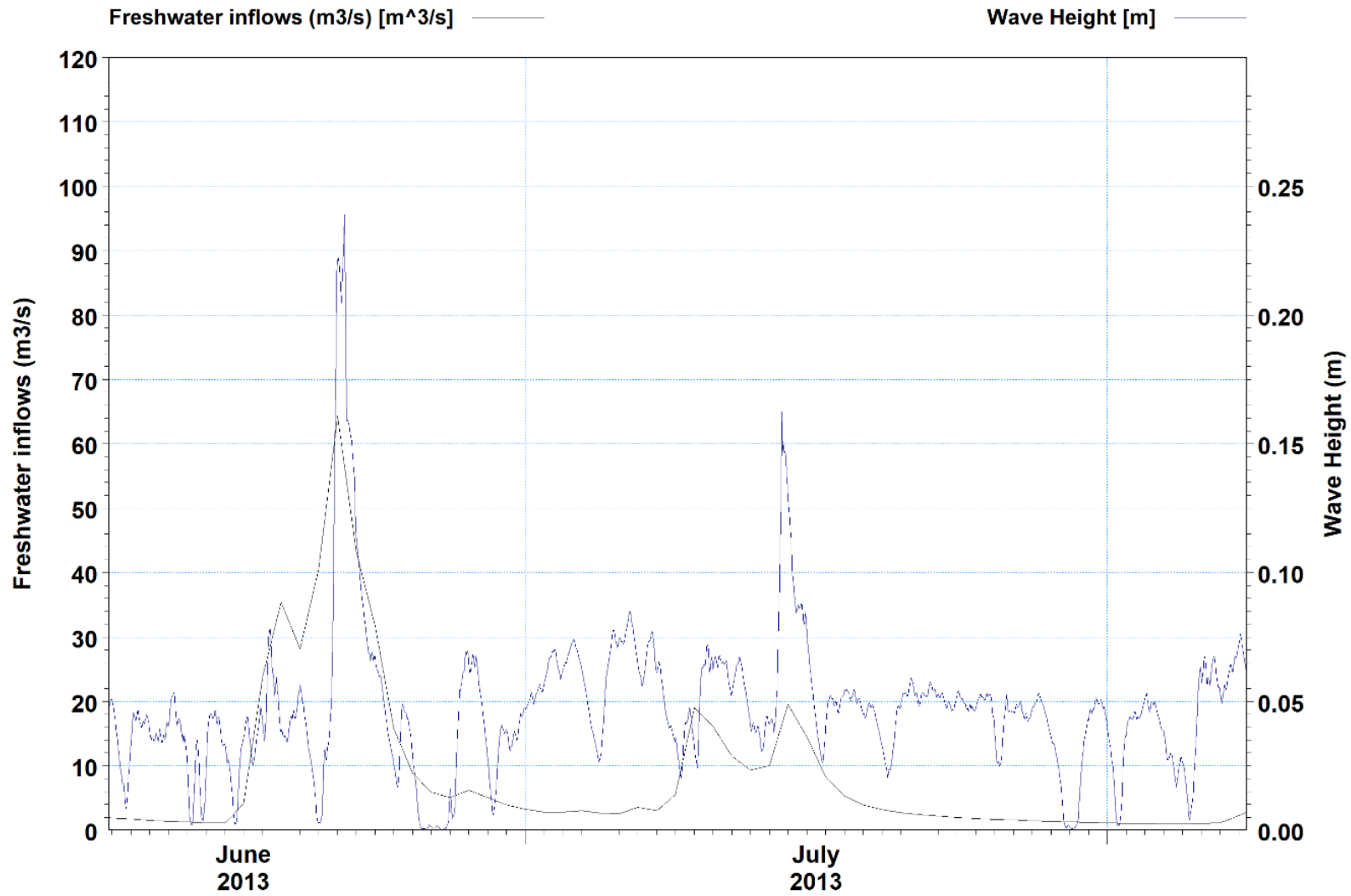
Figure 6-14.   Time-series of predicted wave height at the central Pauatahanui site (Figure 6-5) and sum of all catchment freshwater inputs for the 2013 event.
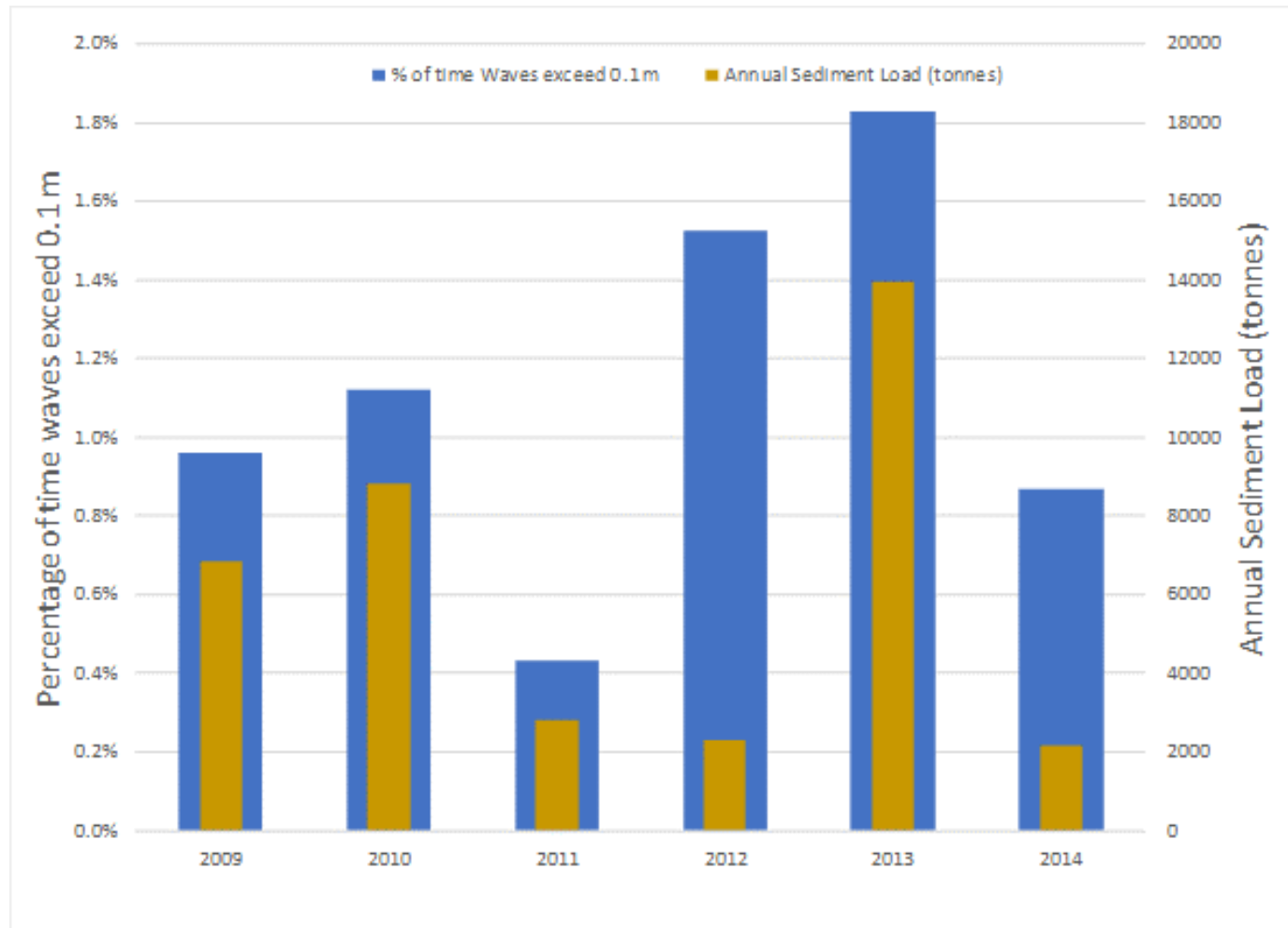
Figure 6-15. Summary of annual sediment load and wave data at Bradeys Bay for the periods between the DML surveys (2009-2014).

6.2 Sediments

The following section of the report provides details of the outputs of the sediment transport model that have been presented to the Whaitua committee.

6.2.1 Basin-Wide Sediment Budget

Data in Table 6-2 shows the overall sediment budget for the two arms of the harbour based on the model outputs from the 2010 simulations.

The mass deposited and exported from the harbour are expressed as both tonnes and as a percentage of total catchment inputs.

The catchment input data is the total catchment load data (summed across all catchment outlets) for all of 2010.

The mass exported from the two arms is the net sediment flux crossing the entrances to the two arms over the full duration of the 2010 simulation. This considers the net effect of the flushing of sediments from the arms on the outgoing tide and the transport back into the arms on the incoming tide. It provides a measure of the quantity of sediment permanently lost from the two arms.

The mass deposited within the two arms is derived from summing the total change in mass on the seabed (of all sediment fractions) that has occurred at the end of the 2010 simulation. This includes the net effect of new sediment being deposited on the seabed and the existing sediments being exported, consisting of both new catchment derived sediments and existing sediments from the harbour.

There is only a small reduction in the mass of sediment exported from the harbour under the Water Sensitive scenario. That is because the mass exported from the harbour is the combination of 1) the suspended sediment concentration across the entrance to the arm and 2) the flux of water exiting and entering the arms on each tidal cycle. As discussed below, the model results show that there is very little difference in the predicted suspended sediment concentration between the scenarios (because this is primarily driven by the resuspension of pre-existing bed sediments). The areas where the largest changes in suspended sediment concentration occur are close to the catchment outlets. Near the entrances to the two arms of the harbour, any changes in suspended sediment concentration will be minimal. In addition, the flux of water exiting and entering the arms on each tidal cycle is totally dominated by the offshore tidal and wind forcing (which does not change between scenarios). The effect of the small changes in freshwater inflows (Table 3-3) will be minimal.

The BAU and Water Sensitive scenarios do result in a marked reduction in the mass of sediment deposited within each arm of the harbour. As discussed below, this primarily comes about because of the reduced deposition rates predicted to occur in the area in the vicinity of the catchment outlets and within the main subtidal basins of the harbour.

Table 6-2.   Overall sediment budget for the 2010 simulation.

Scenario	Onepoto Arm	Pauatahanui Inlet
Catchment Inputs (tonnes)		
BASELINE	3300	5500
BAU	2800	5400
Water Sensitive	1400	3000
Export (tonnes)		
BASELINE	750 (23%)	1500 (27%)
BAU	750 (27%)	1500 (28%)
Water Sensitive	690 (49%)	1450 (48%)
Deposited (tonnes)		
BASELINE	2550 (77%)	4000 (73%)
BAU	2050 (73%)	3900 (72%)
Water Sensitive	710 (51%)	1550 (52%)

6.2.2   Harbour-Wide Patterns of Bed Level Change

In this section of the report, the spatial distribution of the predicted changes in bed level over the duration of the simulated events and during 2010 are discussed. Positive changes in predicted bed level over the duration of a model run indicate areas where there has been net accretion over the duration of the model simulation and negative changes in predicted bed level over the duration of a model run indicate areas where there has been net erosion of the seabed over the duration of the model simulation.

Figures 6-16 to 6-20 show the change in bed level at the end of the 2004, 2005, 2006, 2013 events and at the end of the annual 2010 simulation. Overall, certain patterns are evident.

For all the model simulations, deposition occurs within the main subtidal basins of the Onepoto Arm and the Pauatahanui Inlet and just outside the entrance to the harbour. Areas of highest deposition outside these depositional basins are near the major catchment outlets of the Porirua Stream, Duck Creek and the Pauatahanui Creek. The predicted level of deposition is directly related to the magnitude of the catchment load associated with the adjacent sub-catchment.

Areas of erosion are seen around the fringes of the harbour and near the harbour entrance (in the areas where maximum predicted tidal currents occur). Certain differences are also evident in the figures.

For example, the significant sediment load delivered during the 2004 event results in nearly all the southern portion of the Onepoto Arm being a depositional zone (Figure 6-16) and very high levels of deposition in the south-east section of the Pauatahanui Inlet.

Similar patterns of deposition and erosion are observed for the 2006 event (Figure 6-17) compared to the 2004 event because, as discussed above the wave climate for the two events is similar. However, the overall level of deposition is much less due to the lower sediment load delivered during this event and areas of net erosion are seen around the fringes of the Onepoto Arm. This indicates that for the 2006 event, erosion processes outstrip the delivery of sediment in these areas of the Onepoto Arm.

The 2005 event has relatively low sediment input and a lower wave activity. As such it shows much less erosion around the fringes of the harbour (Figure 6-18) compared to the 2004, 2006 events.

Finally, the patterns of deposition and erosion for the 2010 annual simulation (Figure 6-19) and the 2013 event (Figure 6-20) are very similar with the biggest difference being more erosion occurring around the fringes of the harbour during 2010 compared to the 2013 event. This is because there are long periods in 2010 when very little sediment is being delivered to the harbour (Figure 3-14). Under such conditions, tides and wave act to slowly erode these outer fringes of the harbour.

These figures all show that the model predicts deposition in the subtidal area offshore of Bradeys Bay for all the events and the annual simulation, which is not reflected in the DML survey data (as discussed in Section, 5.1, Figure 5-4). As discussed in Section, 5.1, model results in this part of the harbour (i.e. low levels of deposition) should be treated with caution. Based on the DML survey data (i.e. extent and magnitude of the 5-year change in bed level) and the model predictions, this area represents only a relatively small portion (< 0.5%) of the overall sediment budget of the harbour. Overall, the sediment transport model provides good robust estimates of subestuary-scale deposition and erosion rates.
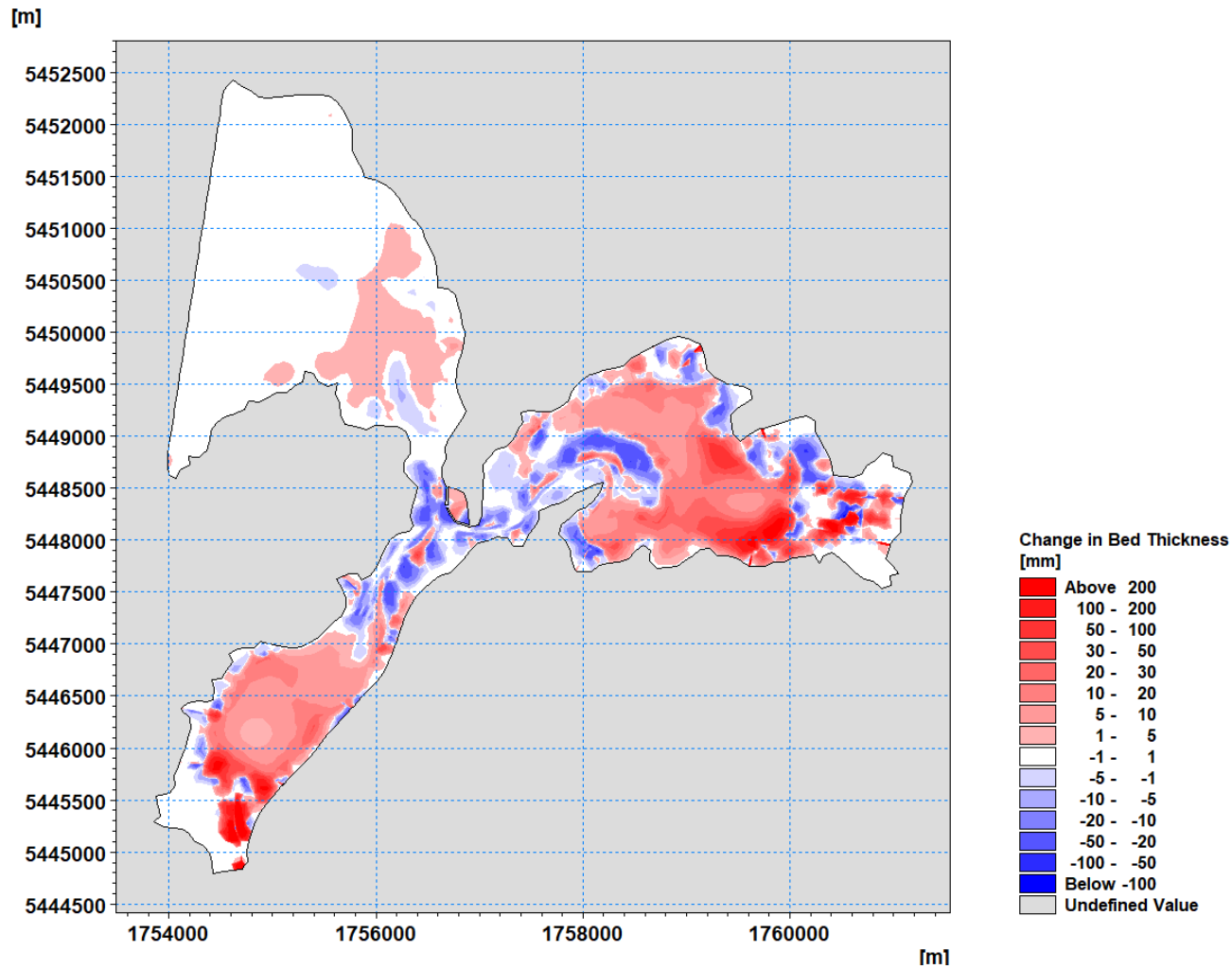
Figure 6-16.   Predicted change in bed level (mm) at the end of the 2004 event. Positive values (shaded red) indicate areas where there has been net deposition over the period of the simulation while negative values (shaded in blue) indicate areas where there has been net erosion of the seabed of the period of the model simulation.
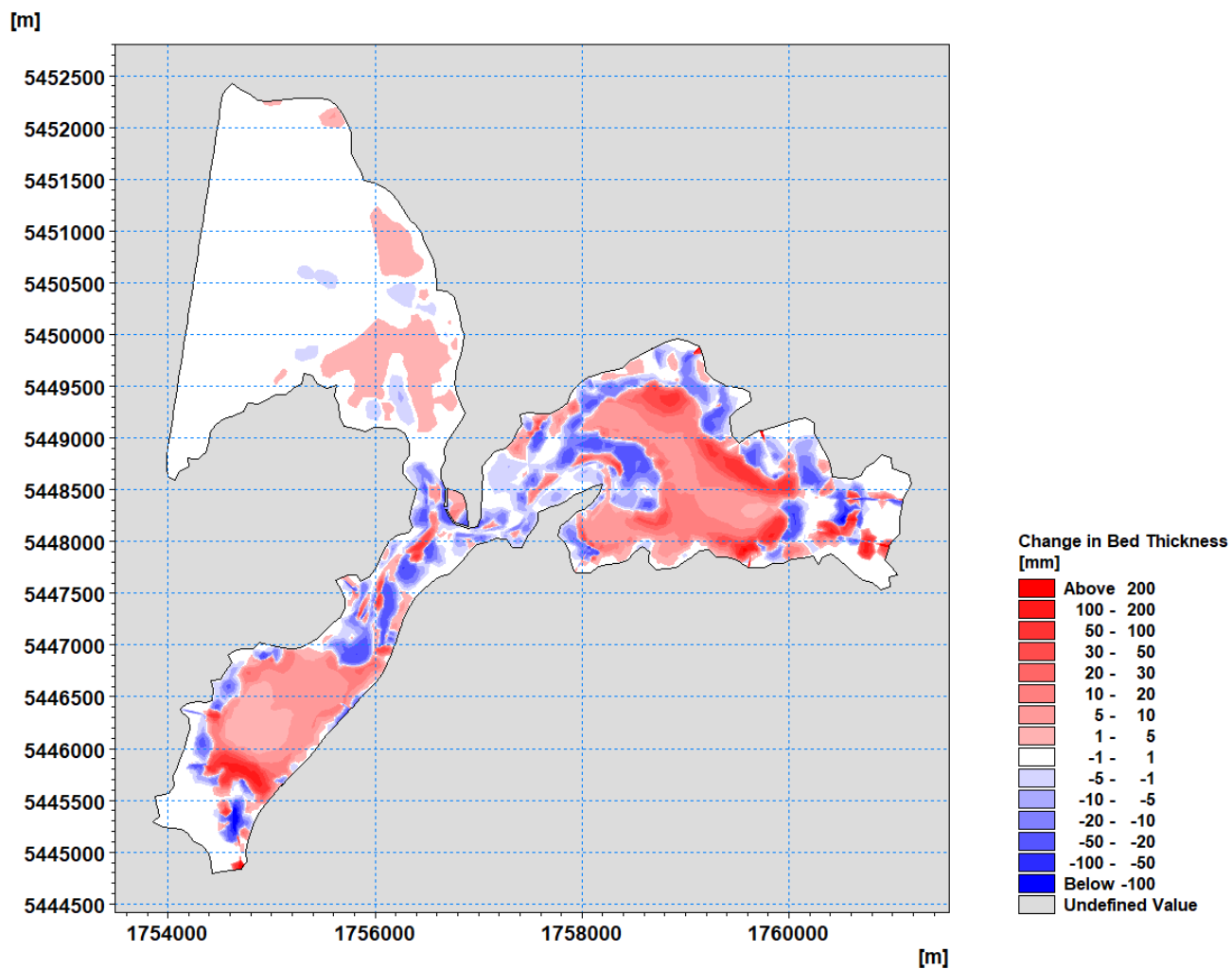
Figure 6-17. Predicted change in bed level (mm) at the end of the 2006 event. Positive values (shaded red) indicate areas where there has been net deposition over the period of the simulation while negative values (shaded in blue) indicate areas where there has been net erosion of the seabed of the period of the model simulation.
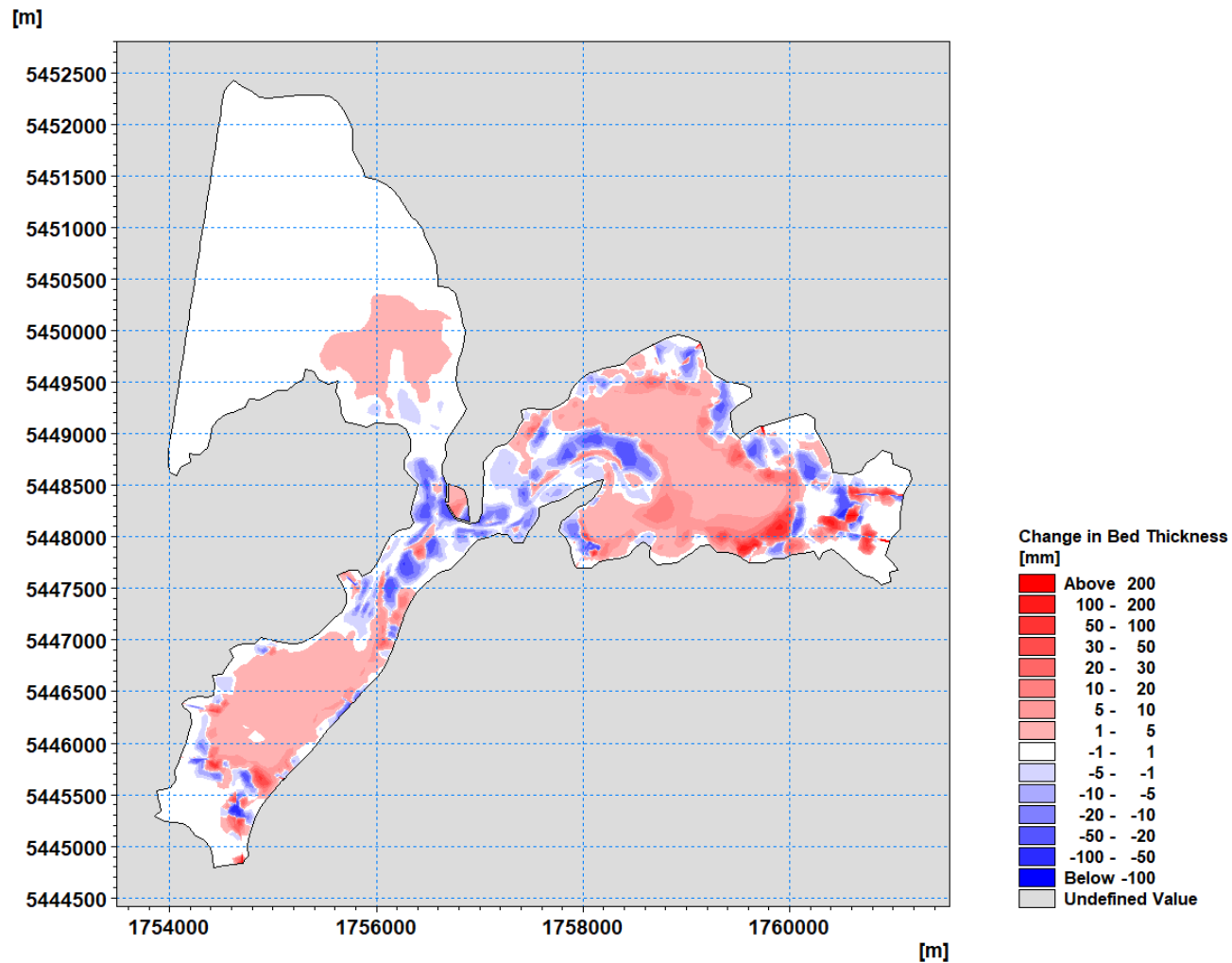
Figure 6-18. Predicted change in bed level (mm) at the end of the 2005 event. Positive values (shaded red) indicate areas where there has been net deposition over the period of the simulation while negative values (shaded in blue) indicate areas where there has been net erosion of the seabed of the period of the model simulation.
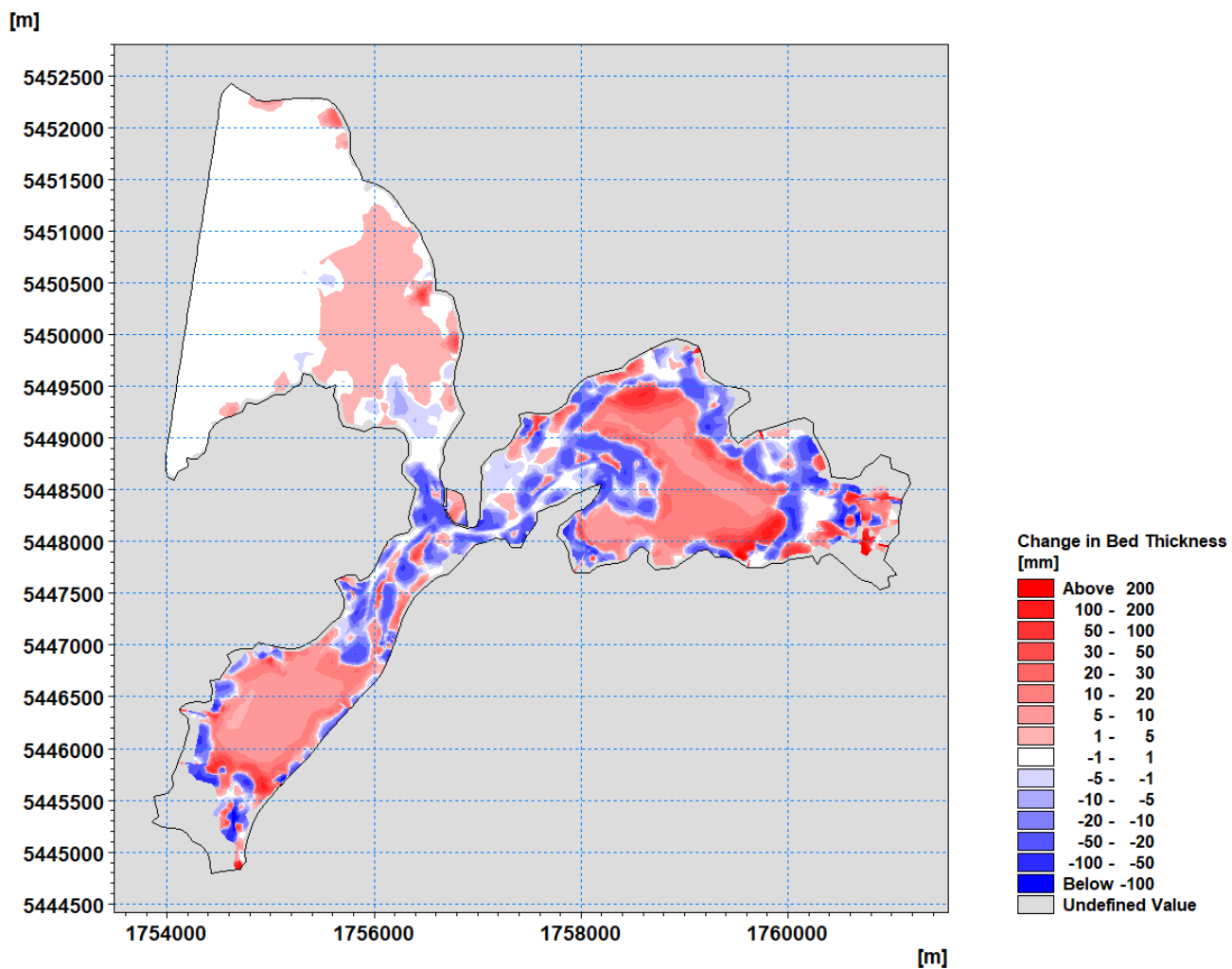
Figure 6-19. Predicted change in bed level (mm) at the end of the 2010 model simulation. Positive values (shaded red) indicate areas where there has been net deposition over the period of the simulation while negative values (shaded in blue) indicate areas where there has been net erosion of the seabed of the period of the model simulation.
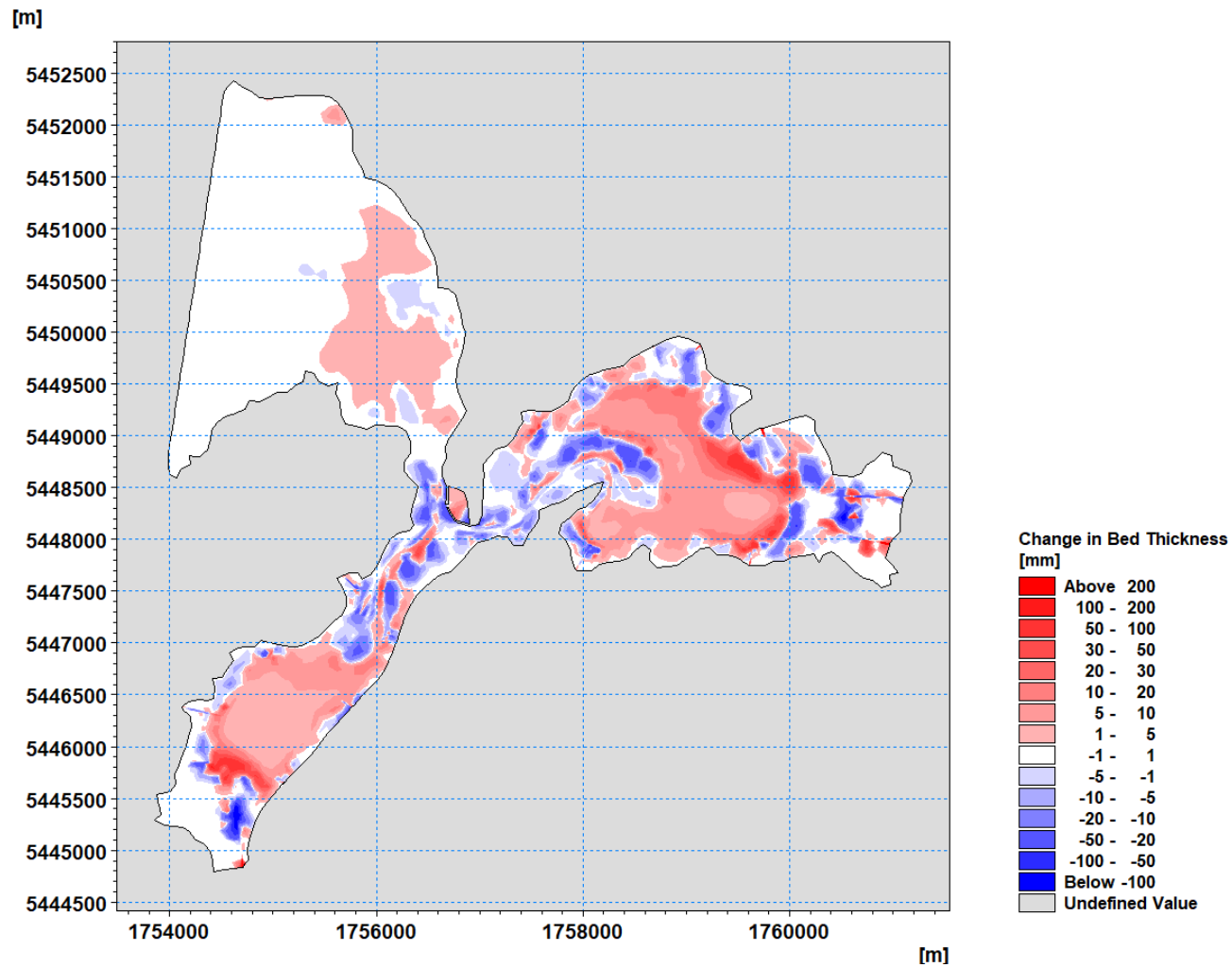
Figure 6-20.   Predicted change in bed level (mm) at the end of the 2013 event. Positive values (shaded red) indicate areas where there has been net deposition over the period of the simulation while negative values (shaded in blue) indicate areas where there has been net erosion of the seabed of the period of the model simulation.

6.2.3 Subestuary Deposition Rates

To develop an understanding of the spatial pattern of deposition and the variability associated with individual events (Section 5.1), the Onepoto Arm and Pauatahanui Inlet have been divided into the subestuaries as shown in Figure 6-21.
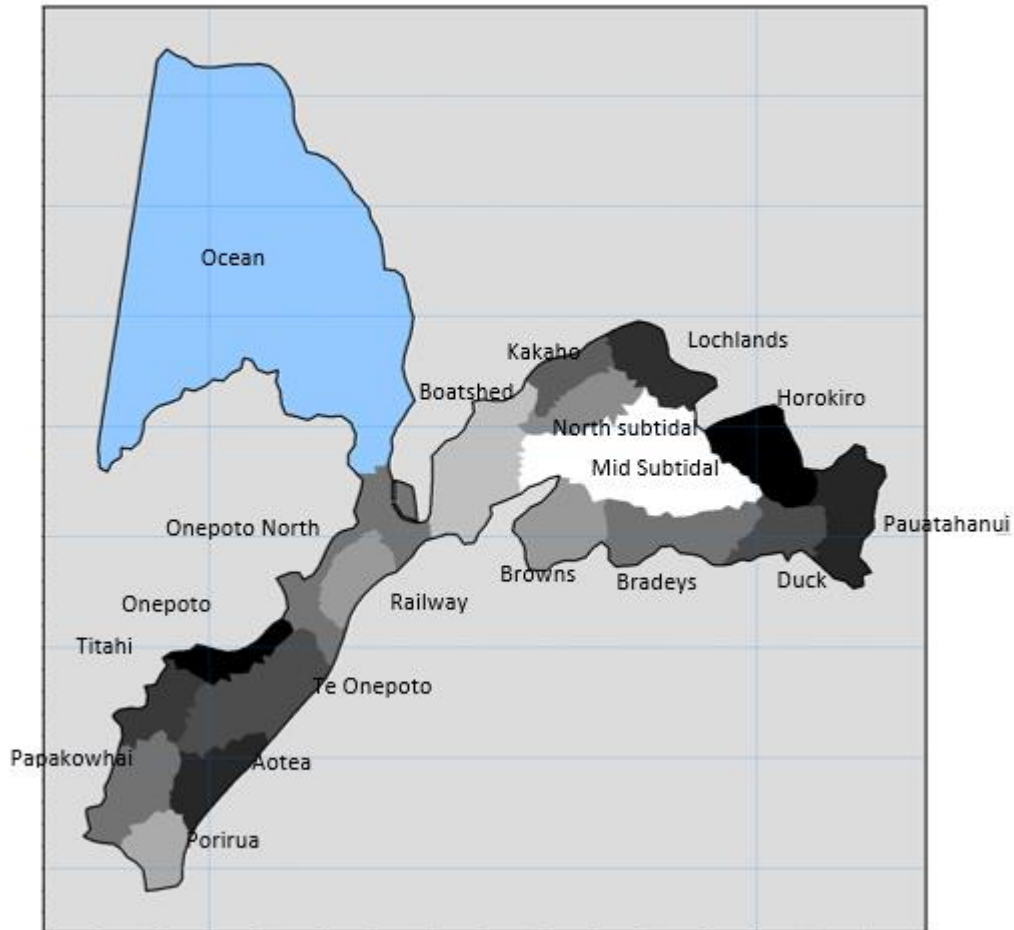
Figure 6-21. Subestuaries of the Onepoto Arm and Pauatahanui Inlet.

Data in Table 6-3 through to Table 6-11 show the predicted spatially averaged bed level change across each of the subestuaries that occur at the end of each of the events and at the end of the 2010 simulation for each of the scenarios considered.

The tables also show the predicted basin-wide average deposition rates in the Onepoto Arm and Pauatahanui Inlet under the three scenarios.

To aid with the interpretation of these results the predicted changes in deposition under the Water Sensitive scenario are presented in Figure 6-22 through to Figure 6-26 for each of the events and the 2010 simulation. The figures show the areas where there has been a reduction of more than 1 mm in deposition due to the Water Sensitive scenario.

The model outputs show that, under the existing land use, there is net erosion for the events and the annual simulation within the Onepoto North, Railway and Boatsheds subestuaries (Table 6-3 and Table 6-4). These are the subestuaries closest to the entrances. This indicates that the net result of the resuspension of sediment in these subestuaries (driven by stronger tidal currents and waves), the input of sediments from elsewhere in the harbour and the export of sediment from the harbour entrance results in an overall loss of sediments within these subestuaries. As discussed above, there are areas of deposition within these subestuaries (e.g. Figure 6-19) but the extent of the areas of erosion and the magnitude of erosion within those areas is such that there is a net loss of sediments.

Data in Table 6-3 and Table 6-4 also shows that there are a number of subestuaries where there is net deposition for all of the events and the annual simulation under the existing land use. These subestuaries can therefore be considered sinks for sediments under a range of different conditions.

These are all of southern subestuaries in the Onepoto Arm except for the Porirua subestuary (which shows net erosion for the 2013 event, discussed below) and Pauatahanui subestuaries to the west of the Pauatahanui Arm along with the two subtidal basins (North and Mid). In addition, the Bradeys Bay and Browns Bay subestuaries show net deposition for all of the events and the annual simulation under the existing land use – but the eastern end of the Bradeys Bay and Browns Bay need to be treated with some caution given the uncertainties around the potential for sub-tidal erosion in these subestuaries.

There are areas of erosion around the fringes of the Browns Bay, Bradeys Bay and Pauatahanui subestuaries (e.g. Figure 6-19) but the extent of the depositional zones and the magnitude of predicted deposition within those areas result in the net gain of sediments.

The response of the other subestuaries (Porirua, Duck Creek, Horokiro, Lochlands and Kakaho) are different for the different events and the 2010 annual simulation. This indicates that there is more of a balance between depositional processes and erosional processes.

For the Porirua subestuary, we see large net deposition for the 2004 event with nearly all of the subestuary showing net deposition at the end of the event (Figure 6-16).

For the other events and the 2010 annual simulation (Figure 6-17 to Figure 6-20), we see areas of net erosion around the fringes of this subestuary which (depending on the extent and level of erosion) leads to either reduced levels of deposition compared to the 2004 event (for the 2005, 2006 events and the 2010 simulation) or net erosion for the 2013 event.

For the Browns Bay subestuary, we see net deposition following the individual events but a small net erosion at the end of the 2010 simulation (Table 6-4). This indicates the importance of the influence of the longer-term erosional processes compared to time scales of the deposition during the events.

For the Duck Creek subestuary, there is net deposition for the 2004, 2005 and 2006 events but for the annual simulation and the 2013 event there is net erosion (Table 6-4).

For the Horokiro subestuary, there is net deposition for the 2004 and 2013 events but for the other events and the 2010 simulation there is net erosion (Table 6-4).

For the Lochlands subestuary, it is only for the 2004 event that we see net deposition across the subestuary (Table 6-4). For all the other simulations the net balance of

sediment delivery and erosion and transport away from the subestuary results in net erosion across this subestuary.

These results indicate that, to achieve a better understanding of the long-term sediments dynamics in the harbour, a range of conditions (i.e. sediment load, sequencing of winds and waves following an event and timing of the event relative to tide range) do need to be modelled. This will provide robust estimates and a good framework for quantifying the potential changes associated with the scenarios being considered.

To provide further understanding of the connectivity of the harbour and the subcatchments, the 2010 model simulation was modified so that the sediment from each of the subcatchments could be tracked separately. This was done by labelling the sediment fractions of the subcatchment of interest separately to the sediment fractions from all the other subcatchments. A separate model run was then completed for each subcatchment allowing the dynamics of the subestuary sediments to be tracked while still modelling the same overall total sediment input to the harbour. Appendix C provides figures showing the estimated deposition footprint for each of the subcatchments. The figures show the area where sediments from each subcatchment are deposited at the end of the 2010 simulation (defining the depositional footprint) and the mass of sediment deposited (kg/m^2) which relates directly back to the relative sediment loads delivered by each subcatchment as detailed in Table 3-3.

Table 6-12 and Table 6-13 show the sediment connectivity matrices for the Onepoto Arm and the Pauatahanui Inlet based on an analysis of the 2010 model simulations.

The matrices show the percentage of the total deposition within each arm of the harbour and the contribution that each catchment outlet makes to the deposition in a given subestuary.

For example, the first **column** of Table 6-12 shows that 22.62% of the total deposition in the Onepoto Arm is derived from sediments arriving from the Porirua Mouth subcatchment and the majority of that sediment is deposited in the Porirua subestuary.

Similarly, the **row** labelled Pauatahanui Mouth in Table 6-12 indicates that 55.75% of the sediment being deposited in the Pauatahanui Inlet is derived from the Pauatahanui Mouth subcatchment. Sediment from this subcatchment is widely dispersed across a number of subestuaries with the majority of that sediment being deposited in the Bradeys Bay, Duck Creek and Pauatahanui Park subestuaries.

These tables provide useful information in terms of where reductions in catchment derived sediments may have a direct benefit in the Onepoto Arm and Pauatahanui Inlet. They also form the basis of developing the metal accumulation model by defining the mass of sediment (and therefore metal) arriving in each subestuary.

Table 6-3.   Predicted change in bed level (mm) in the Onepoto Arm subestuaries for individual events and the 2010 simulation for the Baseline scenario. Highlighted cells show subestuaries where net deposition is predicted to occur.

Simulation	Porirua	Papakowhai	Titahi	Onepoto	Aotea	Te Onepoto	Railway	Onepoto North
2004 event	105.45	13.81	4.32	4.95	19.76	6.13	-3.99	-4.91
2005 event	1.45	0.86	0.32	0.76	3.02	2.24	-3.36	-4.75
2006 event	7.52	9.47	0.97	2.53	19.40	2.49	-3.04	-4.23
2010 annual	2.14	3.72	1.88	2.76	9.64	4.47	-8.13	-6.75
2013 event	-3.44	6.87	0.83	2.02	6.27	2.74	-3.64	-3.47

Table 6-4.   Predicted change in bed level (mm) in the Pauatahanui Inlet subestuaries for individual events and the 2010 simulation for the Baseline scenario. Highlighted cells show subestuaries where net deposition is predicted to occur.

Simulation	Boatsheds	Browns Bay	Bradeys Bay	Duck Creek	Pauatahanui Park	Horokiro	Lochlands	Kakaho	North subtidal	Mid Sub tidal
2004 event	-2.52	4.71	51.63	24.23	17.92	3.37	2.74	3.85	5.54	8.95
2005 event	-2.48	1.50	14.84	4.62	3.27	-2.47	-1.00	0.73	2.35	1.15
2006 event	-2.49	2.46	17.60	3.32	7.38	-0.37	-1.55	-6.05	15.16	7.36
2010 annual	-4.36	-0.04	20.67	-2.39	2.70	-5.67	-5.23	-4.79	22.18	2.47
2013 event	-2.43	1.84	7.89	-7.00	2.60	0.46	-1.19	1.02	7.94	6.48

Table 6-5.   Predicted deposition (mm) in the Onepoto Arm and Pauatahanui Inlet for individual events and the 2010 simulation for the Baseline scenario.

Simulation	Onepoto Arm	Pauatahanui Inlet
2004 event	14.13	11.55
2005 event	0.09	1.99
2006 event	3.93	4.82
2010 annual	0.97	2.40
2013 event	1.19	2.51
Overall Average	4.06	4.66

Table 6-6.	Predicted change in bed level (mm) in the Onepoto Arm subestuaries for individual events and the 2010 simulation for the BAU scenario. Highlighted cells show subestuaries where net deposition is predicted to occur.

Simulation	Porirua	Papakowhai	Titahi	Onepoto	Aotea	Te Onepoto	Railway	Onepoto North
2004 event	58.64	8.62	3.52	4.39	15.38	5.68	-4.01	-4.94
2005 event	1.34	0.89	0.30	0.72	3.18	2.14	-3.38	-4.77
2006 event	0.94	6.55	0.74	2.34	15.10	2.33	-3.07	-4.24
2010 annual	-0.26	3.35	1.85	2.72	8.60	4.39	-8.11	-6.74
2013 event	-5.29	5.77	0.65	1.84	5.41	2.55	-3.70	-3.49

Table 6-7.	Predicted change in bed level (mm) in the Pauatahanui Inlet subestuaries for individual events and the 2010 simulation for the BAU scenario. Highlighted cells show subestuaries where net deposition is predicted to occur.

Simulation	Boatsheds	Browns Bay	Bradeys Bay	Duck Creek	Pauatahanui Park	Horokiro	Lochlands	Kakaho	North subtidal	Mid Sub tidal
2004 event	-2.53	4.64	46.81	22.28	17.85	3.04	2.38	3.70	5.40	8.49
2005 event	-2.52	1.44	14.59	4.99	3.37	-2.45	-1.00	0.70	2.28	1.10
2006 event	-2.52	2.38	16.67	3.09	7.39	-0.59	-1.67	-6.08	14.95	7.02
2010 annual	-4.38	-0.07	20.04	-2.25	2.80	-5.70	-5.27	-4.83	22.06	2.46
2013 event	-2.49	1.75	7.58	-7.16	2.59	0.29	-1.26	0.92	7.82	6.21

Table 6-8.   Predicted deposition (mm) in the Onepoto Arm and Pauatahanui Inlet for individual events and the 2010 simulation for the BAU scenario.

Simulation	Onepoto Arm	Pauatahanui Inlet
2004 event	8.64	10.75
2005 event	0.07	1.97
2006 event	2.41	4.58
2010 annual	0.58	2.34
2013 event	0.69	2.36
Overall Average	2.48	4.40

Table 6-9. Predicted change in bed level (mm/) in the Onepoto Arm subestuaries for individual events and the 2010 simulation for the Water Sensitive Scenario. Highlighted cells show subestuaries where net deposition is predicted to occur.

Simulation	Porirua	Papakowhai	Titahi	Onepoto	Aotea	Te Onepoto	Railway	Onepoto North
2004 event	7.37	1.44	1.50	2.79	6.60	4.19	-4.17	-5.10
2005 event	0.07	0.72	0.26	0.71	2.47	2.12	-3.40	-4.79
2006 event	-5.91	3.05	0.27	1.94	9.63	2.10	-3.22	-4.35
2010 annual	-3.68	2.13	1.56	2.57	5.62	4.23	-8.20	-6.91
2013 event	-8.49	3.92	0.33	1.59	3.61	2.41	-3.76	-3.35

Table 6-10. Predicted change in bed level (mm) in the Pauatahanui Inlet subestuaries for individual events and the 2010 simulation for the Water Sensitive Scenario. Highlighted cells show subestuaries where net deposition is predicted to occur.

Simulation	Boatsheds	Browns Bay	Bradeys Bay	Duck Creek	Pauatahanui Park	Horokiro	Lochlands	Kakaho	North subtidal	Mid Sub tidal
2004 event	-2.70	3.70	31.12	3.71	6.80	-3.51	-2.92	1.11	2.65	3.45
2005 event	-2.52	1.39	13.10	-0.17	1.09	-3.26	-1.34	0.52	2.13	0.78
2006 event	-2.56	2.14	13.94	-4.68	2.00	-3.57	-3.74	-6.40	12.52	3.79
2010 annual	-4.44	-0.21	17.20	-5.49	0.66	-6.49	-5.92	-4.97	21.54	2.05
2013 event	-2.54	1.57	6.35	-10.31	-0.22	-1.76	-1.96	0.74	7.19	4.17

Table 6-11.   Predicted deposition (mm) in the Onepoto Arm and Pauatahanui Inlet for individual events and the 2010 simulation for the Water Sensitive Scenario.

Simulation	Onepoto Arm	Pauatahanui Inlet
2004 event	1.57	4.43
2005 event	-0.16	1.10
2006 event	0.57	1.93
2010 annual	-0.31	1.38
2013 event	-0.11	0.98
Overall Average	0.31	1.96
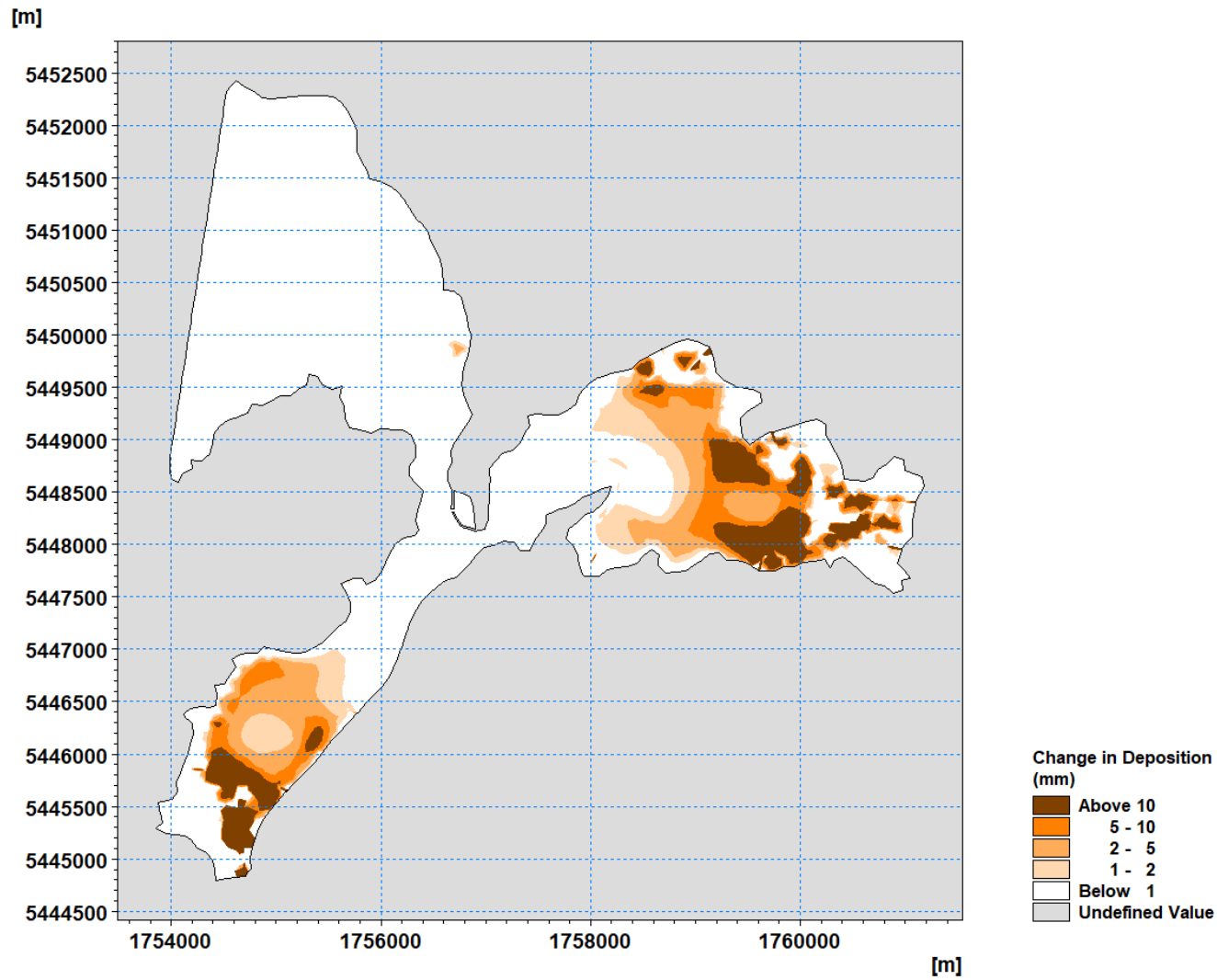
Figure 6-22.   Reduction in predicted deposition rate (mm) due to the Water Sensitive scenario for the 2004 event. Figure shows the change in deposition predicted to occur under the Baseline scenario <u>minus</u> the predicted deposition that occurs under the Water Sensitive scenario.
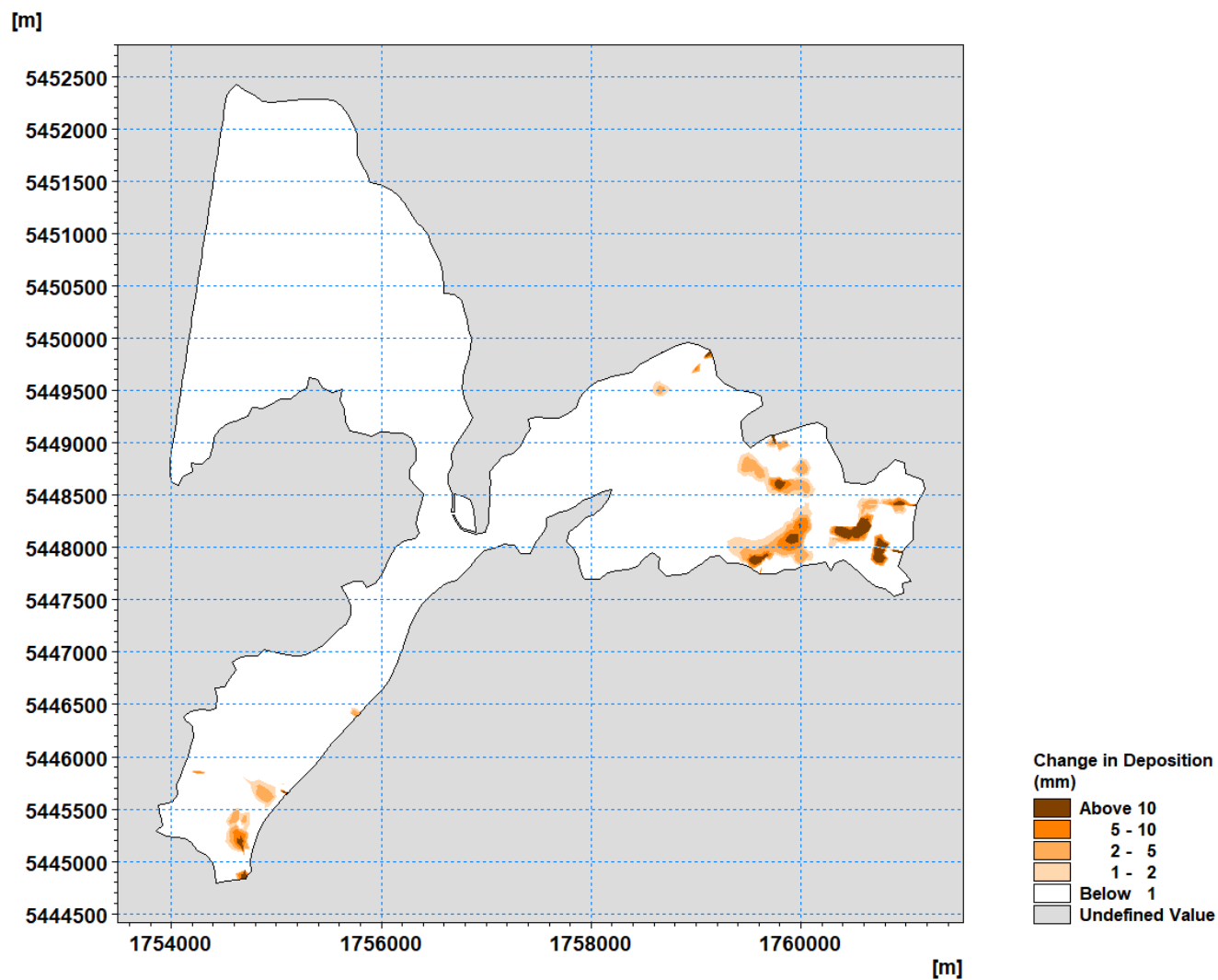
Figure 6-23. Reduction in predicted deposition rate (mm) due to the Water Sensitive scenario for the 2005 event. Figure shows the change in deposition predicted to occur under the Baseline scenario <u>minus</u> the predicted deposition that occurs under the Water Sensitive scenario.
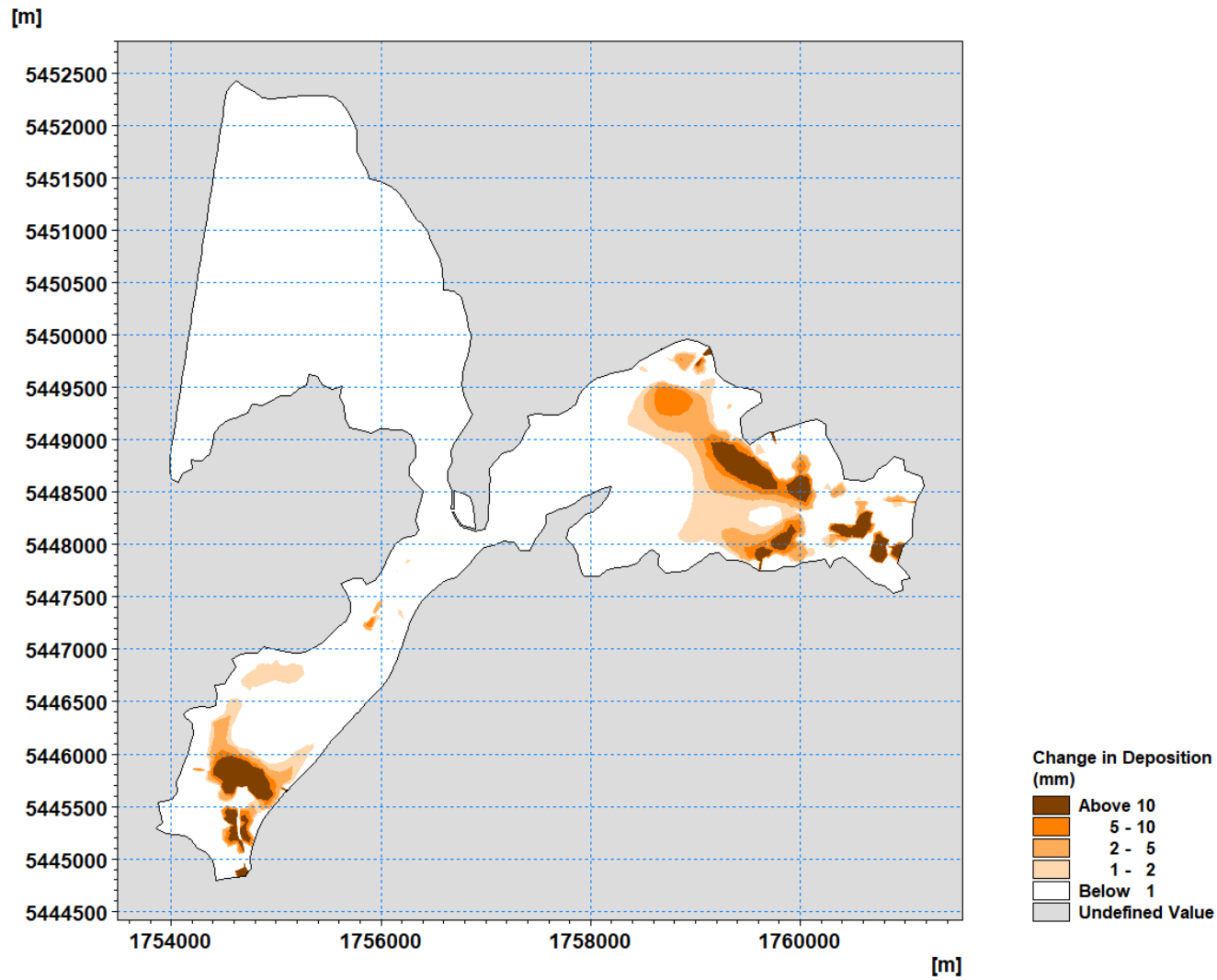
Figure 6-24. Reduction in predicted deposition rate (mm) due to the Water Sensitive scenario for the 2006 event. Figure shows the change in deposition predicted to occur under the Baseline scenario <u>minus</u> the predicted deposition that occurs under the Water Sensitive scenario.
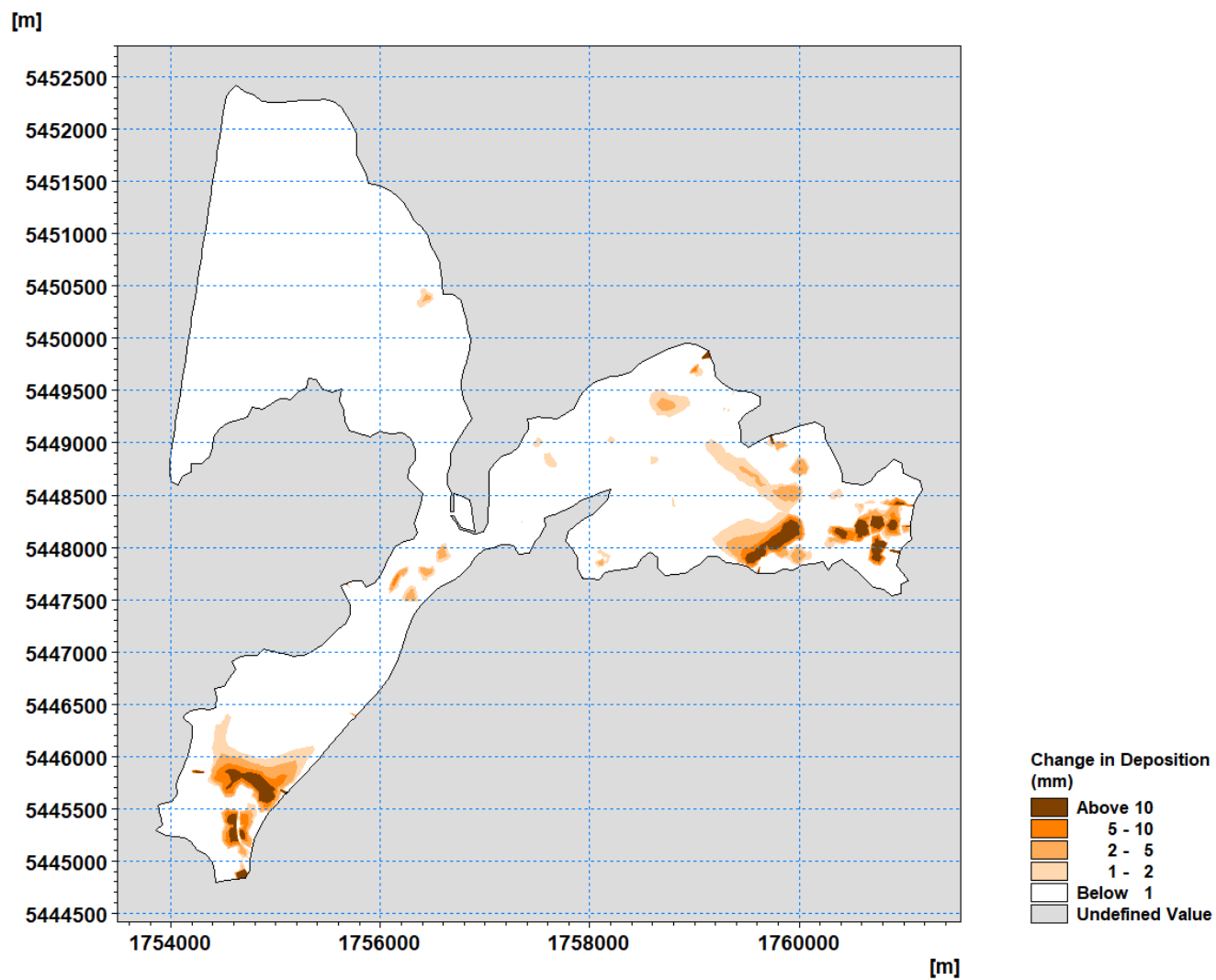
Figure 6-25.   Reduction in predicted deposition rate (mm) due to the Water Sensitive scenario for 2010. Figure shows the change in deposition predicted to occur under the Baseline scenario <u>minus</u> the predicted deposition that occurs under the Water Sensitive scenario.
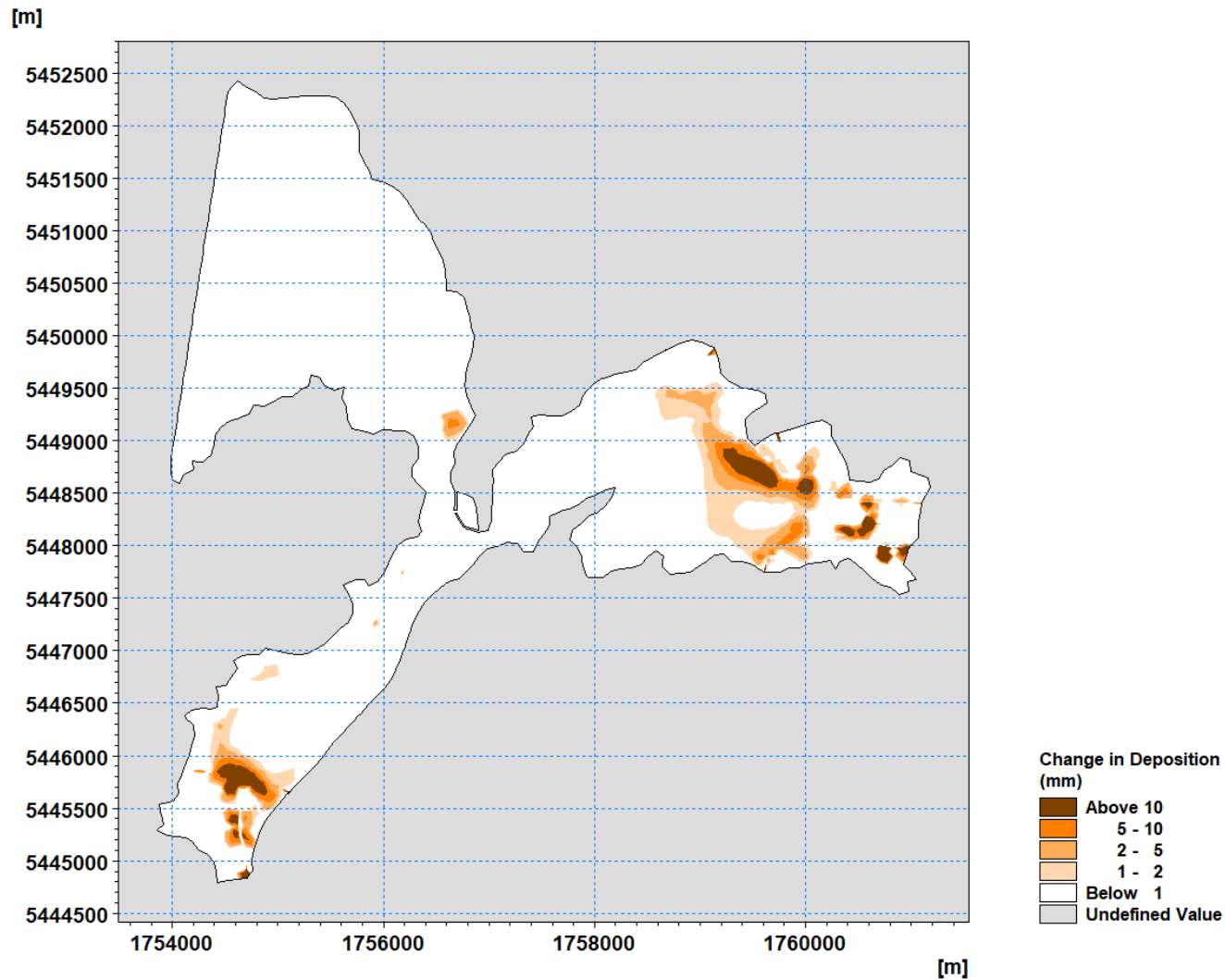
Figure 6-26.   Reduction in predicted deposition rate (mm) due to the Water Sensitive scenario for the 2013 event. Figure shows the change in deposition predicted to occur under the Baseline scenario <u>minus</u> the predicted deposition that occurs under the Water Sensitive scenario.

Table 6-12.   Sediment deposition matrix for the Onepoto Arm. Values are the percentage of the total mass deposited based in all subestuaries within the Onepoto Arm (Figure 6-21).

SUBESTAURY

SUBCATCHMENT	Porirua	Papakowhai	Titahi	Onepoto	Aotea	Te Onepoto	Railway	Onepoto North	% of total deposited
Whitby to Browns Bay	0.000121	0.004617	0.010271	0.006590	0.009055	0.058661	0.013561	0.005221	0.11
Pauatahanui village	0.000010	0.000351	0.000783	0.000477	0.000692	0.004245	0.000861	0.000311	0.01
Lower Duck Creek	0.000395	0.013504	0.028446	0.017657	0.026602	0.153952	0.034851	0.013234	0.29
Horokiri	0.000834	0.027819	0.056424	0.035968	0.056546	0.314363	0.073775	0.028530	0.59
Kakaho	0.000386	0.014985	0.031121	0.019502	0.031575	0.177805	0.045027	0.018263	0.34
Onepoto fringe Elsdon	0.240970	0.205344	0.036445	0.016980	0.353814	0.060519	0.003193	0.001824	0.92
Direct to Onepoto (South)	0.001125	0.019729	0.020660	0.010547	1.446088	0.128027	0.004720	0.002888	1.63
Next to Mahinawa	0.001421	0.139738	0.082057	0.033020	0.047800	0.059189	0.004474	0.002463	0.37
Hukarito	0.000582	0.023233	0.252759	0.045310	0.022586	0.071561	0.006640	0.003821	0.43
Kahetoa (Onepoto Park)	0.000104	0.006157	0.013055	0.080390	0.010695	0.080582	0.009476	0.005178	0.21
Whitireia/Te Onepoto	0.000077	0.003951	0.009521	0.006990	0.008370	0.062731	0.407804	0.004185	0.50
Direct to Onepoto (North)	0.000096	0.005036	0.013018	0.008260	0.012820	0.105619	0.059403	0.021543	0.23
Direct to Onepoto (Mid)	0.000165	0.007591	0.018629	0.011881	0.027613	0.374484	0.010304	0.006637	0.46
Pauatahanui mouth	0.001515	0.048899	0.099238	0.061893	0.096599	0.529193	0.122473	0.047193	1.01
Direct to Pauatahanui (Mid)	0.000003	0.000143	0.000341	0.000221	0.000289	0.002091	0.000531	0.000208	0.00
Motukaraka	0.000003	0.000125	0.000295	0.000181	0.000251	0.001696	0.000403	0.000155	0.00
Direct to Pauatahanui (Water ski club)	0.000004	0.000151	0.000352	0.000222	0.000305	0.002109	0.000509	0.000195	0.00
Direct to Pauatahanui (Boat houses)	0.000003	0.000146	0.000372	0.000232	0.000296	0.002274	0.000594	0.000241	0.00
Porirua Mouth	22.370021	21.586949	3.692487	1.756309	37.074142	5.851213	0.314505	0.177747	92.82
Ration	0.000101	0.003446	0.007389	0.004634	0.006753	0.040130	0.009271	0.003678	0.08
% of total deposited	22.62	22.11	4.37	2.12	39.23	8.08	1.12	0.34	100.00

Table 6-13. Sediment deposition matrix for the Pauatahanui Inlet. Values are the percentage of the total mass deposited based in all subestuaries within the Pauatahanui Inlet (Figure 6-21).

SUBESTAURY

SUBCATCHMENT	Boatsheds	Browns Bay	Bradeys Bay	Duck Creek	Pauatahanui Park	Horokiro	Lochlands	Kakaho	North subtidal	Mid Sub tidal	% of total deposited
Whitby to Browns Bay	0.011253	0.409904	0.138195	0.001429	0.000110	0.001178	0.002457	0.006753	0.046279	0.160495	0.78
Pauatahanui village	0.001562	0.002683	0.052574	0.030361	0.001447	0.002126	0.001239	0.001835	0.009981	0.041611	0.15
Lower Duck Creek	0.058123	0.124722	8.162106	0.317796	0.003689	0.057382	0.039307	0.060127	0.389719	1.776899	10.99
Horokiri	0.155484	0.235604	12.133049	0.547314	0.030414	2.264918	0.148997	0.162420	1.086043	4.502552	21.27
Kakaho	0.117818	0.117681	0.821439	0.066523	0.004117	0.056100	1.409151	0.200346	1.222743	1.788654	5.80
Onepoto fringe Elsdon	0.000603	0.002246	0.002125	0.000033	0.000004	0.000025	0.000057	0.000256	0.001920	0.004428	0.01
Direct to Onepoto (South)	0.000628	0.002233	0.002179	0.000034	0.000004	0.000026	0.000059	0.000260	0.001901	0.004459	0.01
Next to Mahinawa	0.000866	0.003186	0.003026	0.000043	0.000003	0.000031	0.000073	0.000339	0.002559	0.006230	0.02
Hukarito	0.001228	0.004329	0.004111	0.000057	0.000003	0.000039	0.000090	0.000436	0.003381	0.008358	0.02
Kahetoa (Onepoto Park)	0.001672	0.005992	0.005638	0.000075	0.000005	0.000055	0.000127	0.000566	0.004391	0.011265	0.03
Whitireia/Te Onepoto	0.001665	0.006320	0.005891	0.000075	0.000006	0.000057	0.000136	0.000619	0.004703	0.011840	0.03
Direct to Onepoto (North)	0.001485	0.005277	0.004863	0.000062	0.000005	0.000049	0.000117	0.000516	0.003905	0.009890	0.03
Direct to Onepoto (Mid)	0.001123	0.004181	0.003988	0.000052	0.000004	0.000041	0.000102	0.000460	0.003372	0.008119	0.02
Pauatahanui mouth	0.226951	0.409004	17.594776	16.431179	11.959667	0.324091	0.163061	0.229161	1.463165	6.945020	55.75
Direct to Pauatahanui (Mid)	0.002307	0.001003	0.001605	0.000046	0.000005	0.000039	0.000143	0.011322	0.002661	0.003567	0.02
Motukaraka	0.000917	0.001011	0.005474	0.000305	0.000030	0.000329	0.018859	0.001095	0.006415	0.011793	0.05
Direct to Pauatahanui (Water ski club)	0.001504	0.001124	0.004286	0.000252	0.000026	0.000227	0.001725	0.003121	0.007490	0.009521	0.03
Direct to Pauatahanui (Boat houses)	0.003214	0.000849	0.000882	0.000011	0.000001	0.000009	0.000035	0.000246	0.001138	0.001974	0.01
Porirua Mouth	0.057456	0.214857	0.207237	0.003263	0.000319	0.002464	0.005689	0.024870	0.184815	0.428077	1.13
Ration	0.017117	0.029692	1.074426	0.086170	1.983882	0.040942	0.011016	0.016861	0.107709	0.495227	3.86
% of total deposited	0.66	1.58	40.23	17.49	13.98	2.75	1.80	0.72	4.55	16.23	100.00

6.2.4 Predicted Change in Sediment Texture

Table 6-14 and Table 6-15 show the predicted percentage of cohesive sediments within each of the subestuary under Baseline conditions for the Onepoto Arm and Pauatahanui Inlet respectively.

Table 6-16 and Table 6-17 show the percentage change (compared to the the Baseline predictions) in the predicted mass of cohesive sediment in each of the subestuaries. This data gives an indication of the reduction in muddiness that could be expected within subestuaries under the alternative scenarios. As discussed above, the major change in the Onepoto Arm relates to change in deposition rates in the Porirua subestuary (driven by the big reduction in sediment loads from the Porirua Mouth subcatchment). This is reflected in the big reduction in the predicted mass of cohesive sediments seen in this subestuary under both alternative scenarios driven by the reductions in deposition rates (e.g. Table 6-5 and Table 6-11).

Within the Pauatahanui Arm, the largest reductions in muddiness are seen in the fringing subestuaries - Bradeys Bay, Duck Creek, Pauatahanui Park, Horokiro and Lochlands. These are the areas of the harbour where the largest differences in deposition occur between the scenarios.

6.2.5 Suspended Sediment Concentrations

Finally, model outputs from the 2010 simulations have been used to look at the mean suspended sediment concentrations under the Baseline and Water Sensitive Scenarios.

Figures 6-27 and 6-28 show the 50th percentile suspended sediment concentrations over the 2010 model simulation for the Baseline and Water Sensitive Scenario and Figure 6-29 shows the reduction in the 50th percentile suspended sediment concentrations that is predicted to occur in Water Sensitive Scenario.

Figures 6-30 and 6-31 show the 90th percentile suspended sediment concentrations over the 2010 model simulation for the Baseline and Water Sensitive Scenario and Figure 6-32 shows the reduction in the 90th percentile suspended sediment concentrations that is predicted to occur in Water Sensitive Scenario.

The largest changes in suspended sediment concentrations occur closest to the catchment sources associated with the largest catchment sediment loads. Further from the catchment outlets, the reductions in suspended sediment concentrations are much smaller as these reflect the reworking of existing sediment rather than the delivery of new sediment from the catchment.

Table 6-14. Predicted percentage of cohesive sediments in Onepoto Arm subestuaries for the Baseline scenarios based on outputs from the 2010 simulations.

Simulation	Porirua	Papakowhai	Titahi	Onepoto	Aotea	Te Onepoto	Onepoto North	Railway
BAU	79.4%	79.3%	81.6%	81.9%	68.3%	81.0%	60.7%	39.4%

Table 6-15. Predicted percentage of cohesive sediments in Pauatahanui Inlet subestuaries for the Baseline scenarios based on outputs from the 2010 simulations.

Simulation	Boatsheds	Browns Bay	Bradeys Bay	Duck Creek	Pauatahanui Park	Horokiro	Lochlands	Kakaho	North subtidal	Mid Sub tidal
BAU	44.4%	79.4%	79.3%	30.7%	79.8%	31.3%	37.2%	65.2%	82.3%	74.6%

Table 6-16. Predicted change in mass of cohesive sediments (as percentage of Baseline mass) in Onepoto Arm subestuaries based on outputs from the 2010 simulations. Positive values indicate a reduction in the percentage of cohesive sediments in the subestuary.

Simulation	Porirua	Papakowhai	Titahi	Onepoto	Aotea	Te Onepoto	Onepoto North	Railway
BAU	21%	4%	1%	1%	6%	1%	1%	1%
Water Sensitive Scenario	29%	13%	4%	2%	19%	2%	1%	0%

Table 6-17. Predicted change in mass of cohesive sediments (as percentage of Baseline mass) in Pauatahanui Inlet subestuaries based on outputs from the 2010 simulations. Positive values indicate a reduction in the percentage of cohesive sediments in the subestuary.

Simulation	Boatsheds	Browns Bay	Bradeys Bay	Duck Creek	Pauatahanui Park	Horokiro	Lochlands	Kakaho	North subtidal	Mid Sub tidal
BAU	1%	1%	2%	-1%	-1%	1%	1%	0%	0%	0%
Water Sensitive Scenario	1%	1%	10%	21%	14%	11%	13%	1%	2%	4%
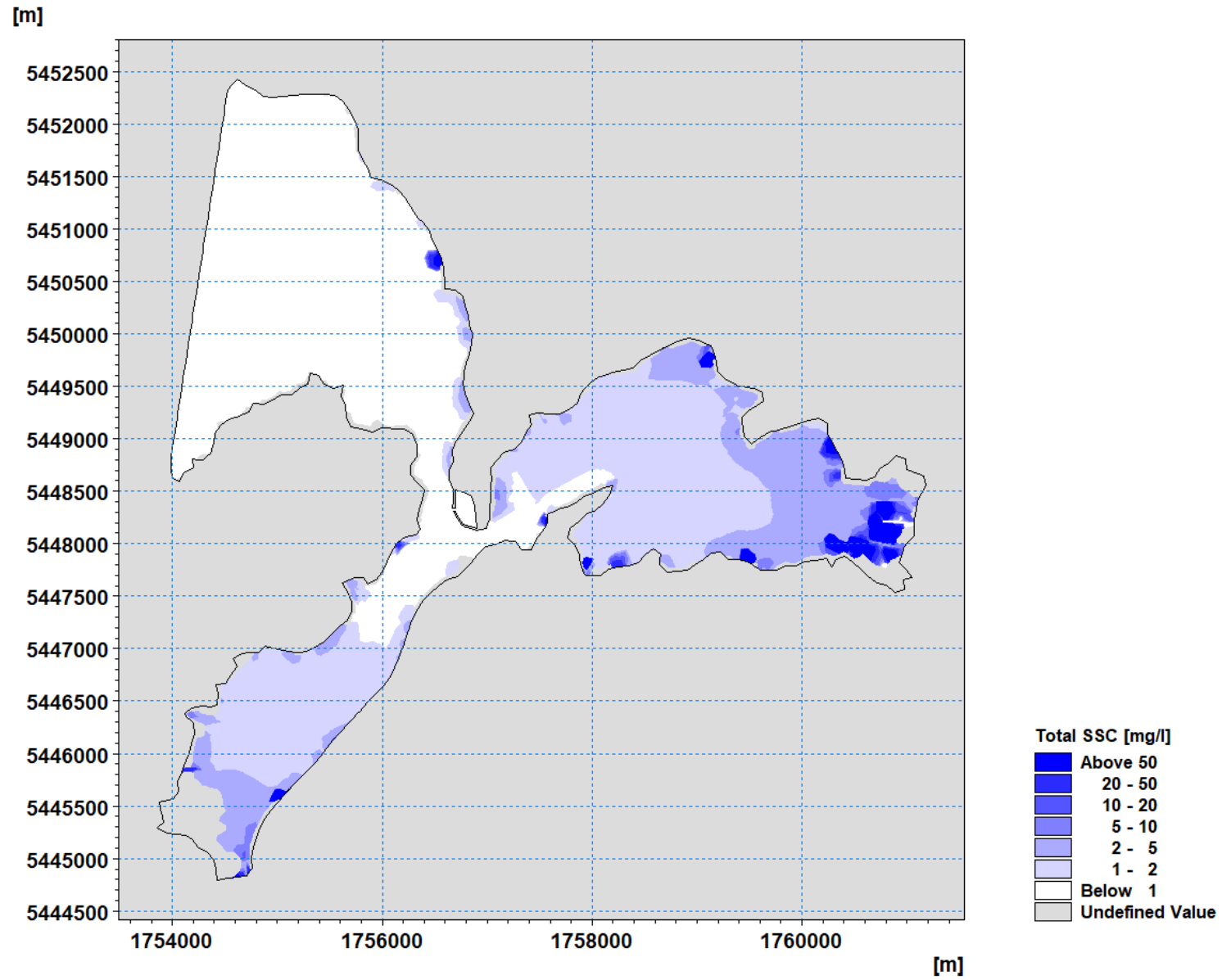
Figure 6-27.   Baseline - 50th percentile suspended sediment concentration.
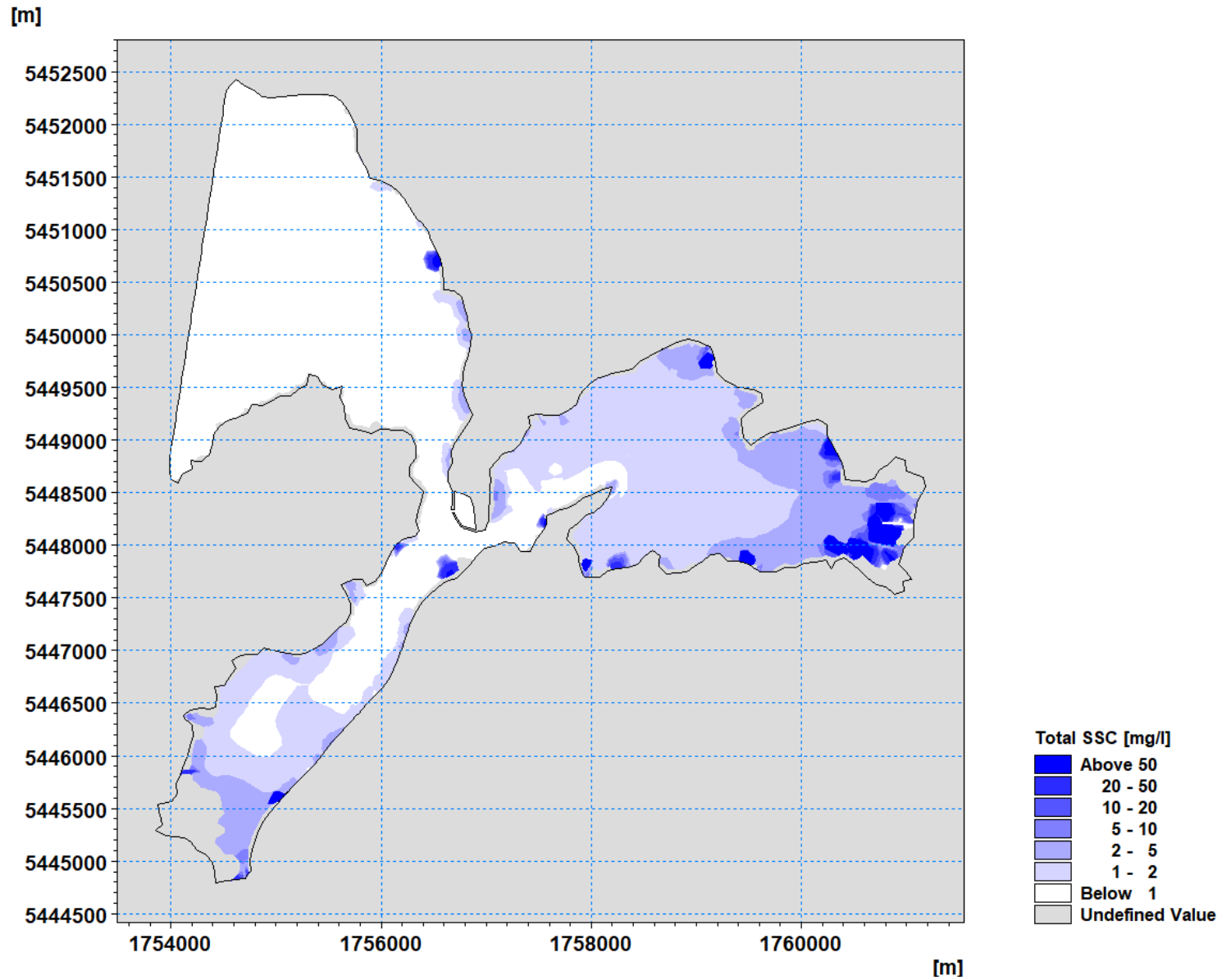
Figure 6-28.   Water Sensitive Scenario - 50th percentile suspended sediment concentration.
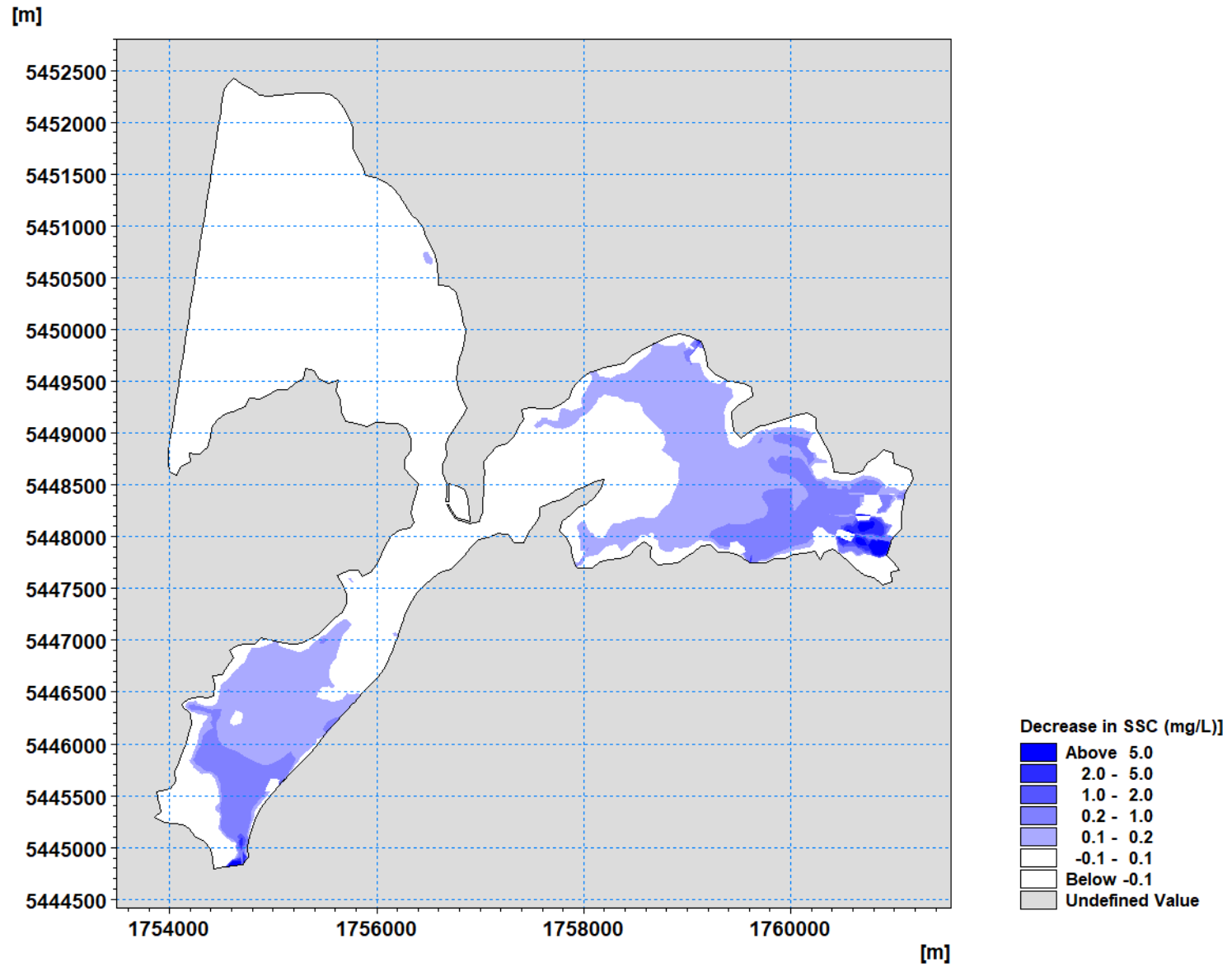
Figure 6-29. Reduction in 50th percentile suspended sediment concentration under the Water Sensitive Scenario.
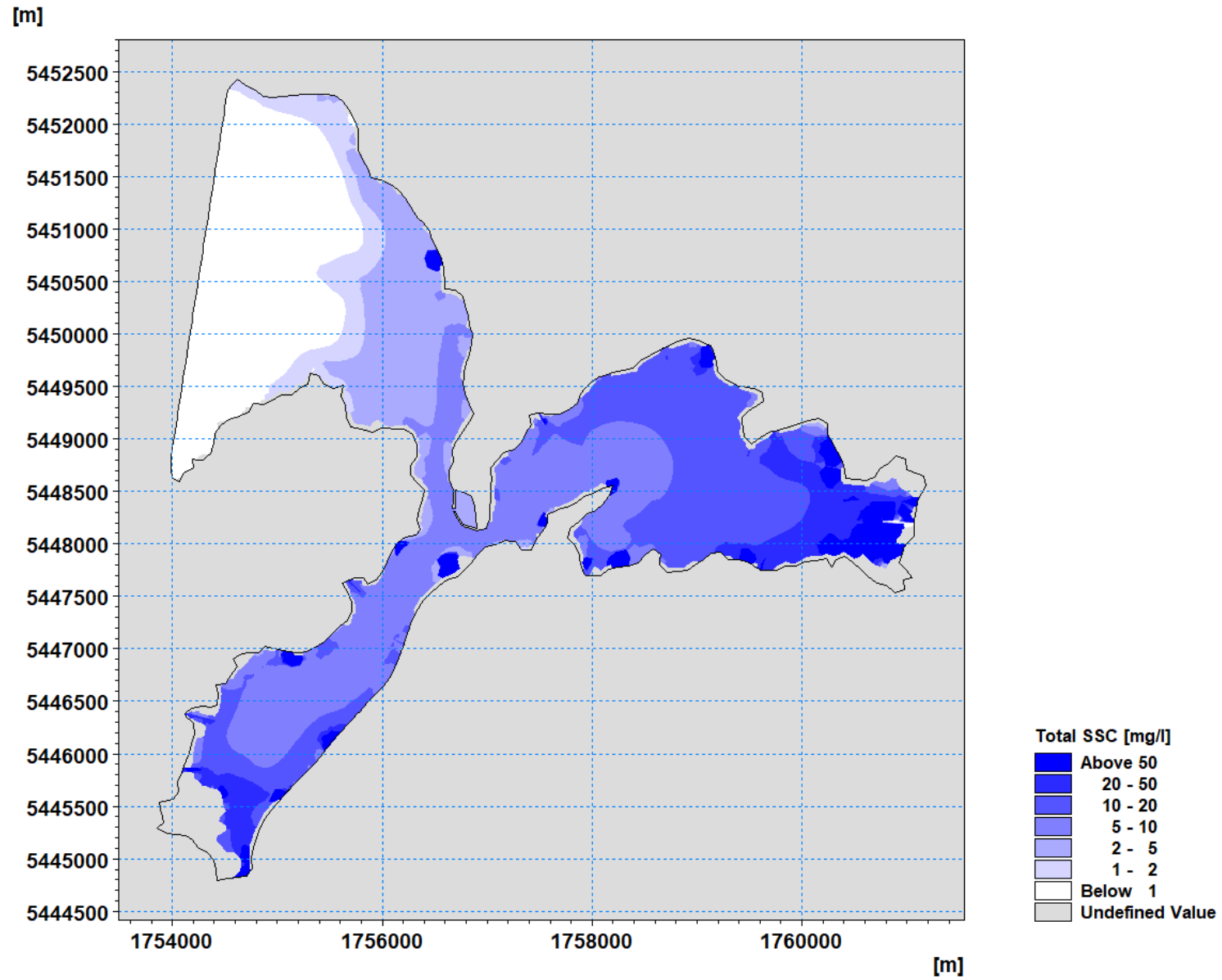
Figure 6-30. Baseline 90th percentile suspended sediment concentration.
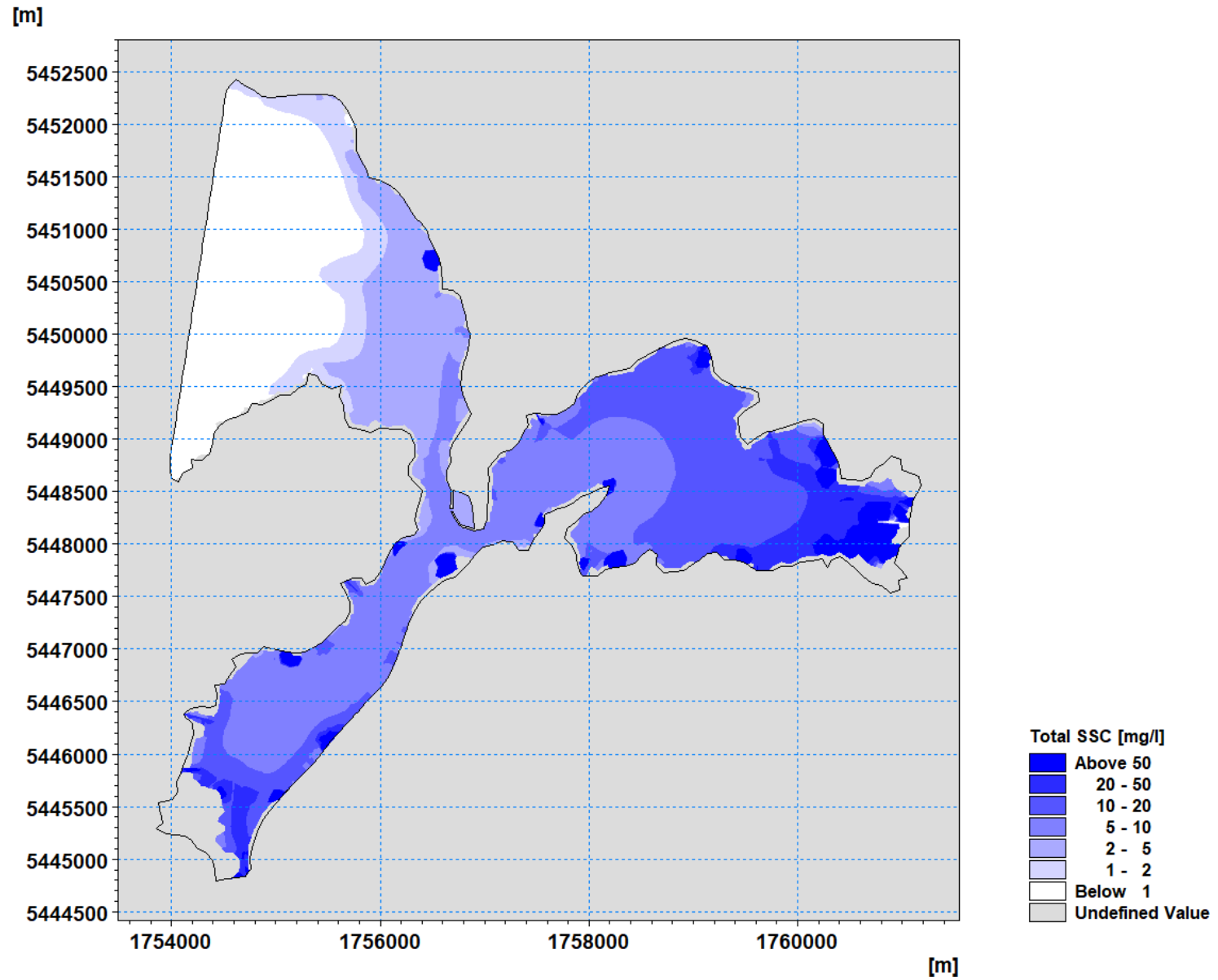
Figure 6-31.   Water Sensitive Scenario - 90th percentile suspended sediment concentration.
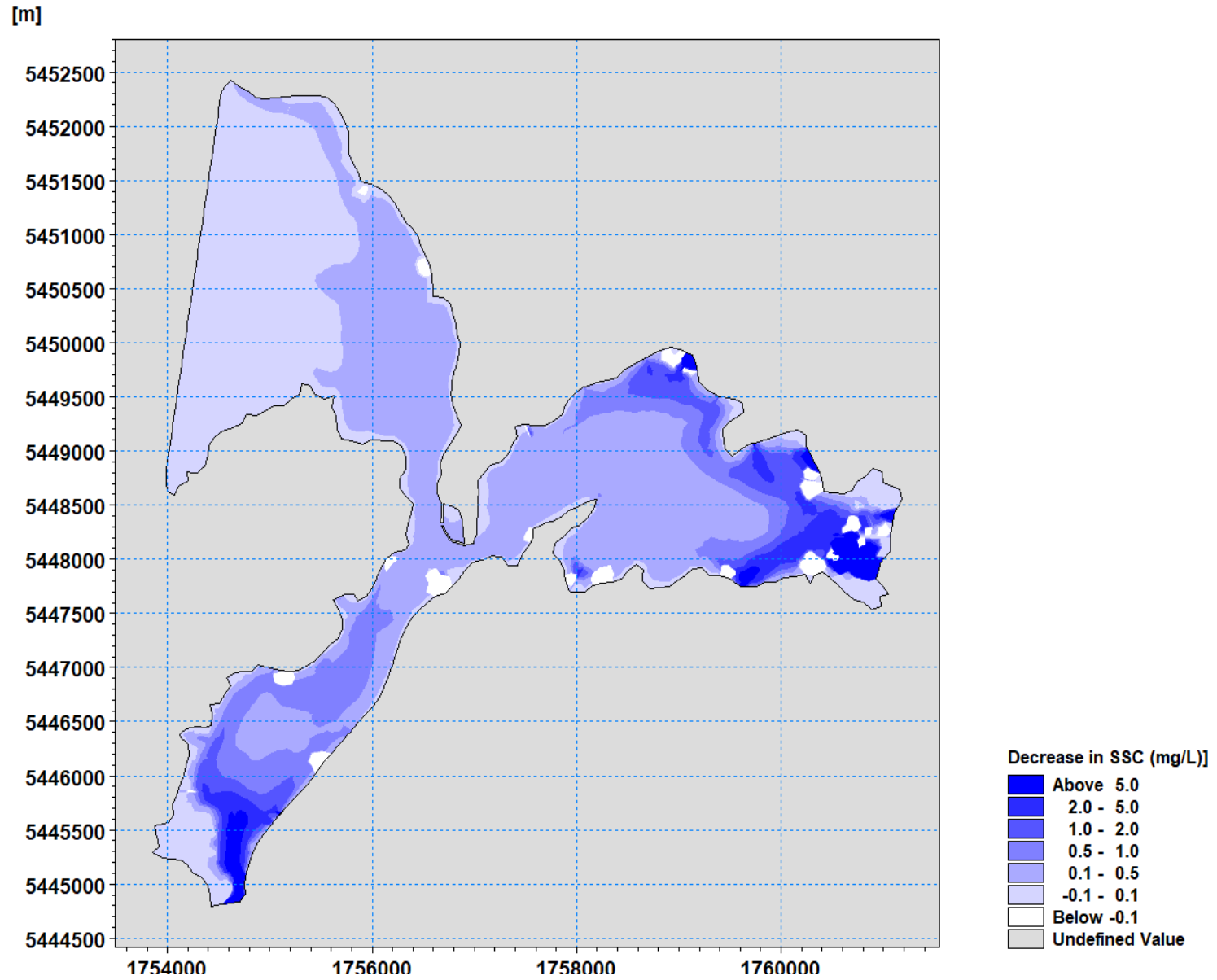
Figure 6-32.   Reduction in 90th percentile suspended sediment concentration under the Water Sensitive Scenario.

6.3 Nutrients

Outputs from the 2010 model simulation have been post-processed to provide the spatial distribution of the predicted 50th percentile concentrations across the whole model domain.

Figures 6-33 to 6-36 show the depth-averaged 50th percentile Total Phosphorous and Total Nitrogen concentrations (mg/l) for the Baseline and Water Sensitive Scenario.

The results show that that highest concentrations occur near the catchment outlets and it is in these areas where any discernible decrease in nutrients are predicted to occur.
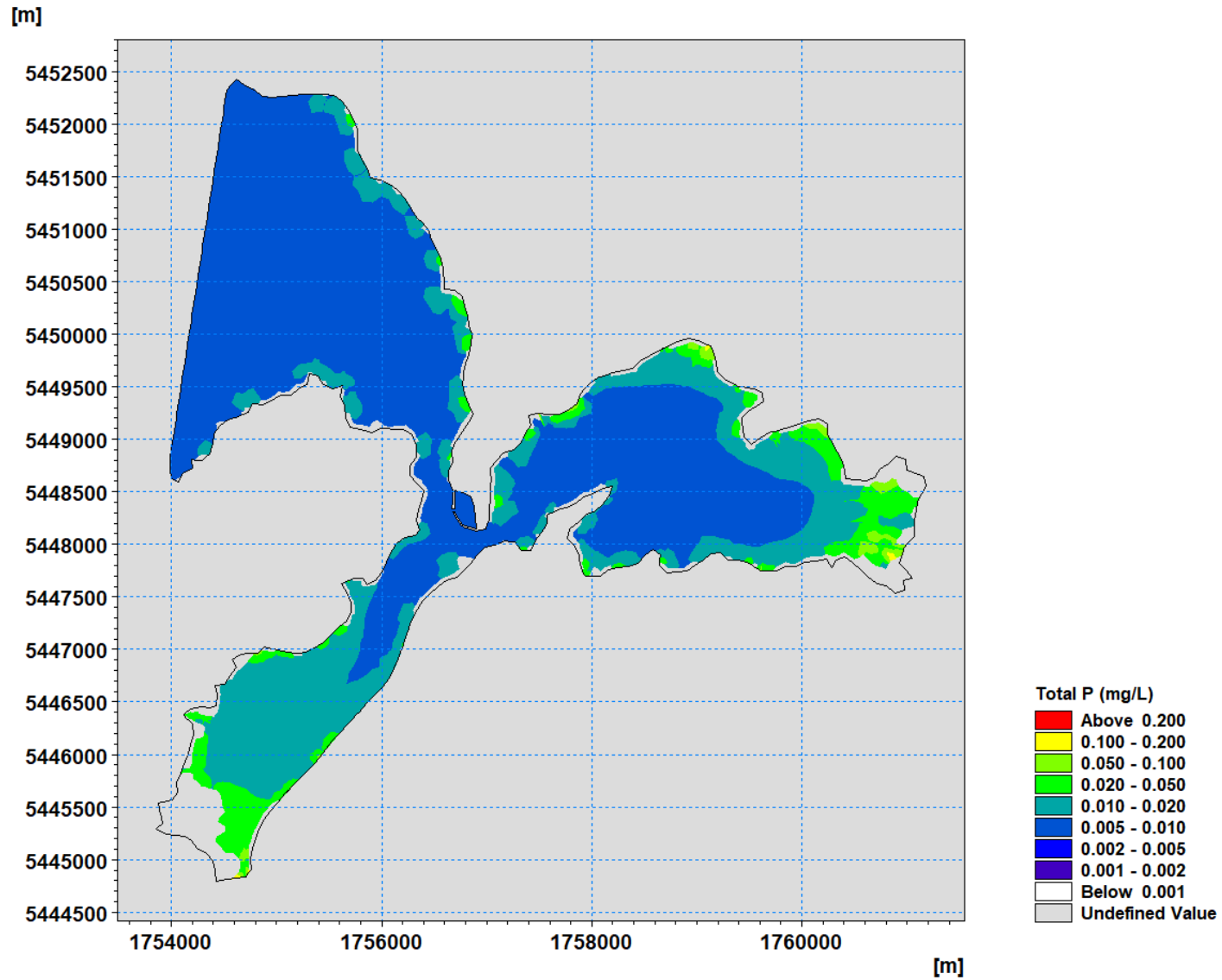
Figure 6-33.   Predicted 50th percentile Total Phosphorous for the baseline scenario.
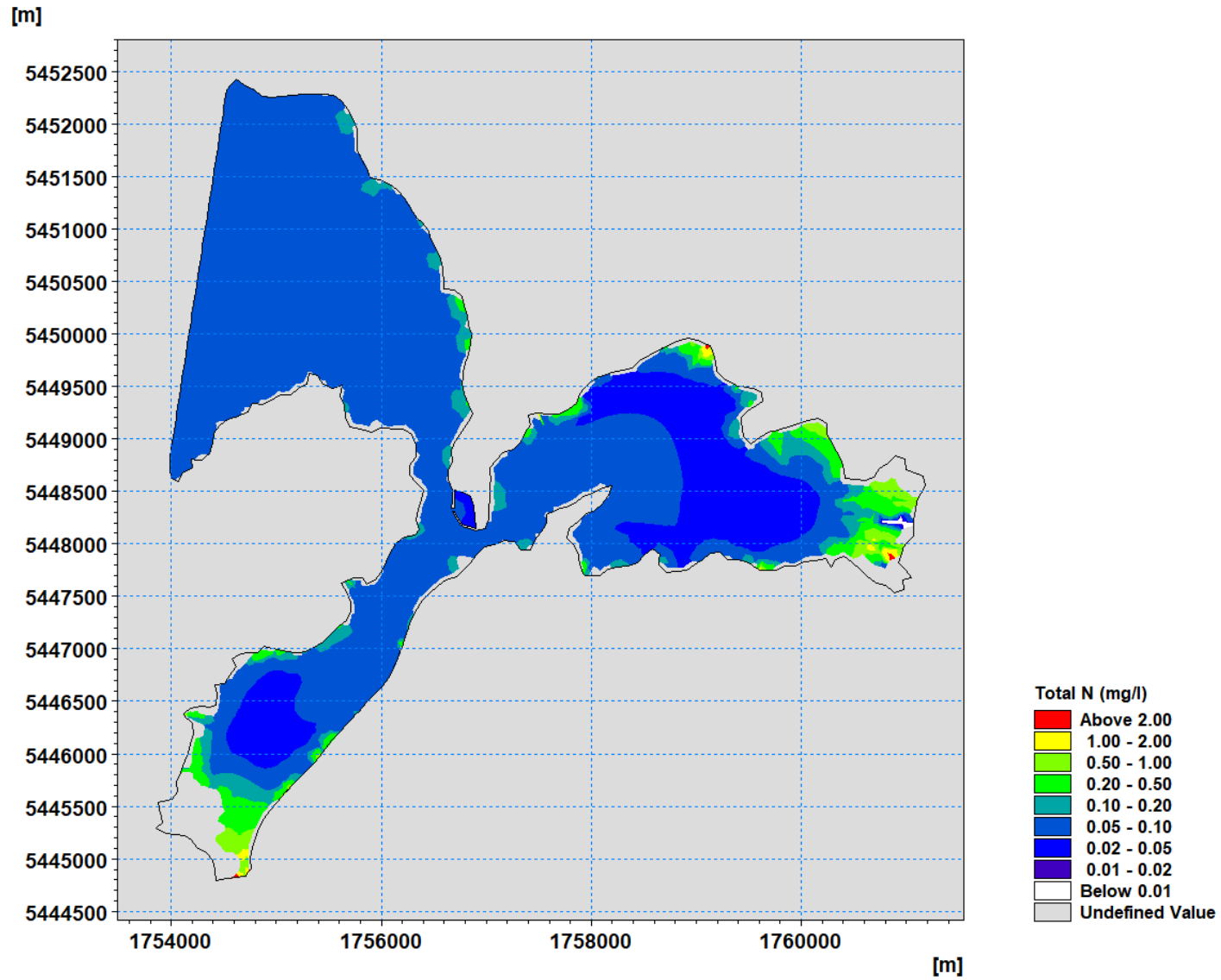
Figure 6-34. Predicted 50th percentile Total Nitrogen for the baseline scenario.
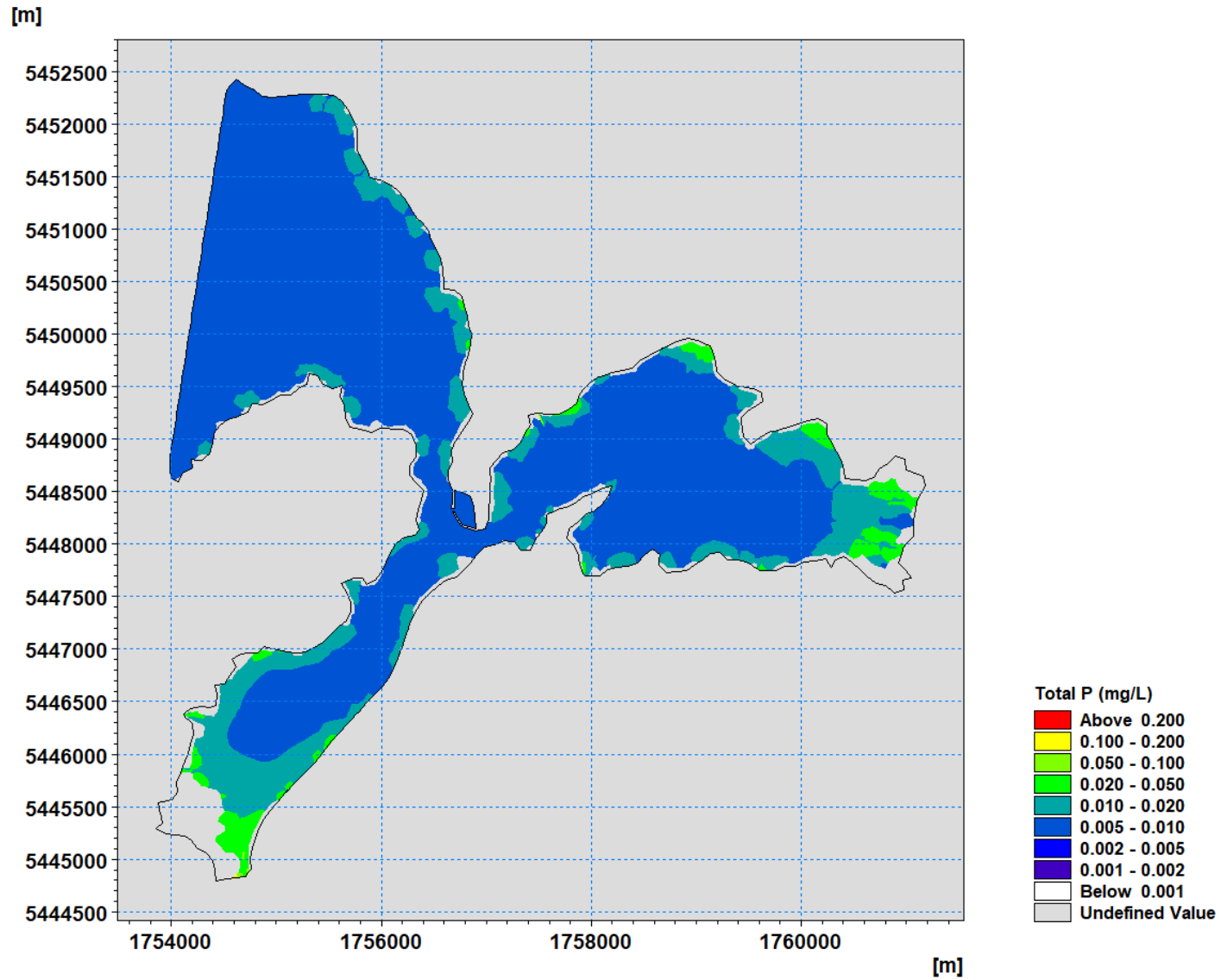
Figure 6-35.   Predicted 50th percentile Total Phosphorous for the Water Sensitive Scenario.
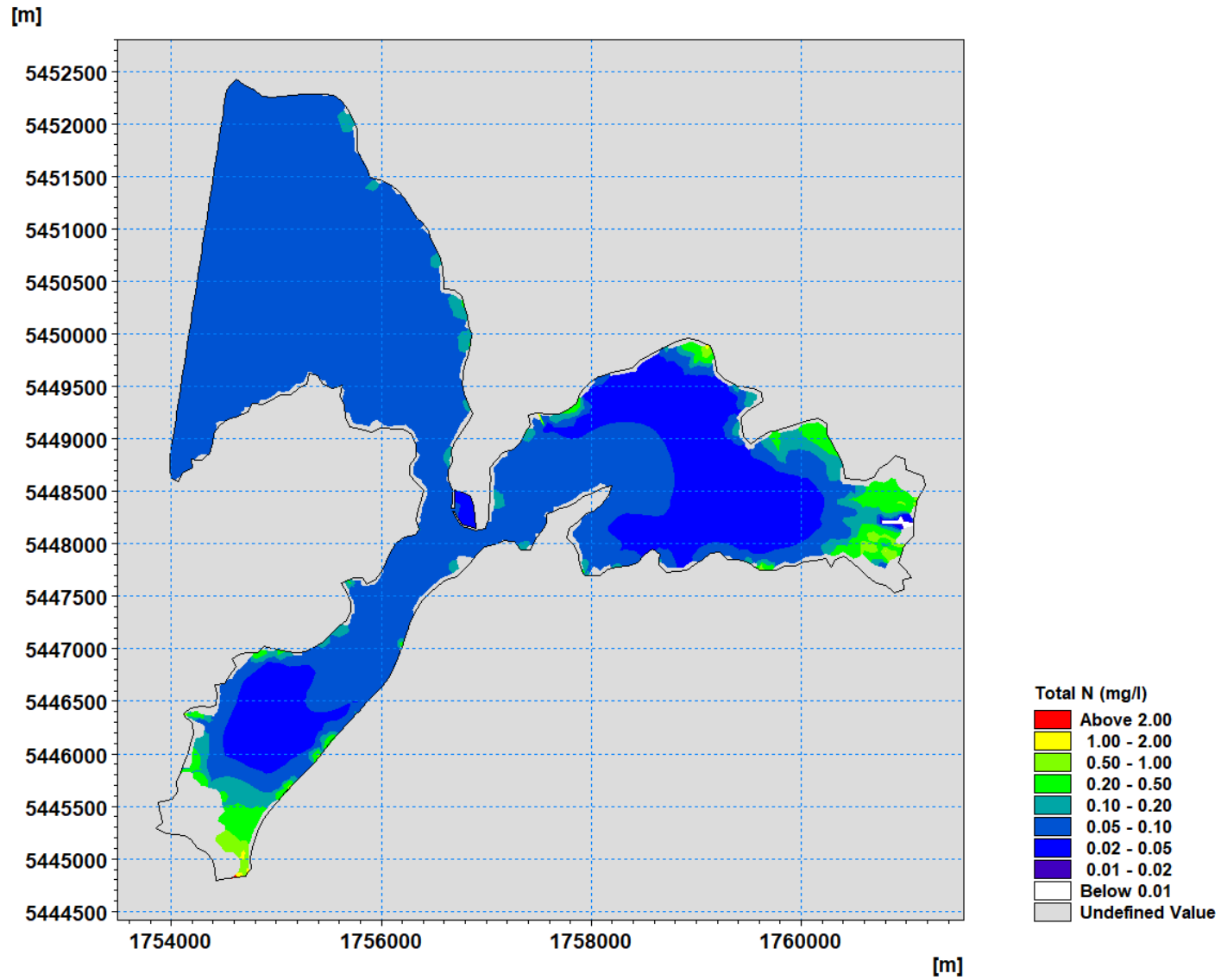
Figure 6-36. Predicted 50th percentile Total Nitrogen for the Water Sensitive Scenario.

6.4 Pathogens

Model results from the 2010 model simulation of *Enterococci* have been extracted at key sites within the harbour (Figure 6-37).
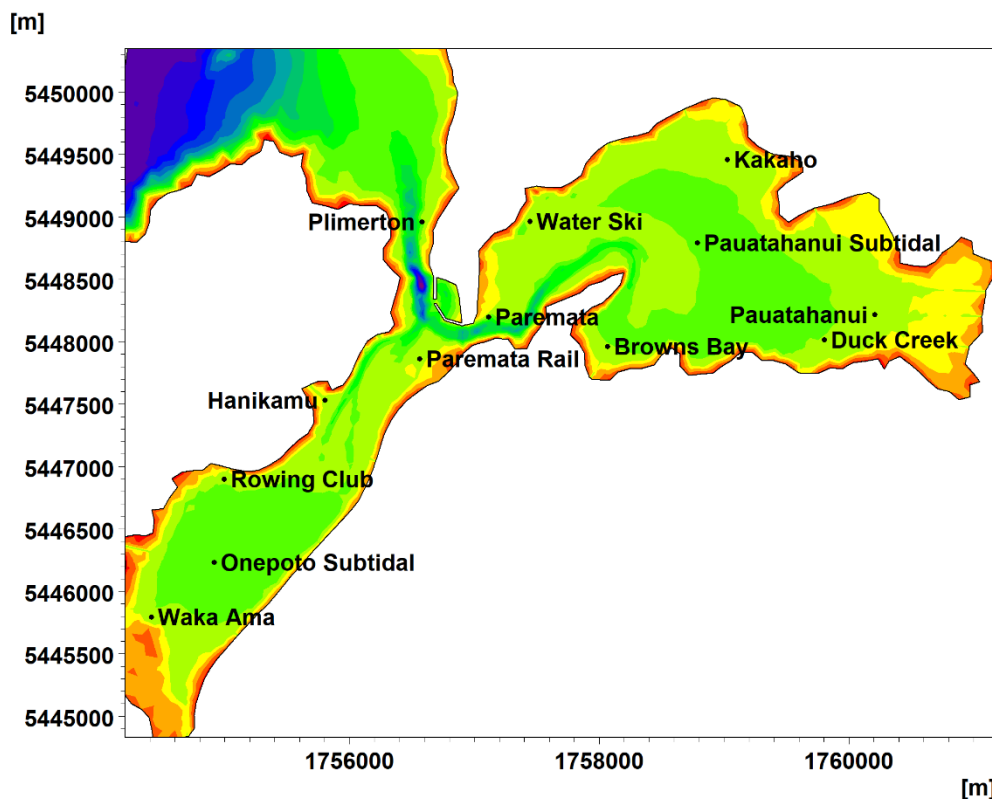
Figure 6-37.   Sites where *Enterococci* predictions have been extracted from the 2010 simulation.

The attribute state and criteria set out in Table 6-18 have been used for the assessment of *Enterococci* concentrations at the key sites. For an attribute state to be achieved, all four criteria must be met.

Table 6-19 shows the model predictions at each of the sites for the attribute criteria and the overall attribute state for each of the Scenarios. For all but the Waka Ama site there is an improvement in the attribute state which is driven mostly by the 95th percentile criteria. This criteria is the one used for assessing water quality for recreational waters (Ministry for the Environment, 2002) to derive a Microbiological Assessment Category grade based on long-term monitoring data – typically spanning a number of years and more than 100 samples.

Figures 6-38 to 6-50 show the distribution of predicted *Enterococci* at each of the sites for each scenario and Figures 6-51 to 6-53 show spatial plots of the 95th percentile concentration for the Baseline, BAU and Water Sensitive Scenario respectively.

Table 6-18.   Attribute State description and attribute state criteria.

Description of Attribute State	Percentage of exceedances over 500 *Enterococci* per 100 ml	Median: *Enterococci* per 100 ml	95th percentile: *Enterococci* per 100 ml	Percentage of samples above 140 per 100 ml	Attribute State
For at least half the time, the estimated Gastro Intestinal risk is <1% and Acute Febrile Respiratory Infection risk is <0.3% The estimated Gastro Intestinal risk is >10% and Acute Febrile Respiratory Infection risk is >4% less than 5% of the time	<5%	<=40	<=40	<20%	Excellent (Blue)
For at least half the time, the estimated Gastro Intestinal risk is <1% and Acute Febrile Respiratory Infection risk is <0.3% The estimated Gastro Intestinal risk is >10% and AFRI risk is >4% between 5 and 10% of the time	5-10%		<=200	20-30%	Good (Green)
For at least half the time, the estimated Gastro Intestinal risk is <1% and Acute Febrile Respiratory Infection risk is <0.3% The estimated Gastro Intestinal risk is >10% and AFRI risk is >4% between 10 and 20% of the time	10-20%		<=500	20-34%	Fair (Yellow)
For at least half the time, the estimated Gastro Intestinal risk is >1% and Acute Febrile Respiratory Infection risk is >0.3%. The estimated Gastro Intestinal risk is >10% and Acute Febrile Respiratory Infection risk is >4% more than 20% of the time	>20%	>40	>500	>34%	Poor (Red)

Table 6-19. Attribute state criteria at each of the key sites.

Location	Scenario	Percentage of exceedances over 500 *Enterococci* per 100 ml	Median: *Enterococci* per 100 ml	95th percentile: *Enterococci* per 100 ml	Percentage of samples above 140 per 100 ml	Attribute State
Waka Ama	Baseline	19.51	33.15	2148.83	33.72	Poor
	BAU	19.38	34.68	2058.34	33.98	Poor
	Water Sensitive	7.18	6.82	679.38	18.62	Poor
Rowing Club	Baseline	12.8	24.28	1372.1	27.12	Poor
	BAU	12.46	24.04	1337.81	26.81	Poor
	Water Sensitive	3.77	3.92	330.8	10.3	Fair
Paremata	Baseline	0.28	0.72	80.44	2.94	Good
	BAU	0.1	0.73	68.75	2.48	Good
	Water Sensitive	0	0.13	22.5	0.55	Excellent
Water Ski	Baseline	1.89	1.69	211.66	7.74	Fair
	BAU	1.45	1.65	180.54	6.7	Good
	Water Sensitive	0.06	0.32	57.62	2.09	Good
Browns Bay	Baseline	1.4	2.16	152.32	5.32	Good
	BAU	1.39	2.11	144.77	5.13	Good
	Water Sensitive	0.02	0.37	36.04	1.07	Excellent
Kakaho	Baseline	5.84	3.61	571.13	16.07	Poor
	BAU	4.65	3.33	461.15	14.06	Fair
	Water Sensitive	0.73	0.89	144.46	5.14	Good
Duck Creek	Baseline	10.57	8.54	910.72	24.49	Poor
	BAU	7.63	8.05	684.77	22.08	Poor
	Water Sensitive	1.88	1.82	225.66	9.23	Fair
Plimmerton	Baseline	0.23	0.58	60.98	2.12	Good
	BAU	0.09	0.6	54.24	1.94	Good

Location	Scenario	Percentage of exceedances over 500 *Enterococci* per 100 ml	Median: *Enterococci* per 100 ml	95th percentile: *Enterococci* per 100 ml	Percentage of samples above 140 per 100 ml	Attribute State
	Water Sensitive	0	0.09	15.75	0.6	Excellent
Paremata Rail	Baseline	0.63	0.91	82.41	3.04	Good
	BAU	0.55	0.91	77.47	2.88	Good
	Water Sensitive	0.11	0.15	21.54	1.44	Excellent
Onepoto Subtidal	Baseline	0.67	1.35	90.51	3.66	Good
	BAU	0.67	1.35	85.95	3.49	Good
	Water Sensitive	0.12	0.24	23.38	1.59	Excellent
Pauatahanui Subtidal	Baseline	0.17	0.78	77.12	2.73	Good
	BAU	0.05	0.75	62.04	2.05	Good
	Water Sensitive	0	0.16	19.93	0.2	Excellent
Hanikamu	Baseline	1.79	1.74	206.55	7.1	Fair
	BAU	1.44	1.66	169.8	6.03	Good
	Water Sensitive	0.73	0.28	47.68	2.5	Excellent
Pauatahanui	Baseline	14.22	10.36	1420.79	26.57	Poor
	BAU	11.11	9.97	1027.33	24.12	Poor
	Water Sensitive	2.59	2.28	360.82	13.37	Fair
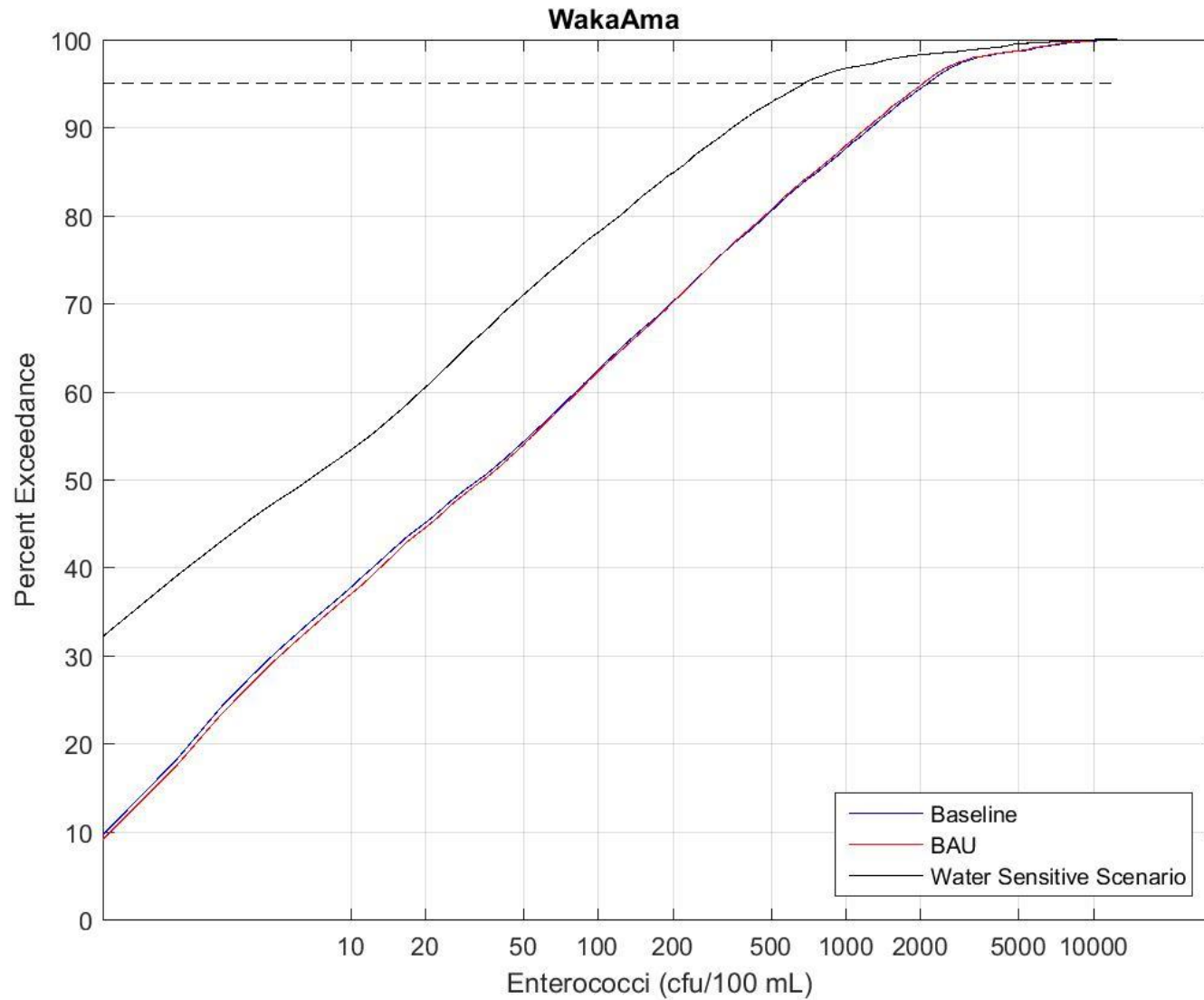
Figure 6-38.   Distribution of predicted *Enterococci* (cfu/100 mL) at the Waka Ama site for each of the scenarios.
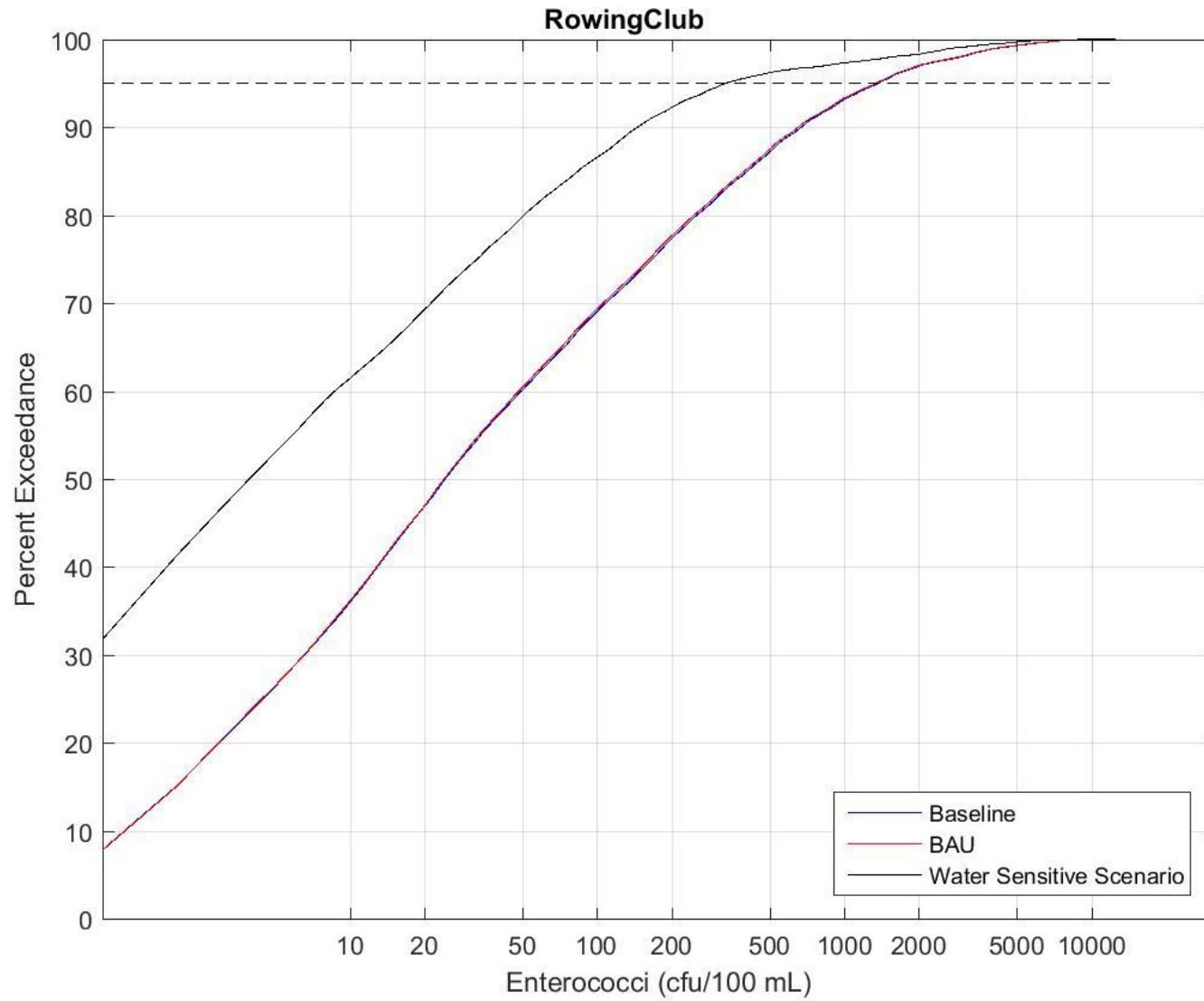
Figure 6-39. Distribution of predicted *Enterococci* (cfu/100 mL) at the Rowing Club site for each of the scenarios.
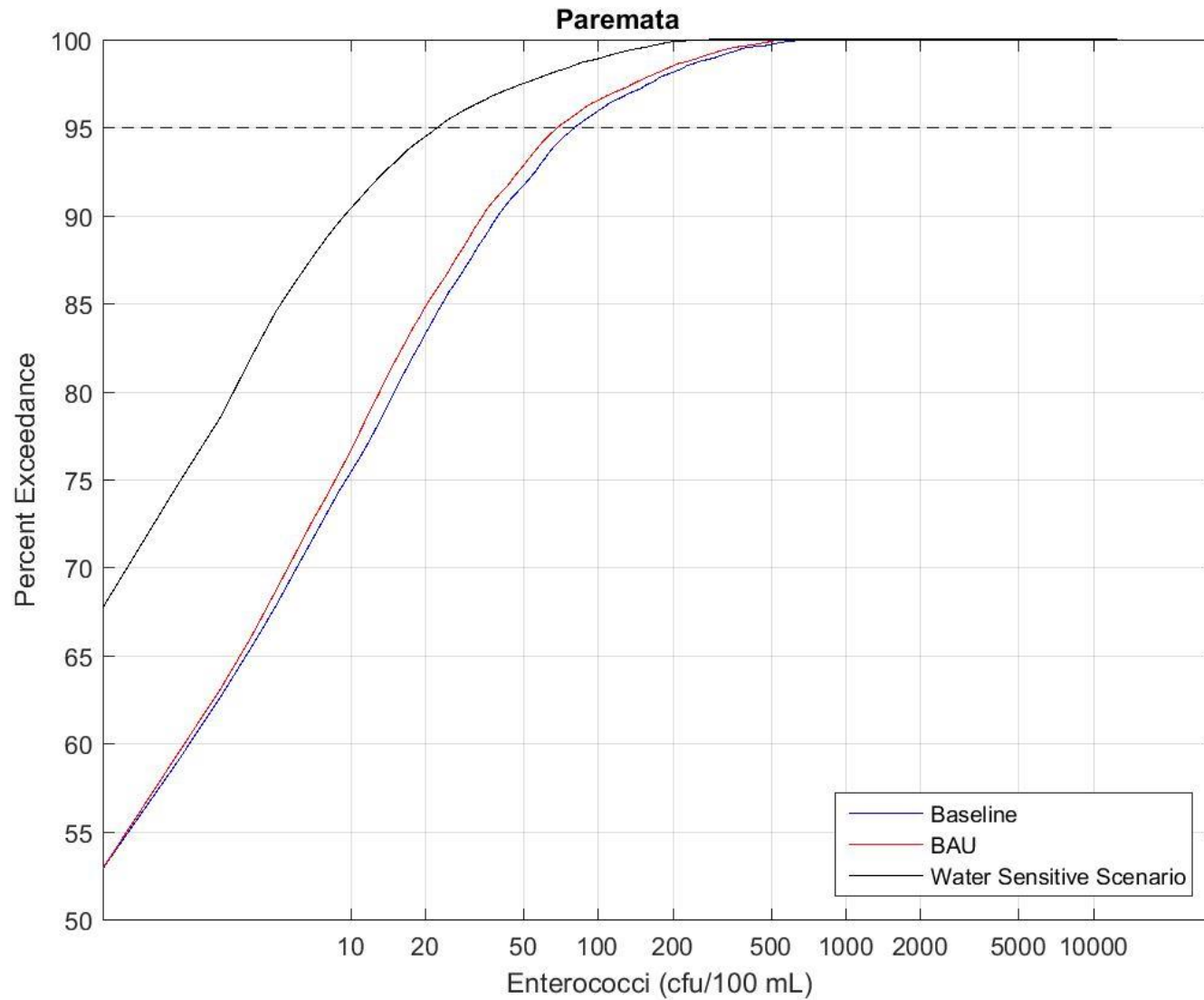
Figure 6-40.   Distribution of predicted *Enterococci* (cfu/100 mL) at the Paremata site for each of the scenarios.
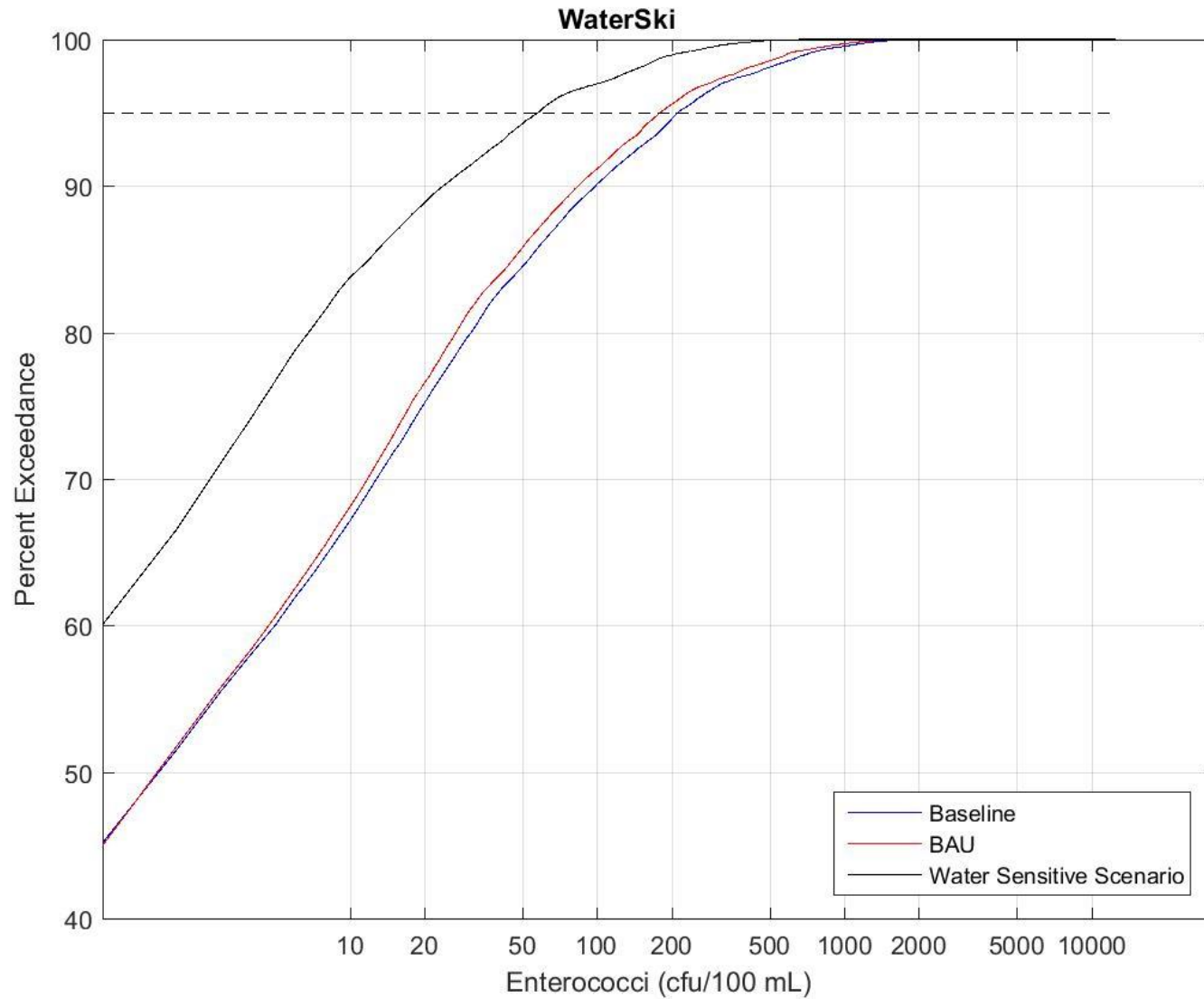
Figure 6-41.   Distribution of predicted *Enterococci* (cfu/100 mL) at the Water Ski site for each of the scenarios.
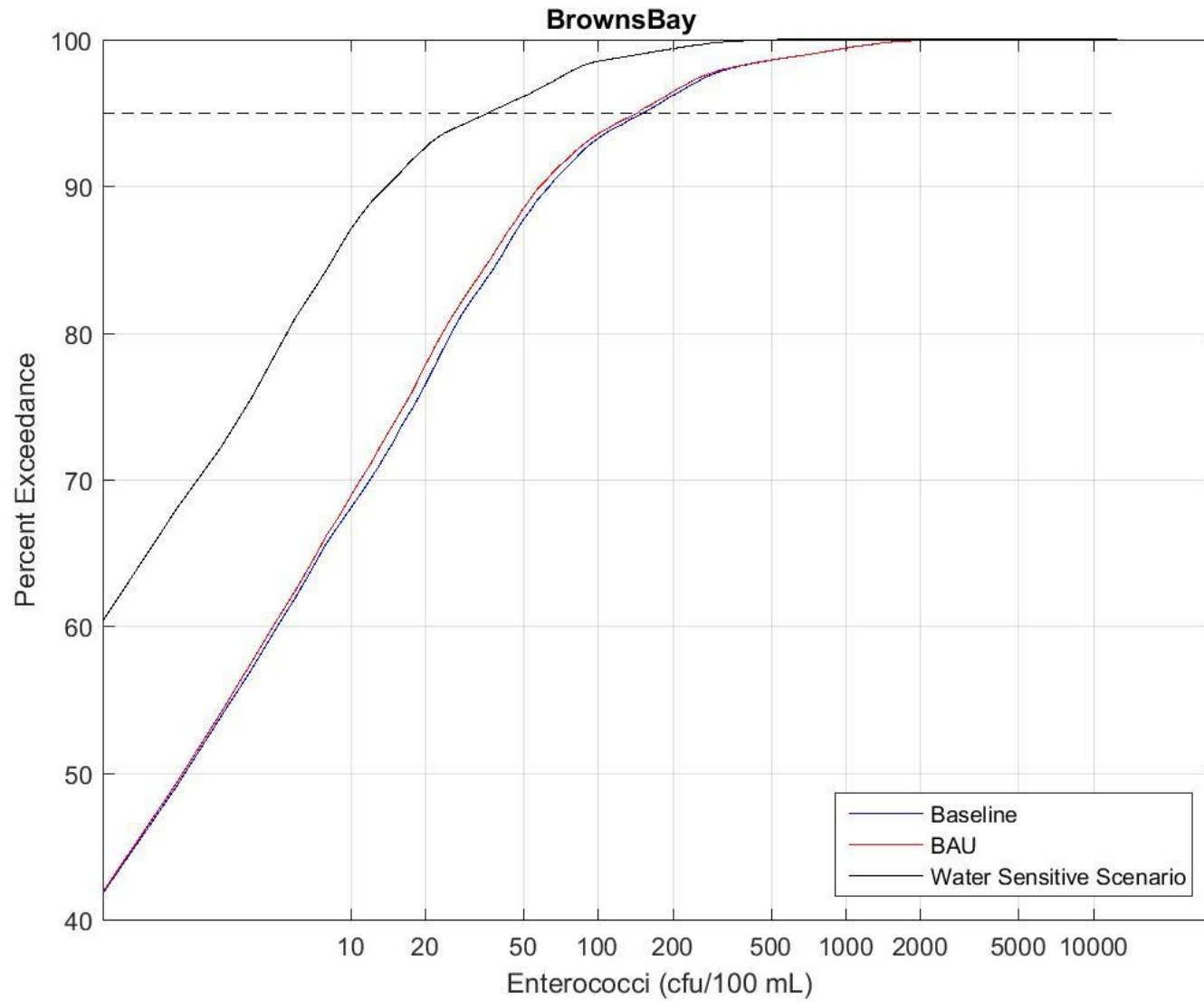
Figure 6-42.   Distribution of predicted *Enterococci* (cfu/100 mL) at the Browns Bay site for each of the scenarios.
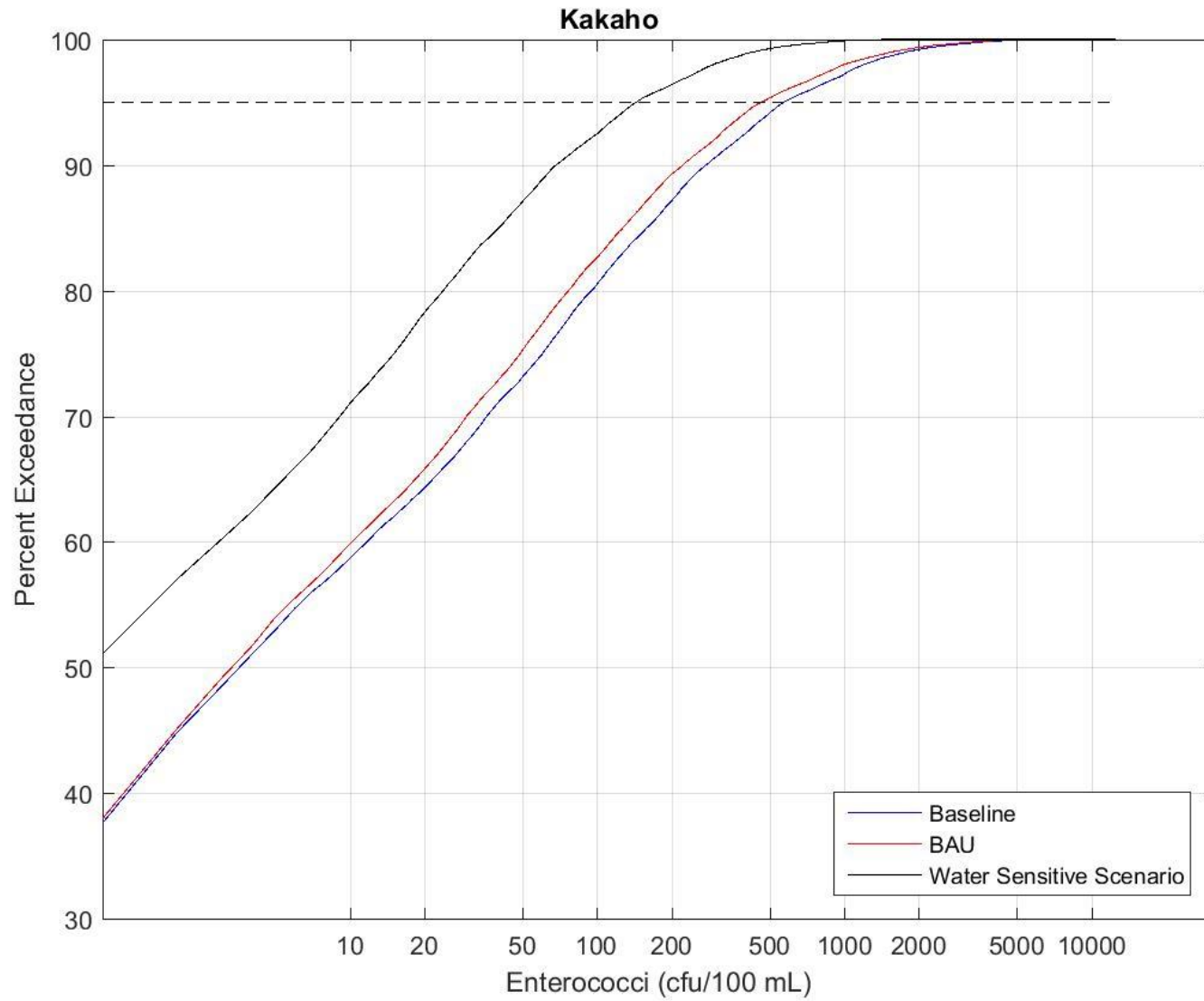
Figure 6-43.   Distribution of predicted *Enterococci* (cfu/100 mL) at the Kakaho site for each of the scenarios.
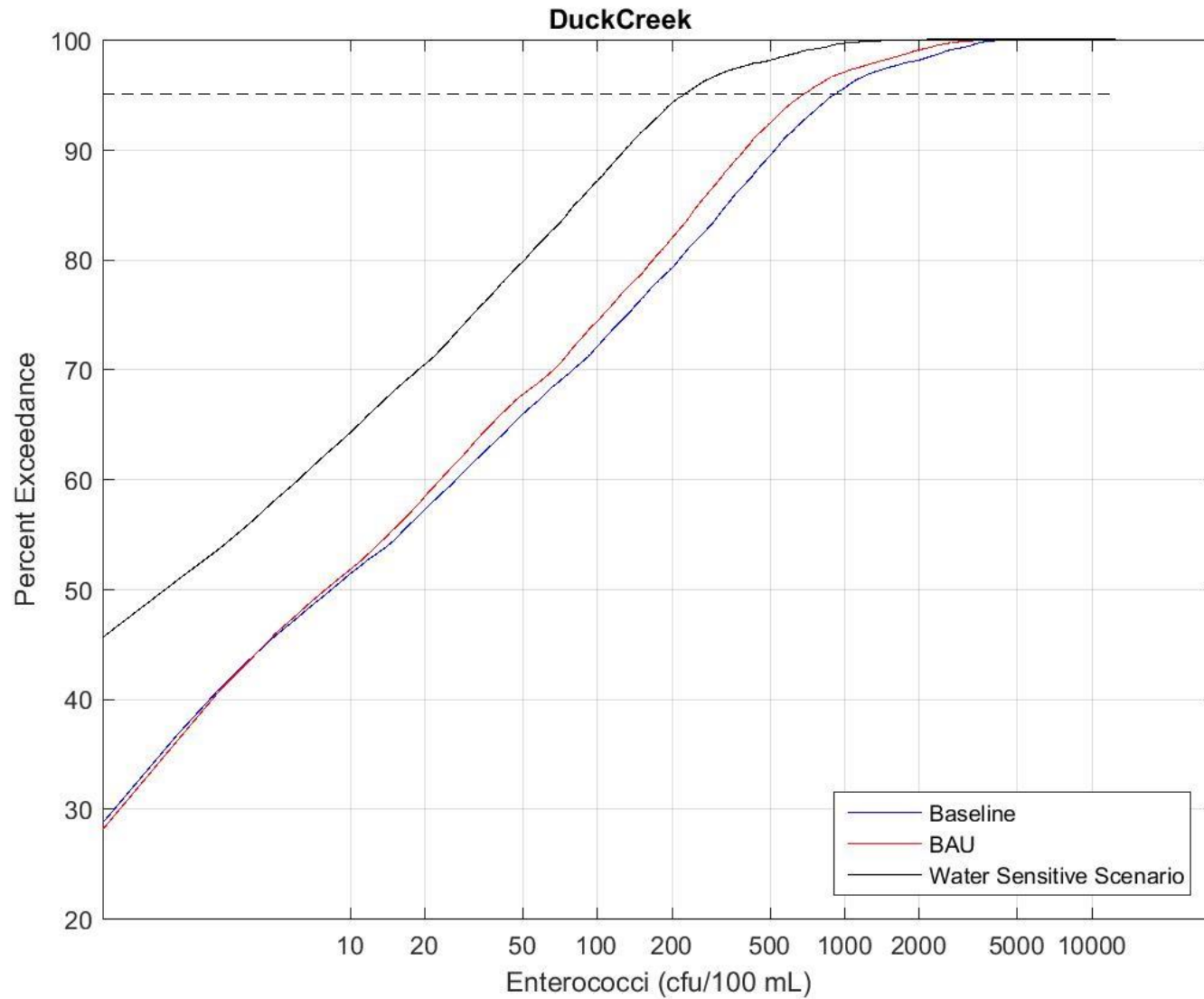
Figure 6-44.   Distribution of predicted *Enterococci* (cfu/100 mL) at the Duck Creek site for each of the scenarios.
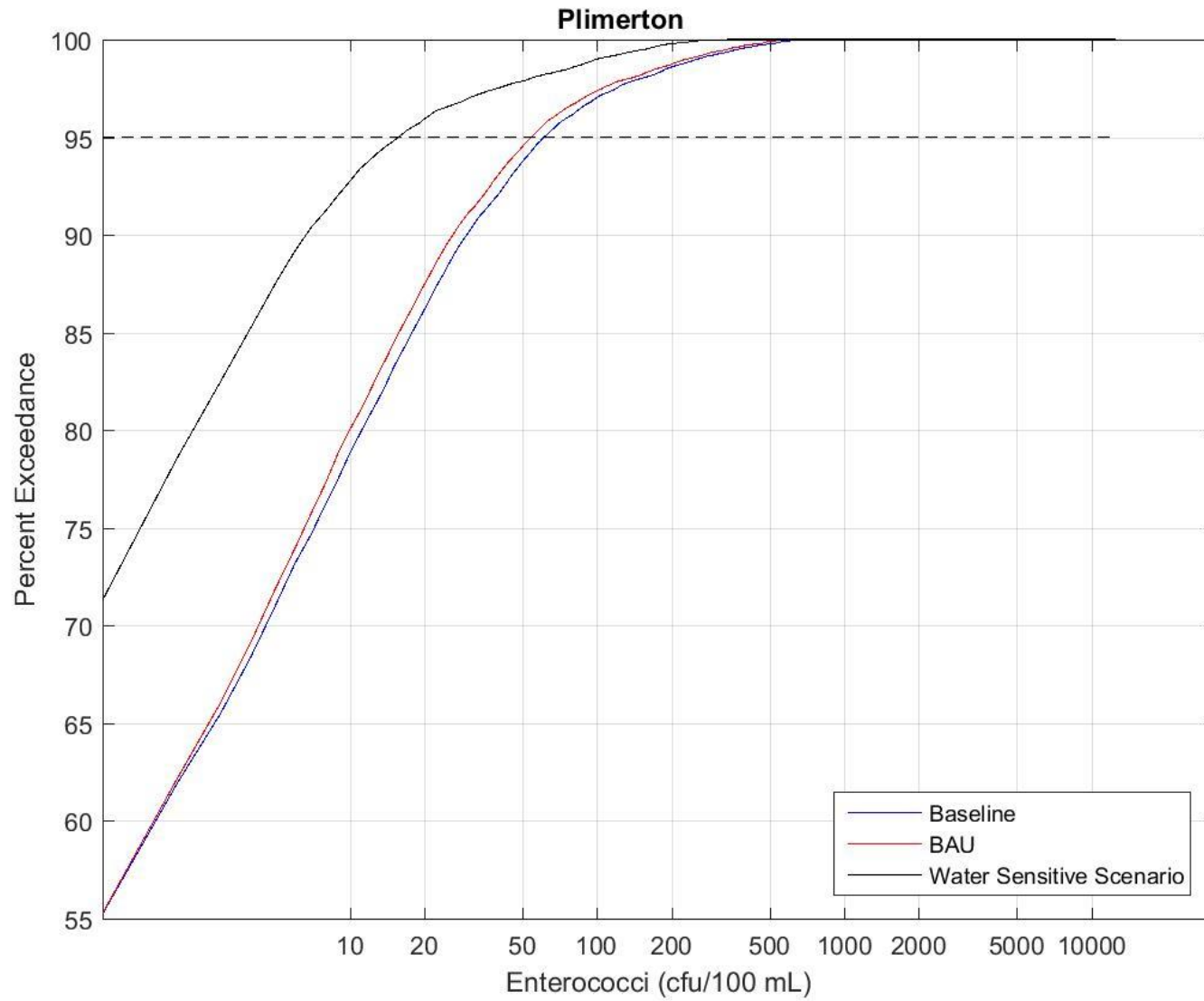
Figure 6-45.   Distribution of predicted *Enterococci* (cfu/100 mL) at the Plimerton site for each of the scenarios.
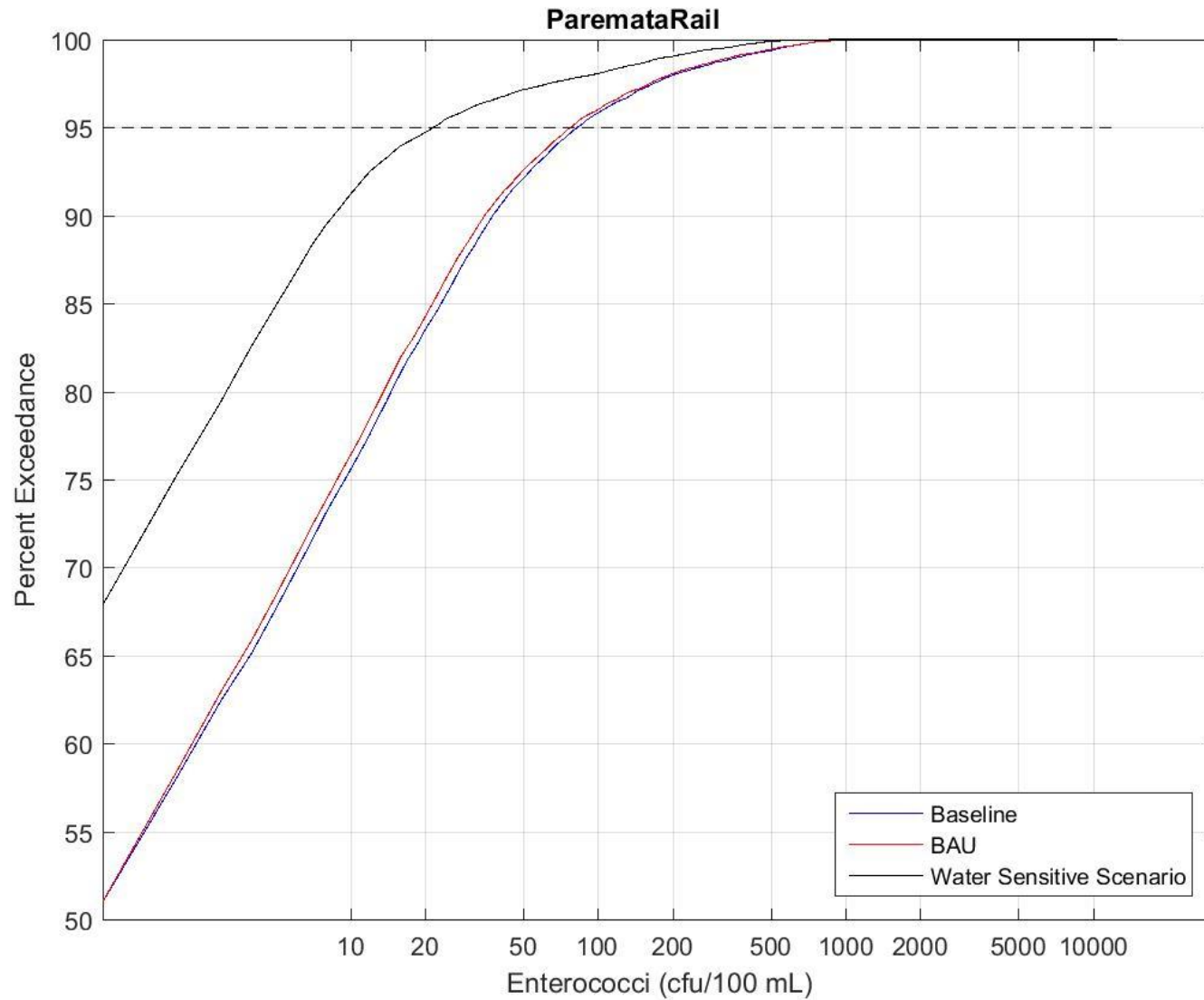
Figure 6-46.   Distribution of predicted *Enterococci* (cfu/100 mL) at the Paremata Rail site for each of the scenarios.
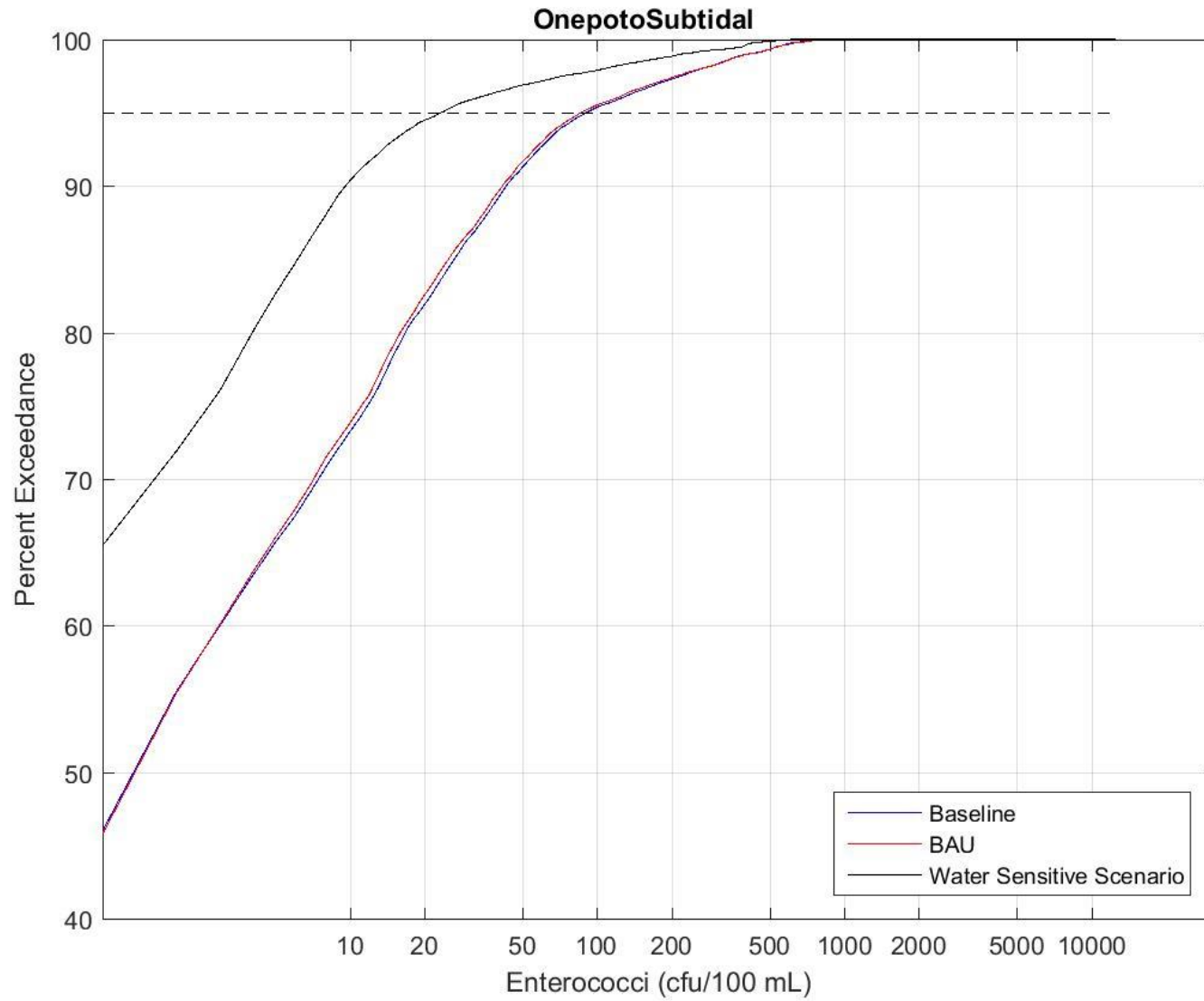
Figure 6-47.   Distribution of predicted *Enterococci* (cfu/100 mL) at the Onepoto Subtidal site for each of the scenarios.
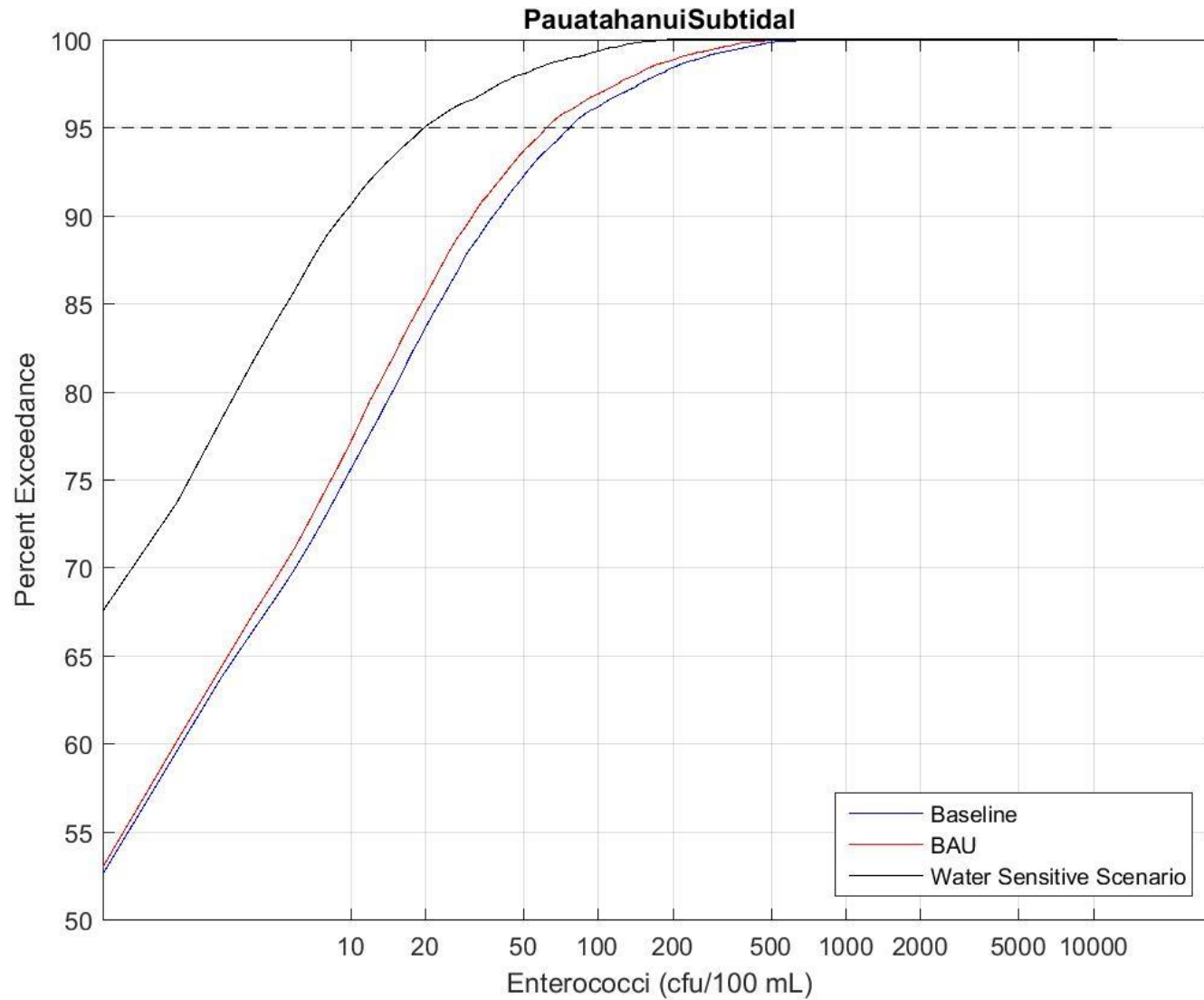
Figure 6-48.   Distribution of predicted *Enterococci* (cfu/100 mL) at the Pauatahanui subtidal site for each of the scenarios.
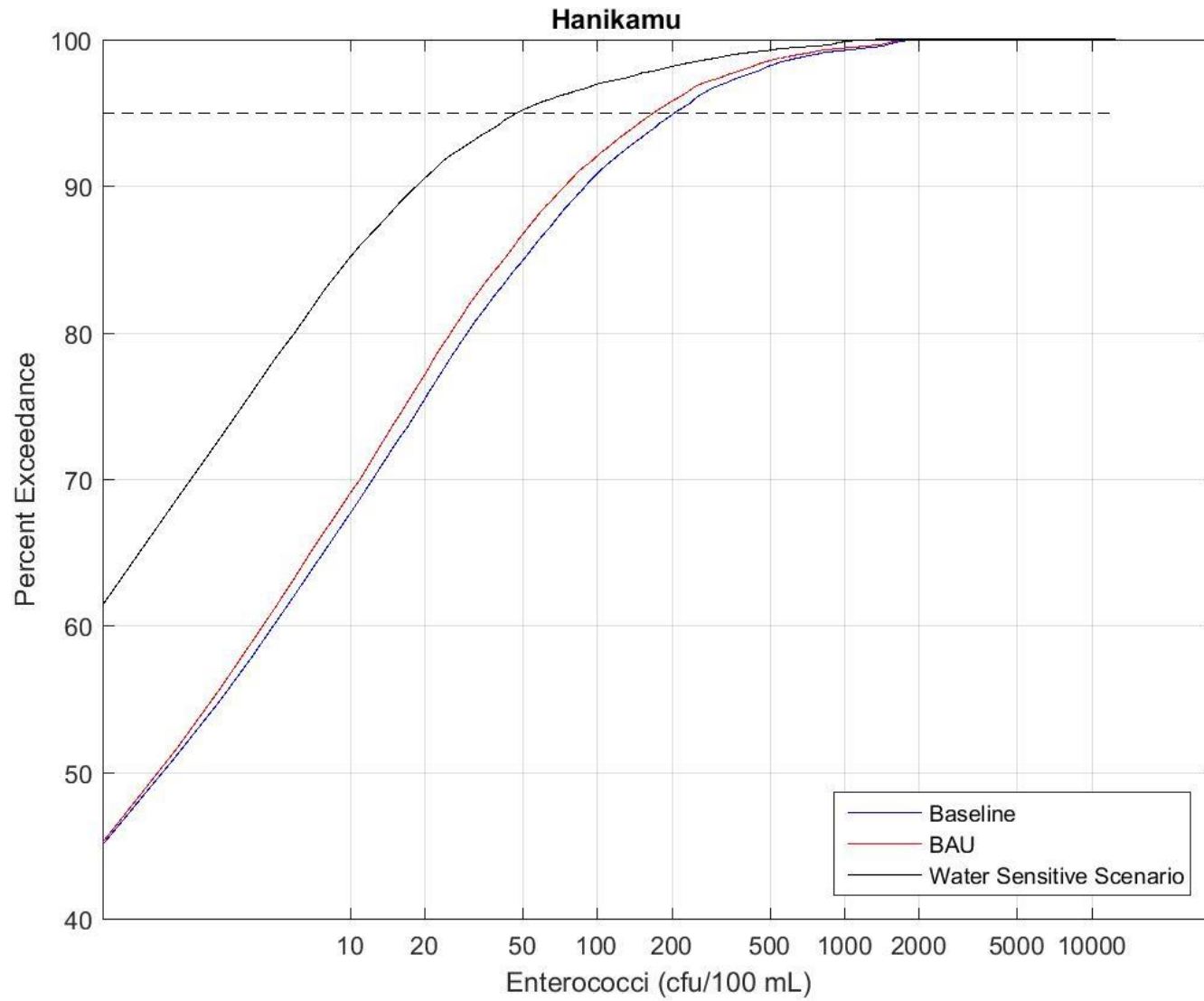
Figure 6-49.   Distribution of predicted *Enterococci* (cfu/100 mL) at the Hanikamu site for each of the scenarios.
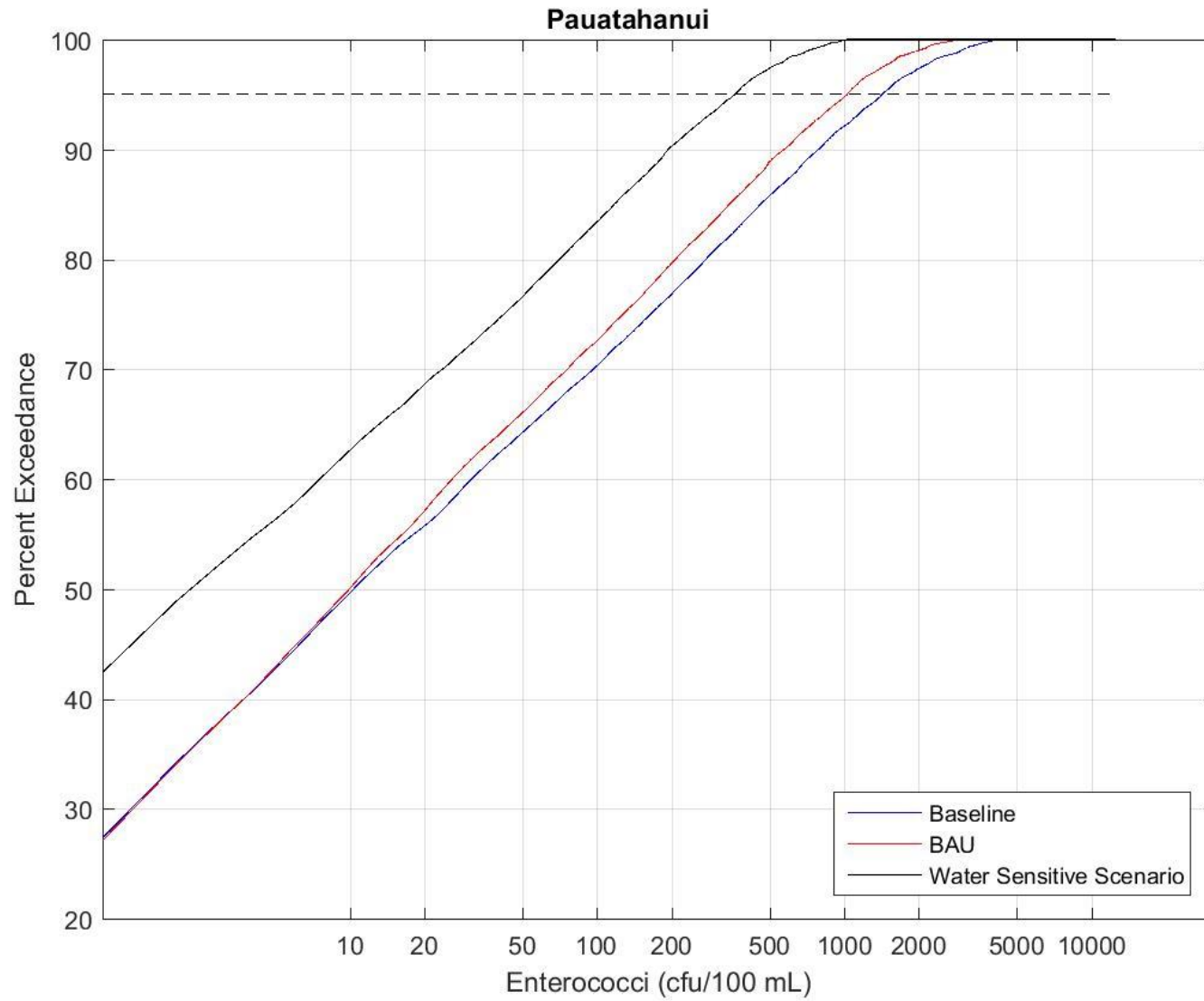
Figure 6-50.   Distribution of predicted *Enterococci* (cfu/100 mL) at the Pauatahanui site for each of the scenarios.
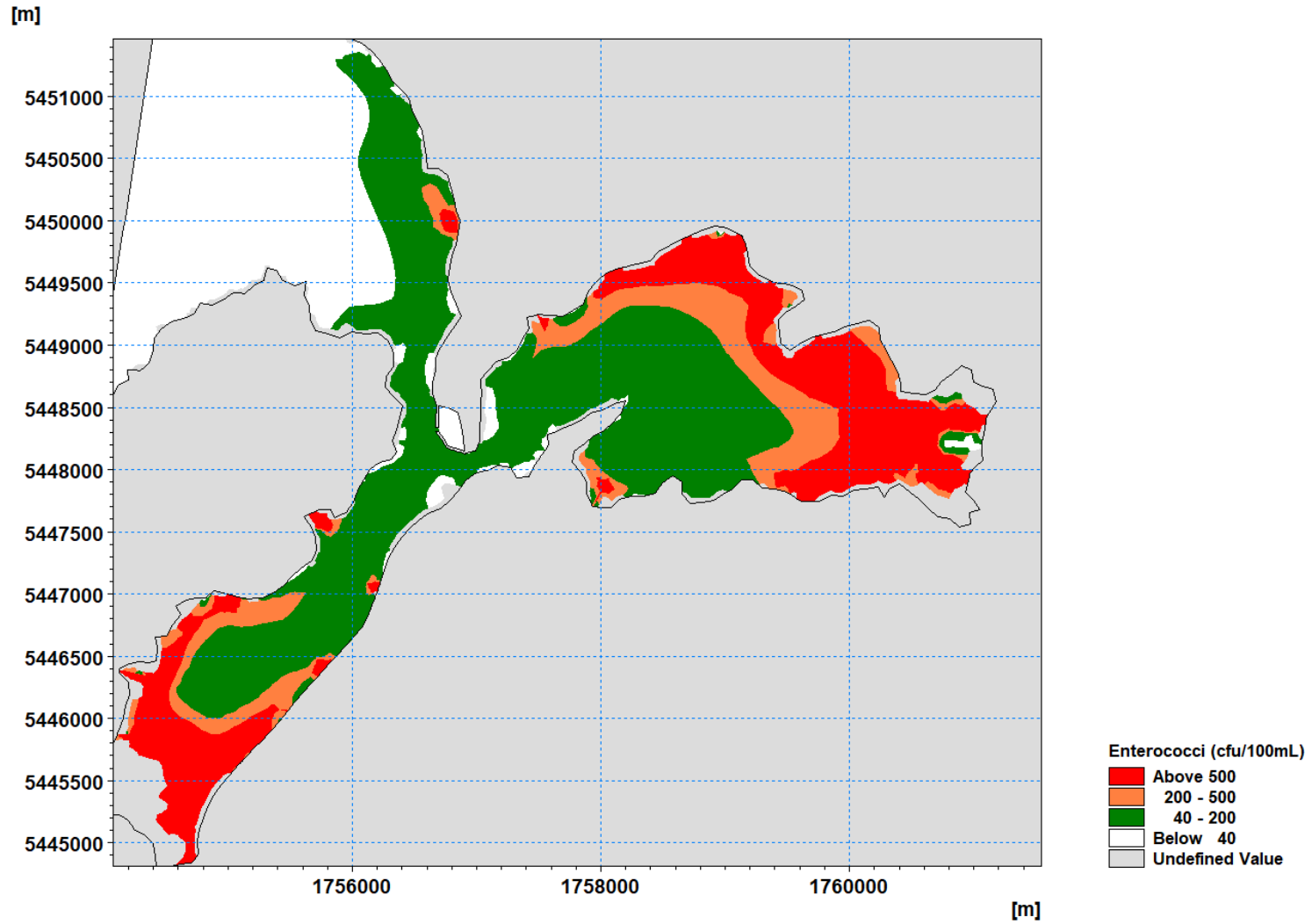
Figure 6-51.   95th percentile *Enterococci* concentration (cfu/100 mL) for the Baseline scenario.
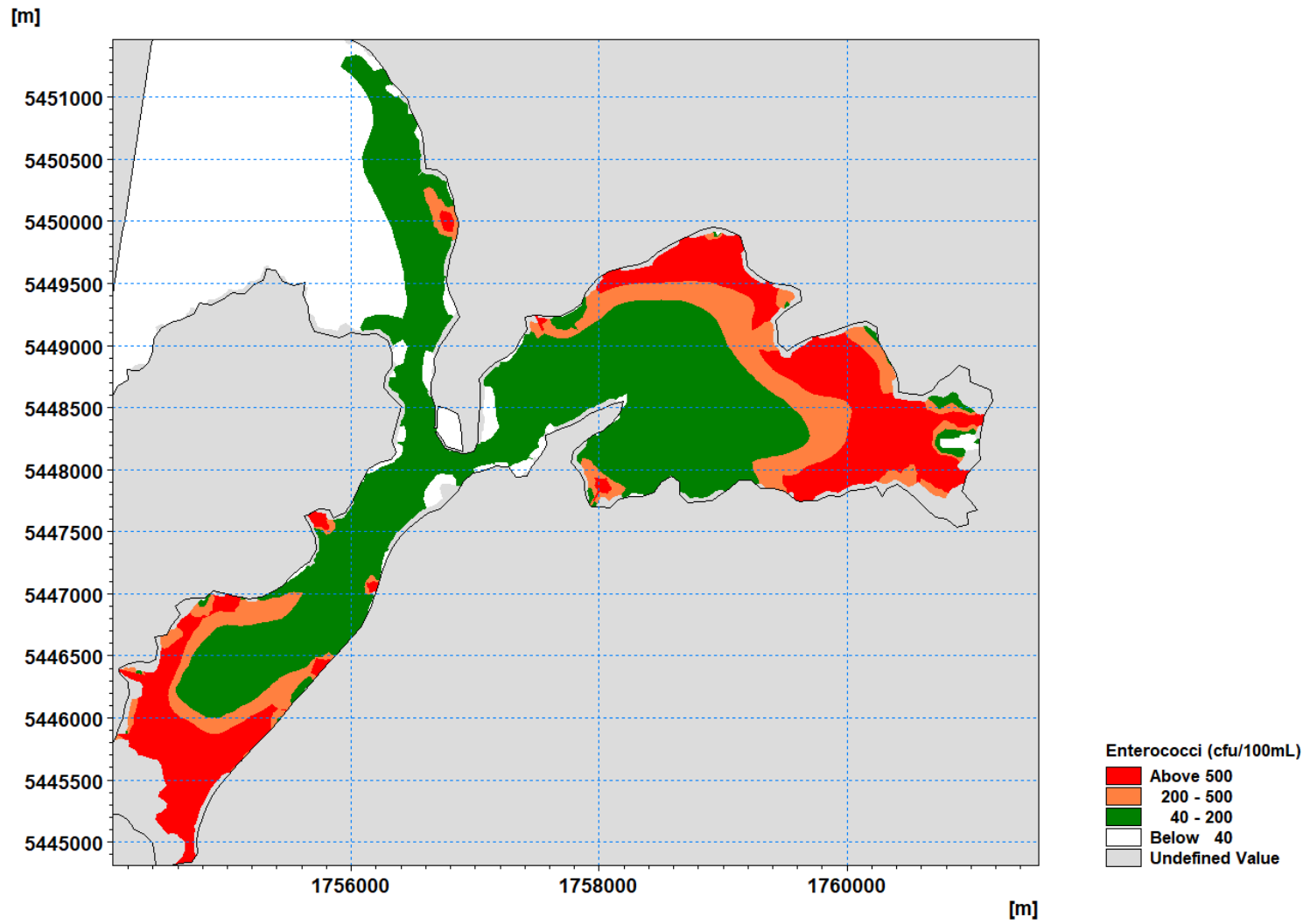
Figure 6-52.   95th percentile *Enterococci* concentration (cfu/100 mL) for the BAU scenario.
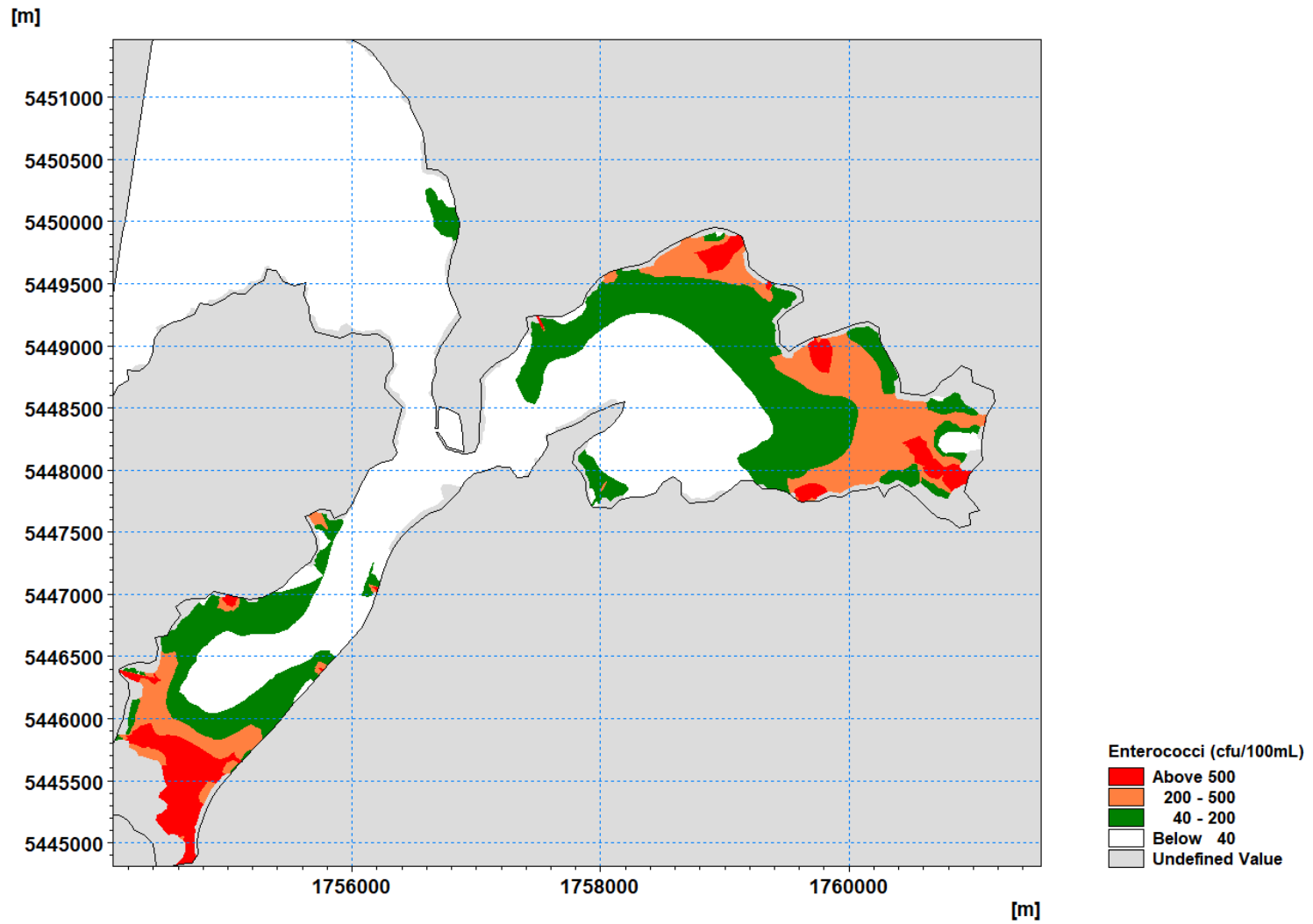
Figure 6-53.   95th percentile *Enterococci* concentration (cfu/100 mL) for the Water Sensitive scenario.

6.5   Metals

In this section the results from the metal accumulation model are presented.

Primarily, the metal accumulation model uses the connectivity matrices (Table 6-12 and Table 6-13) to define how much sediment (and therefore metal) is accumulating in the surface mixed layer of each of the subestuaries of the harbour (Figure 6-54). The source concentrations of metals are defined by dividing the annual metal load for Zinc and Copper for 2010 by the 2010 sediment load for each of the catchment sources.

As a worst-case assumption, it is assumed that all the metal is in the form of particulate and that there is no movement of metal from the particulate phase to the dissolved phased once it is deposited on the seabed.

Table 6-20 shows the source concentrations for Zn and Cu based on the sediment and metal loads delivered via the freshwater inputs to the harbour during 2010. In addition, Table 6-20 also shows the contribution each subcatchment makes to the overall input of sediment to the harbour.
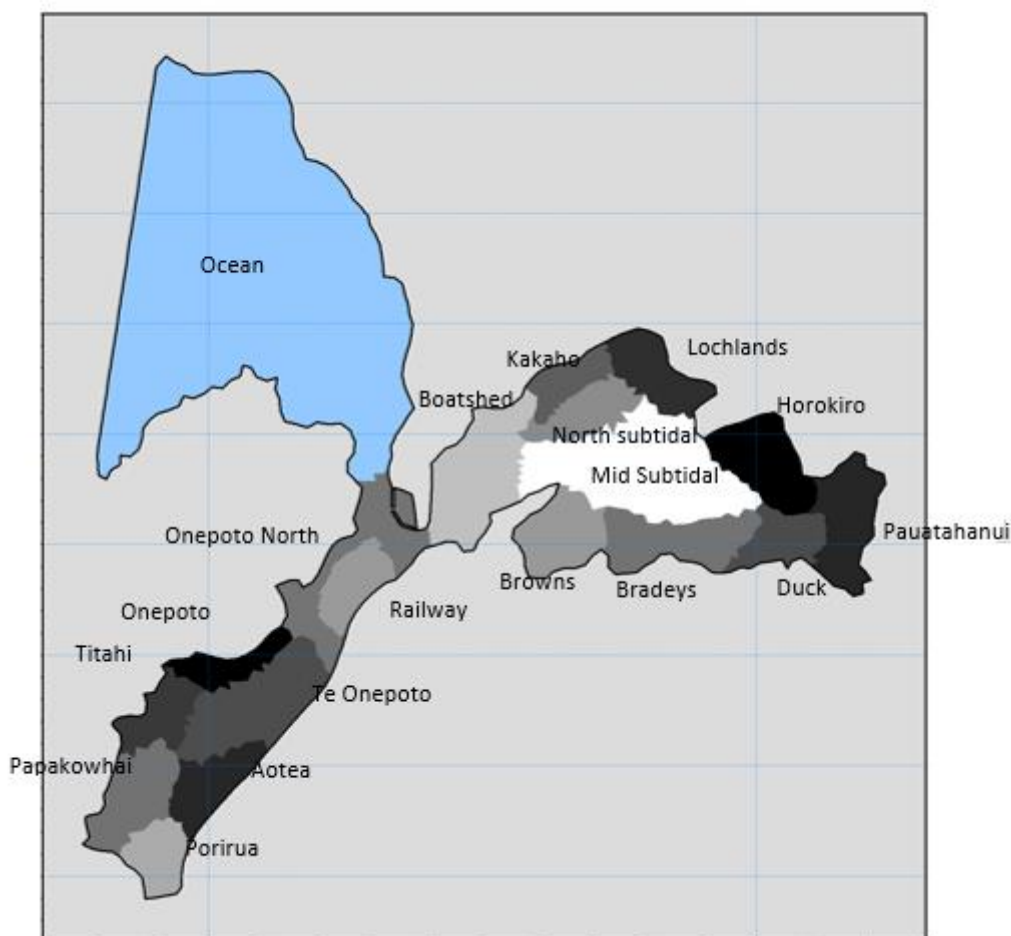
Figure 6-54.   Subestuaries of the Onepoto Arm and Pauatahanui Inlet.

Table 6-20. Baseline metal source concentrations derived from 2010 sediment and metal load data.

Catchment Outlet	Zn Source concentration (mg/kg)	Cu Source concentration (mg/kg)	Contribution to overall sediment input (%)
Whitireia/Te Onepoto	367	35	0.11
Porirua Mouth	744	69	42.48
Onepoto fringe Elsdon	6511	473	0.18
Next to Mahinawa	5425	451	0.08
Kahetoa (Onepoto Park)	7915	788	0.07
Hukarito	1230	124	0.09
Direct to Onepoto (South)	369	56	0.32
Direct to Onepoto (North)	4533	414	0.10
Direct to Onepoto (Mid)	2890	356	0.13
Whitby to Browns Bay	1536	129	0.40
Ration	57	8	1.76
Pauatahanui village	575	67	0.06
Pauatahanui mouth	57	8	32.38
Motukaraka	1101	127	0.02
Lower Duck Creek	332	30	6.99
Kakaho	99	16	3.90
Horokiri	70	11	10.89
Direct to Pauatahanui (Water ski club)	925	167	0.01
Direct to Pauatahanui (Mid)	11184	1050	0.01
Direct to Pauatahanui (Boat houses)	12211	1092	0.01

There is ongoing work associated with setting trigger levels for sediment metal accumulation in coastal waters. Table 6-21 shows the guidelines developed for the Auckland Region (Williamson et al. 2017) and the values from ANZECC (2000).

Table 6-21.   Threshold sediment metal concentrations (mg metal to kg sediment) from Williamson et al (2002).

Threshold	Threshold for Zn	Threshold for Cu
TEL (Threshold Effects Level)	124 mg/kg	19 mg/kg
ERL (Effects Range Low)	150 mg/kg	34 mg/kg
PEL (Probable Effects Levels)	271 mg/kg	108 mg/kg
ANZECC 2000 Guidelines (ISQG-Low)	200 mg/kg	65 mg/kg
ANZECC 2000 Guidelines (ISQG-High)	410 mg/kg	270 mg/kg

Table 6-20 gives an indication of the subcatchments that could contribute to the build-up of metals to levels that exceed the above guidelines. These are the subcatchments with both high sediment inputs and high source concentrations of metals. For example, subcatchment inputs for the Lower Duck Creek and Porirua Mouth have both relatively high sediment loads (compared to other subcatchments) and higher Zn source concentrations than other subcatchments. The connectivity matrices (Table 6-12 and Table 6-13) indicate where in the harbour sediments (and therefore metals) accumulate in the harbour.

Table 6-22 shows the subcatchment outlets where the source concentrations of metals increase under the Water Sensitive scenario. This is due to the relative decreases in sediment loads (~39%, Table 3-4) and metal loads (60% and 20% for Zinc and Copper and Zinc respectively, Table 3-4). This gives an indication of the subcatchments that may contribute to the elevated build-up of metals under the Water Sensitive Scenario.

Applying the metal accumulation model methodology (set out in Section 5.4 and Appendix C), the time series of predicted metal accumulation in each of the subestuaries for the Baseline, BAU and Water Sensitive Scenario over the next 100 years can be made. Current day metal concentrations have been assumed to be the mean of all the available monitoring data (10.50 mg/kg for Cu and 77.0 mg/kg for Zn).

Based on data presented in Swales et al. (2005) and Green et al. (2014), the surface mixed layer for sediment was assumed to be 15 cm.

Figures 6-55 to 6-58 show the time series plots for the Onepoto Arm and Pauatahanui Inlet for each of the subestuary.

The key results from the metal accumulation modelling are that it is unlikely that overall metal accumulation in the Pauatahanui Inlet or the northern sector of the Onepoto Arm will exceed guideline levels under any of the scenarios.

Metal accumulation in the southern sector of the Onepoto Arm will be accelerated under the BAU scenario.

Under the Water Sensitive scenario, there is likely to be an improvement in Zn accumulation but potentially higher levels of Cu accumulation. This is because of the relative decreases in the sediment loads and metal loads for the Water Sensitive scenario leading to higher source concentrations of Cu (i.e. mg of Cu to kg of sediments) under the Water Sensitive Scenario compared to the Baseline conditions (particularly for the Porirua Mouth subcatchment).

These results are a combination of the subestuary deposition results (Section 6.2.3 - where we see several depositional sinks within the Pauatahanui Inlet and the Southern Onepoto Arm) and the relative differences in ratio of sediment and metal loads being delivered to two arms of the harbour. For the Onepoto Arm, we see both high sediment loads and metal loads being delivered by a subcatchment that has high connectivity to the rest of the Onepoto Arm and for the Pauatahanui Inlet we see that the subcatchments with the highest sediment loads have relatively low metal loads (reflecting the land use in the catchment).

Table 6-22.   Water Sensitive Scenario metal source concentrations. Red cells indicate catchment outlets where the metal concentration increases under the Water Sensitive Scenario.

Catchment Outlet	Zn Source concentration (mg/kg)	Cu Source concentration (mg/kg)
Whitireia/Te Onepoto	204	37
Porirua Mouth	742	134
Onepoto fringe Elsdon	1438	256
Next to Mahinawa	1897	343
Kahetoa (Onepoto Park)	4166	756
Hukarito	681	123
Direct to Onepoto (South)	812	142
Direct to Onepoto (North)	1988	360
Direct to Onepoto (Mid)	2175	398
Whitby to Browns Bay	1171	212
Ration	71	13
Pauatahanui village	211	38
Pauatahanui mouth	59	11
Motukaraka	299	52
Lower Duck Creek	369	67
Kakaho	148	25
Horokiri	102	18
Direct to Pauatahanui (Water ski club)	303	57
Direct to Pauatahanui (Mid)	6620	1199
Direct to Pauatahanui (Boat houses)	5033	904
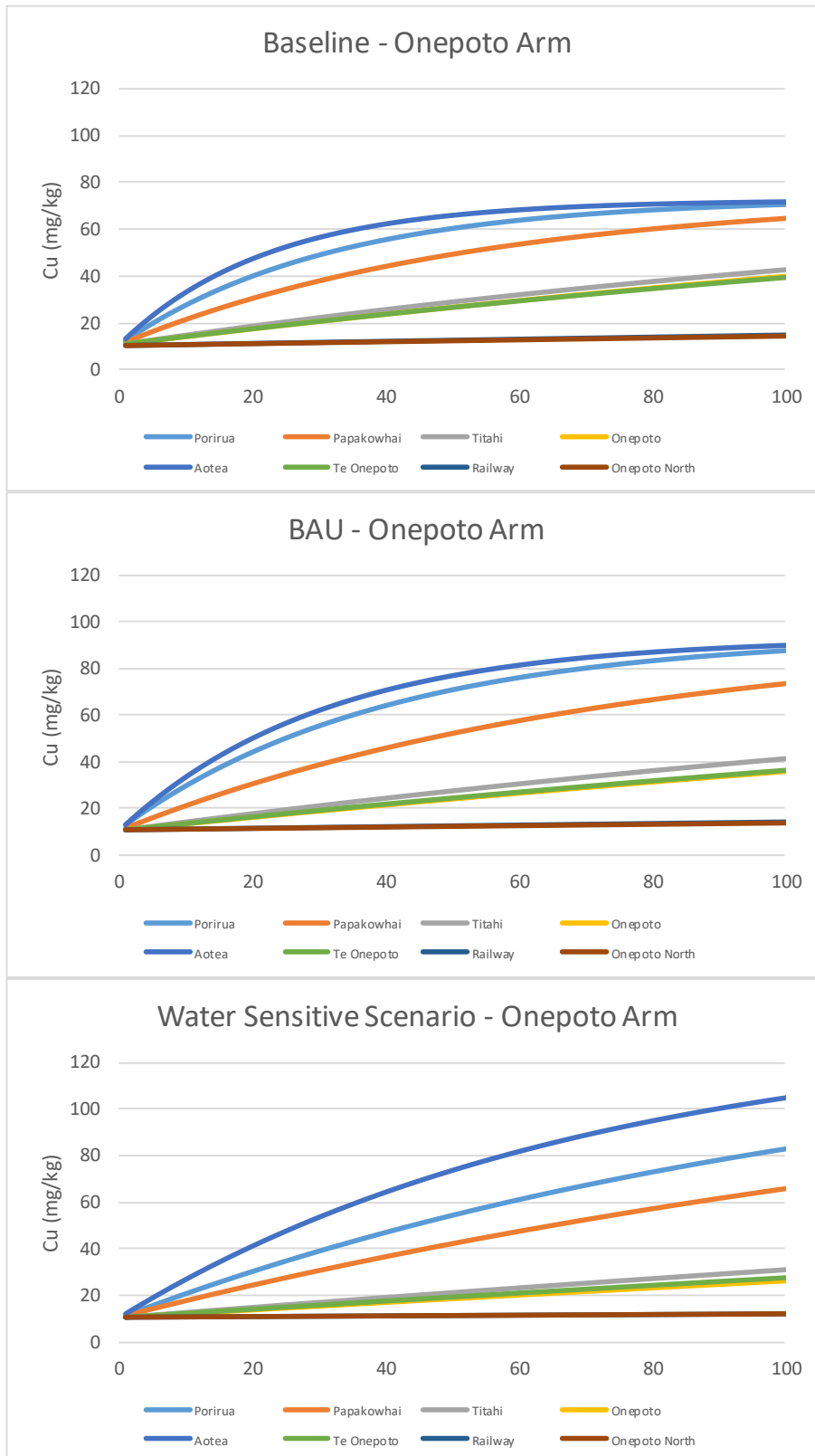
Figure 6-55. Surface mixed layer Copper metal concentration (mg/kg) in the Onepoto subestuary for the Baseline, BAU and Water Sensitive scenarios.
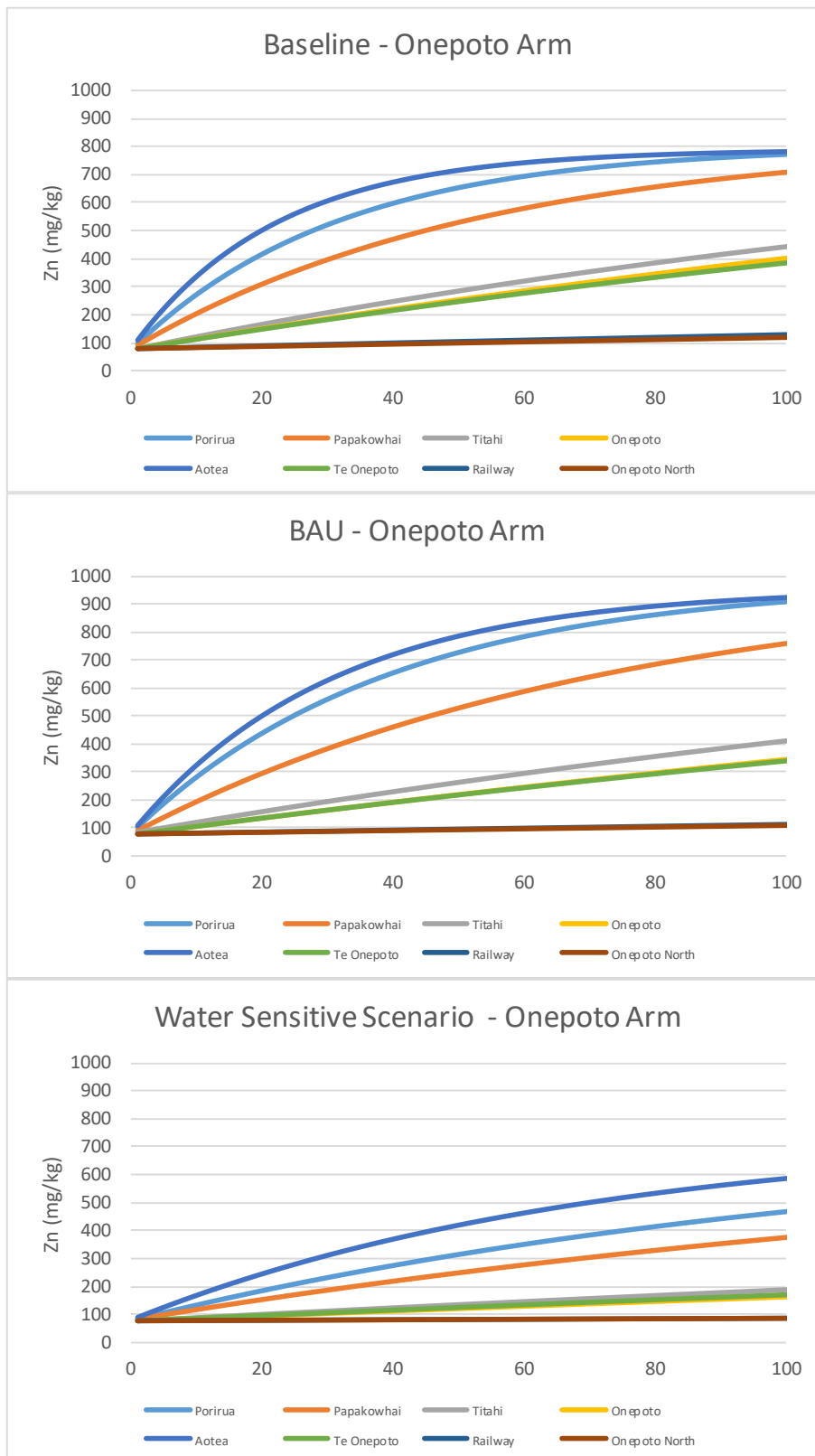
Figure 6-56.   Surface mixed layer Zinc metal concentration (mg/kg) in the Onepoto subestuary for the Baseline, BAU and Water Sensitive scenarios.
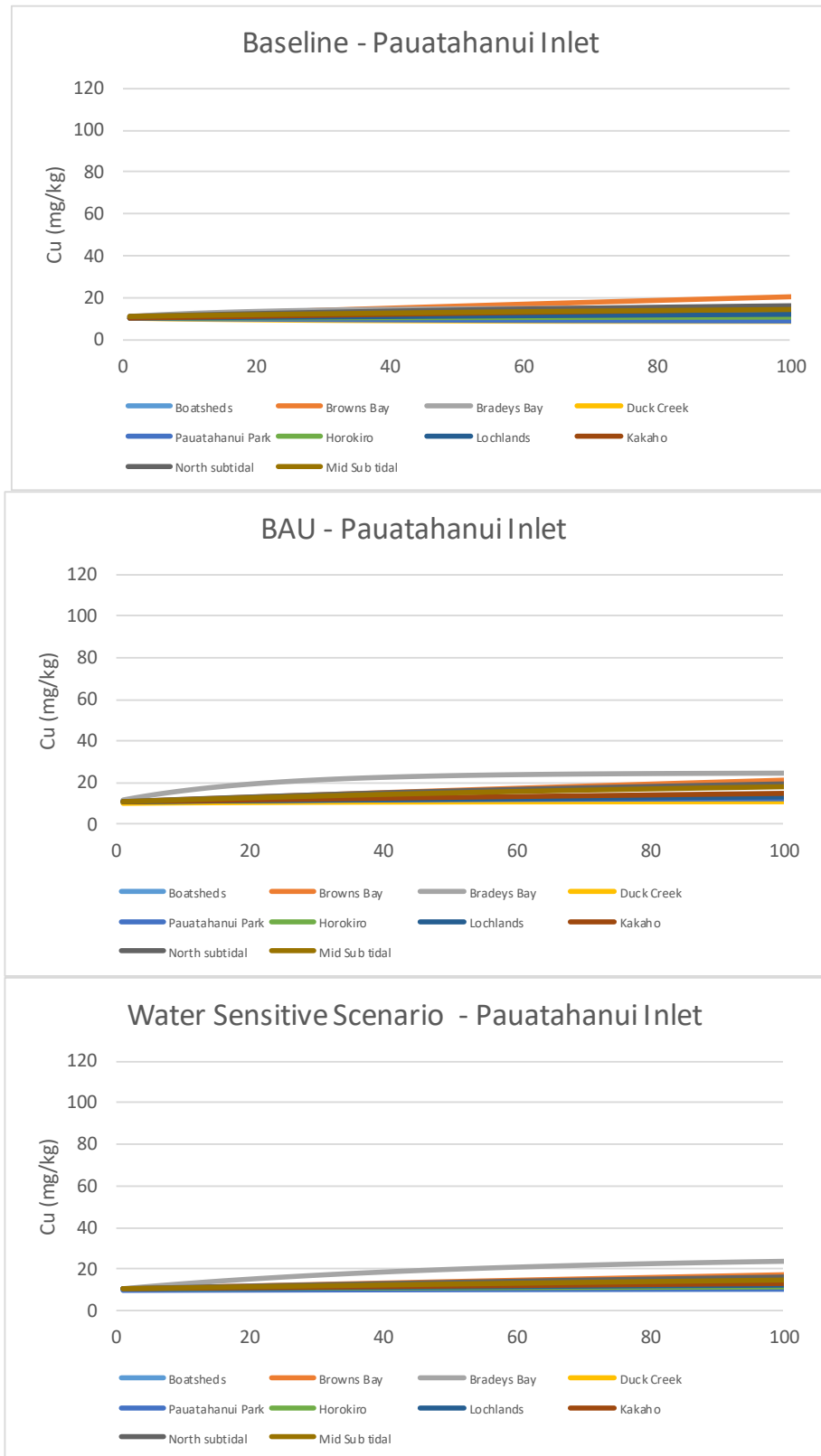
Figure 6-57.   Surface mixed layer Copper metal concentration (mg/kg) in the Pauatahanui subestuary for the Baseline, BAU and Water Sensitive scenarios.
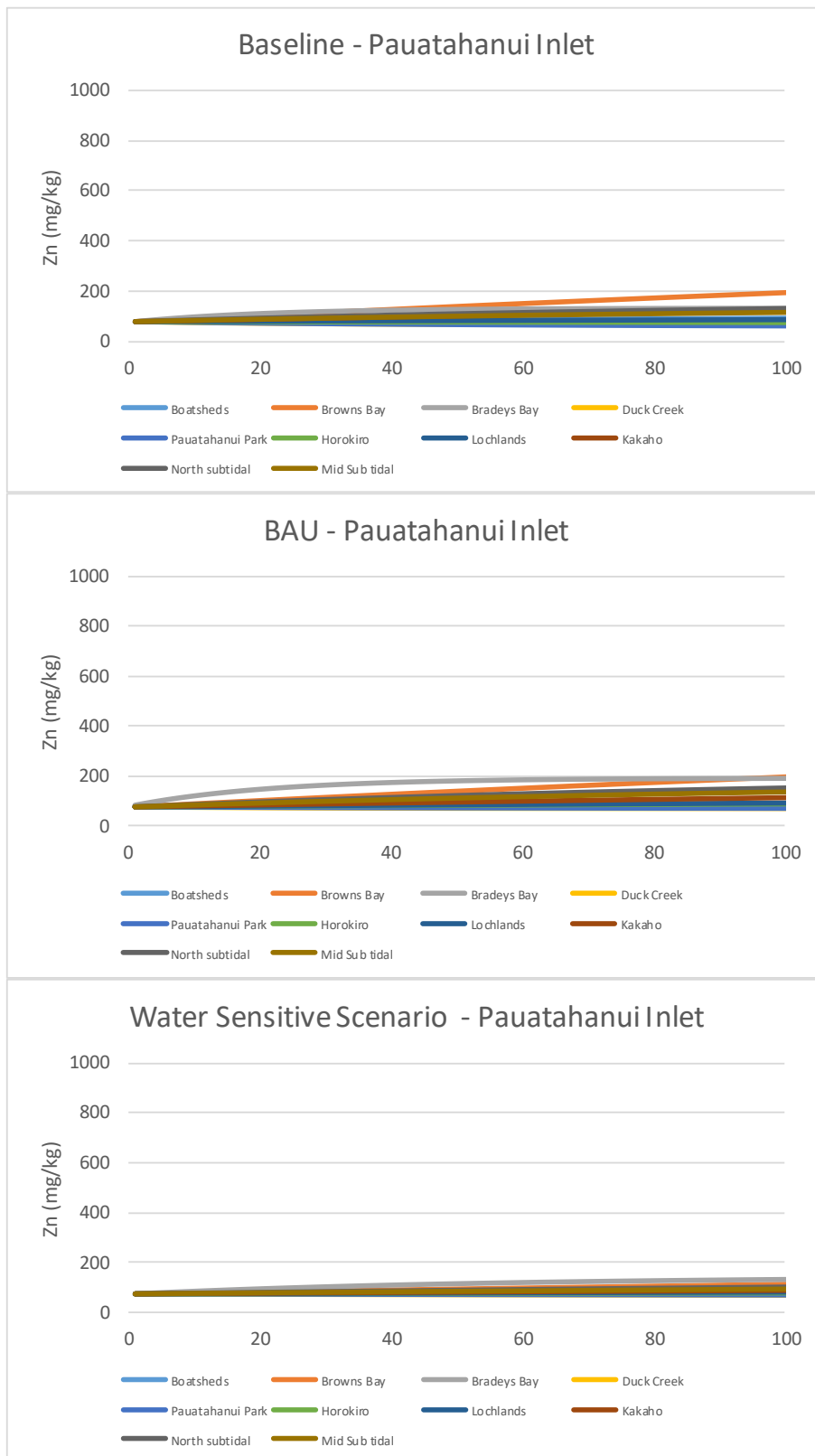
Figure 6-58.   Surface mixed layer Zinc metal concentration (mg/kg) in the Pauatahanui subestuary for the Baseline, BAU and Water Sensitive scenarios.

7   References

ANZECC 2000. Australian and New Zealand Guidelines for Fresh and Marine Water Quality. National Water Quality Management Strategy. Australian and New Zealand Environment and Conservation Council. Agriculture and Resource Management Councils of Australia and New Zealand. Canberra, Australia.

Black, K.P., Bell, R.G., Oldman, J.W., Gorman, R.M., Oulton, D. 1995. Numerical modelling of a future diffuse shoreline discharge option for the Mangere Wastewater Treatment Plant. Report for Watercare Services Ltd, Auckland. NIWA

Broekhuizen, N., Hadfield, M., Plew D. 2015. A biophysical model for the Marlborough Sounds: Pelorus Sound. NIWA report CHC2014-130 prepared for Marlborough District Council.

Burt, T.N. 1986. Field settling velocities of estuary muds. In Estuarine Cohesive Sediment Dynamics. Lecture note son Coastal and Estuarine Studies (Mehta, A.J. ed.) pg 126-150.

DHI 2018. Porirua Harbour Water Quality Forecast Annual Quality Status Report 2018. Technical memo prepared for Greater Wellington Regional Council.

DHI 2019. DHI Eutrophication Model, including sedimentation and benthic vegetation. MIKE ECO Lab template scientific description.

DML 2015. Te Awarua-O-Porirua Harbour Report of Survey & Verification of Sedimentation Rates Project No. SP00041 Report Prepared for Porirua City Council

Edelvang, K., Kaas, H., Erichsen, A.C., Alvarez-Berastegui, D., Bundgaard, K., Jørgensen, P.V. 2005. Numerical modelling of phytoplankton biomass in coastal waters, J. Marine Syst., 57, 13–29.

Gibb, J.G. 2009. Patterns and Rates of Sedimentation Within Porirua Harbour Report Prepared for Porirua City Council

Gillespie P., Knight B., MacKenzie L. 2011. The New Zealand King Salmon Company Limited: Assessment of Environmental Effects – Water Column, Cawthron Report 1985.

Green M., Stevens L., Oliver M.D. 2014. Te Awarua-o-Porirua Harbour and catchment sediment modelling: Development and application of the CLUES and Source-to-Sink models. Greater Wellington Regional Council, Publication No. GW/ESCI-T-14/132, Wellington.

Green, M.O. 2008. Central Waitemata Harbour Contaminant Study. Predictions of Sediment, Zinc and Copper Accumulation under Future Development Scenario 1. Prepared by NIWA Ltd for Auckland Regional Council. Auckland Regional Council Technical Report 2008/043.

Green, M.O. 2016. Assessment of Potential Effects of Land Development on Okura Estuary. Estimates of Metal Accumulation in the Estuary. Extension of Model and Review of Model Parameters. Report TOD1601–1, Streamlined Environmental.

Heath, M., Sabatino, A., Serpetti, N., McCaig, C., O'Hara M.R. 2017. Modelling the sensitivity of suspended sediment profiles to tidal current and wave conditions, Ocean & Coastal Management, 147 p 49-66.

Jacobs 2019a. Porirua Whaitua Collaborative Modelling Project. Baseline Modelling Technical Report.

Jacobs 2019b. Porirua Whaitua Collaborative Modelling Project. Scenario Modelling Technical Report.

Knight B.R., Keeley N.B., Taylor D. 2014. Aquaculture effects modelling in the Hauraki Gulf. Prepared for Waikato Regional Council. Cawthron Report No. 2423. 36 p.

Ministry for the Environment 2002. Microbiological Water Quality Guidelines for Marine and Freshwater Recreational Areas. MfE publication number 474.

Moores, J., Easton, S., Gadd, J., Sands. M. 2017. Te Awarua-o-Porirua Collaborative Modelling Project Customisation of urban contaminant load model and estimation of contaminant loads from sources excluded from the core models. NIWA Client report 2017050AK

Oliver, M.D., Conwell C. 2019. Coastal Water Quality and Ecology monitoring programme Annual data report, 2017/18.

Schlee, J. 1973. Atlantic Continental Shelf and Slope of the United States sediment texture of the northeastern part: U.S. Geological Survey Professional Paper 529-L, 64 p.

Semadeni-Davies, A. 2009. Fall Velocities of Stormwater Sediment Particles. Literature Review. Prepared by NIWA Ltd for Auckland Regional Council. Auckland Regional Council Technical Report 2009/035.

Semadeni-Davies, A., Kachhara, A.S. 2017. Te Awarua-o-Porirua Collaborative Modelling Project: CLUES modelling of rural contaminants. NIWA Client report 2017189AK prepared for Greater Wellington Regional Council.

Sinton L.W., Davies-Colley R.J., Bell R.G. 1994. Inactivation of enterococci and fecal coliforms from sewage and meatworks effluents in seawater chambers. Appl Environ Microbiol. 60(6): 2040-8.

SKM 2016. Transmission Gully Project. Assessment of Hydrology and Stormwater Effects Technical Report 14. Prepared for NZTA and Porirua City Council.

Sorensen P.G., Milne J.R. 2009. Porirua Harbour targeted intertidal sediment quality assessment. Greater Wellington Regional Council.

Stevens L., Robertson, B. 2016. Porirua Harbour Sediment Plate Monitoring 2015/16. Report prepared by Wriggle Limited for Greater Wellington Regional Council.

Swales, A., Bentley, S.J., McGlone, M.S., Ovenden, R., Hermanspahn, N., Budd, R., Hill, A., Pickmere, S., Haskey, R., Okey, M.J. 2005. Pauatahanui inlet: effects of historical catchment land cover changes on inlet sedimentation. National Institute of Water & Atmospheric Research Ltd Client Report HAM2004-149, April 2005 prepared for Greater Wellington Regional Council and Porirua City Council. 135p.

Vant, W.N., Williams, B L. 1992. Residence times of Manukau Harbour, New Zealand. New Zealand Journal of Marine and Freshwater Research 26: 393–404.

Williamson, R.B., Hickey, C.W., Robertson, B.M. 2017. Preliminary assessment of limits and guidelines available for classifying Auckland coastal waters. Prepared by Diffuse Sources, NIWA and Wriggle Coastal Management for Auckland Council. Auckland Council technical report, TR2017/035.

Appendix A - Paper presented at Coast and Ports Conference 2013, Sydney.

Hydrodynamic and Sedimentation Behaviour within Porirua Harbour, New Zealand – Development of a Hydrodynamic and Sediment Transport Model for Multiple Parties and Studies.

Ben Tuckey

DHI New Zealand, Auckland, New Zealand.

Abstract

Porirua Harbour is located on the south-western coast of the North Island of New Zealand, north of Wellington. The harbour contains two arms, Onepoto Arm to the south and Pauatahanui Inlet to the northeast. Pauatahanui Inlet contains an environmentally sensitive wetland area. The current high sedimentation rates within Porirua Harbour are concerning to local authorities and the local community.

A new motorway, known as the Transmission Gully Motorway, has been proposed by the New Zealand Transit Agency, to alleviate traffic congestion and provide a more robust access to Wellington in the event of a major emergency. Some rivers and streams within the catchments of certain sections of the proposed motorway discharge into Porirua Harbour. A study was commissioned to assess the impact of construction works on the sedimentation rates and patterns within the harbour.

Terrestrial sediment loads were provided for specified rainfall events for both existing and construction situations. To predict the fate of sediment discharged into Porirua Harbour for these specified rainfall events with different predominant wind conditions, DHI developed a sediment transport model. The model was validated with data from an extensive data collection campaign, with a reasonable agreement between observations and predictions obtained. Predictions from the model were utilised by ecologists to predict the effects of the additional sediment loads on the ecology within the harbour.

Porirua City Council commissioned a study utilising the existing sediment transport model to investigate whether dredging sand from the flood tide delta within Pauatahanui Inlet will encourage the flushing of silt/clay from terrestrial sources out of the harbour.

This paper shows a good example of successful collaboration across Agencies/Territorial Authorities and provides a successful example where a numerical model is used for multiple parties and studies.

Keywords: sediment transport, estuaries, numerical modelling.

1. Introduction

Porirua Harbour is a natural inlet which is located on the south-western coast of the North Island of New Zealand, north of Wellington. Porirua, one of the four cities within the Wellington region, is located to the south of the harbour.

The harbour has an entrance only approximately 150 m in width, close to the suburb of Plimmerton. It opens up into two arms; Onepoto Arm to the south which has an area of 283 ha (35% of the total harbour area) of which approximately 80% is sub-tidal; and the north-eastern arm, Pauatahanui Inlet, is 524 ha (65% of the total harbour area), of which approximately 60% is sub-tidal.

Pauatahanui Inlet is recognised for its high ecological, aesthetic and recreational values. The wetland within Pauatahanui Inlet located close to where Pauatahanui Stream is the largest remaining estuarine wetland in the lower North Island. There are ongoing efforts to reduce human impact on the wetland and to restore damaged areas. Figure 1 presents an overview of the harbour.

Figure 1. Overview of Porirua harbour.

The harbour has historically been affected by the impact of both rural and urban development with significant increases in sediment loads from the surrounding catchments. The current high sedimentation rates within Porirua Harbour are concerning to local authorities and the local community. Between 1974 - 2009, the net average deposition rates

within Pauatahanui Inlet were 9.1 mm/year and within Onepoto Arm were 5.7 mm/year. Since 1974, the tidal prism for Pauatahanui Inlet has reduced by 8.7% and 1.7% in Onepoto Arm. At current sedimentation rates, Pauatahanui Inlet will fill in during the next 145 – 195 years and the Onepoto Arm will fill in during the next 290 – 390 years [1].

A new motorway, known as the Transmission Gully Motorway, has been proposed by the New Zealand Transit Agency (NZTA), to alleviate traffic congestion and provide a more robust access to Wellington in the event of a major emergency. Some rivers and streams within the catchments of certain sections of the proposed motorway discharge to Porirua Harbour. The proposed location for Transmission Gully Motorway is shown in Figure 2.
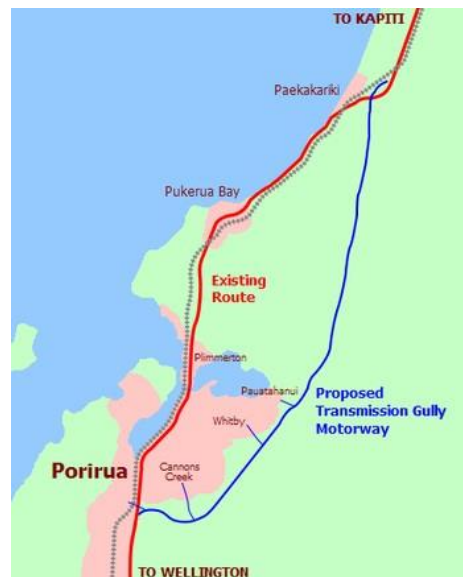
Figure 2. Proposed location for Transmission Gully Motorway.

DHI and Sinclair Knight Merz (SKM) were commissioned by NZTA to undertake a numerical modelling study to assess the impact of construction works of the motorway on the sedimentation rates and patterns within the harbour.

Porirua City Council (PCC) commissioned the collection of a comprehensive detailed bathymetry of the harbour in 2009 [2]. An agreement was made between NZTA and PCC that if the bathymetry data could be utilised for the development of a sediment

transport model for the harbour, NZTA and PCC would jointly own the model.

After the completion of the Transmission Gully Motorway study for NZTA, Porirua City Council commissioned DHI to carry out a study utilising the existing sediment transport model to investigate whether dredging sand from the flood tide delta within Pauatahanui Inlet, will encourage the flushing of silt/clay from terrestrial sources out of the harbour.

2. Data Collection

As outlined above, Discovery Marine Limited (DML) undertook a detailed bathymetric survey for the harbour and its approaches in 2009 [2].

A comprehensive field campaign was carried out by the Cawthron Institute (Cawthron) for the period, 13th January to 3rd March 2010, to obtain a data set suitable for constructing a detailed sediment transport model of the study area. An additional field campaign was undertaken by Cawthron, for the period, 1st July to 1st October 2010. Water level data was also available from a previous study at three locations, while there is a permanent water level gauge at Mana Marina in the entrance to the harbour. An overview of the hydrodynamic and Total Suspended Sediment (TSS) data available for the study is presented in Figure 3. An extensive grab sampling exercise was also undertaken by Cawthron with samples obtained from twenty locations within the harbour and the approaches to the harbour.
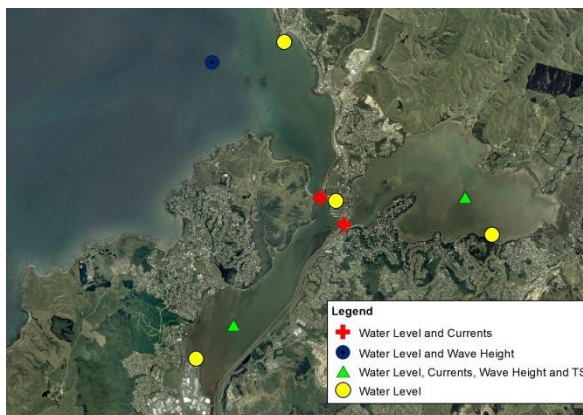
Figure 3. Available data collection overview.

For the first data collection campaign, the instrument locations were selected to

provide information on currents and water levels, wave heights and sediment size distribution throughout the whole study area, including the approaches to the harbour; the entrance to the harbour; and within the harbour arms. At the location of the current and water level measurements within the harbour and Pauatahanui Inlet entrances, ADCP flow transects were also carried out for a full tidal cycle to measure the flow into and out of the harbour and Pauatahanui Inlet.

TSS data was only collected within the arms of the harbour as the study focused on the fate of terrestrial sourced sediment within the harbour and not marine sourced sediment.

A second data collection campaign was undertaken by Cawthron, for the period, 1st July to 1st October 2010, since there were only a few significant wind and rainfall events that occurred during the initial data collection campaign. The data collected in the second campaign focused only on the arms of the harbour, since the data from the first campaign was considered sufficient for calibrating the hydrodynamic model. The data from the second campaign which recorded more significant storm events was used to calibrate the wave and sediment transport models.

3. Sediment Transport Model

A sediment transport model was developed by coupling hydrodynamic (MIKE 21 HD) [3], wave (MIKE 21 SW) [4] and sediment transport (MIKE 21 MT) [5] models using a Flexible Mesh (FM).

3.1   Model Set Up

The model bathymetry, mesh and extent are shown in Figure 4.
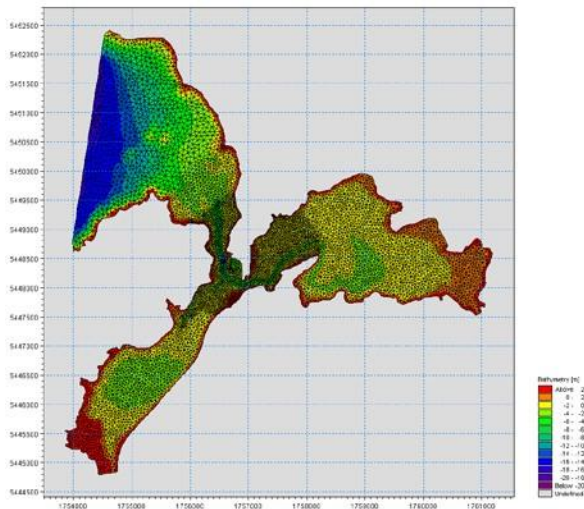
Figure 4. Model bathymetry, mesh and extent (Mean Sea Level).

3.2 Model Calibration / Validation

The hydrodynamic and wave components of the sediment transport model were calibrated using the hydrographic data collected by Cawthron in the vicinity of the harbour mouth and within the harbour arms.

To validate that the model was able to correctly reproduce the tidal prism for Porirua Harbour, the predicted discharge through the main harbour entrance and Pauatahanui Inlet entrance, was compared against discharges that were measured through both entrances 26th February 2010. There was a very good agreement between observed and predicted flow as shown in Figure 5.

The sediment transport model was validated using TSS data collected within the harbour arms. Events were selected when significant suspension of sediment occurred due to wind / wave events or sediment was supplied from significant freshwater inflows to the harbour. An example of one of the validation periods and the agreement between observed and predicted TSS is shown in Figure 6.
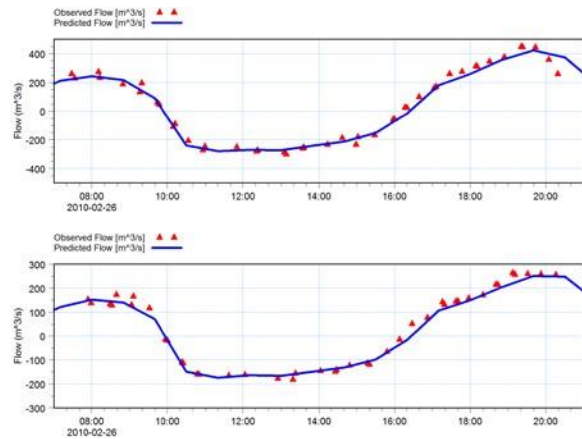
Figure 5. Comparison of observed and predicted flow through main harbour entrance (top) and Pauatahanui Inlet entrance (bottom).
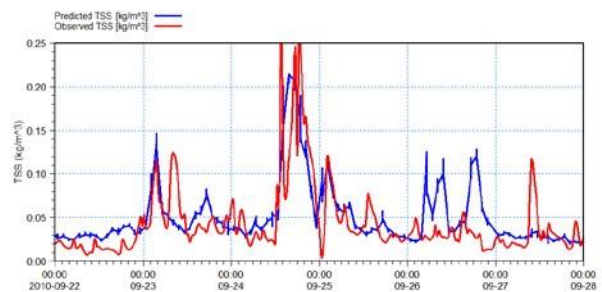
Figure 6. Comparison of observed and predicted TSS for Pauatahanui Inlet.

4. Assessment of Effects for Construction of Transmission Gully Motorway

The sediment transport model was used to carry out both event based and long term assessments to determine the impact of increased sediment loads which may occur during the construction of the proposed Transmission Gully motorway.

Freshwater inflows and the associated sediment loads (combination of mud and sand) were provided by SKM for the event based and long term scenarios [6].

The motorway is likely to take six years to construct. The likely construction programme for the Transmission Gully Project was predicted by Macdonald International. They predicted that the duration of construction within any of the major stream catchments feeding into the harbour is likely to be between two to four years with the peak of construction (period when greatest area of open earthworks exposed) likely to occur over a two year period.

4.1   Event Based Scenarios

A total of 12 event based scenarios were defined by the project team for investigation. The scenarios were a combination of three different predominant wind conditions as determined by local wind records (calm, 90th percentile south-south easterly wind (herein called a southerly wind) and a 90th percentile north-north westerly wind (herein called a northerly wind)) and different rainfall events occurring within the surrounding catchments of the harbour arms.

The following scenarios were defined for the rainfall events occurring within the surrounding catchments:

- Ten year annual recurrence interval (ARI) rainfall event in the Porirua and Kenepuru catchments only with two year ARI rainfall event elsewhere.
- Ten year ARI rainfall event in the Pauatahanui and Duck catchments only with two year ARI rainfall event elsewhere.
- Ten year ARI rainfall event in the Horokiri catchment only with two year ARI rainfall event elsewhere.
- Two year ARI rainfall event in all catchments.

The Kenepuru, Duck and Horokiri catchments were identified as the major stream catchments feeding into the harbour which will have significant open earth works during the construction of the motorway. Figure 7 provides an overview of the catchments surrounding the harbour and the locations for the peak of motorway construction.
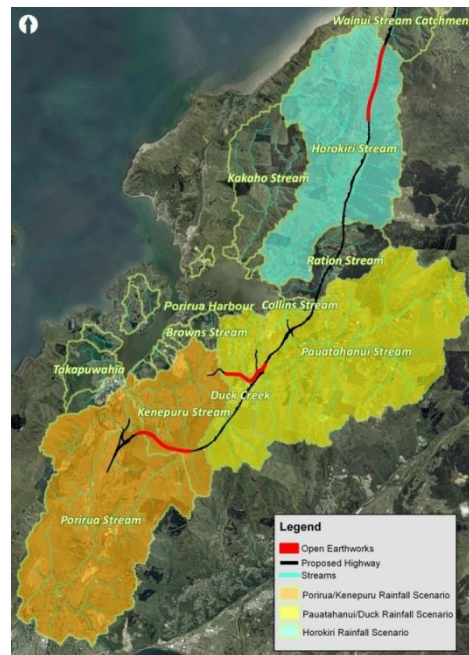
Figure 7. Catchments surrounding the harbour and the locations for the peak of motorway construction.

The sediment loads entering the harbour from the surrounding catchments were calculated for the rainfall scenarios above. For both the two and ten year rainfall events, it was predicted that sediment loads are likely to increase by 11%, 17% and 15% in the Kenepuru, Duck and Horokiri catchments respectively for the peak construction period, with no change in the other catchments.

Results from the model simulations such as bed deposition after one and three days and TSS after one and three days were provided to ecologists at Boffa Miskell (BML), as part of their ecological assessment of the impact of additional sediment loads to the estuary from the construction of Transmission Gully [7].

An example of the bed deposition after three days from a ten year ARI rainfall event in Pauatahanui and Duck Catchments, and a two year ARI event elsewhere with a 90th percentile southerly wind for the existing scenario is presented in Figure 8. The difference in bed deposition between existing and construction scenarios is presented in Figure 9.
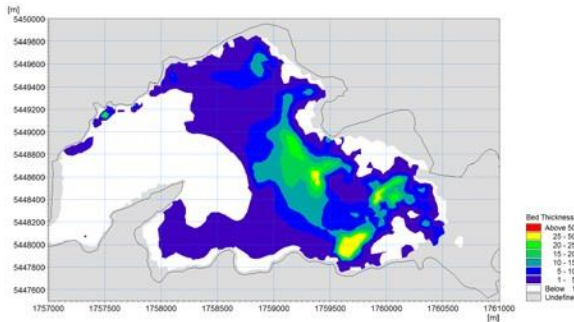
Figure 8. Bed deposition after three days from a ten year ARI rainfall event in Pauatahanui and Duck Catchments, and a two year ARI events elsewhere with a 90th percentile southerly wind for the existing scenario.
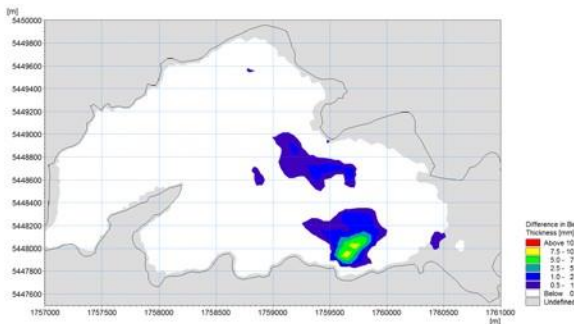
Figure 9. Difference in bed deposition after three days from a ten year ARI rainfall event in Pauatahanui and Duck Catchments, and a two year ARI events elsewhere with a 90th percentile southerly wind, comparing construction and existing scenarios.

4.2   Long Term Assessment

In addition to the event based scenarios, a twenty year long term simulation was undertaken with and without the motorway construction, to quantify the long term effects of the additional sediment from the construction. For the long term assessment, historical rainfall and wind data was used. A coarser resolution model was required due to the long run time of the long term simulations.

The model results indicated that over the twenty year simulation period, the construction of the motorway is likely to have no detectable impact on sedimentation rates within the Onepoto Arm, but is likely to increase the sedimentation within Pauatahanui Inlet by 0.1 and 0.2 mm/year (compared with current sedimentation rate of 9.1 mm/year).

5. Assessment of Effects of Dredging Channel/s through Existing Flood Tide Delta

The existing Porirua Harbour sediment transport model was utilised to assess whether dredging of the flood tide delta would encourage erosion of the muddy basin in the middle of Pauatahanui Inlet or reduce deposition of mud in the central muddy basin during a large flood event [8].

The perception from the local community is that dredging within Pauatahanui Inlet will increase the tidal flushing within the inlet. In reality dredging can only, at the most, change the current patterns within the inlet, since even if the whole of the flood tide delta was removed via dredging, the calculated increase in the tidal prism would be approximately 2% (based on calculated existing tidal volume of 5,184,000 m^3 and dredged volume of 92,000 m^3 to dredge flood tide delta to Mean Low Water Springs (MLWS)). This would not be sufficient to alter the flushing capacity of the inlet.

The only way to significantly increase the tidal flushing of the inlet, would be to either dredge the intertidal regions around the fringes of the inlet, resulting in a maximum increase in the tidal prism of approximately 13% (based on a dredged volume of 676,000 m^3 to dredge the inter tidal regions to MLWS), or increase the surface area of the inlet, both of which are not feasible for logistical, financial and ecological reasons.

The main objective of any realistic dredging in Pauatahanui Inlet would therefore be to modify the current patterns and corresponding sedimentation behaviour within the inlet. Two proposed dredging options were developed in conjunction with PCC:

• dredging existing channels in north west of inlet (Dredging Option One); and
• continuation of the main channel through the flood tide delta (Dredging Option Two).

The model bathymetries for Pauatahanui Inlet that were used for the assessment are presented in Figure 10.

5.1 Impact of Dredging on Central Muddy Basin

The sediment transport model was applied to provide a qualitative indication of whether dredging a channel/s through the flood tide delta would encourage the erosion of the existing central muddy basin within Pauatahanui Inlet.

Figure 10. Pauatahanui Inlet model bathymetry (MSL) – existing (top), Dredging Option One (middle) and Dredging Option Two (bottom).

Both dredging options were shown to have minimal impact on the central muddy basin in Pauatahanui Inlet, with only some erosion occurring at the end of the new channel for Dredging Option Two.

The reason there was minimal impact was that for the muddy basin to erode, current velocities would have to be increased in the vicinity of the central basin. Although it was predicted that the dredging options would change the current pattern (see Figure 11 for example), it would not significantly increase the current velocities, except at the end of the new channel for Dredging Option Two, where the maximum current speed is increased from approximately 0.15 m/s to 0.25 m/s and erosion of the muddy basin is predicted to occur.

5.2 Impact of Dredging on Terrestrial Sediment Entering into Pauatahanui Inlet

The sediment transport model was applied to predict whether dredging of a channel/s through the flood tide delta would keep mud which enters into Pauatahanui Inlet during significant flood events in suspension and not allow the sediment to settle in the central muddy basin as occurs currently.

Figure 11. Maximum current speed for existing situation (top) and Dredging Option Two (bottom) with calm wind condition.

A ten year ARI rainfall event for the Pauatahanui and Duck catchments with associated sediment loads timed to coincide with a spring tide was simulated. Three wind conditions were investigated, a calm condition and the two predominant wind conditions outlined in Section 4.1).

The model results (see Figure 12 for example) indicated that although dredging of the flood tide delta has an impact on the sedimentation patterns of the mud which enters into the inlet, the mud will still

deposit within the inlet, since the current velocities would not be increased significantly enough compared with the existing situation, to keep the mud in suspension and allow the mud to be flushed out of the harbour.

6. Summary

DHI were commissioned by NTZA to develop a sediment transport model of Porirua Harbour able to predict the sedimentation behaviour of terrestrial sourced sediments within the harbour. The model was calibrated / validated with an extensive data collection campaign.

The model was utilised to predict the likely impacts of additional sediment loads to the harbour resulting from the construction of the proposed Transmission Gully Motorway.

PCC commissioned DHI to assess whether dredging channels through the existing flood tide delta in Pauatahanui Inlet are likely to encourage the flushing of terrestrial sourced sediment out of the harbour.

7. Acknowledgements

The author wishes to thank New Zealand Transit Agency and Porirua City Council for allowing this work to be presented and Sinclair Knight Merz for provision of freshwater and sediment loads for the study.
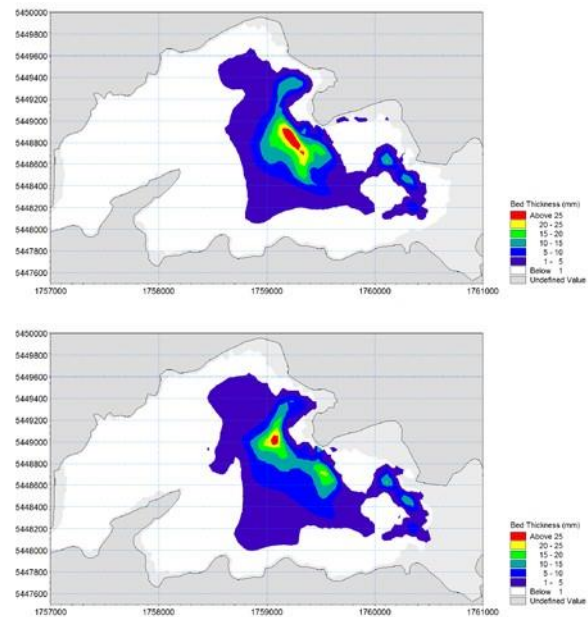
Figure 12. Sedimentation pattern of mud from 10 year ARI rainfall event in Pauatahanui catchment with southerly 90th percentile wind condition for existing situation (top) and dredging option two (bottom).

8. References

[1] Gibb, J.G and Cox G.J, (2009); Patterns and Rates of Sedimentation within Porirua Harbour. Report prepared for Porirua City Council.
[2] DML (2009); Porirua Harbour Survey Report of Survey. Report prepared for Porirua City Council.
[3] DHI (2012), *MIKE 21 & MIKE 3 Flow Model FM, Mud Transport Module, Scientific Documentation*, Hørsholm, Denmark.
[4] DHI (2012), *MIKE 21, Spectral Wave Module, Scientific Documentation*, Hørsholm, Denmark.
[5] DHI (2012), *MIKE 21 & MIKE 3 Flow Model FM, Hydrodynamic and Transport Module, Scientific Documentation*, Hørsholm, Denmark.
[6] DHI and SKM (2011). *Transmission Gully Project, Assessment of Water Quality Effects, Technical Report 15*. Report prepared for NZTA.
[7] BML (2011). *Transmission Gully Project, Ecological Impact Assessment, Technical Report 11*. Report prepared for NZTA.
[8] DHI (2011). *Porirua Harbour - Assessment of Effects on Hydrodynamics from Proposed Dredging*. Report prepared for PCC.

Appendix B – Metal Model Methodology

The metal accumulation model works at a subestuary scale to derive an equilibrium metal concentration. Thus, for each subestuary the following methodology is applied.

It is assumed that there is a surface mixed layer on seabed that is uniformly mixed to a depth of λ (m) during each year by a combination of physical and bioturbation processes. Thus, at the end of each year, the sediment in the surface mixed layer consists of the sediment deposited from the catchment mixed uniformly with the existing bed sediments.

The mass of catchment derived sediment that accumulates on the seabed (S) over the course of a year is given by:

$$S_c = \rho\eta \text{ (kg/m}^2) \tag{1}$$

where η is the sediment deposition rate (m/y) derived from the sediment transport model (e.g. Table 6-3) and ρ is the density (kg/m^3) of the bed sediments (assumed to be 1200 kg/m^3).

At the end of the year (t = 1) the sediment in the surface mixed layer consists of the catchment derived sediment deposited during the year mixed uniformly to a depth of $(\lambda - \eta)$ metres with pre-existing sediments. Hence, at the end of the year, the mass of sediment per unit area of seabed exhumed to a depth of $(\lambda - \eta)$, metres is given by:

$$S_e = \rho(\lambda - \eta) \text{ (kg/m}^2) \tag{2}$$

The total mass of sediment per unit area of seabed in the surface mixed layer at the end of the year (S_t) is given by the sum of sediment deposited (S_c) and sediment exhumed (S_e):

$$S_t = \rho\eta + \rho(\lambda - \eta) \text{ (kg/m}^2) \tag{3}$$

Assuming that the catchment derived sediment deposited during the course of the year carries metal at a concentration of C_c (kg metal / kg sediment), the mass of catchment derived metal that accumulates on the seabed per unit area of seabed over the year is:

$$M_c = \rho\eta C_c \text{ (kg)} \tag{4}$$

At the beginning of the simulation period (time = 0) the metal concentration in the seabed surface mixed layer is C_0 (kg metal / kg sediment). The mass of metal per unit area of seabed that is exhumed from below during the year is:

$$M_e = \rho(\lambda - \eta)C_0 \text{ (kg)} \tag{5}$$

Hence, the total mass of metal in the surface mixed layer at the end of the year is:

$$M_t = \rho[\eta C_c + (\lambda - \eta)C_0] \text{ (kg)} \tag{6}$$

The metal concentration in the surface mixed layer at the end of the year, C_1, is given by the total mass of metal in the surface mixed layer (M_t) divided by the total mass of sediment in the surface mixed layer:

$$C_1 = \frac{\rho[\eta C_c + (\lambda - \eta)C_0]}{\rho\lambda} \text{ (kg metal/kg sediment)} \tag{7}$$

Which reduces to:

$$C_1 = \frac{[\eta C_c + (\lambda - \eta)C_0]}{\lambda} \text{ (kg metal/kg sediment)} \tag{8}$$

For the following year, the initial concentration (C_0) becomes the predicted concentration at the end of year C_1, hence:

$$C_2 = \frac{[\eta C_c + (\lambda - \eta)C_1]}{\lambda} \text{ (kg metal/kg sediment)} \tag{9}$$

Catchment sediment and metal load data is used to define the source concentration for each of the subcatchments (Figures 3-1 and 3-3). Outputs from the sediment transport model are used to determine the contribution that each subcatchment makes to the overall deposition in each subestuary (Table 6-12 and Table 6-13). For each subestuary (Figure 6-21), C_c can then be derived by summing the percent contribution to the overall deposition of each subcatchment by the predicted subcatchment source concentration. For example, for the Porirua subestuary the data in Table A-1 shows how an overall catchment derived metal concentration (C_c) of 805 mg/kg can be determined for this subestuary.

Repeating this calculation for each subestuary we derive C_c for each subestuary.

Data from the sediment transport model is used to define η for each subestuary (e.g. Table 6-3) and global values of C_o and λ are assumed based on observations.

Zinc and Copper concentrations in the surface mixed layer of each subestuary are then derived starting with equation 8 and iterating equation 9 over a 100-year interval.

Table B-1.   Example of the calculation of C_c for the Porirua subestuary.

Subcatchment	Zn Source concentration (mg/kg) from Error! Reference source not found.	Percentage contribution to overall deposition (derived from Table 6-12)	Individual contribution to C_c (mg/kg)
Whitby to Browns Bay	1536	0.001%	0.008
Pauatahanui village	575	<0.001%	<0.001
Lower Duck Creek	332	0.002%	0.006
Horokiri	70	0.004%	0.003
Kakaho	99	0.002%	0.002
Onepoto fringe Elsdon	6511	1.065%	69.372
Direct to Onepoto (South)	369	0.005%	0.018
Next to Mahinawa	5425	0.006%	0.341
Hukarito	1230	0.003%	0.032
Kahetoa (Onepoto Park)	7915	<0.001%	0.036
Whitireia/Te Onepoto	367	<0.001%	0.001
Direct to Onepoto (North)	4533	<0.001%	0.019
Direct to Onepoto (Mid)	2890	0.001%	0.021
Pauatahanui mouth	57	0.007%	0.004
Direct to Pauatahanui (Mid)	11184	0.000%	0.002
Motukaraka	1101	<0.001%	<0.001
Direct to Pauatahanui (Water ski club)	925	<0.001%	<0.001
Direct to Pauatahanui (Boat houses)	12211	<0.001%	0.002
Porirua Mouth	744	98.904%	735.353
Ration	57	<0.001%	<0.001

Appendix C – Depositional Footprint

The following figures provide the estimated sediment deposition footprint for each of the individual catchment outlets. The colour scale is logarithmic ranging from very low values of less than 0.005 kg/m^2 (equivalent to less than 0.01 mm) through to more than 2 kg/m^2 (equivalent to more than 5 mm of deposition).
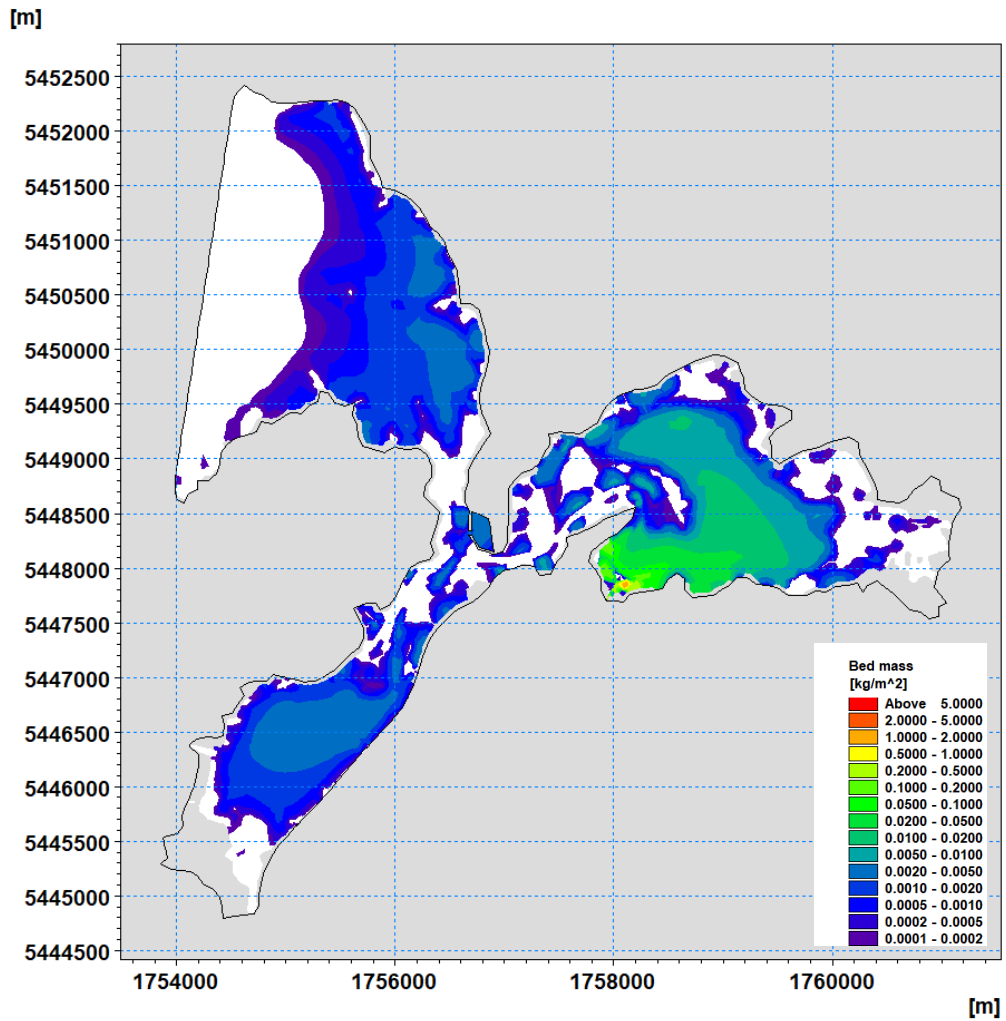
Figure C-1.   Predicted sediment depositional footprint for the Whitby to Browns Bay subcatchment. Graduated colour scale represents the mass of subcatchment deposited on the seabed (kg/m²) over the duration of the 2010 model simulation. 5mm of deposition).
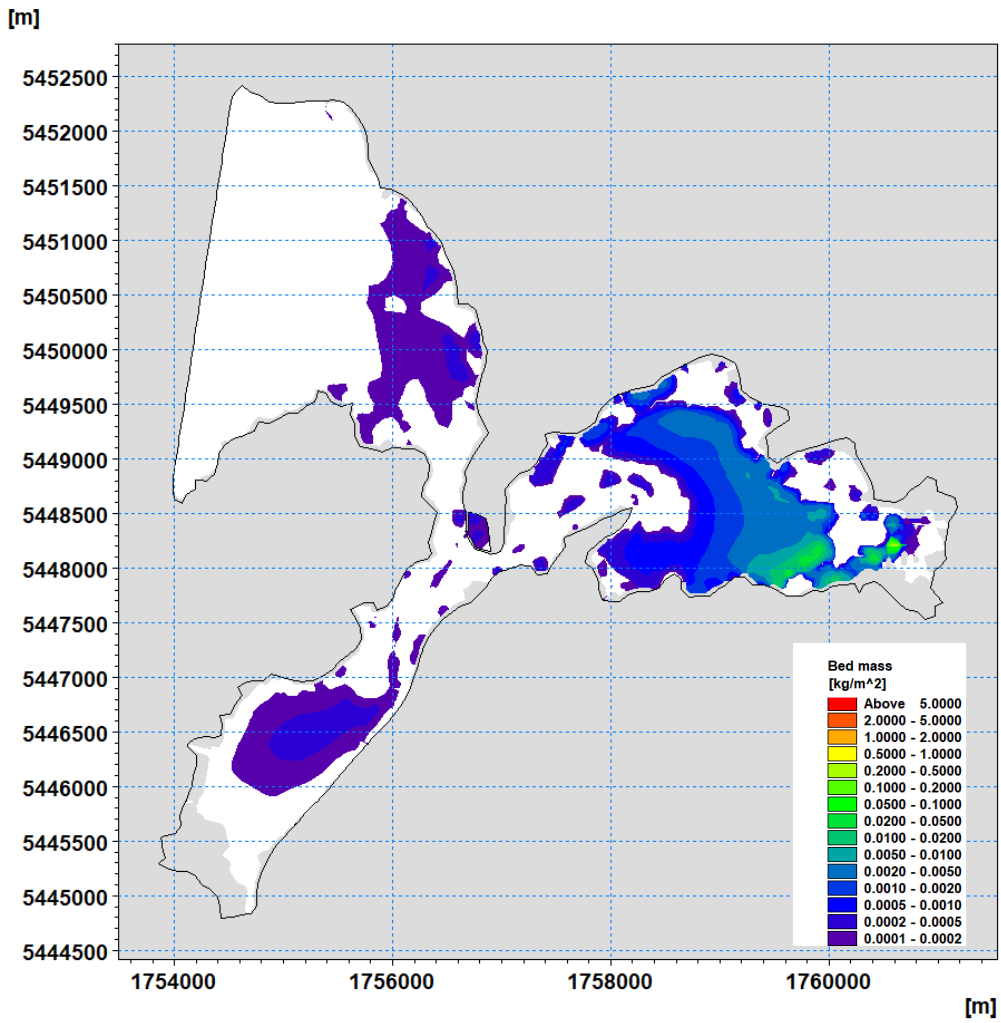
Figure C-2.   Predicted sediment depositional footprint for the Pauatahanui village subcatchment. Graduated colour scale represents the mass of subcatchment deposited on the seabed (kg/m2) over the duration of the 2010 model simulation.
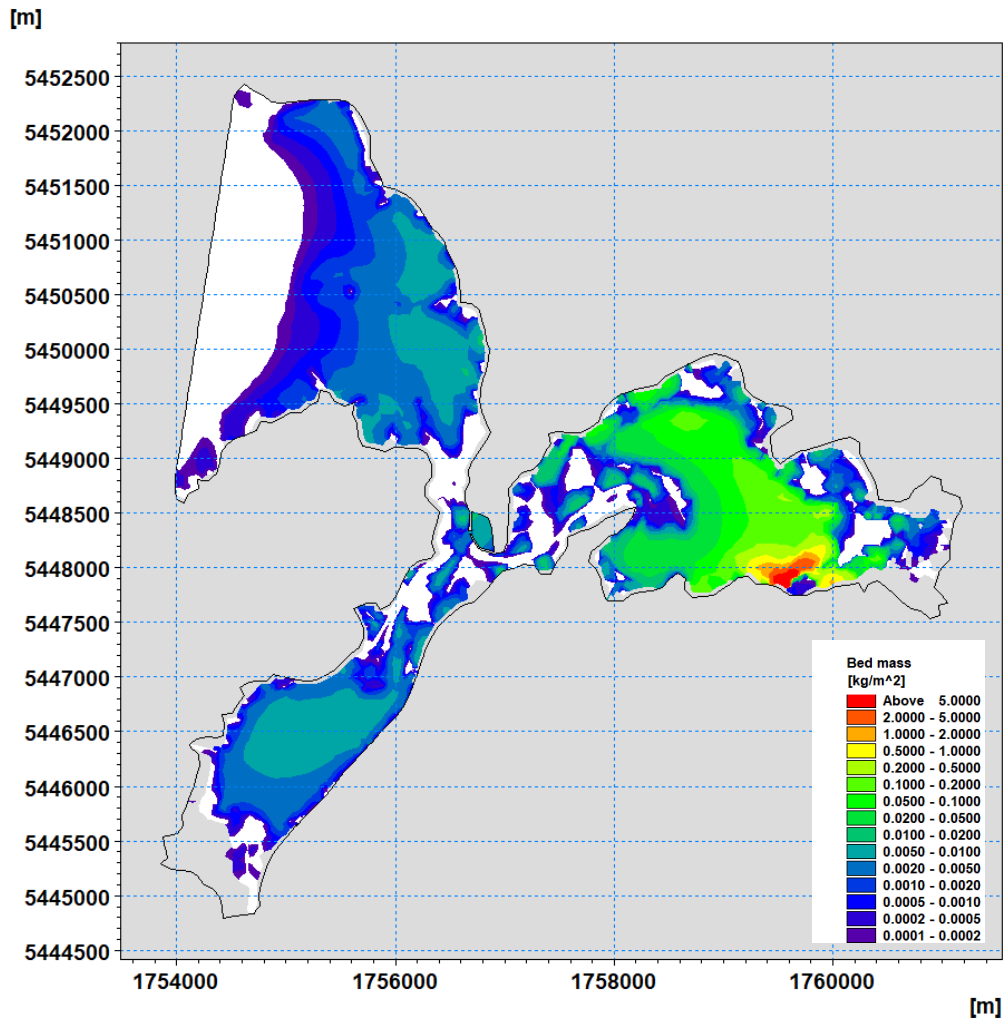
Figure C-3.   Predicted sediment depositional footprint for the Lower Duck Creek subcatchment. Graduated colour scale represents the mass of subcatchment deposited on the seabed (kg/m2) over the duration of the 2010 model simulation.
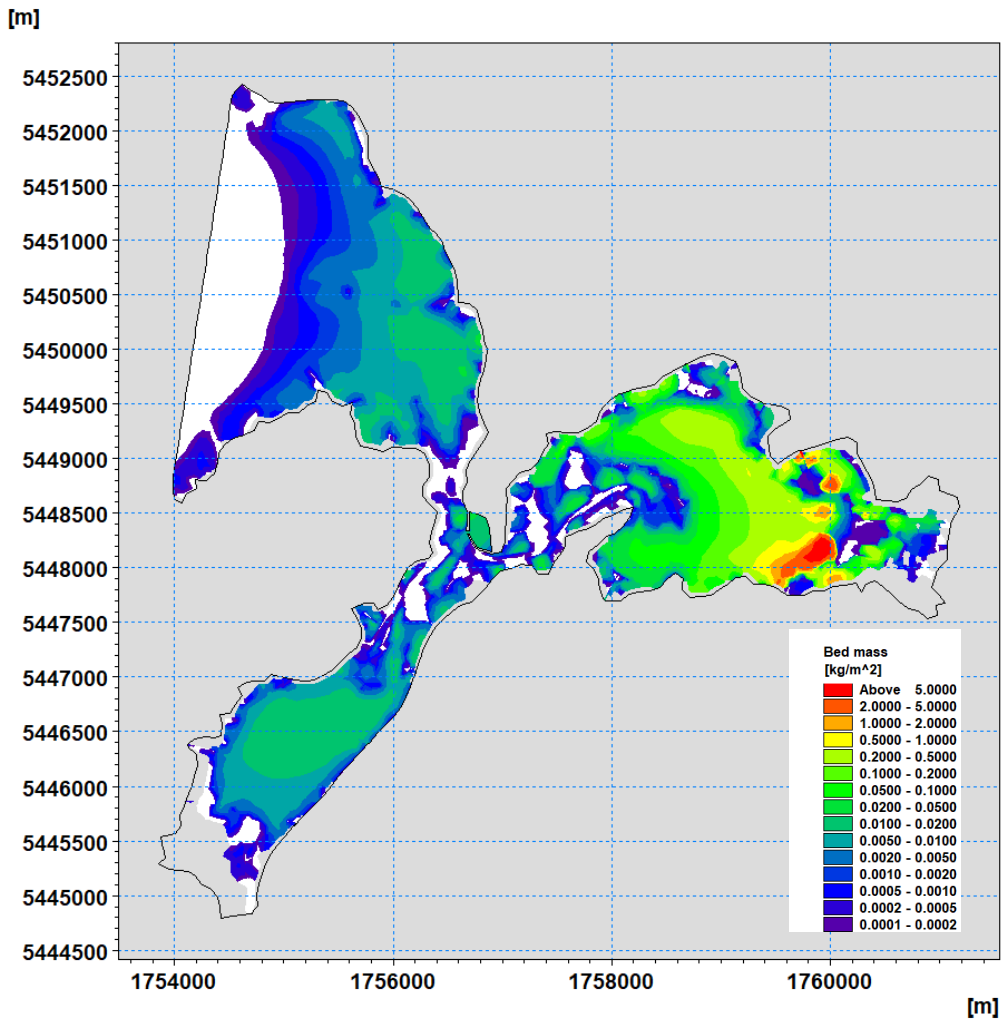
Figure C-4. Predicted sediment depositional footprint for the Horokiri subcatchment. Graduated colour scale represents the mass of subcatchment deposited on the seabed (kg/m2) over the duration of the 2010 model simulation.
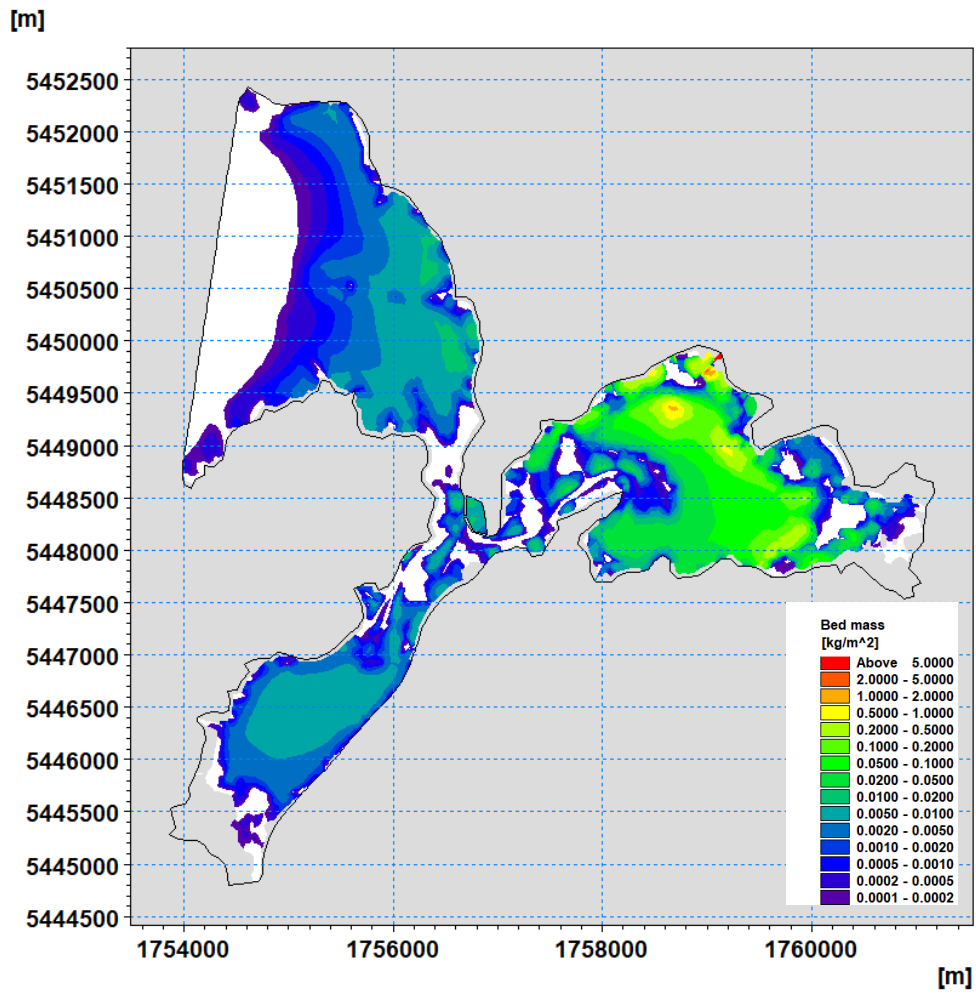
Figure C-5.   Predicted sediment depositional footprint for the Kakaho subcatchment. Graduated colour scale represents the mass of subcatchment deposited on the seabed (kg/m2) over the duration of the 2010 model simulation.
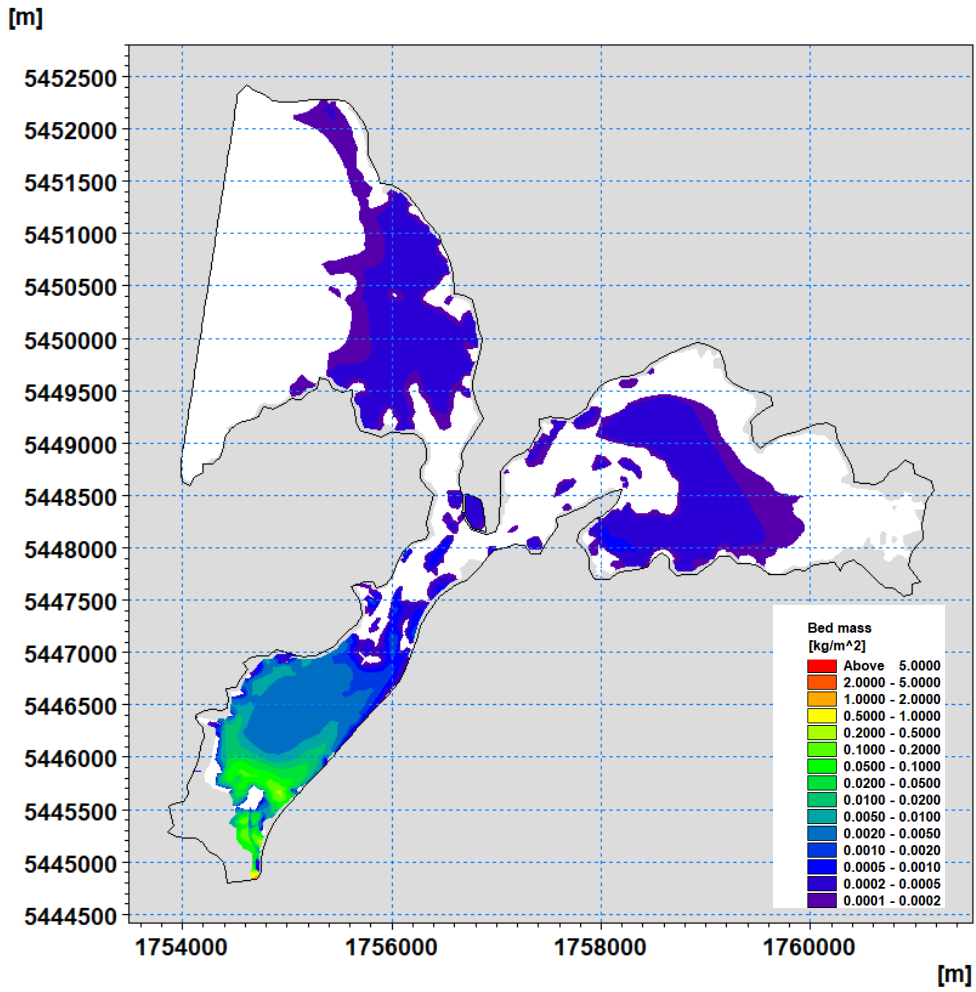
Figure C-6.   Predicted sediment depositional footprint for the Onepoto fringe Elsdon subcatchment. Graduated colour scale represents the mass of subcatchment deposited on the seabed (kg/m2) over the duration of the 2010 model simulation.
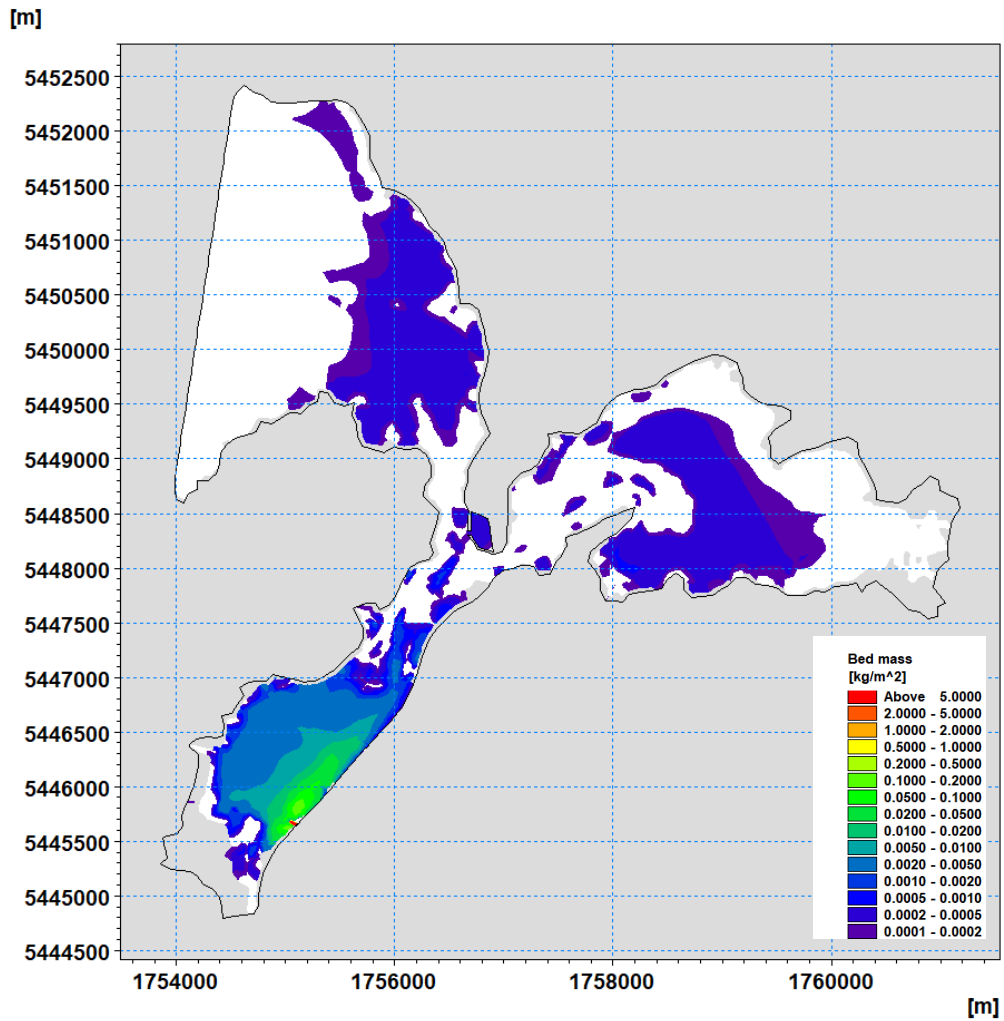
Figure C-7. Predicted sediment depositional footprint for the Direct to Onepoto (South) subcatchment. Graduated colour scale represents the mass of subcatchment deposited on the seabed (kg/m2) over the duration of the 2010 model simulation.
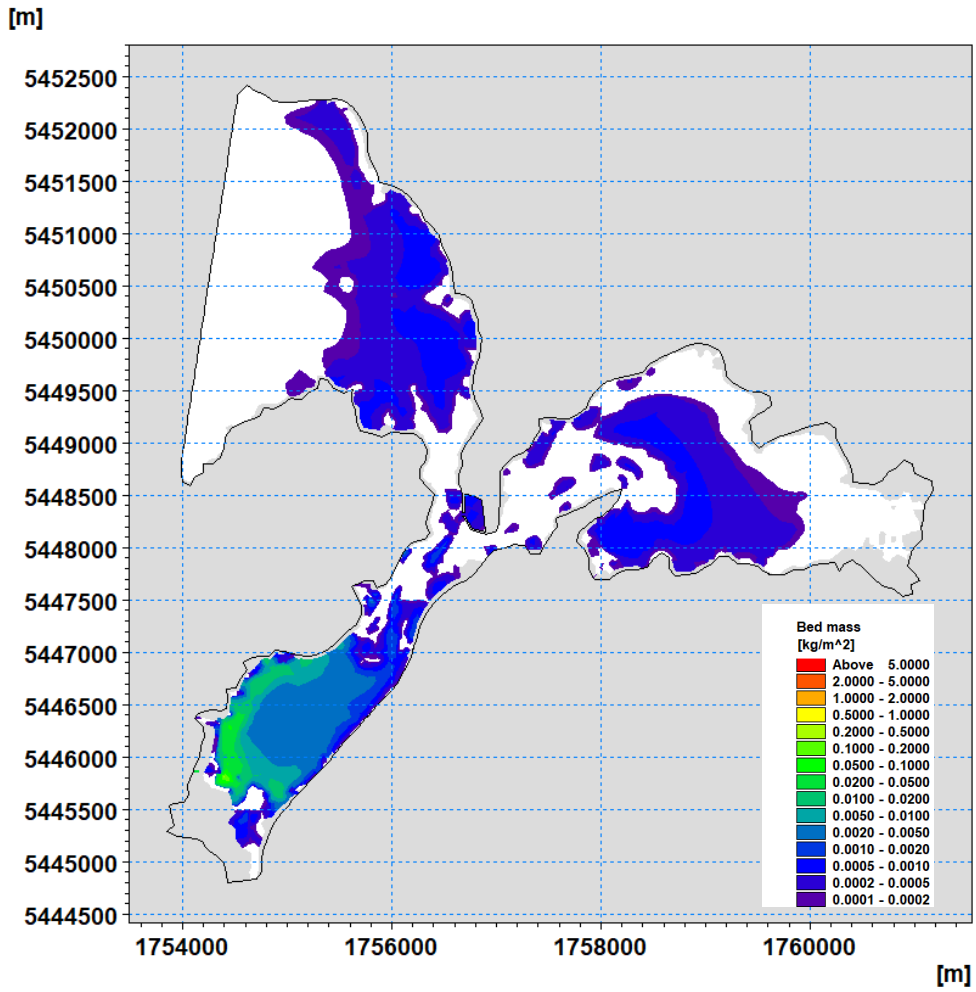
Figure C-8. Predicted sediment depositional footprint for the Next to Mahinawa subcatchment. Graduated colour scale represents the mass of subcatchment deposited on the seabed (kg/m2) over the duration of the 2010 model simulation.
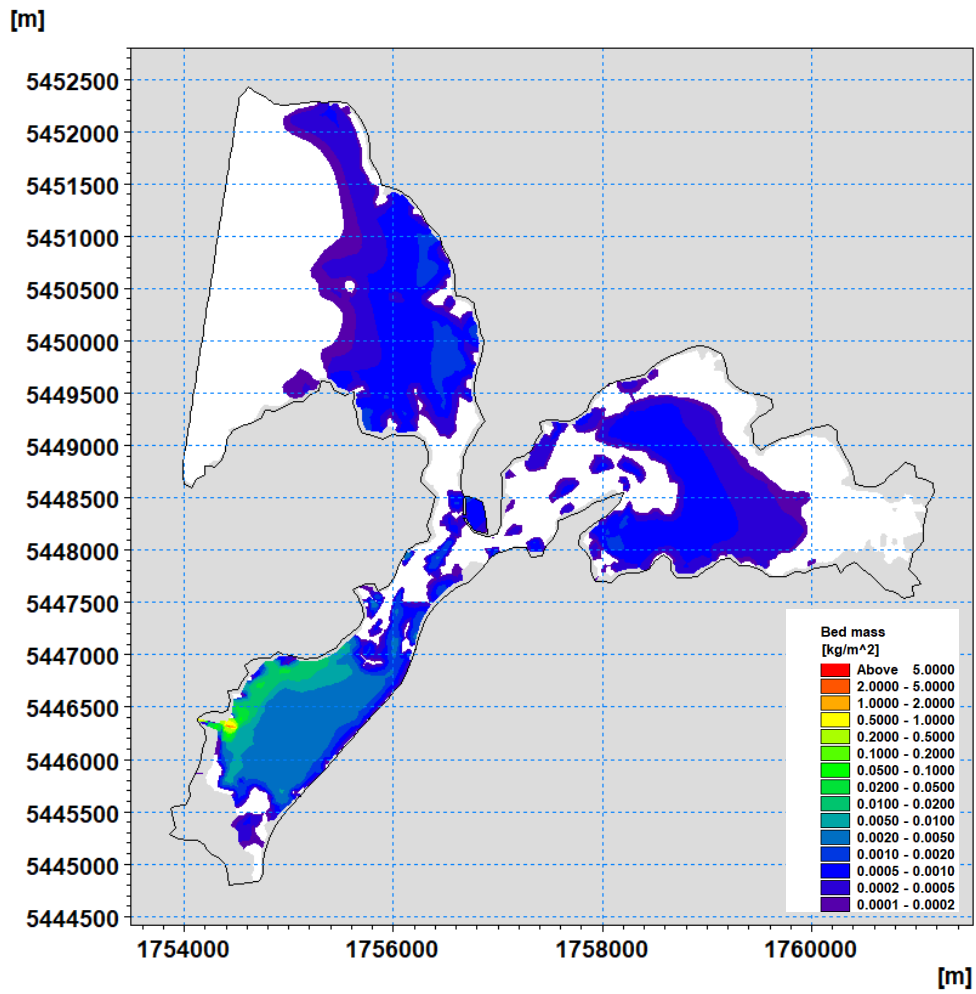
Figure C-9.   Predicted sediment depositional footprint for the Hukarito subcatchment. Graduated colour scale represents the mass of subcatchment deposited on the seabed (kg/m2) over the duration of the 2010 model simulation.
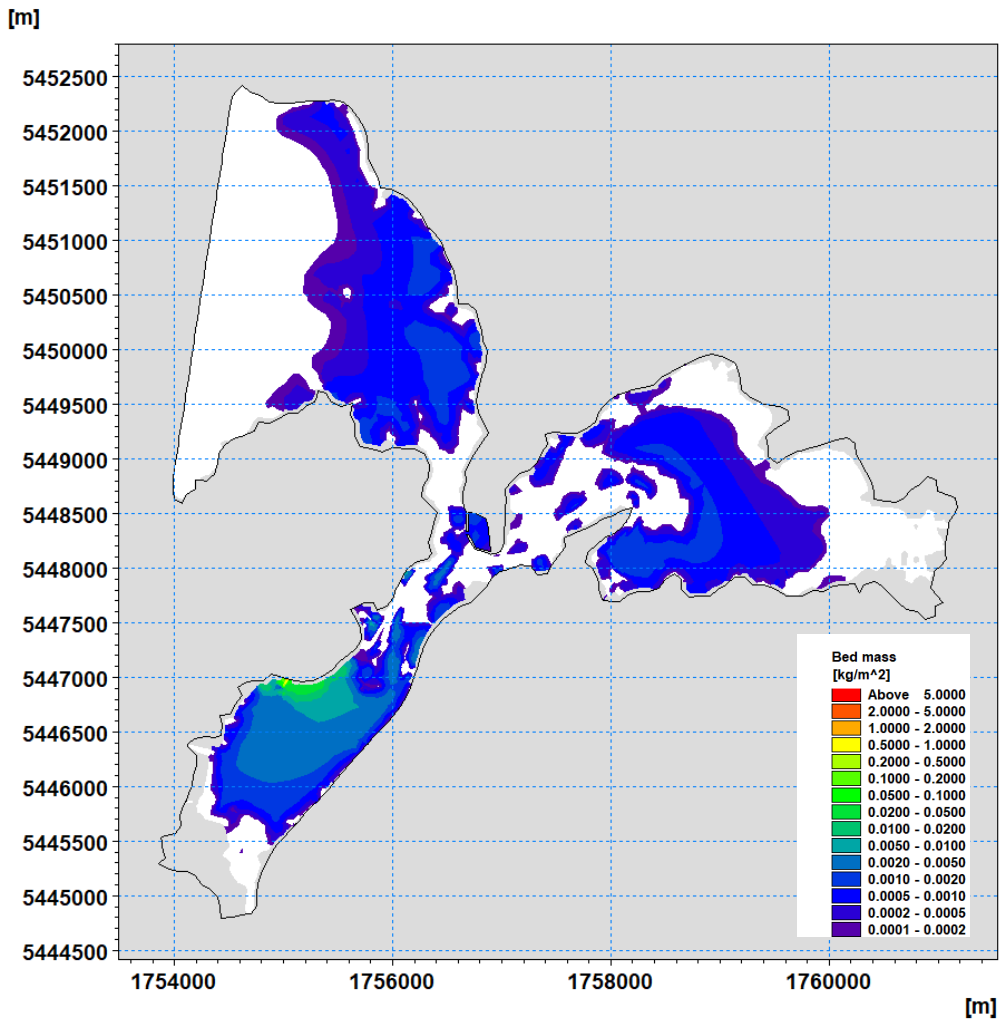
Figure C-10. Predicted sediment depositional footprint for the Kahetoa (Onepoto Park) subcatchment. Graduated colour scale represents the mass of subcatchment deposited on the seabed (kg/m2) over the duration of the 2010 model simulation.
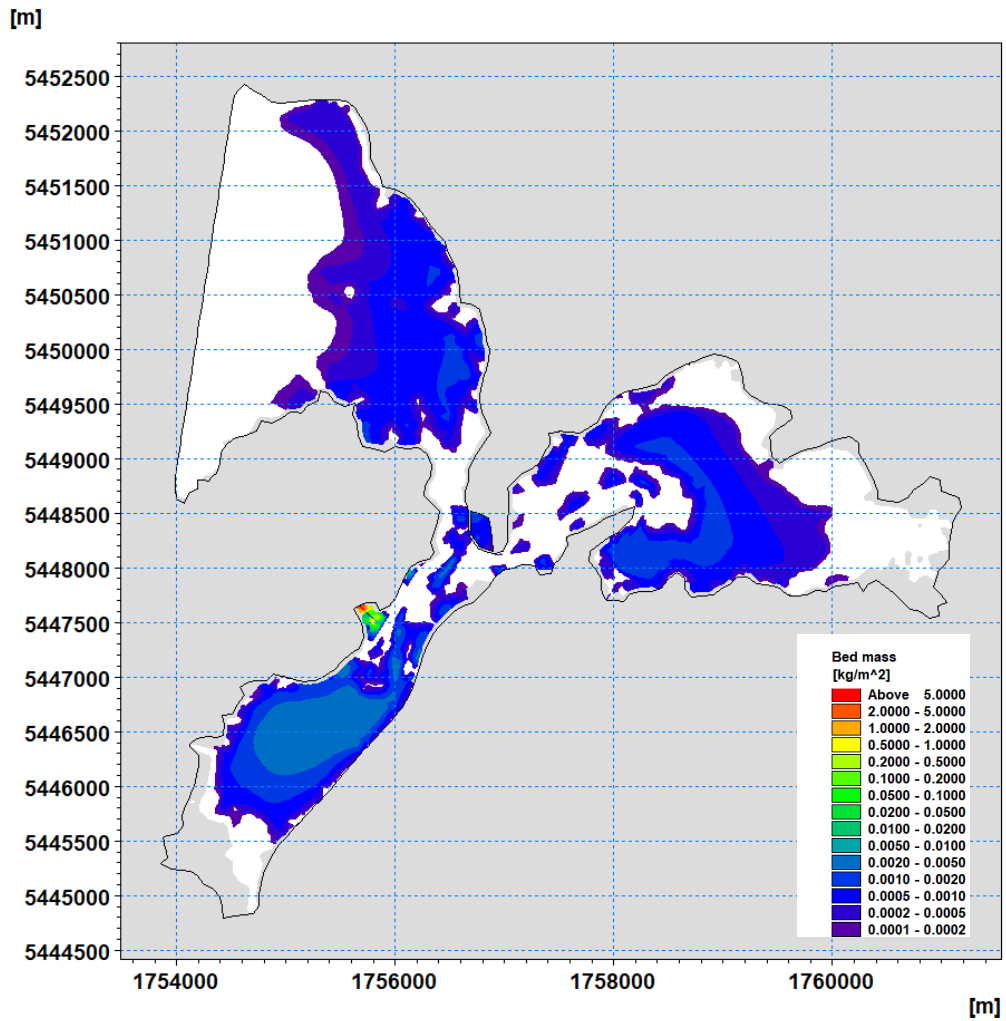
Figure C-11. Predicted sediment depositional footprint for the Whitireia/Te Onepoto subcatchment. Graduated colour scale represents the mass of subcatchment deposited on the seabed (kg/m2) over the duration of the 2010 model simulation.
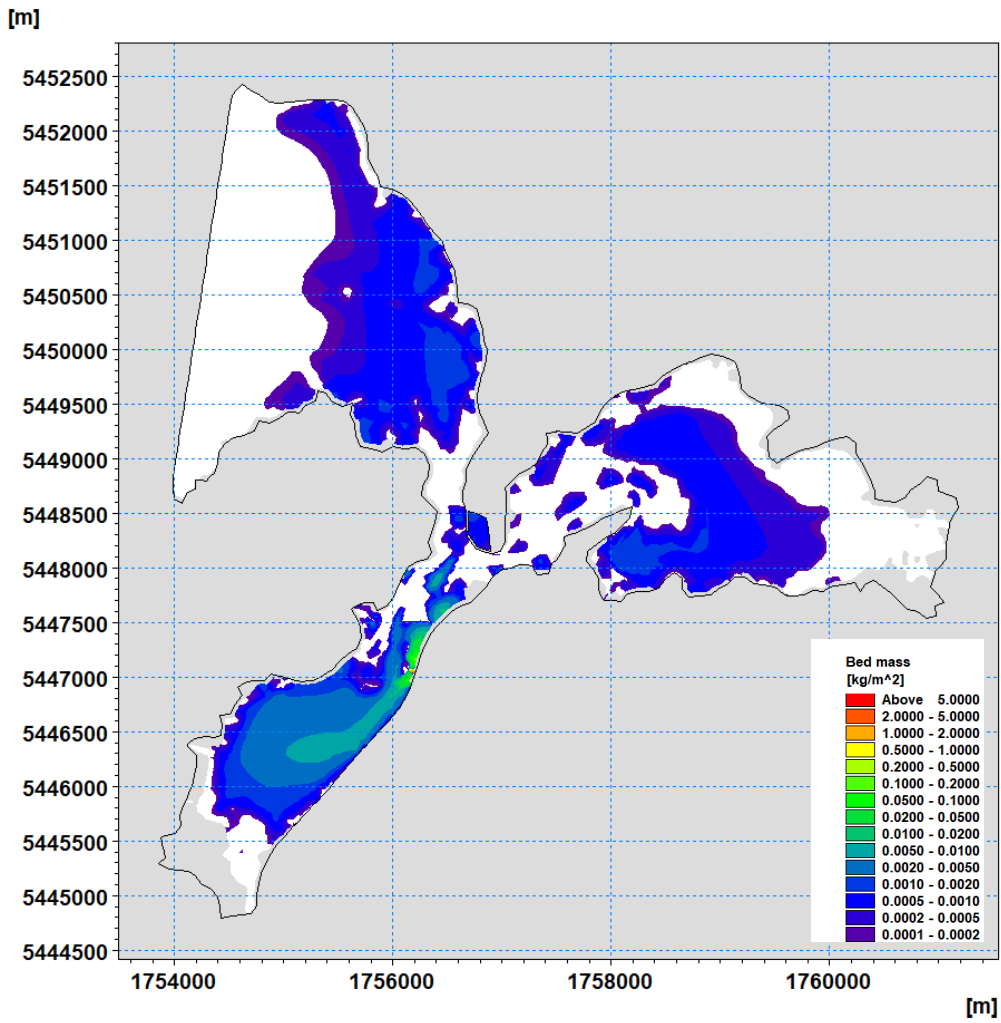
Figure C-12. Predicted sediment depositional footprint for the Direct to Onepoto (North) subcatchment. Graduated colour scale represents the mass of subcatchment deposited on the seabed (kg/m2) over the duration of the 2010 model simulation.
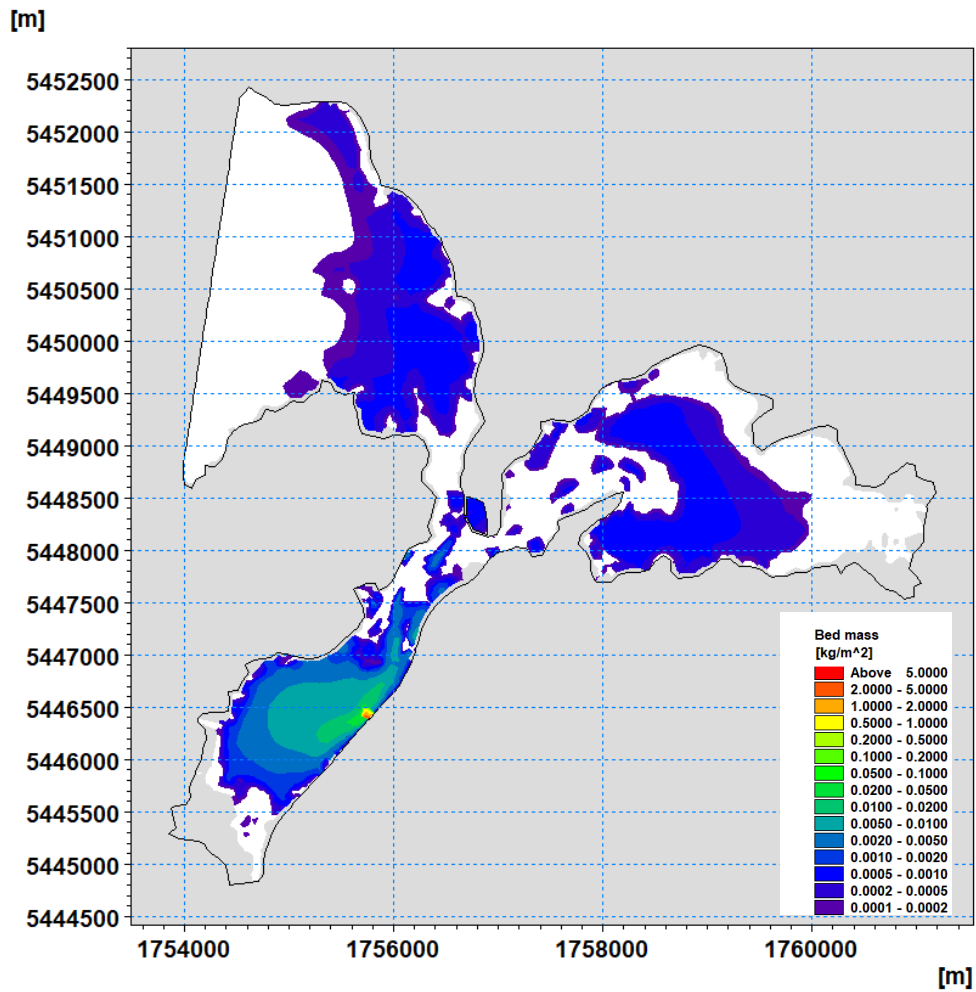
Figure C-13. Predicted sediment depositional footprint for the Direct to Onepoto (Mid) subcatchment. Graduated colour scale represents the mass of subcatchment deposited on the seabed (kg/m2) over the duration of the 2010 model simulation.
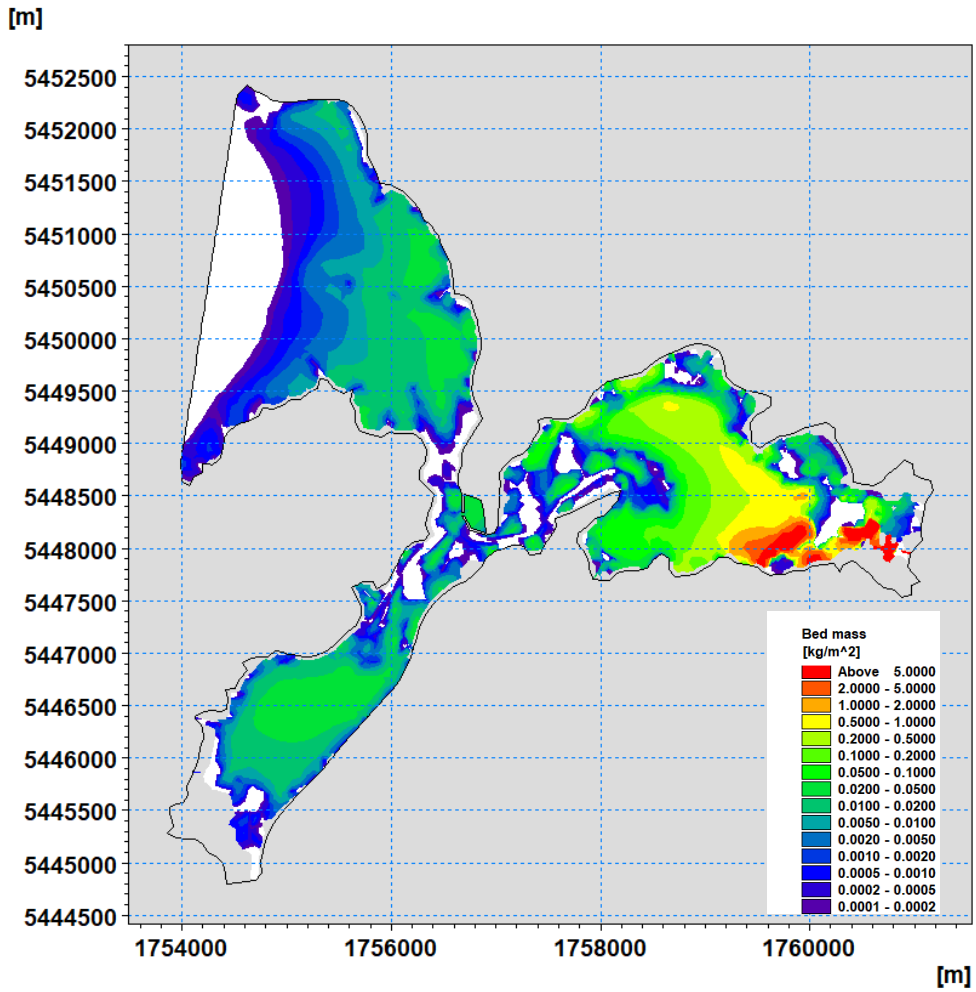
Figure C-14. Predicted sediment depositional footprint for the Pauatahanui mouth subcatchment. Graduated colour scale represents the mass of subcatchment deposited on the seabed (kg/m2) over the duration of the 2010 model simulation.
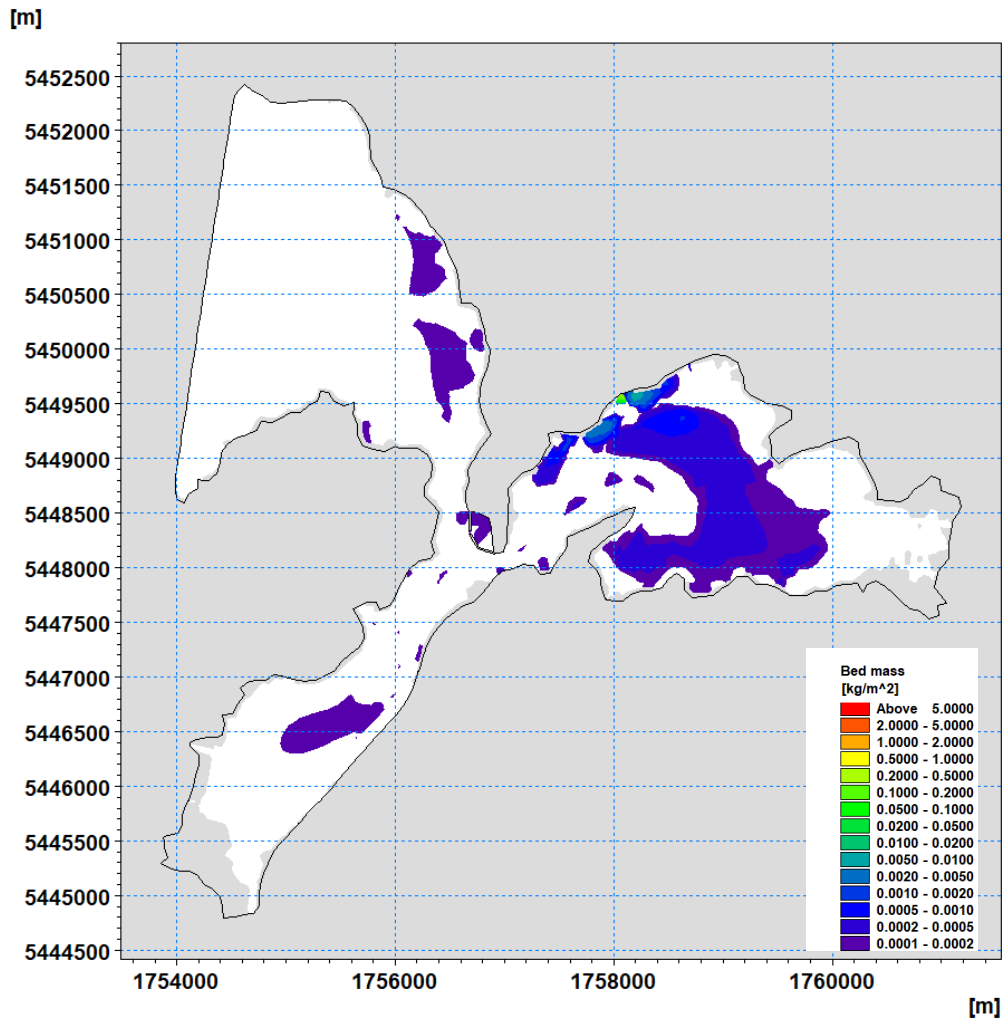
Figure C-15. Predicted sediment depositional footprint for the Direct to Pauatahanui (Mid) subcatchment. Graduated colour scale represents the mass of subcatchment deposited on the seabed (kg/m2) over the duration of the 2010 model simulation.
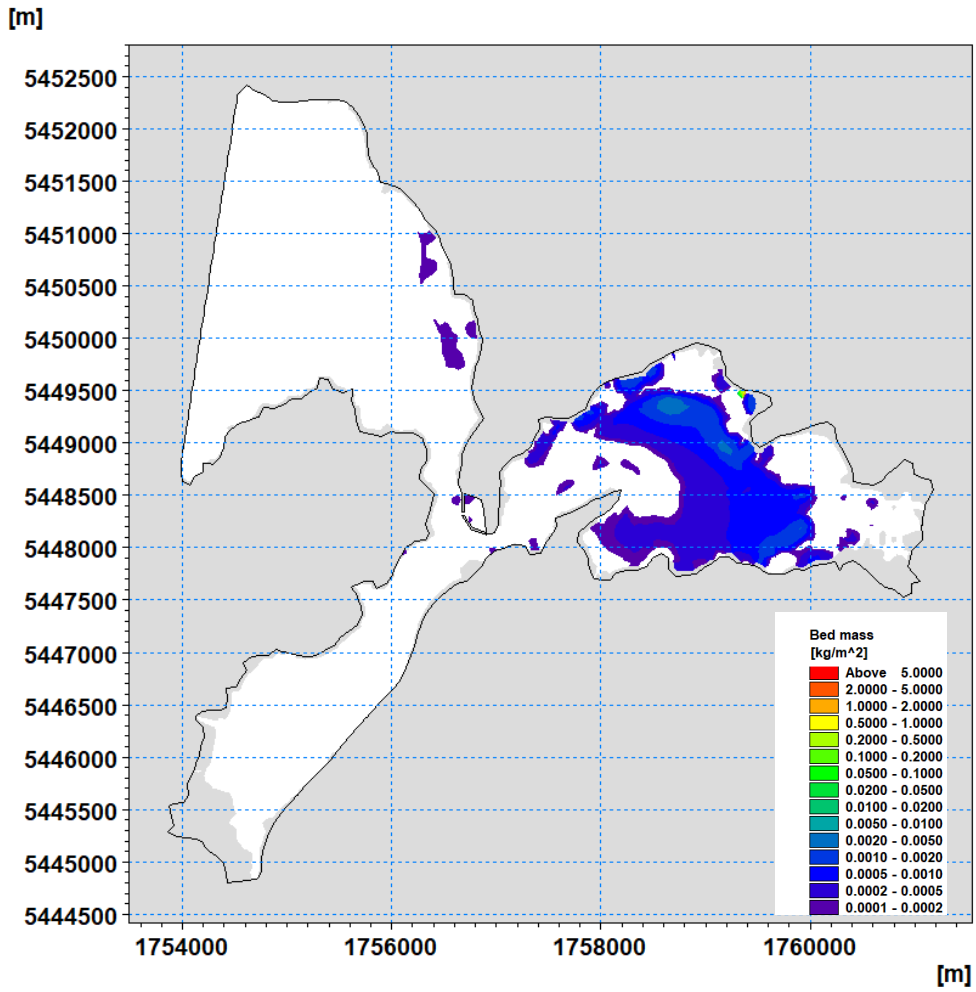
Figure C-16. Predicted sediment depositional footprint for the Motukaraka subcatchment. Graduated colour scale represents the mass of subcatchment deposited on the seabed (kg/m2) over the duration of the 2010 model simulation.
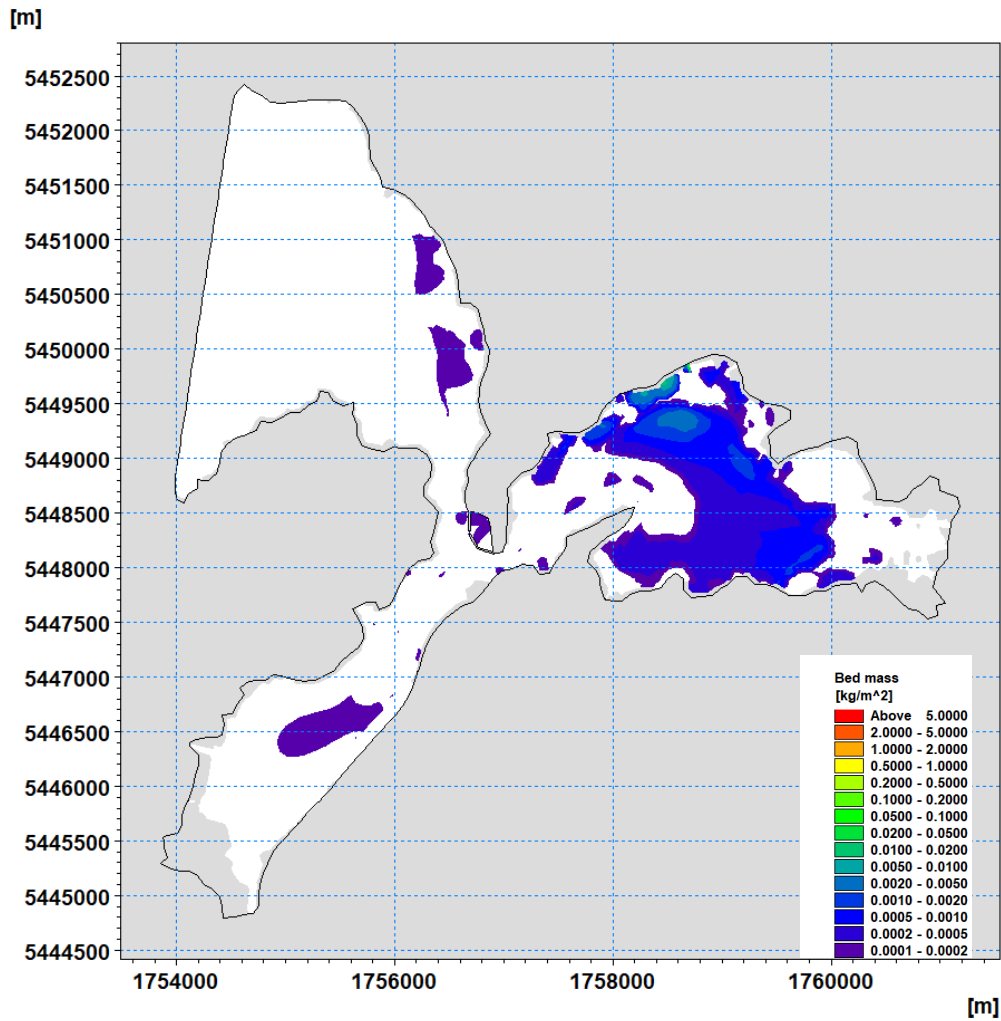
Figure C-17. Predicted sediment depositional footprint for the Direct to Pauatahanui (Water ski club) subcatchment. Graduated colour scale represents the mass of subcatchment deposited on the seabed (kg/m2) over the duration of the 2010 model simulation.
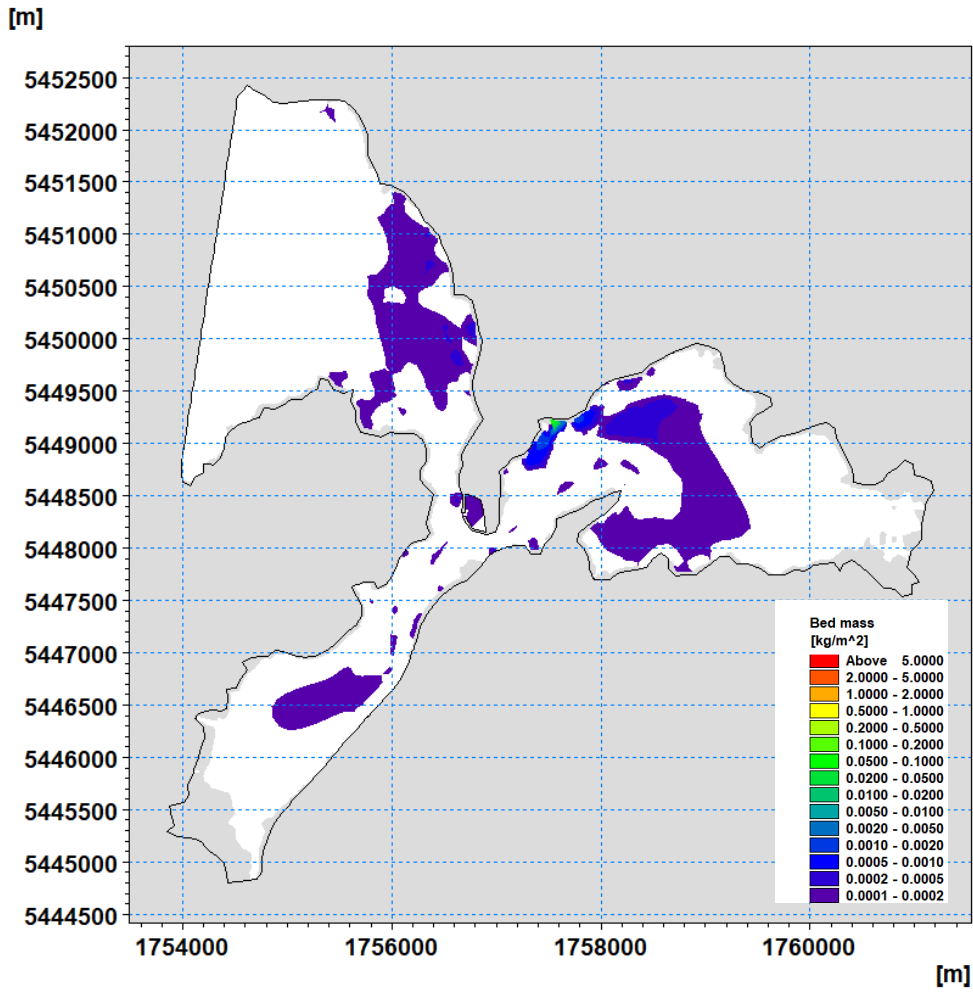
Figure C-18.   Predicted sediment depositional footprint for the Direct to Pauatahanui (Boat houses) subcatchment. Graduated colour scale represents the mass of subcatchment deposited on the seabed (kg/m²) over the duration of the 2010 model simulation.
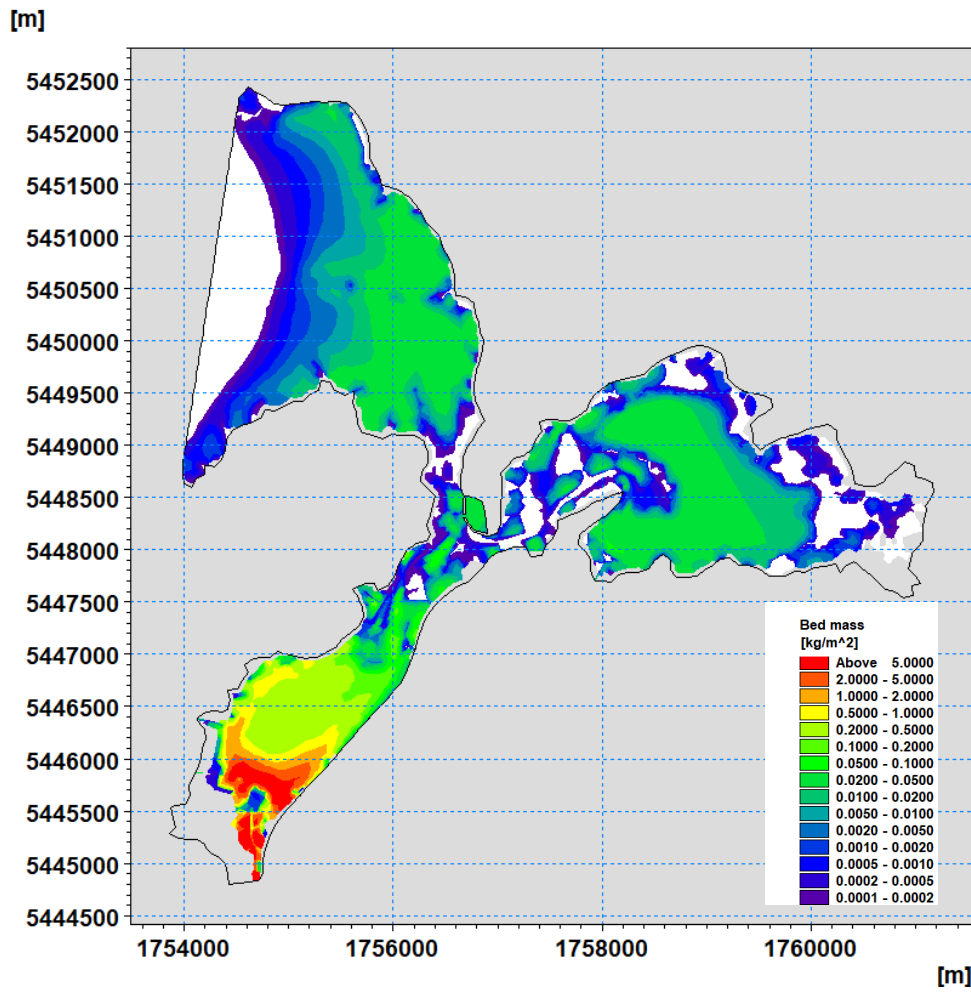
Figure C-19. Predicted sediment depositional footprint for the Porirua Mouth subcatchment. Graduated colour scale represents the mass of subcatchment deposited on the seabed (kg/m²) over the duration of the 2010 model simulation. Scale is logarithmic ranging from very low values of less than 0.005 kg/m² (equivalent to less than 0.01 mm) through to more than 2 kg/m² (equivalent to more than 5 mm of deposition)
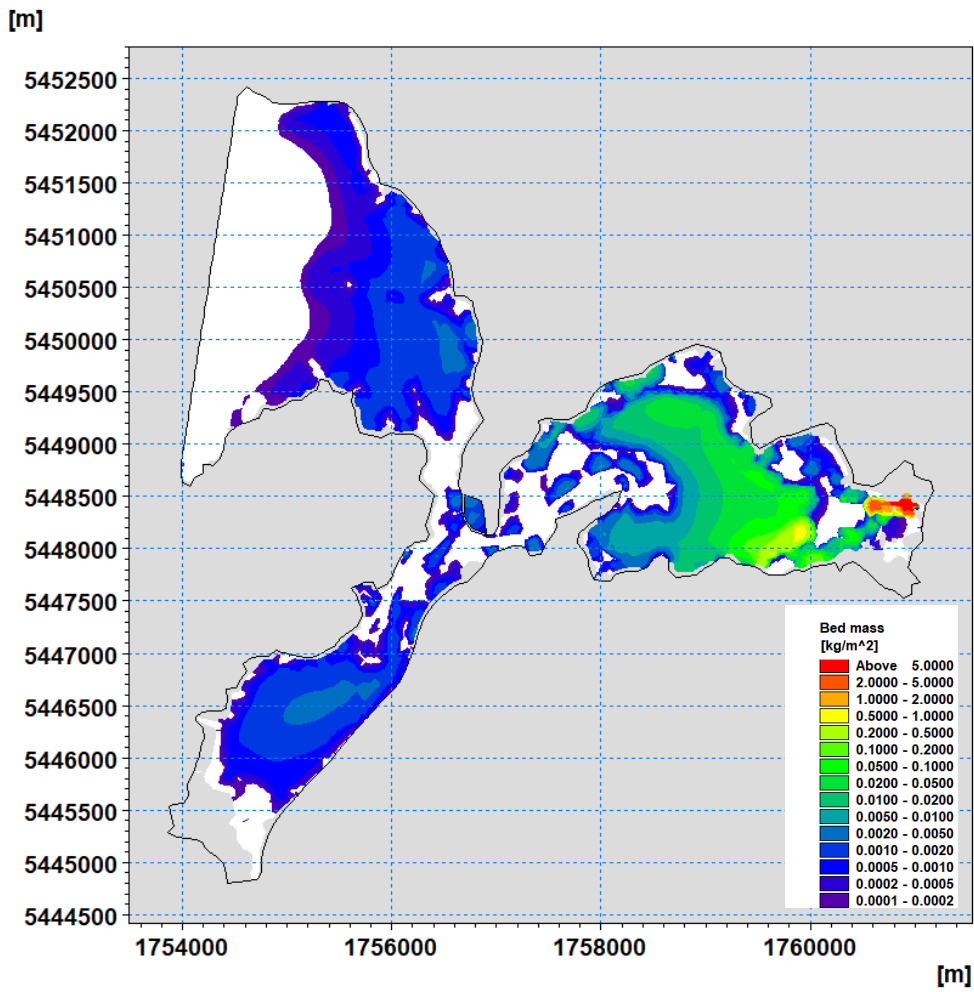
Figure C-20. Predicted sediment depositional footprint for the Ration subcatchment. Graduated colour scale represents the mass of subcatchment deposited on the seabed (kg/m^2) over the duration of the 2010 model simulation.